Australian Rainfall & Runoff

A GUIDE TO FLOOD ESTIMATION

BOOK 5 - FLOOD HYDROGRAPH ESTIMATION

Australian Government

ENGINEERS AUSTRALIA

ISBN 978-1-925848-36-6

How to reference this book:
Ball J, Babister M, Nathan R, Weeks W, Weinmann E, Retallick M, Testoni I, (Editors) Australian Rainfall and Runoff: A Guide to Flood Estimation, © Commonwealth of Australia (Geoscience Australia), 2019.

How to reference Book 9: Runoff in Urban Areas:
Coombes, P., and Roso, S. (Editors), 2019 Runoff in Urban Areas, Book 9 in Australian Rainfall and Runoff - A Guide to Flood Estimation, Commonwealth of Australia, © Commonwealth of Australia (Geoscience Australia), 2019.

PREFACE

Since its first publication in 1958, Australian Rainfall and Runoff (ARR) has remained one of the most influential and widely used guidelines published by Engineers Australia (EA). The 3rd edition, published in 1987, retained the same level of national and international acclaim as its predecessors.

With nationwide applicability, balancing the varied climates of Australia, the information and the approaches presented in Australian Rainfall and Runoff are essential for policy decisions and projects involving:

- infrastructure such as roads, rail, airports, bridges, dams, stormwater and sewer systems;
- town planning;
- mining;
- developing flood management plans for urban and rural communities;
- flood warnings and flood emergency management;
- operation of regulated river systems; and
- prediction of extreme flood levels.

However, many of the practices recommended in the 1987 edition of ARR have become outdated, and no longer represent industry best practice. This fact, coupled with the greater understanding of climate and flood hydrology derived from the larger data sets now available to us, has provided the primary impetus for revising these guidelines. It is hoped that this revision will lead to improved design practice, which will allow better management, policy and planning decisions to be made.

One of the major responsibilities of the National Committee on Water Engineering of Engineers Australia is the periodic revision of ARR. While the NCWE had long identified the need to update ARR it had become apparent by 2002 that even with a piecemeal approach the task could not be carried out without significant financial support. In 2008 the revision of ARR was identified as a priority in the National Adaptation Framework for Climate Change which was endorsed by the Council of Australian Governments.

In addition to the update, 21 projects were identified with the aim of filling knowledge gaps. Funding for Stages 1 and 2 of the ARR revision projects were provided by the now Department of the Environment. Stage 3 was funded by Geoscience Australia. Funding for Stages 2 and 3 of Project 1 (Development of Intensity-Frequency-Duration information across Australia) has been provided by the Bureau of Meteorology. The outcomes of the projects assisted the ARR Editorial Team with the compiling and writing of chapters in the revised ARR. Steering and Technical Committees were established to assist the ARR Editorial Team in guiding the projects to achieve desired outcomes.

Assoc Prof James Ball
ARR Editor

Mark Babister
Chair Technical Committee for
ARR Revision Projects

ARR Technical Committee:

Chair: Mark Babister
Members:
Associate Professor James Ball
Professor George Kuczera
Professor Martin Lambert
Associate Professor Rory Nathan
Dr Bill Weeks
Associate Professor Ashish Sharma
Dr Bryson Bates
Steve Finlay

Related Appointments:

ARR Project Engineer:	Monique Retallick
ARR Admin Support:	Isabelle Testoni
Assisting TC on Technical Matters:	Erwin Weinmann, Dr Michael Leonard

ARR Editorial Team:

Editors:James Ball
Mark Babister
Rory Nathan
Bill Weeks
Erwin Weinmann
Monique Retallick
Isabelle Testoni

Associate Editors for Book 9 - Runoff in Urban Areas

Peter Coombes
Steve Roso

Editorial assistance: Mikayla Ward

Status of this document

This document is a living document and will be regularly updated in the future.

In development of this guidance, and discussed in Book 1 of ARR 1987, it was recognised that knowledge and information availability is not fixed and that future research and applications will develop new techniques and information. This is particularly relevant in applications where techniques have been extrapolated from the region of their development to other regions and where efforts should be made to reduce large uncertainties in current estimates of design flood characteristics.

Therefore, where circumstances warrant, designers have a duty to use other procedures and design information more appropriate for their design flood problem. The Editorial team of this edition of Australian Rainfall and Runoff believe that the use of new or improved procedures should be encouraged, especially where these are more appropriate than the methods described in this publication.

Care should be taken when combining inputs derived using ARR 1987 and methods described in this document.

What is new in ARR 2019?

Geoscience Australia, on behalf of the Australian Government, asked the National Committee on Water Engineers (NCWE) - a specialist committee of Engineers Australia - to continue overseeing the technical direction of ARR. ARR's success comes from practitioners and researchers driving its development; and the NCWE is the appropriate organisation to oversee this work. The NCWE has formed a sub-committee to lead the ongoing management and development of ARR for the benefit of the Australian community and the profession. The current membership of the ARR management subcommittee includes Mark Babister, Robin Connolly, Rory Nathan and Bill Weeks.

The ARR team have been working hard on finalising ARR since it was released in 2016. The team has received a lot of feedback from industry and practitioners, ranging from substantial feedback to minor typographical errors. Much of this feedback has now been addressed. Where a decision has been made not to address the feedback, advice has been provided as to why this was the case.

A new version of ARR is now available. ARR 2019 is a result of extensive consultation and feedback from practitioners. Noteworthy updates include the completion of Book 9, reflection of current climate change practice and improvements to user experience, including the availability of the document as a PDF.

Key updates in ARR 2019

Update	ARR 2016	ARR 2019
Book 9	Available as “rough” draft	Peer reviewed and completed
Guideline formats	Epub version Web-based version	Following practitioner feedback, a pdf version of ARR 2019 is now available
User experience	Limited functionality in web-based version	Additional pdf format available
Climate change	Reflected best practice as of 2016 Climate Change policies	Updated to reflect current practice
PMF chapter	Updated from the guidance provided in 1998 to include current best practice	Minor edits and reflects differences required for use in dam studies and floodplain management
Examples		Examples included for Book 9
Figures		Updated reflecting practitioner feedback

As of May 2019, this version is considered to be final.

BOOK 5

Flood Hydrograph Estimation

Flood Hydrograph Estimation

Table of Contents

List of Figures

List of Tables

Chapter 1. Introduction

James Ball, Erwin Weinmann

Chapter Status	Final
Date last updated	14/5/2019

1.1. Flood Hydrograph Modelling

From the alternative flood estimation approaches introduced in Book 1, Chapter 3, the methods and models covered in this book of Australian Rainfall and Runoff focus on the event-based simulation approach. This approach simulates only the time period covering a single storm event, given the initial conditions for the event, but the storm may consist of several separate rainfall bursts, resulting in a multi-peaked flood hydrograph.

The more general aspects of catchment simulation for design flood estimation are covered in Book 4, and the chapters in this book deal specifically with the models and design inputs required to transform the event-based design rainfall inputs from Book 2 into design flood hydrographs at catchment locations of interest.

This book is an extension of the material covered in Book 3, which deals with the calculation of design flood peak discharges. While peak discharges (without flood hydrographs) are adequate for many applications, such as calculating bridge or culvert capacity, flood hydrographs are essential for many other applications. These applications include those where floodplain storage or artificial storage is an important issue or where the movement and modification of flood events through a catchment is of interest. With the increasing implementation of more advanced hydrological modelling systems and more complex analysis requirements, guidance on flood hydrograph modelling is becoming increasingly important.

The flood hydrograph methods described here provide an alternative method to the flood peak discharge methods covered in Book 3 and allow cross checking between the two methods. There is a place therefore for both peak flow and flood hydrograph estimation for different applications.

1.1.1. Overall Flood Hydrograph Estimation Process

The process of developing and applying an event-based flood hydrograph estimation model involves the following steps:

1. Definition of the flood estimation problem and the model requirements;

2. Assessment of data requirements and data availability, data collation and checking;

3. Study of catchment data and flood information to develop an understanding of the catchment behaviour during floods and to identify important features that need to be represented in the model - Book 5, Chapter 2;

4. Conceptualised representation of the runoff generation phase of flood formation (loss model and baseflow model) - Book 5, Chapter 3 and Book 5, Chapter 4;

5. Conceptualised representation of the flood hydrograph formation phase (the routing elements of the catchment) - Book 5, Chapter 2, Book 5, Chapter 5 and Book 5, Chapter 6;

6. Determination of model parameters by calibration to observed events, from experience values in regions with similar flood producing characteristics or from links with measured catchment characteristics - Book 7, Chapter 5;

7. Validation of the calibrated model to ensure that it is fit for the intended purpose – Book 7, Chapter 6;

8. Application of the model with design rainfalls (Book 2), design losses (Book 5, Chapter 3) and design baseflows (Book 5, Chapter 4) to estimate design flood hydrographs - Book 7, Chapter 7;

9. Interpretation and presentation of model results, including determination of uncertainty – Book 7, Chapter 9 and Book 7, Chapter 8; and

10. The modelled design flood hydrographs will generally form the inputs to a hydraulic model of the study area.

The following chapters of Book 5 introduce the important hydrologic modelling principles that are applied in Steps 3 to 5 of the overall process. Book 5, Chapter 3 (Losses) and Book 5, Chapter 4 (Baseflow Models) also provide guidance on the design values required in Step 7. Detailed application guidance relating to the other steps is provided in Book 7.

1.1.2. Conceptual Representation of Flood Formation

The complex hydrologic processes involved in the formation and modification of flood hydrographs are represented in flood hydrograph estimation models in a highly conceptualised form. The processes involved in the *runoff generation phase*, described in more detail in Book 4, Chapter 2, are represented in *conceptual loss models* (Book 5, Chapter 3, Section 2) in a simplified fashion. These conceptual loss models divide the rainfall inputs into rainfall excess and loss (without modelling what happens with the loss component). As the name implies, the rainfall excess reflects only the surface runoff component that is directly attributable to the event rainfall. The additional component of streamflow originating from recession flows from previous rainfall events or groundwater inflows is referred to as baseflow. This baseflow component is represented in *conceptual baseflow models* (Book 5, Chapter 4). Baseflow contributions to runoff are added to the rainfall excess component either at the sub-catchment scale or, more commonly, as a total baseflow hydrograph at the catchment outlet.

In the *hydrograph formation phase*, the routing of flood contributions from subareas through the various stream reaches, floodplains and natural or artificial storages is modelled by hydrologic or hydraulic routing models of different complexity (Book 5, Chapter 5).

Some flood hydrograph modelling approaches represent the catchment only as a single unit (lumped models). However, the models now typically applied in the event-based simulation approach are semi-distributed in nature; they represent the catchment being modelled by a number of sub-catchments or subareas, where the degree of spatial resolution used typically varies between around 10 to 100 subareas. The processes involved in the *runoff generation phase* are modelled at the sub-catchment or subarea scale, and the resulting runoff hydrographs are then routed along the different stream reaches and storages in the catchment to the point of interest. Node-link type runoff-routing models are the most

common form of these models, where the nodes represent the subareas and stream junctions, and the links the routing reaches (Book 5, Chapter 6). In addition to providing a more detailed and physically based approach to hydrological modelling, distributed models allow the assessment of flood hydrographs for points within the main catchment as well as at the outlet, whereas lumped models allow calculation of hydrographs only at the catchment outlet.

Figure 5.1.1 depicts a schematic representation of how the flood formation processes are conceptualised in event-based flood hydrograph estimation models.

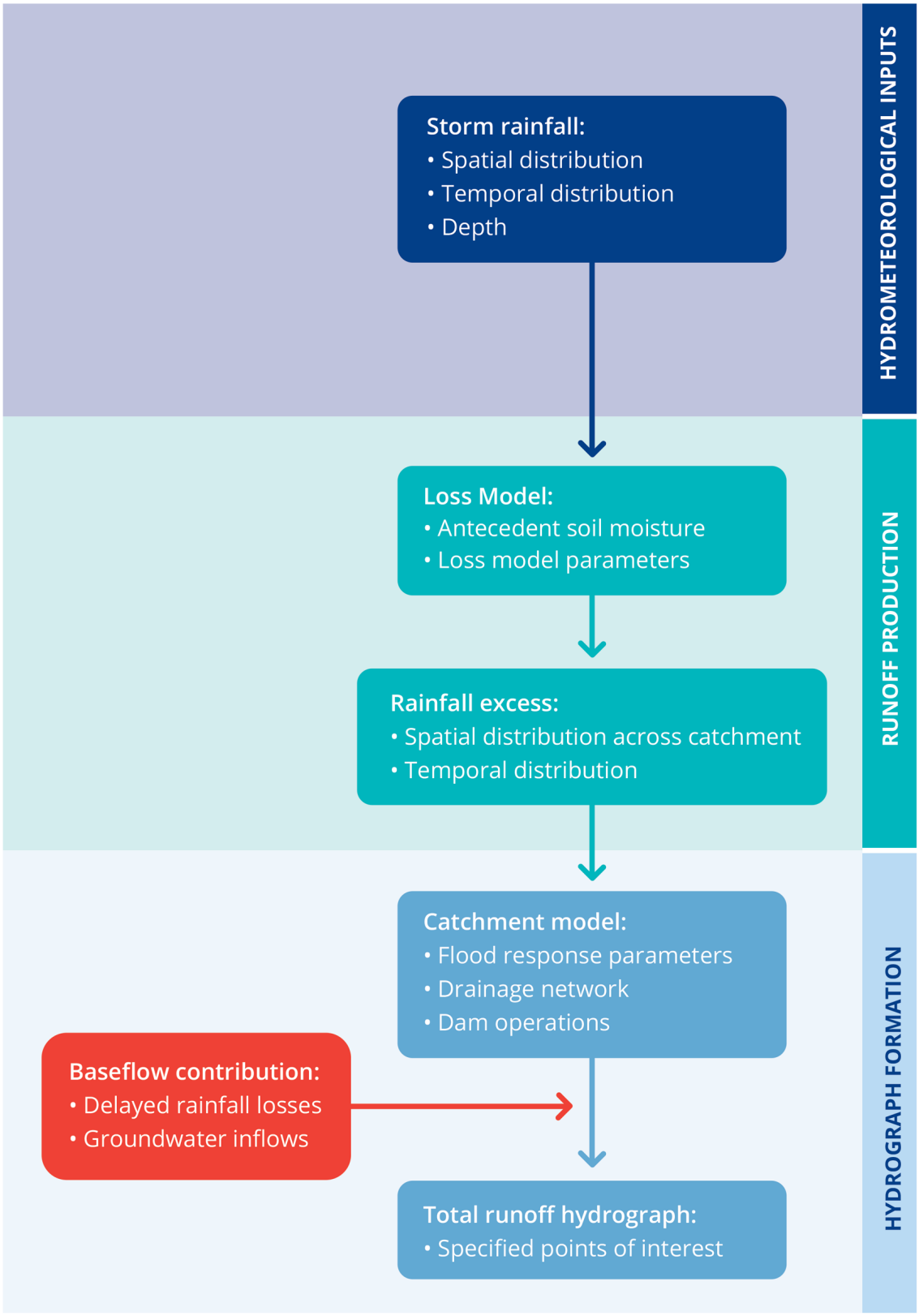

Figure 5.1.1. Conceptual Representation of Flood Formation Processes in the Most Commonly used Event-based Flood Hydrograph Estimation Models (courtesy R Nathan)

1.2. Scope

This book of Australian Rainfall and Runoff provides background information on the basic elements that make up event-based flood hydrograph estimation models, and an overview of the modelling systems most commonly used in Australia. This introductory information is intended to equip practitioners with a clearer understanding of the simplifications and assumptions involved in different model components. Book 5, Chapter 3 and Book 5, Chapter 4 also give guidance on the design loss and baseflow inputs for use with event-based flood hydrograph estimation models. Detailed guidance on other aspects of applying these models to practical flood hydrograph estimation problems is provided in Book 7.

As in other books, the guidance provided here should not be interpreted as being prescriptive, as unusual catchment conditions may require special considerations. Importantly, the application of the models and design data for flood hydrograph estimation should be informed by a good understanding of general hydrologic principles and concepts relevant to flood estimation as well as specific interpretation of local flood data.

1.3. Book Contents

After this introductory chapter, Book 5, Chapter 2 introduces the basic concepts and approaches used in representing catchments for event-based modelling of floods. Book 5, Chapter 3 gives details of the loss models applied in generating surface runoff, and the models used to represent the contribution of baseflow are dealt with in Book 5, Chapter 4. Both chapters are based on research undertaken as part of the ARR Revision Projects funded by the Commonwealth of Australia. The chapters give the background to the selection of the adopted models, then describe the sources of information for the derivation of design values of losses and baseflow, and finally provide guidance for the practical application of loss models and baseflow models. Book 5, Chapter 5 introduces important flood routing principles applied in modelling the movement of flood hydrographs through the stream and floodplain system, linking them with the hydraulic principles covered in Book 6. Finally, Book 5, Chapter 6 describes the most important conceptualisations and approaches used in runoff-routing modelling systems to derive complete flood hydrographs at points of interest.

Chapter 2. Catchment Representation

Erwin Weinmann

Chapter Status	Final
Date last updated	14/5/2019

2.1. Introduction

The representation of a catchment in a flood hydrograph estimation model is, by necessity, highly conceptualised and aims to represent those features and characteristics that are most influential in determining the overall flood response of the catchment. The distribution of storm rainfall over different parts of the catchment and the flood response to it may vary considerably, depending on the details of topography, vegetation cover, land use and drainage network characteristics. However, as the hydrograph inputs from different parts of the catchment are progressively combined on their way to the catchment outlet, only some of these differences in response characteristics are directly reflected in the combined hydrographs at downstream points of interest. Different catchment modelling approaches have therefore evolved to find an appropriate compromise between required model complexity and spatial resolution on the one hand, and desirable modelling efficiency on the other. These different modelling approaches can be applied with different degrees of complexity, and often more simple methods may be quite appropriate.

As is explained in more detail in Book 5, Chapter 5 and Book 5, Chapter 6, the various forms of *temporary flood storage* available in different parts of the catchment play a key role in determining how the runoff inputs from different parts of the catchment are transformed into the flood hydrograph at the catchment outlet. The effect of catchment storage on the routing of hydrographs is twofold and involves:

i. *translation* of the hydrograph peak and other ordinates forward in time and

ii. *attenuation* of the peak as the hydrograph moves along the stream network.

The different catchment representations in flood hydrograph estimation models can therefore be classified on the basis of how the different forms of temporary flood storage are conceptualised and in how much detail they are represented in the model. Other factors such as losses, which determine the flood volume (covered in Book 5, Chapter 3) and baseflow, which may modify the flood hydrograph shape and volume (covered in Book 5, Chapter 4), must also be a part of the modelling of flood hydrographs.

In situations where the interest is only on the combined hydrograph at the catchment outlet and where good flood records for current conditions are available at that point, modelling of the catchment as a single ‘lumped’ response unit may be sufficient. This is the approach adopted by a number of traditional flood hydrograph estimation methods such as the unit hydrograph approach, the time-area approach and the Clark and Nash models of runoff-routing. In these modelling approaches, discussed further in Book 5, Chapter 2, Section 2, the rainfall excess input is ‘lumped’ for the whole catchment and then transformed by some routing method to a hydrograph at the catchment outlet.

For catchments with more complex runoff production and flood hydrograph formation characteristics it is more usual to adopt a semi-distributed rather than a lumped modelling approach. Adoption of a semi-distributed approach allows the key factors that influence flood

response to be represented in a spatially explicit fashion. Common factors represented in a semi-distributed manner include rainfall, losses and routing parameters, though such models also facilitate the representation of influential catchment features that control variation in the timing and/or magnitude of flood runoff from different parts of the catchment. The category of semi-distributed models (or node-link type models), dealt with in Book 5, Chapter 2, Section 3, allows for an appropriate matching of spatial model resolution with the degree of spatial variation of catchment characteristics and inputs.

Finally, developments in computing power and the availability of digital terrain information now allow a fully distributed representation of catchments in grid-based models. The emerging rainfall-on-grid modelling approach is discussed in Book 5, Chapter 2, Section 4.

Many of the following considerations on how to represent catchments in hydrologic flood estimation models apply to both rural and urban catchments. However, modelling of urban catchments is treated in more detail in Book 9.

2.2. Lumped Models

In relatively small catchments (or within each sub-catchment of a larger catchment) there is often only limited spatial variation in rainfall and loss characteristics, and it is thus acceptable to treat the catchment (or sub-catchment) as a homogeneous unit. Models that do not allow for spatial variation in runoff or routing characteristics within a catchment are referred to as ‘lumped’ models. It is possible to link the outputs of several lumped models to form a quasi-distributed catchment model.

The peak flow estimation methods described in Book 3 can be regarded as “lumped” type models, since the flood peaks are calculated at a single point only, without the internal characteristics of the catchment being considered.

In the runoff generation phase of lumped models, the conceptual loss and baseflow models described in Book 5, Chapter 3 and Book 5, Chapter 4 can be applied using the assumption that the rainfall inputs, losses and baseflow contributions are the same over the whole catchment. Such a simplifying assumption may be appropriate when rainfall and streamflow data are only available from a single gauge and it is thus difficult to infer any internal variation of the rainfall and runoff generation characteristics.

In the hydrograph formation or routing phase of lumped models, a range of conceptualisations may be used to represent the hydrograph translation and attenuation effects of the catchment on the runoff hydrograph input. These conceptualisations may aim to represent physical catchment processes, but they are essentially ‘black box’ mathematical representations. The different lumped flood modelling approaches include:

1. *The Time-Area Approach* (Book 5, Chapter 6, Section 2) - in which the different degree of translation (time lag) experienced by runoff from different parts of the catchment is modelled by dividing the catchment into a number of areas with the same delay time to the catchment outlet (‘isochronal areas’). The runoff inputs to the different sub-areas are then lagged accordingly to represent the translation effects of the total catchment, but this routing method does not provide for any attenuation of peak flows on their way to the catchment outlet.

2. *The Unit Hydrograph Approach* (Book 5, Chapter 6, Section 3) - which converts rainfall excess inputs to a flood hydrograph by applying a transfer function (the unit hydrograph). The transfer function is generally inferred from the analysis of observed rainfall inputs and streamflow outputs, and there is limited potential to relate its parameterisation to

measurable catchment characteristics, though the parameters for the method may be developed from recorded data.

3. *Other lumped flood hydrograph estimation methods* - that involve use of a single (concentrated) linear storage (e.g. Clarke) or a distributed form of storage represented by a cascade of several linear storages (e.g. Nash). Variations of these methods with non-linear storages are also used. The fundamental flood routing concepts applied in these methods are further explained in Book 5, Chapter 5, Section 2 to Book 5, Chapter 5, Section 4.

While lumped flood hydrograph estimation models have the advantage of simplicity, they are limited in their application to the following situations:

- Catchments with relatively uniform spatial rainfall, loss and baseflow characteristics or where the variation of these characteristics between events is relatively minor, so that the derived unit hydrograph or other model parameters are applicable to a range of design events;
- Catchments with no significant artificial storages (reservoirs or flood detention basins);
- Applications where a flood hydrograph is only required at the catchment outlet, as for the design of drainage structures on roads and railway lines; and
- Applications that do not require extrapolation to the range of Very Rare to Extreme floods.

To the extent that they adopt a ‘black box’ approach (ie. the functions used to transform rainfalls to streamflows do not have direct links to physical catchment characteristics), lumped models depend on the availability of observed flood hydrographs for their calibration. The scope for application to ungauged catchments is thus more limited but the Clark-Johnstone synthetic unit hydrograph method (Book 5, Chapter 6, Section 3) has in the past been widely used for catchments on the east coast of Australia (Cordery et al., 1981).

The semi-distributed (node-link type) models described in the next section offer a broader range of application but are also more demanding in terms of model development, data requirements and understanding/skill of the practitioner. The lumped flood hydrograph estimation approach can be seen as a simplified version of the semi-distributed flood hydrograph estimation approach, and it is worth noting that the most widely used runoff-routing models (described in Book 5, Chapter 6, Section 4) can be configured to represent catchment response in a lumped fashion.

2.3. Semi-Distributed (Node-Link Type) Models

Semi-distributed models allow the spatial variation of inputs and key processes to be modelled explicitly. This is particularly important in large catchments and in catchments where the natural flooding characteristics have been significantly modified by various forms of development, including the construction of reservoirs, flood mitigation works and transport and drainage infrastructure.

Because of their flexibility and ability to calculate flood hydrographs throughout the catchment and to model land use and catchment changes, as well as being relatively straightforward to establish and run, node-link type models are currently the most widely used modelling approach for flood hydrograph estimation in Australia. A range of ready-to-use modelling systems (Book 5, Chapter 6, Section 4) are available to set up models for catchments of different size and complexity. These modelling systems allow the influential

features and characteristics of a catchment to be represented in the model but in a highly conceptualised form. All conceptualisations involve some degree of lumping in terms of the processes modelled and spatial averaging of inputs, but the different modelling systems differ in the way they divide the catchment into various conceptual elements and in the methods they use to model the processes represented by these elements.

Figure 5.2.1 shows a simple conceptual representation of the runoff-routing process in a node-link type model. Each subarea receives a rainfall excess input which is converted to a runoff hydrograph at the node representing this subarea. The hydrographs are then routed successively through the links representing the drainage network to form the hydrograph at the catchment outlet.

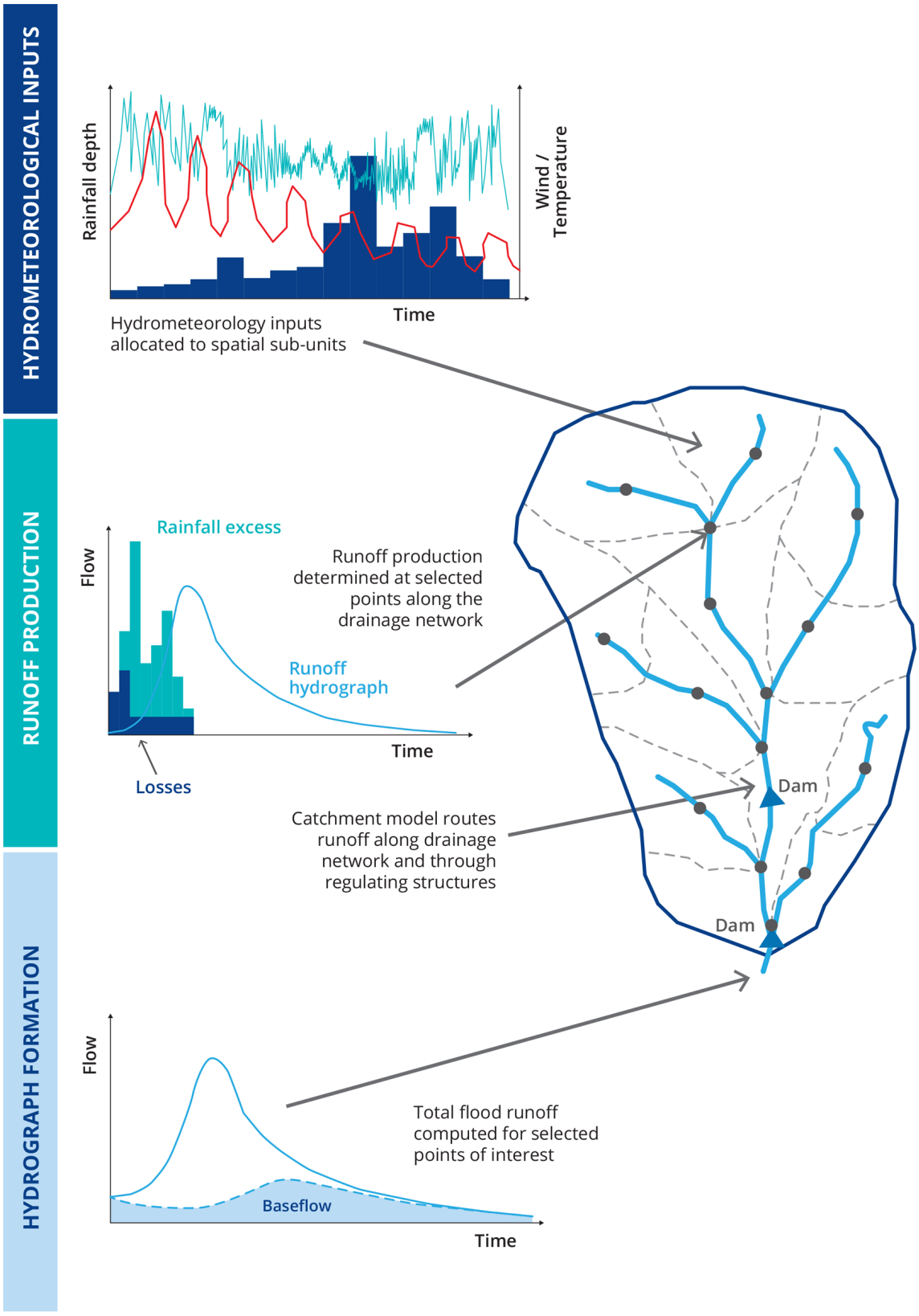

Figure 5.2.1. Conceptual Representation of the Runoff Routing Process in a Node-Link Type Model

2.3.1. Conceptual Model Elements

To build a semi-distributed model, the real catchment has to be conceptually represented as a system of nodes and links, each representing a different element of the actual catchment system. The following set of basic nodes and links can be used in different catchment models, but different models vary in how these basic elements are applied.

Nodes:

- Input nodes for hyetographs of rainfall excess or hydrographs of direct runoff (and possibly baseflow) from model sub-areas;
- Input nodes for inflow hydrographs from separately modelled catchments;
- Junction nodes – where different branches of the drainage network join (or where diversion flows re-enter);
- Diversion nodes – points where some of the flow is diverted or abstracted from the network;
- Reservoir routing nodes;
- Flood detention routing nodes; and
- Nodes for hydrograph outputs (including at gauging locations for comparison of modelled and observed hydrographs).

Links:

- Stream or channel routing links;
- Bypass links; and
- Floodplain storage links.

2.3.2. Catchment Sub-Division

The basic principle applied in dividing the catchment into a number of sub-areas for semi-distributed modelling is to provide a simplified but physically-based representation of the spatial features of the catchment, using a relatively small number of sub-areas (typically 10 to 100). The delineation of these sub-areas should generally follow topographic features that control the movement and storage of flood waters. Relevant land use features, such as the urban sections of the catchment, or areas inundated by large water bodies, need to be specifically delineated. The features that control flowpaths in relatively flat catchments may not be evident, and careful analysis of available topographic and flood data is required to define the sub-area boundaries. Detailed survey as well as aerial or satellite images may assist the catchment delineation in areas where the drainage characteristics are unclear.

The catchment sub-division should also have regard to the prevailing land uses in different parts of the catchment and should aim at sub-areas that are essentially homogeneous in terms of their runoff characteristics. This is particularly relevant in urban or urbanising catchments. Large areas with immediate runoff response, such as natural lakes and reservoirs also require special consideration. Book 7, Chapter 4 provides more detailed guidance.

2.3.3. Modelling of Runoff from 'Hill Slopes' (Overland Flow)

The term “contributing areas” is used to describe those areas of catchments where surface runoff occurs in the form of overland flow, sheet flow or flow in small channels that are not significant enough to be modelled separately (Book 4, Chapter 2, Section 2). There are two distinctly different methods used to model this runoff component:

i. The input hyetograph (areal average rainfall excess) for the sub-area is directly converted into a runoff hydrograph at a representative point within the sub-area (usually at or close to the centroid). This assumes that all runoff from the sub-area reaches this input node without any delay and there is no flow attenuation within the sub-area. Any translation and attenuation effects occurring within the hill slope elements thus need to be represented in the routing through the drainage network from the subarea input node to downstream points of interest; and

ii. The input hyetograph to the sub-area is transformed to an output hydrograph using one of the lumped catchment models introduced in Book 5, Chapter 2, Section 2. Different models use time-area, unit hydrograph or different forms of storage routing or kinematic wave routing concepts for this transformation.

Method (i) has the advantage of simplicity in that it avoids having to determine additional model parameters for runoff from contributing areas. In catchments with relatively uniform land use, when the interest is mainly on flood hydrographs at the catchment outlet for a limited range of flood magnitudes, this method can be expected to provide satisfactory results. However, it may provide conservatively high estimates of hydrograph peaks at internal points in the upper parts of the catchment due to the neglect of routing effects in the contributing areas of the catchment. Book 5, Chapter 6, Section 4 provides more detailed discussion of this method.

Method (ii) allows for better representation of processes that contribute to hydrographs in the upper parts of the catchment but it requires additional parameters. It is also better able to deal with the effects of significant land use changes in parts of the catchment and with changed runoff behaviour in Very Rare to Extreme flood events (Book 8, Chapter 5). A more detailed discussion of this approach is provided in Book 5, Chapter 6, Section 4.

2.3.4. Routing Through Network of Stream/Channel/Floodplain Elements

Except in small rural catchments, most of the translation and attenuation effects in the transformation of rainfall inputs to hydrograph outputs occur in the routing of hydrographs through the network of streams/channels, floodplains and major storages. The capability of a modelling system to adequately reflect the translation and attenuation involved in this transformation is therefore an important prerequisite for accurate flood hydrograph estimation.

Two distinctly different groups of flood routing approaches are used in node-link type flood hydrograph estimation models:

i. *Hydrologic Routing Approaches*- these flood routing methods are based on the storage routing principles described in Book 5, Chapter 5, Section 4 (linear storage routing) and Book 5, Chapter 5, Section 5 (non-linear storage routing). An important characteristic of hydrologic flood routing models is that their parameters are generally inferred from observed flood hydrographs, but it is possible to infer their parameters through close links

with hydraulic methods (e.g. Muskingum-Cunge Method, Book 5, Chapter 5, Section 4) or from the results of hydraulic modelling; and

ii. *Hydraulic Routing Approaches* - these flood routing methods are based directly on the full unsteady flow equations or various simplified forms of these equations, as described in Book 5, Chapter 5, Section 5. Their parameters are inferred from the cross-sectional characteristics of streams, channels and floodplains, and the hydraulic characteristics of controlling features. The kinematic wave and diffusion wave approaches described in Book 5, Chapter 5, Section 5 are the most widely used hydraulic routing approaches incorporated into flood hydrograph estimation models.

The hydrologic routing approaches have the advantage that, by deriving their parameters from observed hydrographs, they represent an integrated routing response from the complex stream and floodplain system that is often too complex to be represented in detail. However, application of such calibrated parameters to conditions outside the ones reflected in the observed hydrographs (ie. for changed catchment conditions or significantly different flood magnitudes) involves assumptions that may not be justifiable. The hydraulic routing methods have closer links to the physical characteristics of the routing reaches, but their application still involves a significant degree of conceptualisation and some form of calibration.

Modelling of the flood routing effects over a range of flow conditions requires a clear understanding of the flood dynamics so that the simulated response can be appropriately matched to the actual flooding behaviour. Specifically this means that the adopted network should represent any breakout flows and bypass flows occurring during larger floods, as well as the effects of significant floodplain storage areas activated during large events. The additional storage availability in large flood events may be counter-balanced by increased flow efficiency as the flow depth increases. Where backwater effects are likely to have a significant impact not only on flood levels but also on the routing of flood flows through the drainage network, hydraulic routing methods based on the full unsteady flow equations may be required.

The model should also represent the varying impact of flow restrictions for different flow magnitudes. In some cases the results of detailed hydraulic modelling may be required to develop a clear understanding of the changes in flood flow behaviour with flood magnitude, so that they can be adequately reflected in the hydrologic catchment model.

One important limitation of node-link type models is that the different routing elements are conceptualised as one dimensional flow links. This means that a dominant flow direction needs to be assumed when the routing elements are defined. In cases where the flow direction changes for floods of different magnitudes, it may be necessary to introduce more complexity into the channel network so that different flowpaths are activated at different flow magnitudes. The two dimensional rainfall-on-grid approaches discussed in Book 5, Chapter 2, Section 4 are in principle better equipped to deal with changes in flow direction during a flood event and between flood events of different magnitude, but this advantage may be off-set by the difficulty of using such models to adequately represent loss processes and roughness characteristics at the scale of individual grid cells.

Whatever routing method is used, it is important to ensure that any application of the model outside its range of calibration is guided by consideration of changes in hydraulic characteristics and then reflected in the adopted network conceptualisation and parameter values. This is further discussed in Book 7, Chapter 4 and Book 7, Chapter 5.

2.3.5. Routing Trough Special Storages

When flood storage occurs in a concentrated form, such as in lakes, reservoirs, detention basins and large natural or artificial flood storageage areas, it is appropriate to model the flood modifying effects of such storages by a 'special storage' routine. Where the relevant survey and hydrographic data are available, the storage-discharge characteristics of such special storages may be defined by storage rating curves and discharge rating curves in terms of depth or elevation. In other situations, simplified storage-discharge relationships need to be derived from observed inflow and outflow hydrographs or by trial and error during model calibration. Methods for deriving storage-discharge relationships for different conceptual storage elements are discussed in Book 5, Chapter 6, Section 4.

2.4. Grid-based (Distributed) Models

In the fully distributed or grid-based flood hydrograph estimation models (also referred to as 'rainfall-on-grid' models) the catchment is represented by a large number of grid cells, based on topographic data from a Digital Elevation Model (DEM). More detailed survey information on the drainage network and flow controlling features of the catchment may be superimposed on the DEM data.

Different models vary in the degree of detail adopted in modelling the runoff generated from rainfall falling on a grid element. In principle the method allows more physically-based representations of runoff processes; however, this is only likely to be valid at larger depths of overland flow. Such models currently represent saturation and ponding processes in a simplistic fashion, and similar simplifications are adopted in modelling the baseflow contribution at the scale of individual cells.

The routing of runoff from individual cells through the catchment and the stream network is then based on the principles of two dimensional dynamic wave modelling introduced in Book 5, Chapter 5, Section 5 and described in more detail in Book 6, Chapter 4, Section 7. Particular issues to be dealt with in these models are the significantly larger data requirements than for node-link type models to give a realistic representation of the catchment, characterisation of hydraulic roughness for different catchment elements, and how to deal with computational stability problems that arise when runoff is generated from initially dry cells.

As the direction of the flow between cells is determined as part of the solution process at each time step, drainage paths do not need to be pre-defined as in traditional one dimensional runoff-routing approaches. The application of hydraulic methods in the runoff-routing process also means that there is no need for linking the hydrologic model with a hydraulic model of the floodplain area.

In most catchments the catchment boundaries and the drainage network are quite well defined in the upper part of the catchment, and traditional runoff-routing models can thus adequately describe the flood hydrograph formation for these parts of the catchment. A 'hybrid' approach, where a two dimensional model is only used for runoff-routing in the flatter or urbanised parts of the catchment that are influenced by complex hydraulic controls, may be the most efficient approach in these situations.

The theoretical advantage of grid-based models is that a lesser degree of conceptualisation in the catchment representation is required, thus requiring less hydrologic expertise of the practitioner. However, the modelling of the overland flow phase at the scale of individual grid cells still poses challenges and requires further research. The principles applied in rainfall-

on-grid models and their advantages and limitations are discussed in more detail in Book 5, Chapter 6, Section 5. While grid-based methods are apparently more directly based on physical catchment data than alternative methods, they still need to be calibrated with recorded data, and there is still uncertainty in the results from their application. This is discussed further in Book 7.

At the current stage of development of these models and with the limited level of experience gained with their practical application, it is considered premature to recommend their general use in these Guidelines. However, it is expected that further development and testing will allow rainfall-on-grid models to be more widely applied.

2.5. References

Cordery, I, Pilgrim, D.H. and Baron, B.C. (1981), Validity of use of small catchment research results for large basins. Instn. Engrs. Australia, Civil Engg. Trans., CE23: 131-137.

Chapter 3. Losses

Peter Hill, Rhys Thomson

Chapter Status	Final
Date last updated	14/5/2019

3.1. Introduction

This chapter provides advice on loss models and values for design flood estimation. It deals with the fundamental hydrologic question – how much rainfall becomes runoff? Design floods are typically derived either using flood frequency analysis or rainfall-based flood event models. Continuous simulation is covered in Book 4 and the focus of this chapter is losses for event based design flood estimation.

The loss is just one of the number of inputs to the design process (such as the critical storm duration, areal reduction factor, spatial pattern, temporal pattern, runoff routing model, model parameters and treatment of baseflow) that can affect the magnitude of the calculated design flood. These other inputs are discussed in other books.

This chapter is structured as follows:

- Book 5, Chapter 3, Section 2 – discusses how loss processes are represented in different conceptual loss models, ranging from empirical models through to more complex process models
- Book 5, Chapter 3, Section 3 – discusses the selection of conceptual loss models and different approaches to estimating loss values
- Book 5, Chapter 3, Section 4 – describes the estimation of effective impervious areas for urban catchments
- Book 5, Chapter 3, Section 5 – summarise different sources of information on loss values for rural and urban catchments that can be used to help select values for design
- Book 5, Chapter 3, Section 6 – discusses different approaches to characterising the distribution of loss values
- Book 5, Chapter 3, Section 7 – discusses a range of other considerations for selecting loss values for design flood estimation

3.2. Conceptual Loss Models

3.2.1. Loss Processes

3.2.1.1. Physical Processes

Loss is defined as the precipitation that does not appear as direct runoff, and is attributed to the following key processes (refer to Figure 5.3.1):

- Interception by vegetation;

- Infiltration into the soil;
- Retention on the surface (depression storage); and
- Transmission loss through the stream bed and banks.

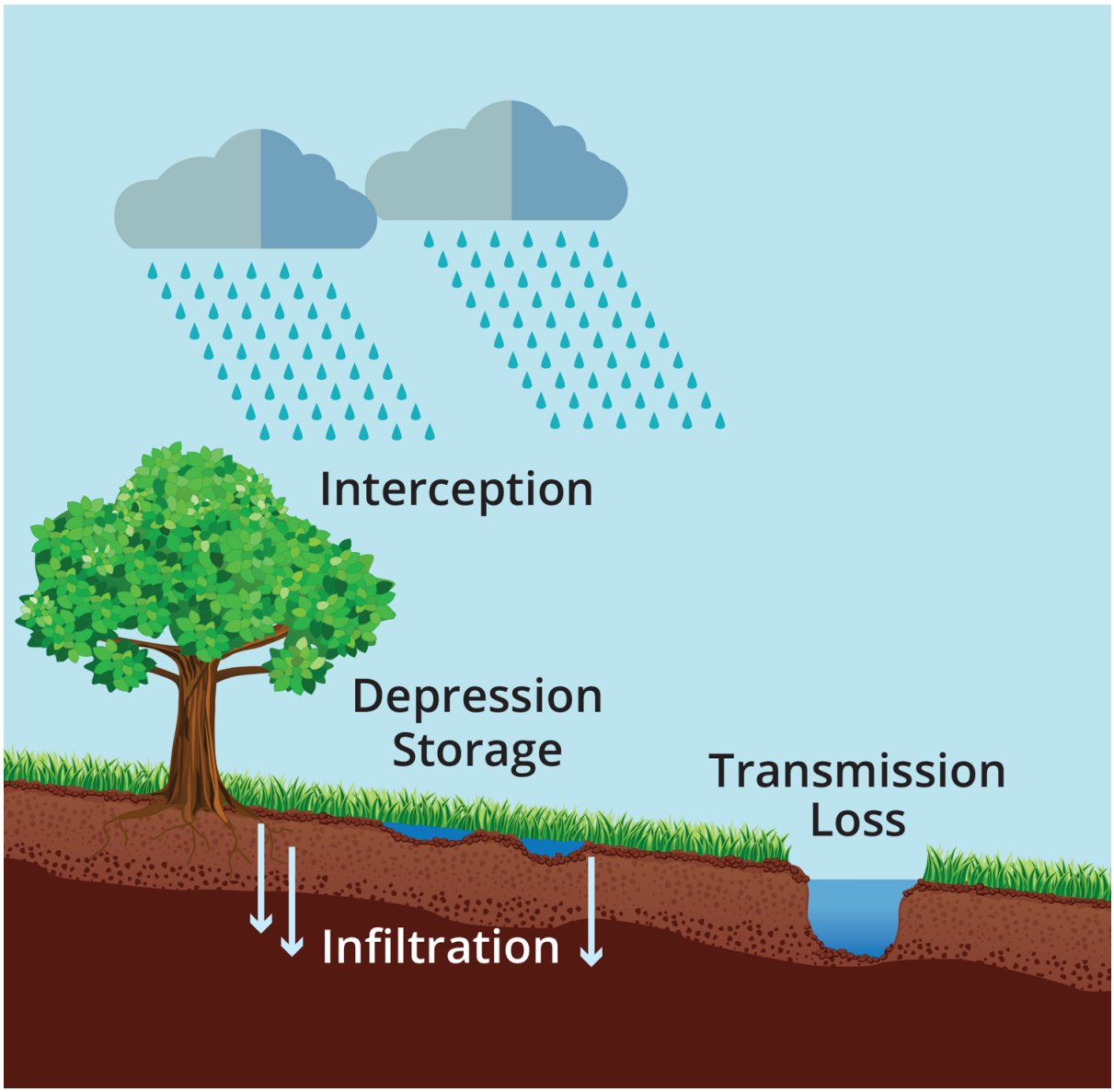

Figure 5.3.1. Physical Processes which Contribute to Rainfall Loss

More details on the runoff process are described in Book 4, while this section focuses on specific processes associated with estimation of losses.

Runoff has generally been considered to consist of surface runoff produced by rainfall excess which occurs at the ground surface when the rainfall intensity exceeds the infiltration capacity. This is known as Horton-type runoff and Fleming and Smiles (1975) provide a review of infiltration theory and its application to practical hydrology.

Over the last twenty years the classical concept of storm runoff has been challenged as a result of observations on natural catchments during storm periods and many detailed studies of instrumented plots and small areas. Two alternative types of storm runoff mechanism have been proposed:

- Saturated overland flow occurs when, on part of the catchment, the surface horizon of the soil becomes saturated as a result of either the build-up of a saturated zone above a soil horizon of lower hydraulic conductivity, or due to the rise of a shallow water table to the surface; and

- The other type of storm runoff is throughflow, which is water that infiltrates into the soil and percolates rapidly, largely through macropores such as cracks, root holes and worm and animal holes, and then moves laterally in a temporarily saturated zone above a layer of low hydraulic conductivity. It reaches the stream channel quickly and differs from other subsurface flow by the rapidity of its response and possibly by its relatively large magnitude.

Associated with the recognition of these two alternative types of storm runoff, is the concept that storm runoff may be generated from only a small part of many catchments. Additionally, this source area may vary in its extent from time to time, in different seasons and during the progress of a storm.

There are no practical methods for estimating storm losses and runoff that would take explicit account of different runoff processes, partial and variable source areas and small-scale variations in characteristics. The various existing methods assume uniform or average conditions, not accounting non-homogeneity of the catchment. Though each model attempts to simplify the overall process by different degrees, however, it is important to understand the complexity of these physical processes when reviewing the different loss models that are available (refer Book 5, Chapter 3, Section 2).

3.2.1.2. Urban Runoff

Urban runoff, even at the allotment level, is complex, involving contributions from roofs, yards, adjacent road and pavement areas. The effective rainfall excess from the various areas is subject to significantly different infiltration regimes (Goyen and O'Loughlin, 1999a; Goyen and O'Loughlin, 1999b) and these units are interconnected by complex and often transitory pathways (Riley and Fanning, 1997). Further discussion on these complex processes is discussed in Book 5, Chapter 3, Section 4.

3.2.1.3. Transmission Loss

The estimation of transmission (or channel) losses may be required in systems where the volume along a reach is required. Stewart and Boughton (1983) identified that the processes contributing to transmission losses were water hole storage, infiltration, evaporation and bank storage.

Majority of research on transmission losses for rural catchments was focused on long term losses relevant for water resource modelling and planning, rather than flood estimation. For example, there has been work done on gaining and losing river reaches within the Murray Darling Basin. Boughton (2015) explored transmission losses for 100 catchments from the east-coast of Australia.

The research on transmission losses tend to focus on specific reaches and hence the results are site specific. For very large arid catchments, transmission losses can be substantial, for example Knighton and Nanson (1994) found transmission losses of 75% for a reach of the Cooper Creek. However, for most design flood applications the channel losses will not be significant and can be combined with other processes that are implicitly covered by lumped conceptual models.

Urban catchments may also be subject to transmission losses. While the losses identified for rural catchments are generally less pronounced in urban catchments, transmission losses can occur along the drainage system. This may include leakages and ageing infrastructure, particularly when the soil around the drainage system is highly permeable.

3.2.2. Types of Loss Model

For the purposes of this chapter, loss models are broken into three broad classes:

- Empirical Models - designed to ensure depths of direct runoff and rainfall excess are in equilibrium. These types of models have minimal factors that would influence the values for an individual catchment.
- Simple Models - attempt to quantify a portion of the processes in a simplified manner. These include, for example, Hortonian Infiltration models where all losses are assumed to relate to infiltration.
- Process Models - attempt to represent the complex behaviour of losses within the catchment, and consider flow through the soil layers and over the catchment surface.

Given their complexities, process models have a large number of parameters that makes them difficult to apply to estimate design floods. In Australia, there is limited experience in applying process models for design flood estimation and therefore they are not covered in this section.

3.2.3. Empirical Models

Empirical loss models focus less on the loss processes themselves, rather more on representing their effects in producing flows. Rainfall excess models typically fall within this category.

In many of these models, the initial loss occurs in the beginning of the storm, prior to the commencement of surface runoff. It is assumed to be composed of interception losses, depression storage and infiltration before the soil surface is saturated; a continuing loss rate is then applied for the remainder of the storm. This model is consistent with the concept of runoff produced by infiltration excess, ie runoff occurs when the rainfall intensity exceeds the infiltration capacity of the soil.

These models apply the losses directly to the rainfall, subtracting from the rainfall itself, to produce a rainfall excess that is subsequently applied to the hydrological model. This concept of rainfall excess is important, as it does not consider the changing catchment characteristics during the period of rainfall (compared with Simple and Process models).

There is typically a wide range of initial loss values observed for a catchment (Rahman et al., 2002; Phillips et al, 2014; Hill et al., 2014a). This variability reflects the importance of antecedent conditions but uncertainties in the estimation of the timing and distribution of the catchment average rainfall also contribute to the range of values. This potential variability in the initial loss value is an important consideration, particularly in application of historical storms to hydrological models.

A number of these models are described further below.

3.2.3.1. Initial Loss - Continuing Loss

The continuing loss is the average loss rate throughout the remainder of the rainfall event after the initial losses are satisfied. Previous research and guidance suggests that constant

loss rates are most applicable to large storm events, where a significant proportion of rainfall becomes runoff. Figure 5.3.2 provides an example of the application of a typical Initial Loss – Continuing Loss model.

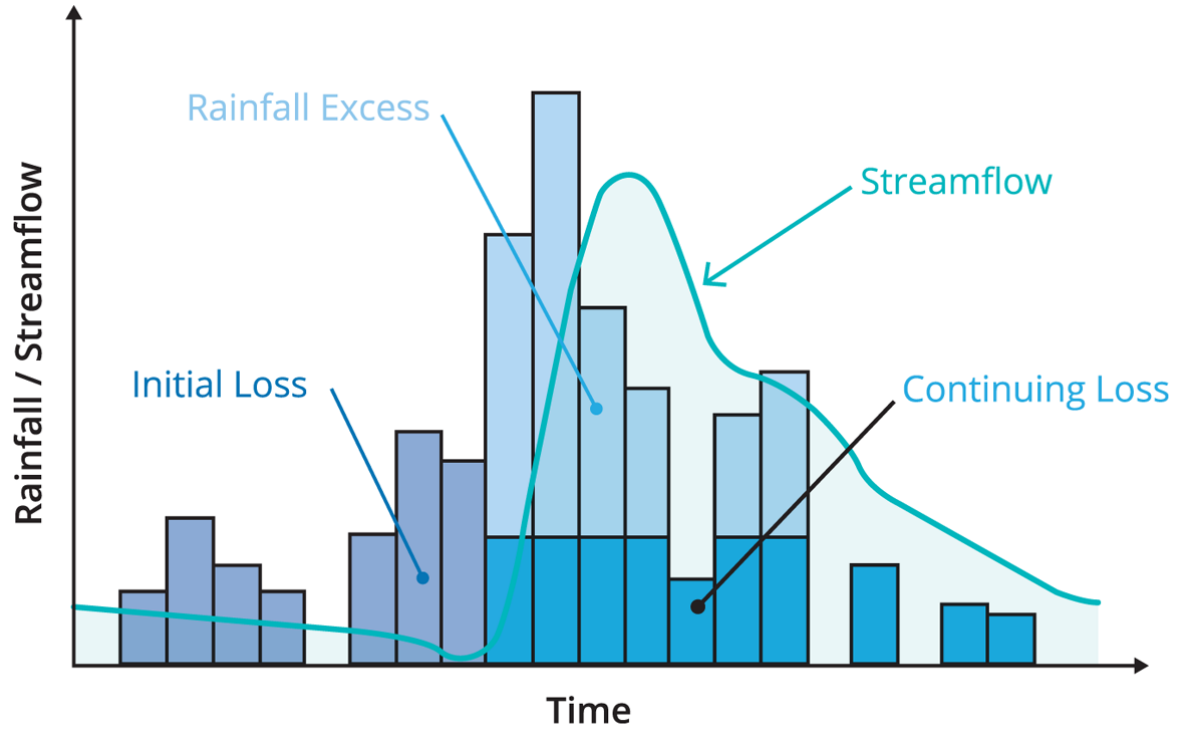

Figure 5.3.2. Initial Loss – Constant Continuing Loss Model

Despite the simple conceptual nature of the IL/CL model, there are a number of challenges in estimating continuing loss directly from recorded streamflow and rainfall.

The continuing loss rate should not be based simply on a water balance of runoff volume less initial loss divided by the duration of the event. This will underestimate the loss rate; as illustrated in Figure 5.3.2 there will likely be timesteps in which the rainfall is less than the continuing loss rate (or even zero) and hence the full value is not taken up.

Although not immediately apparent, the definition of CL also means that its magnitude is dependent on the timestep used in the analysis. This is because as the timestep reduces, there is an increased likelihood that there will be some timesteps in which the rainfall depth is less than the CL rate. Thus, to achieve the same volume of rainfall excess, the CL will typically need to be increased for shorter timesteps. This is discussed further in Book 5, Chapter 3, Section 7.

3.2.3.2. Initial Loss – Proportional Loss

The proportional loss models assume that a fixed proportion or percentage of the rainfall is lost at each time step, after the initial loss has been satisfied, which means that losses throughout the event may vary depending on the temporal patterns of rainfall. For simplicity, the proportional loss coefficient for a storm is usually taken as a constant.

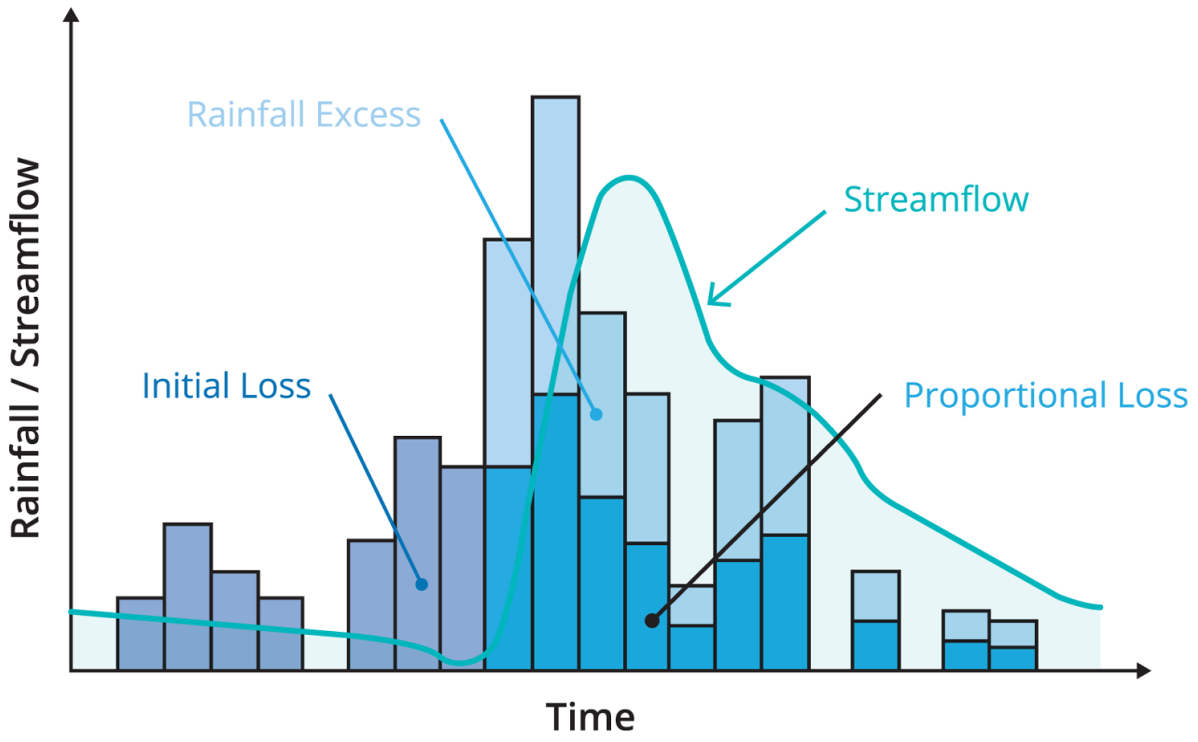

Figure 5.3.3. Initial Loss - Proportional Loss Model

Proportional loss models are consistent with runoff being generated by saturated overland flow. This assumes that runoff is generated from saturated portions of the catchment; this contributing area is expected to increase the duration and severity of the storm (Mein and O'Loughlin, 1991; Mag and Mein, 1994).

3.2.3.3. Variable Continuing Losses

In the application of the constant continuing loss and proportional loss models, it has typically been assumed that the loss rates are a constant, after the initial loss is satisfied. However, based upon consideration of physical processes it might be expected that the loss rates should decrease throughout the event as the catchment becomes wetter and infiltration reduces and/or the size of source areas enlarges.

For the IL/CL model this would suggest that the continuing loss should decrease as the event progresses and such a reduction with duration (as a surrogate for volume of infiltration) is observed from the empirical analysis of data by Ishak and Rahman (2006) and Ilahee and Imteaz (2009). The variation of continuing loss with event duration is discussed further in Book 5, Chapter 3, Section 7.

3.2.3.4. SCS Curve Number

The SCS runoff curve number (CN) is widely used in the US as well as some countries in South-East Asia. Soils in the US are classified in four hydrologic groups (A, B, C, D) according to their infiltration rate. A CN is estimated from the hydrologic soil group, the treatment of the soil (effect of cultivated agricultural lands) and the hydrologic condition (the effect of vegetation density) to add more definition to the groupings (Boughton, 1989; Woodward et al, 2002; Van Mullem et al., 2002; Ward et al., 2009).

A number of studies such as Eastgate et al. (1979) and Rajendran et al. (1982) have applied the SCS to Australian soils. There is however a lack of information on how Australian soils are classified in the SCS hydrologic groups, which limits its application in Australia.

3.2.3.5. Probability Distributed Storage Capacity Models

Most conceptual loss models are lumped so that a similar parameter value is assumed over a catchment or sub-catchment. Moore (1985) introduced the concept of probability distributed models, which can be used to account for the spatial variability in runoff generation across a catchment. This variability can arise either from:

- Differences in overall water storage capacity between sub-catchments (topography, soils, vegetation);
- Spatial variation of water storage capacity within sub-catchments (potential loss distribution);
- Stochastic variation of initial water storage status between events (different antecedent conditions); or
- Gradual variation in water storage status during an event (progressive wetting).

These models are run in a continuous or semi-continuous fashion (updated during an event) and therefore can explicitly account for antecedent conditions, as well as for variation within an event.

In general, the runoff mechanism in drier catchments is more likely to be controlled by infiltration rate whereas saturated excess is more likely to generate runoff for wetter catchments (Hill et al., 2013). The dominant mode of runoff production will depend on a range of factors including climate, soil, vegetation and topography. Those based on variable storage capacity reflect the subsurface saturation excess mechanism and include Xinanjiang (Ren-Jun et al., 1992), SWMOD (Stokes, 1989; Water and Rivers Commission, 2003) and the Revitalised Flood Hydrograph (ReFH) model in the UK (Kjeldsen et al., 2005).

These models are based on the assumption that the catchment consists of many individual storage elements with a soil moisture capacity. The depth of water in each element increases with rainfall and decreases with evaporation. When rainfall exceeds the storage capacity, direct runoff is produced. The model assumes that the soil moisture is redistributed between the elements between rainfall events.

The simplest form assumes a linear distribution of soil moisture in the catchment, from zero to its maximum capacity. This form of probability distributed model is incorporated in ReFH model in the UK. However, the above approach assumes that a portion of the catchment has zero storage capacity and hence there is no initial loss. Many catchments in arid and semi-arid areas exhibit a significant initial loss and therefore the conceptual model is extended such that the capacity varies between a minimum and maximum of the catchment. The simpler models assume that the capacities vary linearly while other models have introduced a shape parameter to describe the form of variation with capacity

3.2.3.6. SWMOD

SWMOD (Soil Water balance MODel) is developed by Stokes (1989) for the Northern Jarrah forest of Western Australia, where saturation excess overland flow is held to be the dominant runoff mechanism for storm events (Water and Rivers Commission, 2003). The model

incorporates the ability of different landforms in the catchment to store water during the storm event. When the accumulated rainfall is greater than its infiltration capacity, the sub-catchment will generate saturation-excess overland flow. Infiltration capacity is assumed to vary within an area due only to soil depth.

$$C_f = C_{\max} - (C_{\max} - C_{\min}) \times (1 - F)^{1/b} \quad (5.3.1)$$

Where:

C_f is the infiltration capacity at fraction *F* of the sub-catchment

F is the fraction of the subcatchment

b is the shape parameter

*C*max is the maximum infiltration capacity

*C*min is the minimum infiltration capacity

The infiltration capacity is taken to mean the maximum depth of water that can be stored in the soil column. Where the accumulated rainfall is greater than the infiltration capacity that fraction of the sub-catchment will have saturation-excess overland flow.

Large infiltrations ponds (10 to 15 m^2) were used in conjunction with a ring infiltrometer and a well permeameter to determine the infiltration characteristics of a complex lateritic soil profile in the Jarrah forest of Western Australia (Ruprecht and Schofield, 1993). The logs from the construction of observation bores were able to characterise the shape of *b* parameter. Hill et al. (2014b) outlines the application of SWMOD to 38 catchments across Australia.

3.2.4. Simple Models

In many loss models, the interception, depression storage and transmission losses are not directly accounted for, while the loss is treated as infiltration into the soil. The main factors affecting the soil infiltration process are the soil properties, antecedent moisture conditions, layered soils, rainfall intensity and surface sealing, vegetation cover and entrapment of air, and the soil slope and land use (Siriwardene et al., 2003). Simple models attempt to incorporate this infiltration into the soil through various models.

Various representations to the complex equations for the water movement in the soil (such as Philip and Green-Ampt, Horton etc) are used to express the reduction of infiltration capacity with time (Maidment, 1992).

Skukla et al. (2003) analysed ten infiltration models including Green-Ampt and Horton's models, using double-ring infiltrometer tests and reported that Horton's model gave the best results for most land use conditions.

Siriwardene et al. (2003) undertook field infiltrometer tests at 21 sites in eight Victorian urban catchments in order to estimate the infiltration parameters related to Horton's infiltration model. They acknowledge the difficulty in selecting representative values for the infiltration parameters because of the 'significant variability with respect to soil type and land use in the catchment'.

Mein and Goyen (1988) note that despite the obvious attraction of using Simple Models, 'the problem is to specify parameters (which relate to soil type) and initial conditions which are

satisfactory for design use on a given catchment. In practice, the uncertainties of soil behaviour and the areal variability of soil properties do not justify the use of anything more than the simplest model'.

3.2.4.1. Horton Model

Horton's equation has been used and modified over the years to provide an estimate of losses due to infiltration into pervious surfaces. It is based on a diminishing continual loss, as described in Equation (5.3.2) below.

$$f_t = f_c + (f_0 - f_c)e^{-kt} \tag{5.3.2}$$

where:

f_t is the infiltration capacity (mm/h)

f_c is the minimum or ultimate value of f_t(mm/h)

f_0 is the maximum or initial value of f_t (mm/h)

k is a decay coefficient (per hour)

t is the time from the beginning of the storm (h)

3.2.4.2. Green-Ampt

The most commonly used approximate theory based infiltration model is the one developed by Green and Ampt (1911), which is an approximate model utilising Darcy's law and is further discussed in Mein and Larson (1973), Chu (1978), Lee and Lim (1995) and King (2000).

William (1994) describes a pilot study for nine Victorian catchments to determine if application of the Green-Ampt equation provides a superior results to simplified models, when applied at catchment scale. Although the Green-Ampt equation was successfully applied to each catchment, the results produced were not on average superior to those produced using the simple empirical models.

3.2.4.3. Australian Representative Basin Model (ARBM)

The Australian Representative Basin Model (ARBM) was developed with the aim to classify and select hydrologically diverse basins at a significant scale for resource development (Fleming, 1974; Mein and McMahon, 1982). Furthermore, the model sought to increase the understanding of the hydrological processes in each basin.

The ARBM is structured to represent the passage of water over and through the catchment, as illustrated in Figure 5.3.4. It is based on Chapman's work (Chapman, 1968; Chapman, 1970), which originally sought to optimise certain parameters, while measuring others. However, developers Boyd et al. (1993) began optimising all parameters as it was believed that measurements were difficult, uncertain, costly and impractical (Mein and McMahon, 1982).

The model uses a deterministic mathematical model intended to represent physical processes and relationships between rainfall and runoff for the catchment. It operates in a continuous mode, considering both rainfall events and initial estimations of soil moisture

conditions for each wetting event. This is done by simulating soil moisture depletion by evaporation between rainfall events (Fleming, 1974). It is expected that the parameters used would be related to physical catchment characteristics, therefore making the model applicable to any Australian gauged or ungauged catchment.

Despite being developed, the optimised parameters have not exhibited uniqueness. Mein and McMahon (1982) however, do not believe that this particular model produces outcomes that are any different to other process models developed for the same purpose.

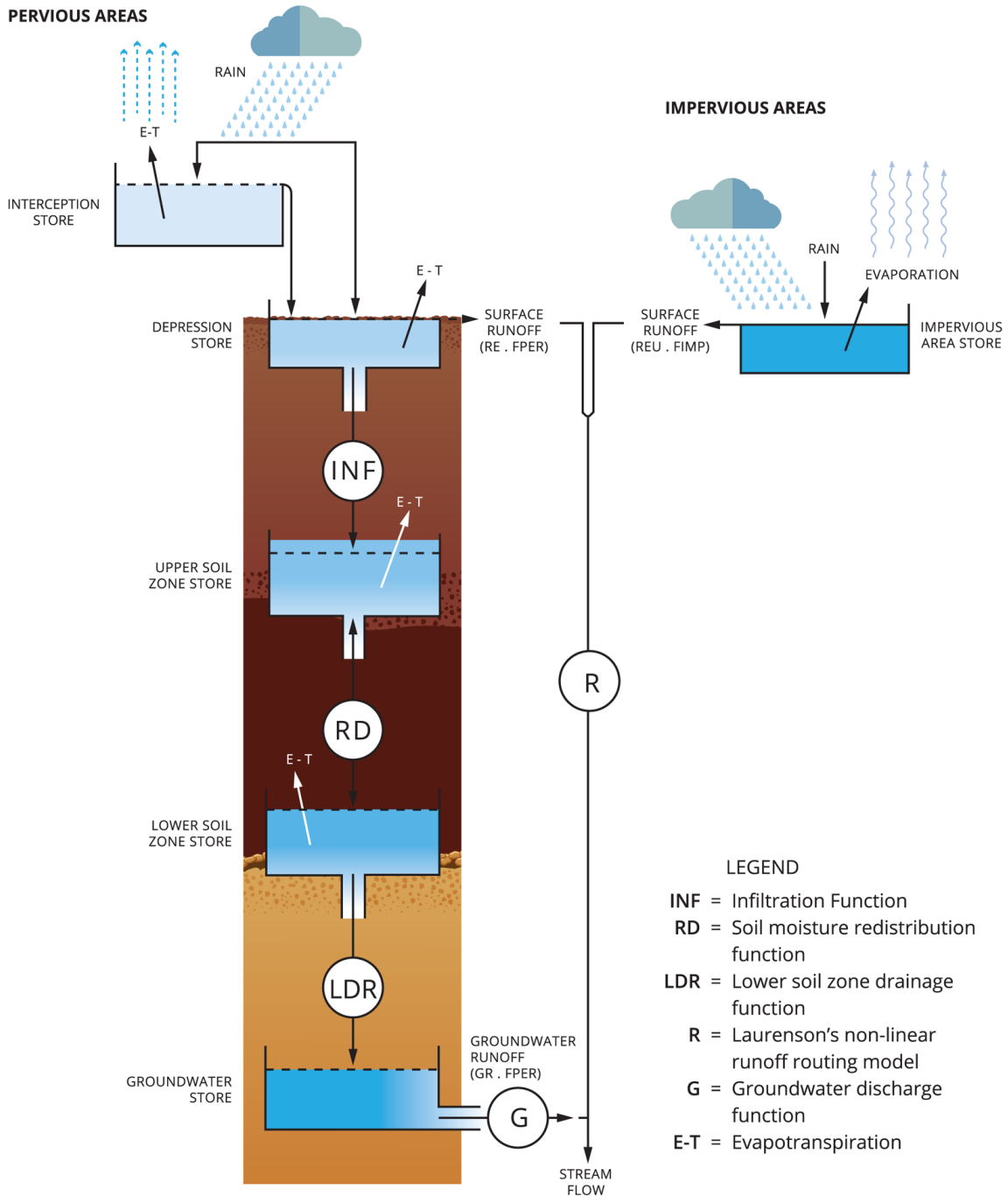

Figure 5.3.4. The model structure of the Australian Representative Basins model based on the work of Chapman (1968). Diagram obtained from Black and Aitken (1977) and Mein and McMahon (1982).

3.2.5. Process Methods

Continuous simulation is covered in Book 2, Chapter 7 and therefore the following brief overview concentrates on the loss modelling aspects.

These models typically estimate the losses from rainfall and the generation of streamflow by simulating the wetness and dryness of the catchment on a daily, hourly and occasionally sub-hourly basis. Continuous simulation eliminates the need to select representative values of loss, since the loss is explicitly included in the modelling. The focus of loss conceptualisation in continuous rainfall-runoff simulation models is less on the representation of the loss process, rather than on representing the effect on producing floods.

The majority of continuous simulation applications are for flood forecasting, rather than for design flood estimation. The development of stochastic rainfall generation techniques has encouraged their application for design flood estimation (Boughton et al., 1999; Kuczera et al., 2006).

A number of Australian studies have applied a continuous simulation approach to estimate design floods and compared the results to those from flood frequency analysis such as Boughton and Hill (1997), Muncaster et al. (1999), Boughton et al. (1999) and Heneker et al. (2003). The reported applications of continuous simulation for design flood estimation have typically involved calibration against recorded data, however,to extend the use to ungauged catchments, it will require developing regional relationships for model parameters.

3.3. Approach to Selection of Loss Model and Values

3.3.1. Selection of loss model

For real-time flood forecasting or calibration of a hydrologic model, the focus is on selection of models and parameter values that replicate the observed hydrograph. However, for design flood estimation, the objective is the derivation of unbiased estimates of specific characteristics of a design flood (typically the peak).

Thus, the key objectives of loss models and their parameterisation for design flood estimation are to:

- Close the volume balance in a probabilistic sense such that the volume of the design flood hydrograph for a given AEP should match the flood volume derived from frequency analysis of flood volumes;
- Produce a realistic time distribution of runoff to allow the modelling of peak flow and hydrograph shape;
- Reflect the effects of natural variability of runoff production for different events on the same catchment, to avoid probability bias in flood estimates; and
- Reflect the variation of runoff production with different catchment characteristics to enable application to ungauged catchments.

As discussed in Book 5, Chapter 3, Section 2, there are a range of different conceptual loss models that were derived with different conceptualisation and varying degrees of complexity from simple lumped rainfall excess models to more detailed process models.

The above objectives are important when selecting loss models for design flood estimation. It is therefore helpful to consider the following criteria when selecting a loss model for design flood estimation:

- The model produces a temporal distribution of rainfall-excess that is consistent with the effect of the processes contributing to loss;
- Suitable for extrapolation beyond calibration and is hence applicable to estimate floods over the required range of AEPs;
- Inputs are consistent with readily available data;
- Small number of parameters that need to be selected (preferably no more than 2);
- Parameters have been linked to catchment characteristics, or it is considered reasonable that such a link could be established so that the parameters can be regionalised;
- Have the potential to be easily incorporated into rainfall-runoff models; and

Considerations of such issues have typically resulted in adoption of simple rainfall excess models.

Dyer et al. (1994) compared the performance of the constant continuing loss and proportional loss models for 24 catchments using RORB and found that the proportion loss model resulted in generally improved calibrations. This finding was supported by Hill et al. (1996), who calibrated RORB models for 11 Victorian catchments. However, analyses undertaken by Phillips et al (2014) and Hill et al. (2014a), concluded that the results were inconclusive in regards to the best model. Even for catchments where one of the loss models was preferred for a majority of events, there were some events for which the alternate model was preferred. Similarly, there was no obvious relationship between the preference for a particular model and hydroclimatic or catchment characteristics that could explain the preference for a particular approach.

A number of Australian studies have demonstrated that the IL/CL model is suitable for design flood estimation where in it can be used to estimate design flood estimates over a range of AEPs. However, it is often difficult to derive unbiased estimates of floods using the IL/PL model over a range of AEPs. Specifically, the IL/PL model has the potential to underestimate peak flows for events rarer than used in the derivation of the values; this suggests that PL should vary with the AEP of the event.

Furthermore, studies that have analysed a large number of events and catchments such as Phillips et al (2014) and Hill et al. (2014a) have found that there can be a large variation in PL values, which makes it difficult to recommend a representative value for design Book 5, Chapter 3, Section 5.

Given the difficulties in characterising how PL should vary with AEP, it is considered that the IL/CL model is the most suitable of these simple rainfall excess models for design flood estimation for both rural and urban catchments. Probability distributed loss models such as SWMOD demonstrate promise and should also be considered for rural catchments where there is reliable and consistent description of hydraulic properties of soils.

If alternate loss models are to be adopted then they should be evaluated against the above criteria. An important consideration is how the loss model performs when extrapolated to events outside of the range of events used in deriving the loss values.

3.3.2. Design Rainfall Bursts v Complete Storms

In selecting loss values for design flood estimation, it is important to consider the nature of the design rainfall information. The Intensity Frequency Duraton data in Book 2 is derived from the analysis of rainfalls for standard durations, rather than complete storms. In some cases, these events represent complete storms but also include cases of bursts of rainfalls within a much longer duration storm.

The conceptual difference between the initial loss for a rainfall burst (IL_b) and for a storm (IL_s) is illustrated in Figure 5.3.5. The initial loss for the storm is assumed to be the depth of rainfall prior to the commencement of surface runoff. The initial loss for the burst however, is the portion of the storm initial loss, which occurs within the burst.

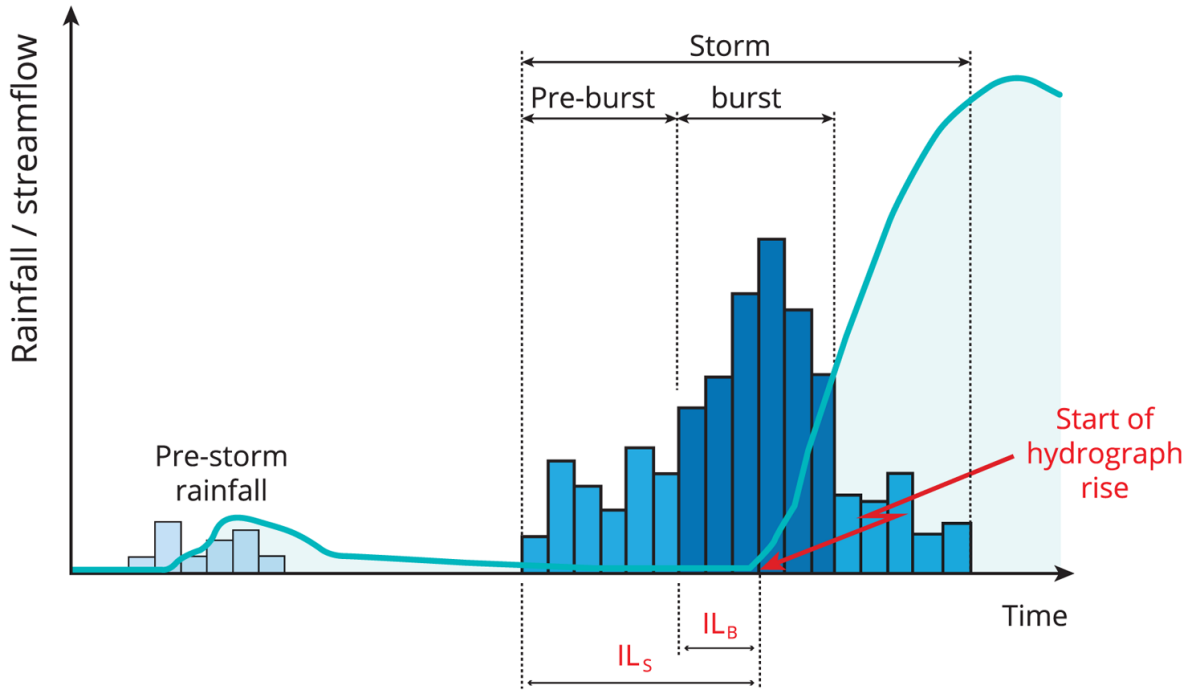

Figure 5.3.5. Distinction between Storm and Burst Initial Loss

If pre-burst rainfalls are included, then the design rainfalls will represent (near) complete design storms and therefore the storm losses can be directly applied without adjustment. The design values recommended in Book 5, Chapter 3, Section 5 are intended for application with complete storms and therefore, requires the pre-burst depths to be included.

However, if design bursts, rather than complete storms, are used in design then the burst initial loss needs to be reduced to account for the pre-burst rainfall. For the same reason, the initial moisture content for storage capacity models (such as Horton and SWMOD) need to be increased to account for this pre-burst rainfall.

This has implications for all design flood situations, but is particularly important for design situations where the outcome is sensitive to the flood volume, such as the design of retarding basins (Rigby and Bannigan, 1996). The failure to recognise the rainfall prior to design rainfall bursts has the potential to significantly underestimate the design flood.

3.3.3. Approaches to Estimating Loss Values

The most appropriate approach to estimating loss values will depend upon the objectives and required rigour of the study, and the quality and availability of at-site and regional flood data. The different approaches can be considered in the following broad classes:

1. Empirical analysis of at-site rainfall and streamflow records;

2. Information from regional analysis of data; and

3. Reconciliation of design values with independent flood frequency estimates.

3.3.3.1. At-site Event Data

If there is long-term pluviograph and streamflow data available at the site of interest it may be possible to directly estimate loss values for a number of events. In order to undertake such an analysis the streamflow should be free of significant regulation or diversion and land use within the catchment should be stationary over the period of data being analysed.

The events to be analysed should be selected carefully to ensure that the sample of events is not biased. The selection of high runoff events for loss derivation is likely to be biased towards wet antecedent conditions (ie. losses tend to be too low). Ideally, events should be selected on the basis of rainfall to remove this bias. However the selection and analysis of events by rainfall is problematic because it requires consideration of a representative duration of the rainfall and there may be little or no runoff generated from some intense bursts of rainfall if the antecedent conditions are dry.

The main limitation of deriving losses directly from the analysis of recorded data is that they may not be compatible with the other design inputs and hence suitable for design flood estimation. That is, although the loss values may reflect the loss response observed for a number of events on the catchment, this does not guarantee that their application with other design inputs results in unbiased estimates of floods. For this reason, it is also desirable to reconcile design values with independent flood frequency estimates where possible (refer Book 5, Chapter 3, Section 3).

3.3.3.2. Regional Data

Deriving loss values from an analysis from multiple catchments has the advantage that there is the opportunity to be more selective in selecting the data sets to be analysed and the larger sample allows the distribution of values to be explored. However the results from these regional analyses need to be transposed to the catchment of interest which relies on relationship being developed between the loss values and physical characteristics – a link which has generally proved to be elusive.

Loss values have been estimated for a large number of urban (Phillips et al, 2014) and rural catchments (Hill et al., 2014a). These two studies represent the most comprehensive regional studies of losses covering Australia and hence the recommended loss values summarised in Book 5, Chapter 3, Section 5 are largely based upon these studies.

As with the estimation of losses from a single site, their application with other design inputs does not guarantee unbiased estimates of floods and for this reason, it is therefore also desirable to reconcile design values with independent flood frequency estimates where possible (refer Book 5, Chapter 3, Section 3).

3.3.3.3. Reconcile Design Values with Independent Flood Frequency Estimates

Deriving loss values by comparison with flood frequency estimates has the advantage of producing design losses which are consistent with the other design parameters and the design objective of deriving peak flows of a given AEP. Indeed the use of design rainfalls to estimate design floods is in fact the sole objective of rainfall-based flood event modelling. The only difference between calibration of the model in this manner and its application is in the magnitude of the events being considered.

The fundamental limitation of this approach is that all the uncertainty in the each of the design inputs (e.g. IFD, ARF, temporal patterns, spatial patterns), modelling (model conceptualisation and parameterisation) and the flood frequency analysis (e.g. rating curve, choice and fitting of the distribution) is reflected in the resulting loss values. The loss simply becomes an error term to compensate for all of the uncertainty and biases in all other inputs. It is therefore not surprising that the values derived from such an approach (e.g. Walsh et al. (1991); Flavell and Belstead (1986)) typically display a large range and relating such values to physical catchment characteristics (that should influence infiltration and interception) has proven intractable.

A further limitation of such approach is that the resulting loss values are a function of the design flood estimation method itself and are therefore only suitable for application with the same set of inputs. For example, if new or alternate information is available on any of the inputs such as IFD, ARF then the analysis needs to be repeated. Thus, the values only work with a single combination of design inputs.

3.3.3.4. Summary of Approaches

The advantages and disadvantages of these different approaches are summarised in the table below.

Table 5.3.1. Summary of Different Approaches for Estimating Loss Values

Approach	Advantages	Disadvantages
1. Empirical analysis of at-site rainfall and streamflow records	• Data is directly relevant to the location of interest and explicitly accounts for the catchment characteristics.	• Only applicable where the catchment is free of significant regulation and diversions and the land use has been stationary • Most catchments do not have a long period of concurrent pluviograph and streamflow data • Difficulty in selecting an unbiased sample of events • Does not guarantee that values result in unbiased estimates of floods

Approach	Advantages	Disadvantages
		• Small sample of events makes it difficult to explore distribution of loss values
2. Regional information	• Can be more selective in choice of data sets for analysis • Larger sample of events allows distribution of values and relationships with characteristics to be explored	• Considerable effort required • Difficulty in selecting an unbiased sample of events • Does not guarantee that values result in unbiased estimates of floods • Difficultly in linking loss values to rainfall and catchment characteristics
3. Reconciliation of design values with independent flood frequency estimates	• Checks that, when combined with the other design inputs, the loss values produce unbiased estimates • Loss values implicitly account for the nature of the design rainfall; whether rainfall bursts or complete storms	• Unlikely to have a long-term stationary streamflow record at the location of interest • If sufficient streamflow is not available, reliance on estimates of regional flood frequency analysis introduces additional uncertainty • Different combination of loss values can result in same flood estimates but has different impact when applied outside of the magnitude used for reconciliation • All of the uncertainty in the design process is attributed to the loss which makes it difficult to infer link with rainfall and catchment characteristics • Unlikely to have sufficient information to be able to define distribution of loss values

If there is a long-term stationary streamflow record at the site, reconciliation of design values (Option 3) is preferable but if the distribution of loss values is required this will typically need to be inferred from previous studies (Option 2). In majority of cases, there will be insufficient streamflow data available at the site and therefore a combination of regional information

(Option 2) and reconciliation of design values with regional flood frequency estimates (Option 3) will typically be the most appropriate approach.

For urban catchments it is more difficult to obtain independent flood frequency estimates and therefore values will often need to be inferred from at-site data (Option 1) or values obtained from regional information (Option 2).

3.4. Estimation of Effective Impervious Area

3.4.1. Overview

3.4.1.1. Surface Types

In estimating runoff from urban catchments, four separate types of surfaces are generally recognised and are referred to in this chapter as the following:

- Directly Connected Areas, which consist of:
  - impervious areas (e.g. roofs and paved areas) which are directly connected to the drainage system – referred to as Direct Connected Impervious Areas (DCIA).
- Indirectly Connected Areas, which consist of:
  - impervious areas which are not directly connected, runoff from which flows over pervious surfaces before reaching the drainage system (e.g. a roof that discharges onto a lawn) – referred to as Indirectly Connected Impervious Areas (ICIA).
  - Pervious areas that interact with Indirectly Connected Impervious Areas, such as nature strips, garden areas next to paved patios, etc.
- Pervious areas consisting of parklands and bushland that do not interact with impervious areas.

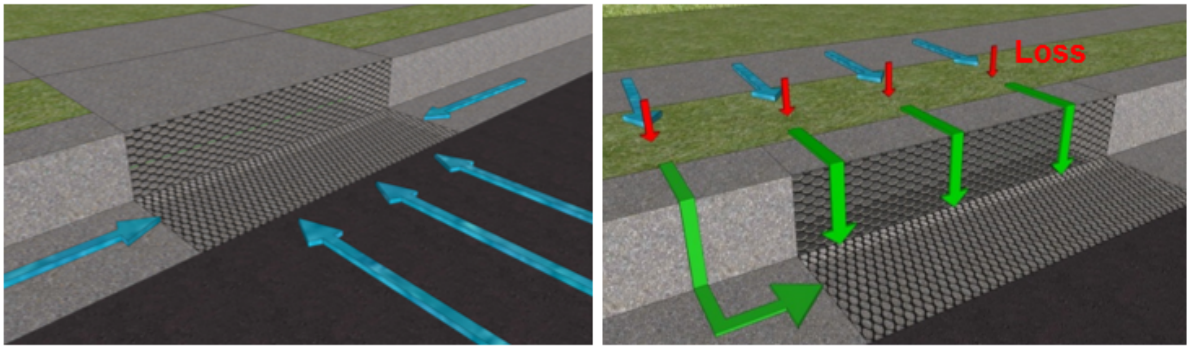

Figure 5.3.6. Example of a Directly Connected Impervious Surface (Left) and an Indirectly Connected Impervious Surface (Right)

3.4.1.2. Challenges with Total Impervious Area

Estimating the catchment imperviousness is an important step in urban rainfall runoff modelling, particularly given the sensitivity of simulated runoff to this parameter in many models (Alley and Veenhuis, 1983). Traditionally, the Total Impervious Area (TIA) is used with the assumption that, neglecting depression losses, this area contributes fully to

generating runoff. This is despite the research dating back to the 1970s, identifying the importance of the Effective Impervious Area (EIA) over the TIA (refer to Cherkaver (1975); Beard and Shin (1979)).

Use of the TIA, which includes impervious areas with no direct connection to the drainage network, can result in the overestimation of urban runoff volumes and peak flows. Although definitions vary, the EIA is generally considered to be representative of the area of the catchment that generates a rapid runoff response in rainfall events. It incorporates the impervious area with a hydraulic connection to the drainage network (DCIA), plus a contribution comprising discharges from an impervious area onto a pervious area (ICIA), which rapidly saturates and acts in a similar manner to an impervious area. The EIA therefore provides a more realistic measure of the impervious area that generates runoff at the catchment outlet.

3.4.1.3. Conceptualisation of Runoff Process

As rainfall continues to fall, it would be expected that additional indirectly connected impervious areas would start to contribute to runoff. A simplified representation of this is shown in Figure 5.3.7. In this schematic, when the initial loss for the Indirectly Connected Area is saturated, the Indirectly Connected Area (comprising pervious and impervious areas) will start to contribute to the runoff. Similarly, once the initial loss of the pervious area is saturated, the pervious area will start to contribute to runoff.

This conceptualisation was observed in Phillips et al (2014) by plotting cumulative runoff of the observed rainfall, the observed discharge, and the estimated runoff based on the calculated EIA estimate (Figure 5.3.8). The deviation of the cumulative observed discharge form the calculated cumulative EIA discharge would suggest the point of Indirectly Connected Area contribution.

It is noted that in Phillips et al (2014), the Indirectly Connected Area incorporated all residential components of the catchment outside of the EIA. Only areas such as large parklands, bushland areas etc were separated out of the analysis. This was following a detailed review of the behaviour, identifying only two discernible responses from within the urban components of a catchment. This approach is recommended.

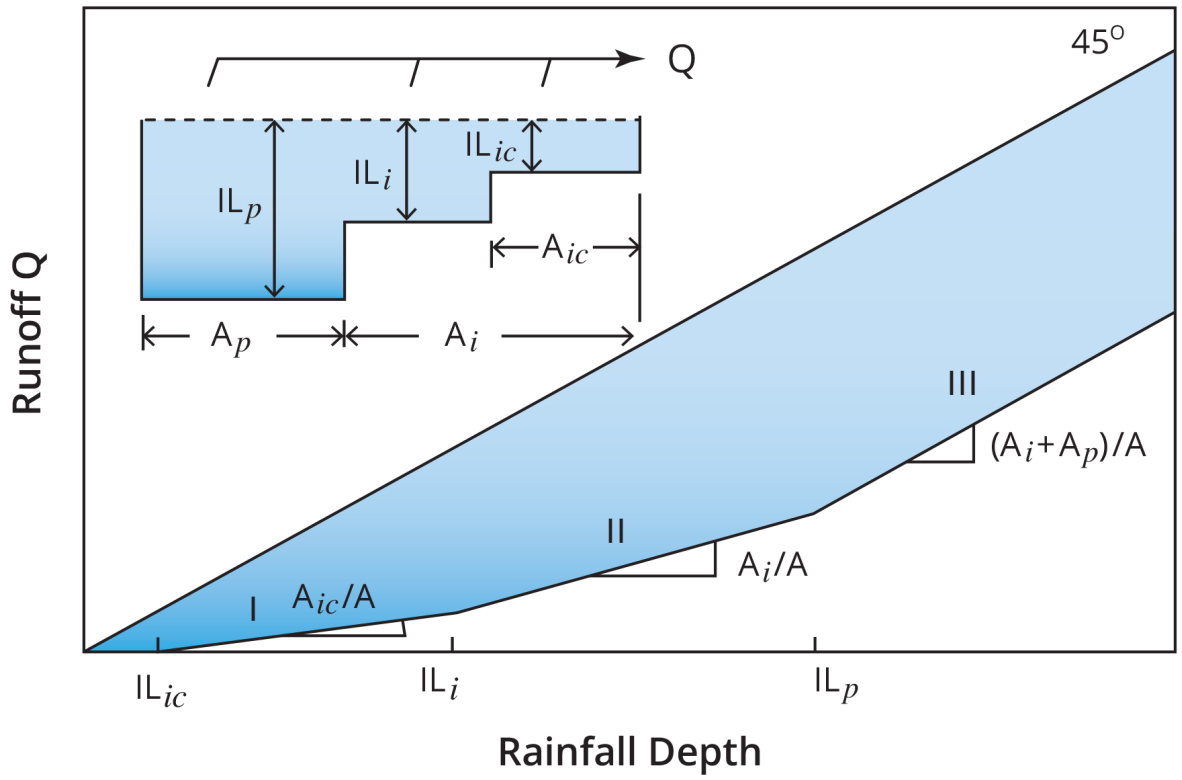

A = Area
IL = Initial Loss
i = Impervious
p = Pervious
ic = Indirectly Connected Impervious

Figure 5.3.7. Schematic of Rainfall Depth v Runoff, from Boyd et al. (1993)

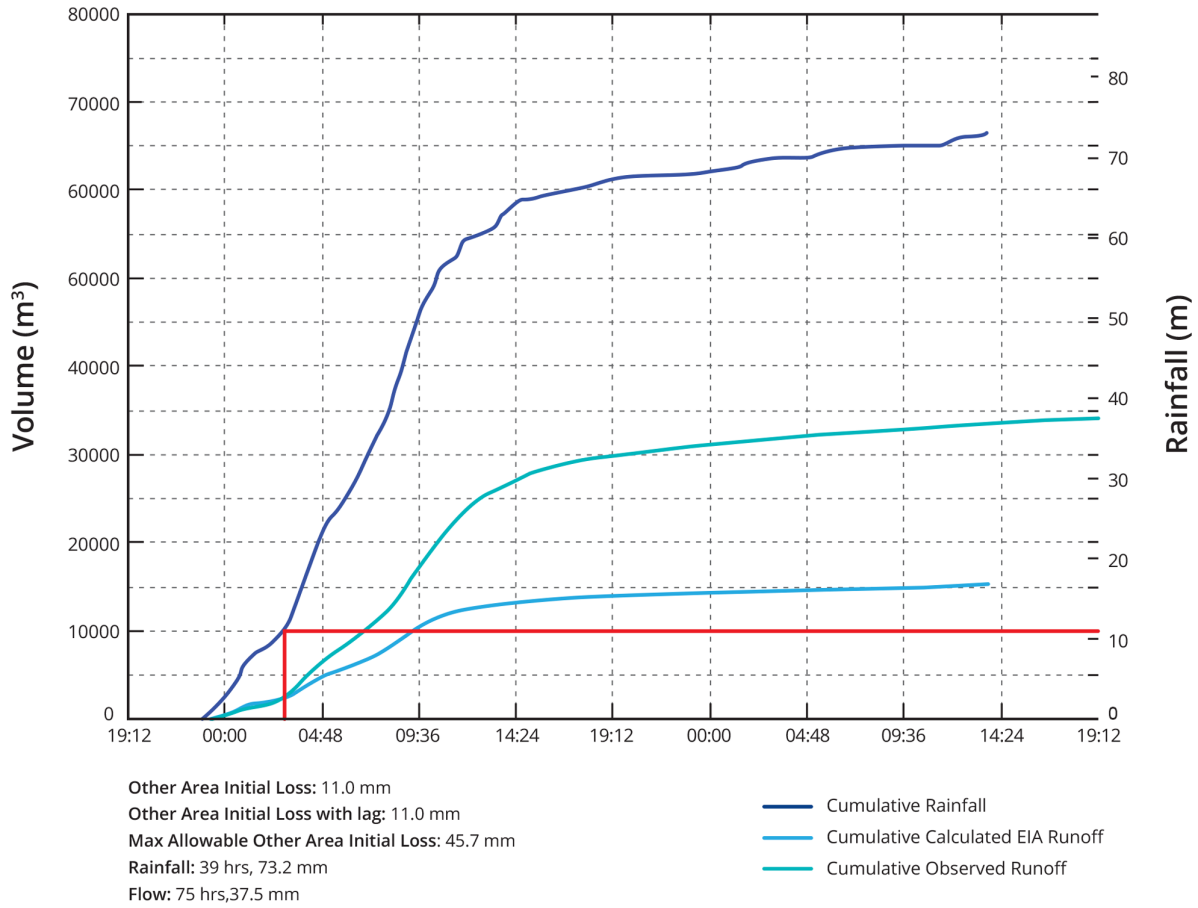

Figure 5.3.8. Cumulative Discharge Plot from Giralang (ACT), showing Cumulative Rainfall, Observed Runoff and Estimated EIA runoff (Phillips et al, 2014)

3.4.2. Estimating Effective Impervious Area

There are a number of methods for estimating EIA. These include:

- Regression analysis of streamflow and rainfall records, where sufficient data exists;
- Adoption of typical EIA/TIA ratios, based on available literature;
- GIS Mapping of TIA areas.

These are described in more detail below.

3.4.2.1. Regression Analysis

The EIA can be estimated using regression techniques on gauged urban catchments, where there are sufficient gauging records to do so. This method provides the most accurate method for estimating EIA for a specific catchment, as it does not require the extrapolation of relationships from other catchments.

This method is done by comparing flow records with a representative rain gauge that is located within or very near the catchment. The key to this method is isolating the runoff that occurs only from the EIA, and not from the other impervious and pervious areas. A method for doing this is detailed in Phillips et al (2014), with an overview of the general approach

provided in Figure 5.3.9. An example of the output of this kind of analysis is provided in Figure 5.3.10.

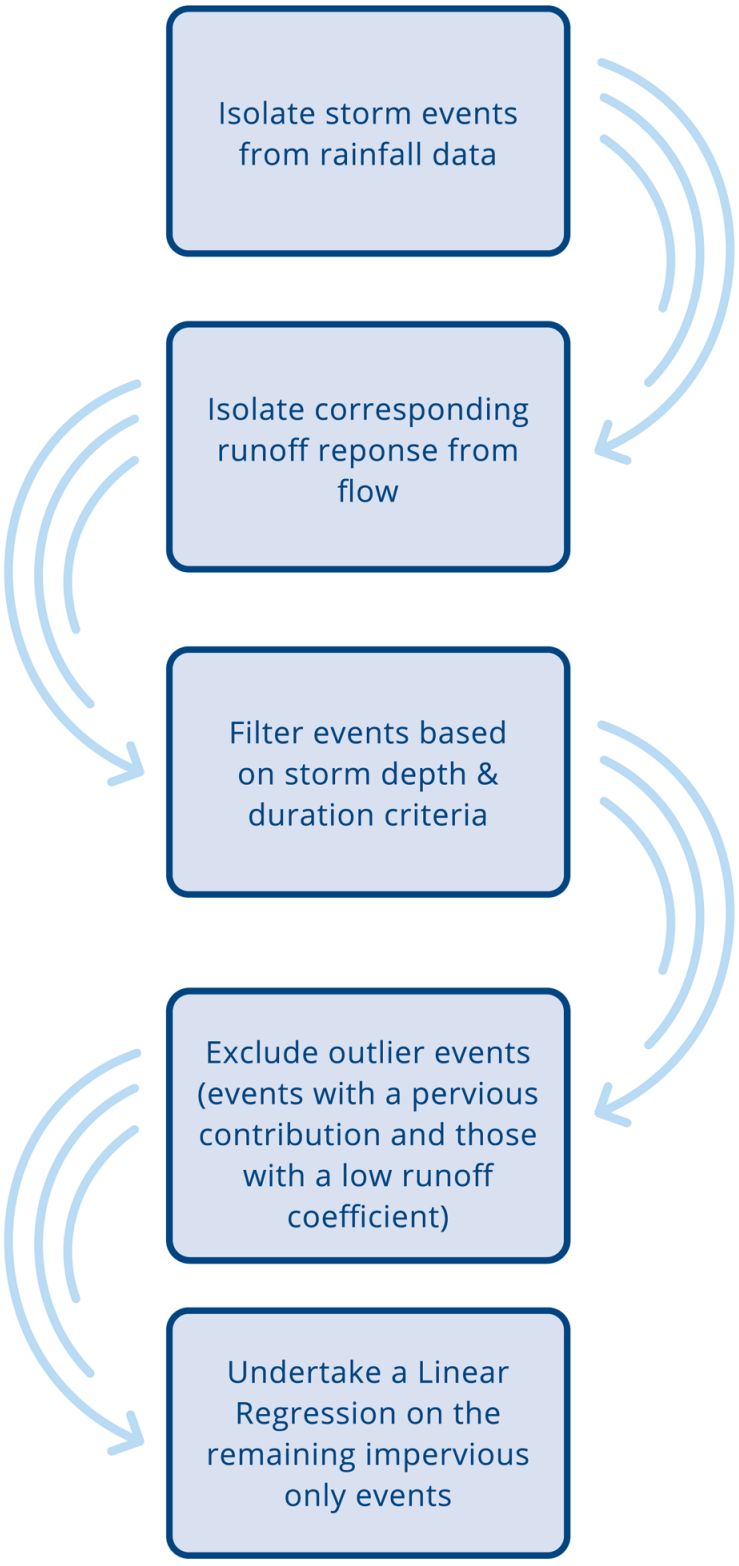

Figure 5.3.9. Overview of Regression Analysis Approach

As identified in Phillips et al (2014), the key requirements for this method are:

- A sufficient gauging (both rainfall and flow) record to undertake the analysis. Phillips et al (2014) adopted a 10 year record as a minimum, although the technique that was applied for the EIA estimation could potentially be used for much shorter records. Where shorter records are adopted, the data should also be checked to ensure that there are sufficient range of rainfall events in terms of magnitude, in order to create a reasonable regression.

- The catchment must have an acceptable gauge rating. Further details on this are discussed in Book 3, Chapter 2. It is noted that because of the technique to isolate EIA events, very large events are generally excluded due to the presence of pervious area runoff. In the absence of any detailed studies on this, a gauge that has an acceptable rating up to around an AEP of 20% may provide a reasonable representation, as long as all events above the acceptable flow level of the gauge are excluded. It is important that engineering judgement is undertaken in reviewing the suitability of the data set.

- A relatively small catchment area. A catchment area of 5 km^2 was used as a target catchment area for the Phillips et al (2014) analysis, although there is no strict guide as to what is appropriate. Larger catchment areas result in a number of potential issues:

  - Greater likelihood for influences of hydraulic controls, catchment storages etc. influencing the runoff;

  - Greater difficulty in isolating the EIA runoff due to longer lag periods from upper catchment areas;

  - More potential for baseflow which will need to be excluded from the analysis;

  - Spatial variation of rainfall becomes more important, and therefore more gauges should potentially be used in the analysis. This will require spatial averaging techniques for rainfall, as discussed in Book 2, Chapter 4.

- A relatively stationary upstream catchment during the period of record (ie. minimal changes in land-use, development intensity etc.).

This process is analytically intensive and is unlikely to be applied in simple applications.

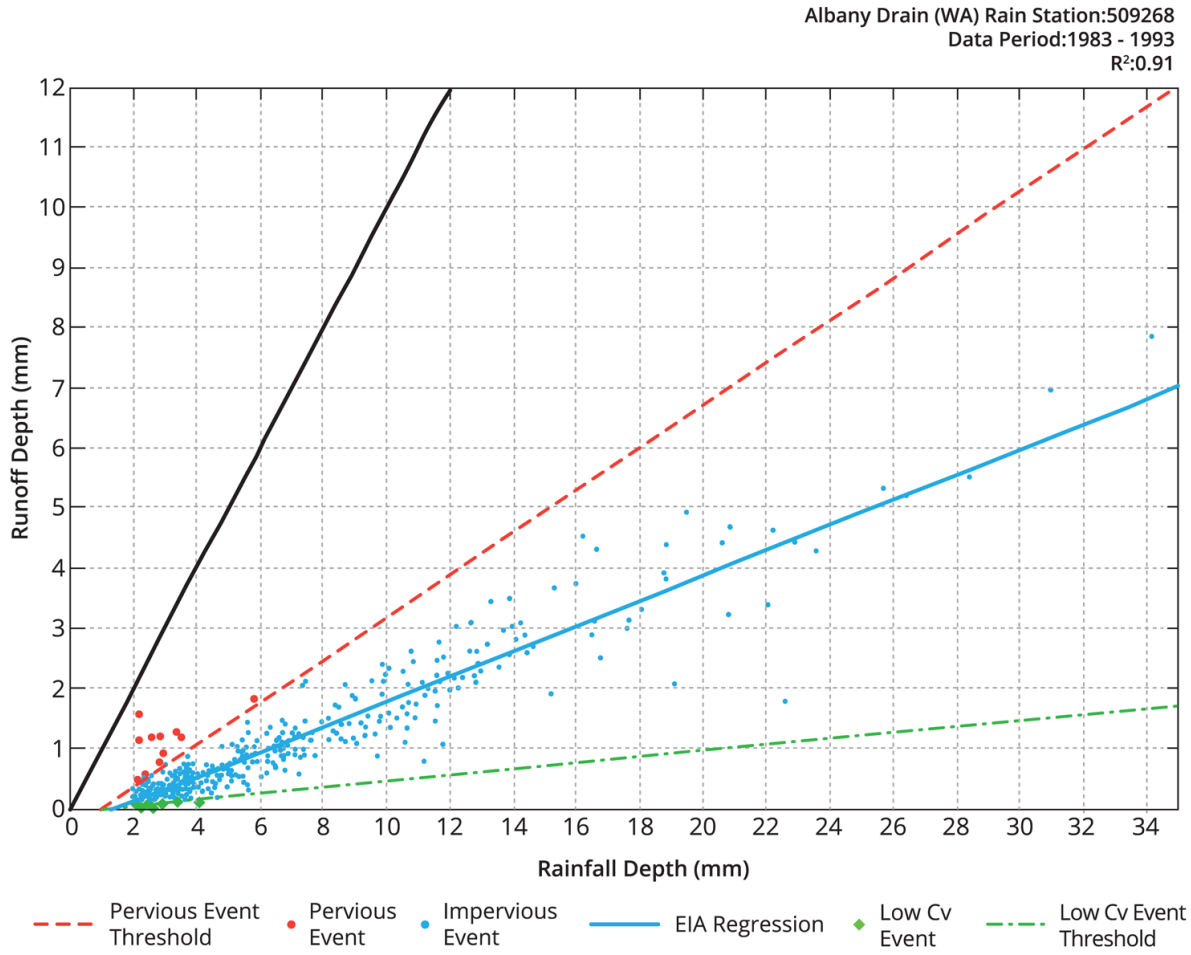

Figure 5.3.10. Example Regression Analysis for Albany Drain Catchment in Western Australia

3.4.2.2. Adoption of Typical EIA/TIA Ratios

Where appropriate flow gauging and rainfall data does not exist, an alternative method for estimating EIA is based on available research on similar catchments.

3.4.2.2.1. Relevant Research

EIA/ TIA

The EIA/ TIA ratio has been found in a number of studies (e.g. Phillips et al (2014); Ball and Powell (1998); Boyd et al. (1993)) to be a good indicator, removing the variability of total imperviousness to create a measure that can be extrapolated to other catchments.

Australian Estimates

Phillips et al (2014) analysed 8 separate catchments throughout Australia using the regression analysis discussed in Book 5, Chapter 3, Section 4. These catchments spanned across all 8 states and territories. However, it is noted that there is only limited representation from the northern part of Australia, with only one catchment from Darwin in the Northern Territory included. This is a reflection of the general urban densities throughout Australia.

This study identified that EIA is typically 55 to 65% of the TIA for most of the catchments identified. This range was recommended in the study in estimating the EIA for most Australian catchments. Based on a sensitivity analysis undertaken within Phillips et al (2014) of some of the key assumptions, the estimates of EIA are expected to fall within +/- 5% to 10% of this estimated range.

It is noted that one catchment from the ACT was identified to have a higher ratio of 74% to 80%. It was theorised that this is likely due to the higher degree of connected surfaces (as discussed in Goyen (2000)), although there were insufficient additional catchments to confirm this hypothesis.

The Phillips et al (2014) study also estimated the DCIA using GIS methods, which primarily included road, roof and driveways (where these driveways drained to the street). It is noted that the road and roof area represents the majority of this area. The analysis suggested that the EIA was roughly in the range of 70 to 80% of this area, suggesting that not all of the roof and road area contributed to runoff.

A summary of results from Phillips et al (2014) are presented in Table 5.3.2.

In order to derive the estimates of EIA/ TIA, Phillips et al (2014) used detailed mapping of different land-uses and aerial photography to estimate the TIA. This was undertaken by taking representative areas within the catchments, detailing the impervious areas, and then extrapolating this to the wider catchment based on land-use mapping which was also derived from aerial photography.

Table 5.3.2. Summary of Effective Impervious Areas Results

Catchment	Total Area (ha)	Urban Area[a] (ha)	TIA (ha)	Urban TIA Fraction[b]	EIA/TIA	DCIA (GIS)/ TIA	EIA (Reg.) / DCIA(GIS)
Albany Drain (WA)	8.2	8.2	2.9	35%	59%	83%	71%
McArthur Park (NT)	144	120	53.7	45%	66%	93%	70%
Giralang (ACT)	91	61.8	28.4	46%	74 to 80%	95%	82%
Parra Hills Drain (SA)	55.1	48.5	26.9	55%	56%	87%	64%
Kinkora Road (VIC)	202	184	122	66%	59%	87%	68%
Powells Creek (NSW)	232	223	152	68%	59 to 63%	81%	75%
Ithaca Creek (Qld)[c]	926	262	128	49%	55%	95%	58%

Catchment	Total Area (ha)	Urban Area[a] (ha)	TIA (ha)	Urban TIA Fraction[b]	EIA/TIA	DCIA (GIS)/ TIA	EIA (Reg.) / DCIA(GIS)
Argyle Street (TAS)	1900	491	292	59%	63%	93%	68%

[a]The urban area for these catchments was based on the residential developed areas, excluding parklands, bushland etc.

[b]The Urban TIA fraction is defined as the percentage of impervious area in the urban area and was based on the desktop GIS method.

[c]Note that Ithaca (QLD) and Argyle St (Tas) were noted to be limited due primarily to large pervious (bushland) areas in these catchments, which influences the results

Ball and Powell (1998) estimated the EIA for Powells Creek in NSW (also analysed by the Phillips et al (2014) research). The analysis of rainfall and runoff data was undertaken by also comparing the antecedent moisture (AMC) in the catchment, based on rainfall in the days leading up to the storm event (refer Book 5, Chapter 3, Section 4). The analysis showed an EIA percentage of the total catchment area (not the TIA) of ranging from 35% to 44% depending on the AMC. Based on the TIA estimated in Table 5.3.2 for the same catchment, this represents an EIA/ TIA of around 53% to 67%, depending on the AMC. This range is very similar to that found under Phillips et al (2014), both for Powells Creek as well as for the wider catchments analysed. Similarly, Chiew and McMahon (1999) undertook an analysis of Powells Creek and found an EIA to total catchment area of around 40%.

Zaman and Ball (1994) undertook a study on Salt Pan Creek in NSW (Southern Sydney). This study estimated the EIA using two alternative methods. The first looked at estimates using orthophoto maps and applying estimates of the EIA to different land-uses. The second analysed rainfall and runoff records to estimate the EIA. Both methods estimated an approximate EIA to Total Area of 39% to 41% of the total catchment area. However, it is noted in the description of this catchment that there are open space areas, making it difficult to directly compare this to other studies. Also, there was no clear description of the TIA to be able to provide a comparative EIA/TIA ratio. Chiew and McMahon (1999) by comparison estimated an EIA to Total Area of 27% for this catchment.

Boyd et al. (1993) analysed 26 catchments, 9 located within Australia (Sydney, Canberra and Melbourne), while the others were international (USA, Canada, UK, Japan and a number of European countries). This study undertook a similar analysis to that of Phillips et al (2014). A regression analysis was undertaken on the EIA/Total Area versus the TIA/Total Area and estimated that the EIA/ TIA ratio of around 74%. A summary of the results is provided in Book 5, Chapter 3, Section 8.

One key thing to note from this study is that there were a number of catchments where the EIA was identified as being greater than the TIA. This is unlikely to be the case in reality, unless the pervious areas have little infiltration. This was not discussed in the paper, but it assumed that the TIA estimated based on aerial photography may not have been appropriate. The data from this study was re-analysed where EIA > TIA catchments are excluded from the analysis, with the results shown in Figure 5.3.12 (the Australian catchments are circled for reference). This was also mapped against Urban Area (ie excluding large pervious areas like bushland and parks), rather than Total Area, to normalise it with the Phillips et al (2014) study and exclude the effects of bushland etc. in the catchments. The re-analysed EIA/TIA ratio is 71%, which is close to the 55% to 65% range identified in Phillips et al (2014).

Dayaratne (2000), which is also referenced in O'Loughlin and Stack (2014), obtained relationships with housing density from modelling storms on 16 gauged residential catchments in four Victorian municipalities:

$$\mathrm{DCIA}/_{\mathrm{TA}}\ (\%) = -0.85\mathrm{hhd}^2 + 23.38\ \mathrm{hhd} - 101.19\ \left(R^2 = 0.90\right) \quad (5.3.3)$$

$$\mathrm{ICIA}/_{\mathrm{TA}}\ (\%) = -0.04\mathrm{hhd}^2 + 1.13\ \mathrm{hhd} - 3.79\ \left(R^2 = 0.91\right) \quad (5.3.4)$$

Where hhd = number of houses per hectare.

It is important to note that this study was based on a range of 7 to 14 houses per hectare. Beyond this range, the equation has significant limitations, as demonstrated in Figure 5.3.11 (ie DCIA reduces with increasing households per hectare for households greater than around 15 per hectare. Also, DCIA reduces below 0% for less than 5 households per hectare). The Phillips et al (2014) results are also shown on this graph for reference.

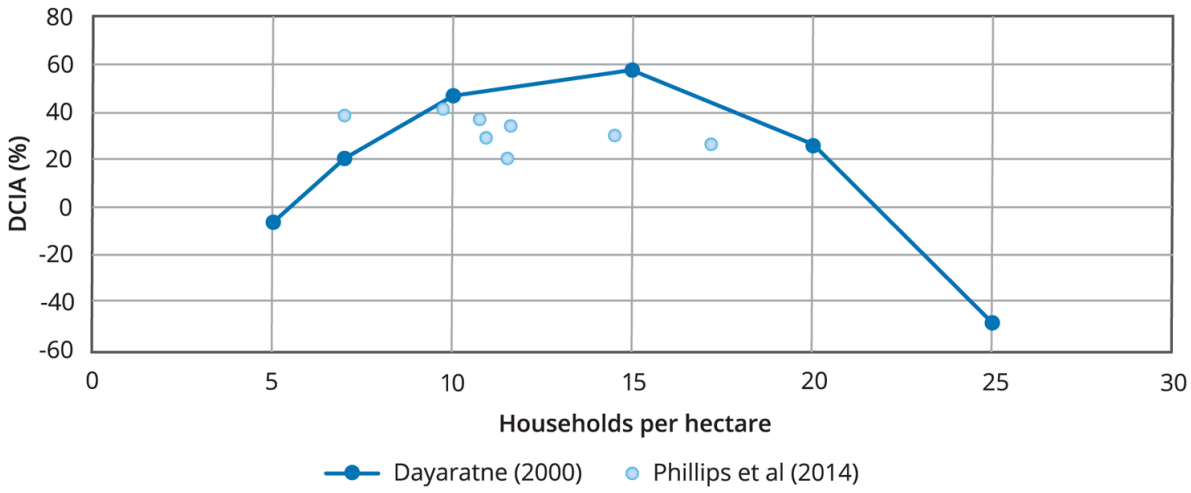

Figure 5.3.11. Representation of Dayaratne (2000) Relationship for DCIA

A further review of just the Australian data from the Boyd et al. (1993) study was compared with that of the Phillips et al (2014) study. The results of this review are shown in Figure 5.3.13 (and removing those catchments which overlap in both studies). The EIA/ Urban Area from this analysis is estimated to be around 60%.

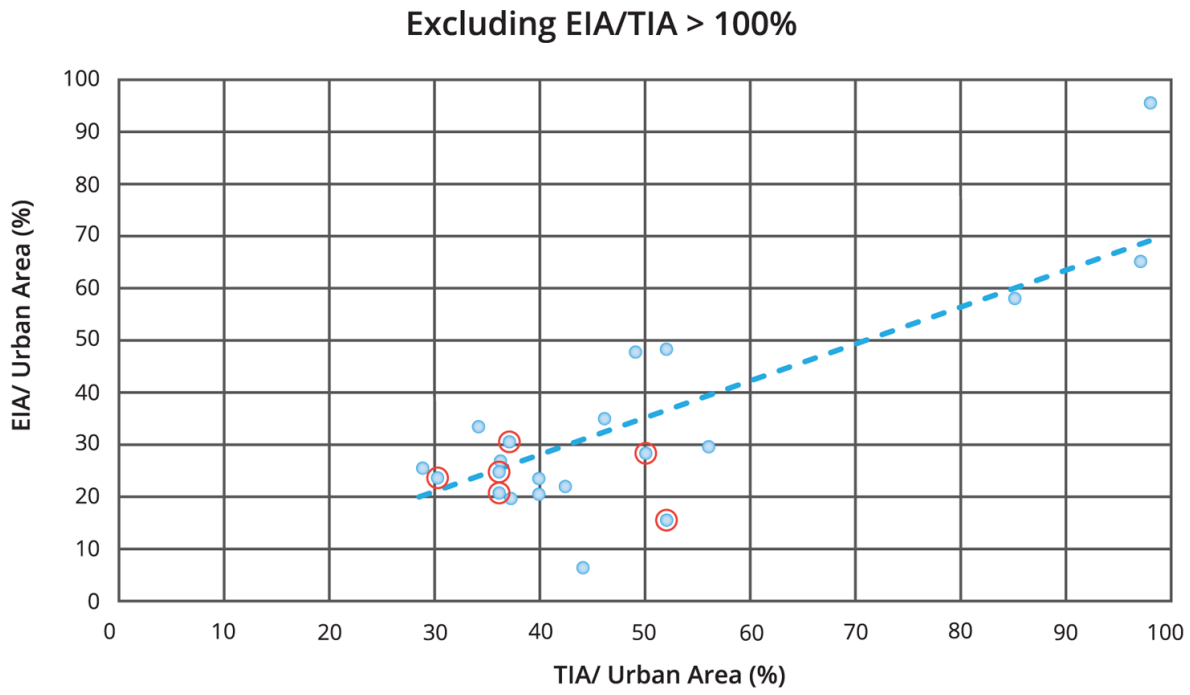

Figure 5.3.12. Re-Analysis of Boyd et al. (1993) Data[1]

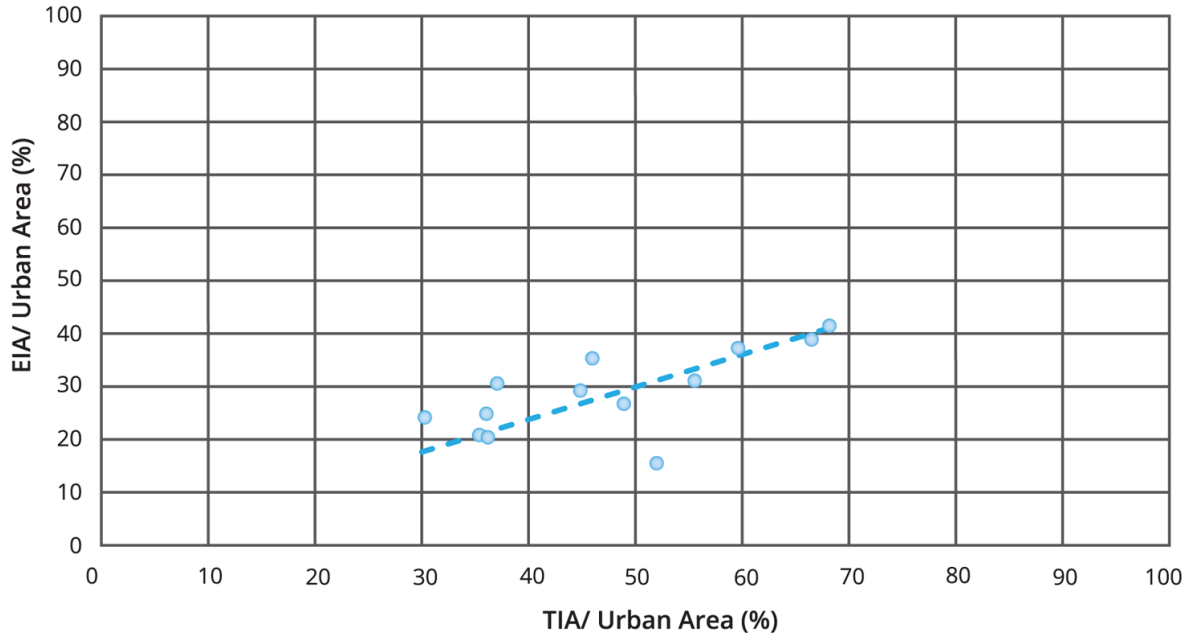

Figure 5.3.13. Australian data from Phillips et al (2014) and Boyd et al. (1993)

International Estimates

Table 5.3.4 provides an overview of international literature on the estimation of EIA/TIA.

The research by Alley and Veenhuis (1983) shows close correlation with the Australian studies for residential catchments (between 53% to 77%, refer Table 5.3.4). This study also incorporated commercial and industrial land-uses, indicating 94% and 77% respectively. As

[1]Australian catchments circled for reference

many of the studies have been undertaken in residential (or predominantly residential) areas, this provides a useful comparison for commercial and industrial land-uses.

Alley and Veenhuis (1983) also derived a relationship between the TIA/TA ratio versus the EIA/TA ratio as a combination of all 19 catchments analysed. This equation is as follows:

$$EIA/TA = 0.15\,(TIA/EA)^{1.41} \quad (5.3.5)$$

It is noted that when applying this relationship both the TIA/TA and EIA/TA should be expressed in terms of the percentage multiplied by 100.

In the Boyd et al. (1993) research, 23 of the 26 catchments were predominantly residential (although some had low rise apartments). Non-residential catchments included Sample Road (highway, industrial), Fort Lauderdale (large shopping mall) and Vika (city centre). Both Sample Road and Fort Lauderdale resulted in much higher EIA/TIA, with 74% and 98% respectively. With Fort Lauderdale being nearly completely impervious, this high value of EIA/ TIA would seem reasonable.

Pompano Creek (USA) in the Boyd et al. (1993) data was identified as having limited pipe infrastructure, and where water flowed through grass swales prior to reaching this infrastructure. This may provide some basis for suggesting greater infiltration through WSUD style features, although there is insufficient data to draw any detailed conclusions.

A compilation of the available data (where individual catchment data is available) is provided in Figure 5.3.14. Both the Alley and Veenhuis (1983) (the equation for which was derived from data from Denver USA) and the USA/ Canada data from Boyd et al. (1993) generally align, and are generally higher than the European and Australian data. The reason for the difference unknown, and may come down to variations in methods as well as catchment characteristics and rainfall patterns.

Table 5.3.3. Overview of International Literature on EIA/TIA

Country	Catchments	Authors	EIA/TIA	Comments
Finland	7	Melanen and Laukkanen (1981)	75%	As quoted in Boyd et al. (1993)
Denmark	6	Jensen (1990)	90%	As quoted in Boyd et al. (1993)
USA	2	Janke and Wilson (2011)	32 to 33%	Both catchments around 50% impervious.
USA	19	Alley and Veenhuis (1983)	56 to 94%	Analysis undertaken in Denver. See Table 5.3.4. Residential between 56% to 65%.
USA, Canada, UK, France, Denmark,	17	Boyd et al. (1993)	Variable	Refer to Table 5.3.15 and Figure 5.3.12

Country	Catchments	Authors	EIA/TIA	Comments
Sweden, Italy, Norway, Yukoslavia, Japan				

Table 5.3.4. EIA Results of Alley and Veenhuis (1983) for 19 Catchments in Denver, as summarised in Shuster et al. (2005)

			Total Impervious Area (TIA) (%)		Effective Impervious Area (EIA) (%)			Effective impervious area/Total impervious area	
Land Use	Lot size, in acres	Number of Basins[a]	Mean	Range	Mean	Range	Mean predicted using mean total impervious area[b]	Mean	Range
Single-family residential	< 1/4	12	39	30-49	23	18-32	26	0.66	0.52-0.66
	1/4 - 1/2	2	26	22-31	15	11-19	15	0.56	0.52-0.61
	1/2 - 1	2	15	13-16	8.5	7-10	6.8	0.58	0.54-0.62
Multifamily residential	-	3	60	53-64	42	33-52	48	0.65	0.57-0.77
Commercial	-	4	88	66-98	83	51-98	83	0.94	0.78-1.0
Industrial	-	1	60	-	46		48	0.77	-

[a]A total of 19 basins were used to derive these averages. However, certain basins had more than one land use type, so that the sum number of basins studied exceeds the sample set

[b]$\mathrm{EIA} = 0.15\ (\mathrm{TIA})^{1.41}, r^2 = 0.98$

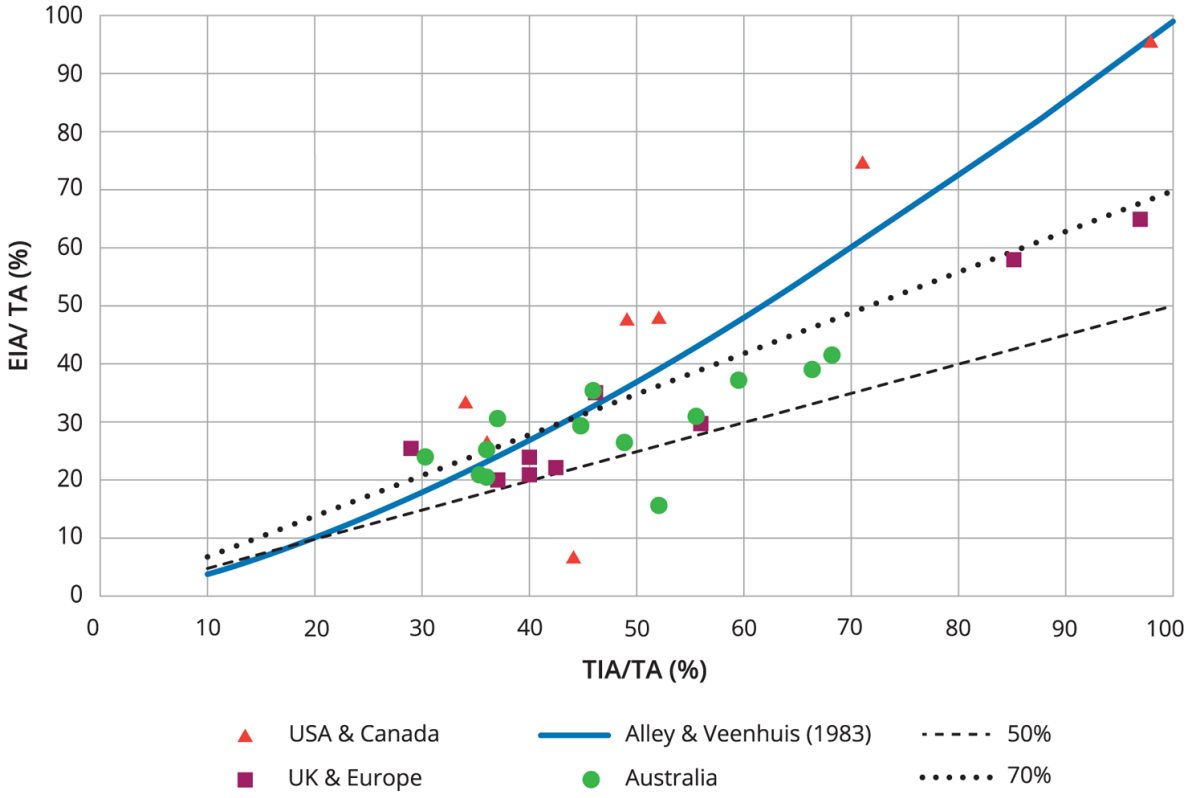

Figure 5.3.14. Compilation of Available EIA Data[2]

3.4.2.2.2. Recommended Values

EIA/TIA

Based on the international literature, and in the absence of any local streamflow and rainfall data, an EIA/ TIA ratio of 50% to 70% would appear to be appropriate for the large majority of urban catchments. Most values from the recent Phillips et al (2014) study fit within a more refined range of 55% to 65%, and this range could be used if the catchments are similar to those described in Phillips et al (2014) (primarily single lot residential).

In choosing the value of EIA/ TIA, the following should be considered:

- Whether the roof areas are connected to the stormwater infrastructure. Where this is not the case, it is likely to be on the lower end of the range; and

- If the drainage infrastructure is piped or whether WSUD features (eg swales) are adopted. Some international studies would suggest that large lengths of drainage swales (rather than pipes) results in a lowering of EIA/TIA, although there is insufficient data to adequately characterise this effect.

The following additional points should be noted in relation to the recommended range of values:

[2]Australian data derived from Boyd et al. (1993) and Phillips et al (2014). USA, Canada and European data is from Boyd et al. (1993). TA = Urban Area for Boyd et al. (1993) and Phillips et al (2014)

The 50% and 70% lines provide the recommended ranges in Book 5, Chapter 3, Section 4

- This range has been adopted primarily from residential catchments, and generally catchments with TIA/ total area of between 30% to 70%. There are no Australian catchments in the literature identified with percentage impervious greater than 70%;

- In one situation in Phillips et al (2014), a catchment in Canberra exhibited EIA/ TIA in the 74% to 80% range. It is possible that this catchment had a higher proportion of "connected" areas, although there is insufficient data to explore this further; and

- Results from US based catchments suggests that for highly impervious industrial and commercial areas, there is a higher level of connectivity, resulting in a much higher EIA/ TIA. In one catchment, nearly 100% EIA/ TIA was observed (although the total imperviousness was also around 100%). However, this was not observed in data from Europe, and the US data does not appear to correlate with European or Australian results. There are insufficient results from Australia with catchments with industrial/ commercial land-uses and high total imperviousness to compare with the international studies. However, it may be appropriate to adopt higher values for EIA/TIA for highly impervious industrial, commercial as well as metropolitan areas (ie total imperviousness greater than 80%).

Estimating the TIA

The above method estimates the EIA as a proportion of the TIA, and therefore needs a reasonable estimate of the TIA. Most of the research undertaken as summarised in Book 5, Chapter 3, Section 4 estimated the TIA based on a detailed analysis of aerial imagery. In most applications, this will be the most appropriate method for estimating TIA. Further discussion on the use of GIS and mapping methods to estimate TIA are provided in Book 5, Chapter 3, Section 4.

3.4.2.3. GIS/ Mapping Methods

GIS methods use data such as aerial photography, drainage maps, land-use maps, cadastral information and terrain to derive estimates of TIA and EIA.

3.4.2.3.1. Overview of GIS Methods

There are different approaches that can be undertaken with the use of GIS. Two different levels of analysis have been identified here:

- Level 1 – undertake mapping of land-use areas within a catchment, and use references to derive the proportion of TIA based on these land-use types; and

- Level 2 – undertake detailed mapping of representative sub-areas within the catchment, and apply the estimated imperviousness from this mapping to the land-use maps from Level 1 analysis.

The Level 2 analysis provides a higher level of certainty, but requires additional work in undertaking the mapping.

The following is a step by step process for a Level 2 analysis:

1. Undertake GIS mapping of key land-use areas in the catchment;

2. Identify small representative areas within the catchment that represent the different land-uses;

3. Undertake detailed mapping of these representative areas. Refer Figure 5.3.15 for an example. Use this mapping to estimate the TIA for the sample area;

4. Apply the estimates from Step 3 to the land-use areas from Step 1, to identify the overall TIA within the catchment; and

5. Using this TIA estimate, the EIA can be estimated from the recommended ratio of EIA/ TIA from Book 5, Chapter 3, Section 4.

Figure 5.3.15. Example Sample Area Analysis for Residential and Commercial Land Use for the Giralang Catchment (ACT)

3.4.2.3.2. Estimating EIA based on GIS Estimate of TIA

Based on the TIA estimates from either Level 1 or Level 2 analysis, the EIA can be estimated based on the EIA/ TIA recommendations as identified in Book 5, Chapter 3, Section 4.

3.4.2.3.3. Estimating EIA using GIS Estimate of DCIA

A Level 2 GIS method will allow identification of different types of impervious areas, which can be identified as being potentially DCIA or ICIA. For example, the impervious areas can be broken into rooves, roads, driveways drainage to the street, footpaths etc. The key challenge in attempting to identify DCIA areas using these methods is that it relies on an interpretation of what is directly connected. Studies such as Phillips et al (2014), Goyen (2000) and Ball and Powell (1998) have shown that DCIA from these methods are generally over-estimates.

Phillips et al (2014) showed that the large majority of what was estimated to be DCIA using GIS mapping of the catchments analysed was road and roof area. The EIA calculated from

regression analysis represented approximately 70% (+/-5%) of this area. However, it is noted that this general rule did not apply to all catchments. For example, Giralang (ACT) had a higher EIA/DCIA ratio of around 82%, although this is likely due to the higher degree of connected surfaces (as discussed in Goyen (2000) and also as evidenced by the higher EIA(regression)/TIA ratio of around 78%).

The outcomes of these studies effectively suggest that areas that are traditionally thought of DCIA (e.g. roof areas), are in fact not directly connected. This is likely due to a number of factors, such as transmission loss (e.g. cracks in stormwater pipes), poorly connected roof drainage, drainage swales along roads etc.

The result is that the use of GIS methods to estimate DCIA and subsequently EIA can be problematic. In general, if GIS methods are to be used, then a reduction factor will be required in order to convert the estimated DCIA to the EIA.

In the absence of other information or data, then a range of 70% to 80% could be adopted in converting the GIS DCIA estimate to EIA.

3.4.3. Additional Considerations

3.4.3.1. Antecedent Conditions

Antecedent conditions have the potential to influence the EIA. Ball and Powell (1998), analysing Powells Creek in NSW (Sydney), showed the EIA to total area ranged from around 35% for six days or greater of no rainfall preceding the storm, to around 44% for less than six days of no rainfall preceding the storm. However, other studies have not reported on this effect. In undertaking sensitivity testing on the EIA, Phillips et al (2014) did not identify a clear influence of the antecedent rainfall on the EIA. The relative importance of antecedent conditions is discussed further in Book 5, Chapter 3, Section 7.

3.4.3.2. Changes in Urban Density

Changes in the urban development over time can alter the density of development. This has the potential to influence results of EIA estimates.

For the regression analysis, as identified in Book 5, Chapter 3, Section 4, it is important that this be taken into account. Ideally a stationary catchment (i.e. limited or not change in density) for the period of the gauging record should be used to estimate the EIA.

For GIS methods, consideration should be made on changes to the catchment since the date of the aerial photography. Where the aerial photography is older, it may no longer be representative of the existing development. Alternatively, for analysis of historical flooding, the aerial photography may not be representative of the development at that time.

3.4.3.3. Water Sensitive Urban Design

Water Sensitive Urban Design is common practice for most new development. WSUD principles would be expected to counteract, to some degree, the increase in imperviousness as a result of the development.

The literature in estimating EIA/ TIA ratios is based on catchments with reasonably long flow gauge records (typically greater than 10 years), and with stationary catchment conditions (i.e. limited new development). WSUD has increased in prevalence in design over the last 10 years or so. As a result, it is unlikely that any of these catchments in the research

incorporate a large proportion of WSUD features, and even if one or two did, there would be insufficient data to establish any trends.

Therefore, while it is expected that WSUD may influence the estimate of EIA in catchments, there is insufficient data at this time to fully understand the impact.

3.5. Regional Loss Information

3.5.1. Introduction

Book 5, Chapter 3 describes the different approaches to selecting loss models and suitable parameter values for design flood estimation. In most cases there is insufficient data to undertake a detailed analysis of the data and therefore loss values should be inferred from consideration of regional information as well as reconciliation of design values with other independent flood estimates (such as at-site or regional flood frequency estimates). However, if losses are to be derived for the specific study of interest then the analysis should be cognisant of the issues discussed in Book 5, Chapter 3, Section 3.

The recommendations in this chapter have been drawn largely from regional studies of loss values undertaken by Phillips et al (2014) for urban catchments and Hill et al. (2014a), Hill et al. (2015), and Hill et al. (2016) for rural catchments.

These 2 studies concluded that the IL/CL model is typically the most suitable for design flood estimation and hence the recommendations in this chapter relate to this model. If other loss models are to be used for design then it is important that consideration is given to the requirements discussed in Book 5, Chapter 3, Section 2.

The loss values recommended in this chapter are intended for application to complete design storms. Thus the initial loss is denoted as IL_s to indicate that it is applicable to a complete storm. However, if design bursts, rather than complete storms, are used in design then the burst initial loss needs to be reduced to account for the pre-burst rainfall Book 5, Chapter 3, Section 2.

3.5.2. Rural Catchments

This section describes the recommended values of median IL_s and CL for rural catchment. Further description of the development of the prediction equations used to estimate these values is available in Hill et al. (2016).

3.5.2.1. Prediction Equations

The prediction equations used to develop the recommended loss values utilised attributes from the Australian Water Resource Assessment – Landscape (AWRA-L) model system which was developed by CSIRO and the Bureau of Meteorology (Frost et al., 2015). The AWRA-L model simulates the water balance on a continental scale with a spatial resolution of ~5km×5km and daily temporal resolution from 1911 to present (Smith et al., 2016). Model outputs include soil moisture, runoff, actual and potential evapotranspiration (ET), deep drainage and leaf area index (LAI) (Smith et al., 2016). AWRA-L was used to explain the variability of loss for its consistency, continuity and availability on the national scale.

Initial attempts to derive prediction equation using all 35 catchment across Australia resulted in considerable uncertainty in the estimated loss values and therefore prediction equations were developed for different regions which were based upon soil moisture characteristics

from AWRA-L. Assessing regions on the basis of differences soil moisture characteristics provides a more logical basis for regionalisation than rainfall alone, as changes in soil moisture reflect the combined influence of climate regime and catchment storage.

The hydrologic similarity was assessed on the basis of two measures representing the seasonality and magnitude of variations in soil moisture. Regional differences in soil moisture characteristics were determined using cluster analysis, and mapping of the identified groups revealed that catchments allocated to the same group were located in largely geographically contiguous regions.

Four regions were defined (refer Figure 5.3.16). Regions 1 and 3 represent the primary summer- and winter-dominant regions, and region 4 largely represents catchments in the south-west of Western Australia. Region 2 represents a more uniform climate: while the region is very large, information is only available on catchment losses for a small eastern portion of this region. The seasonality of average gridded soil moisture in each of the 4 regions is shown in Figure 5.3.17.

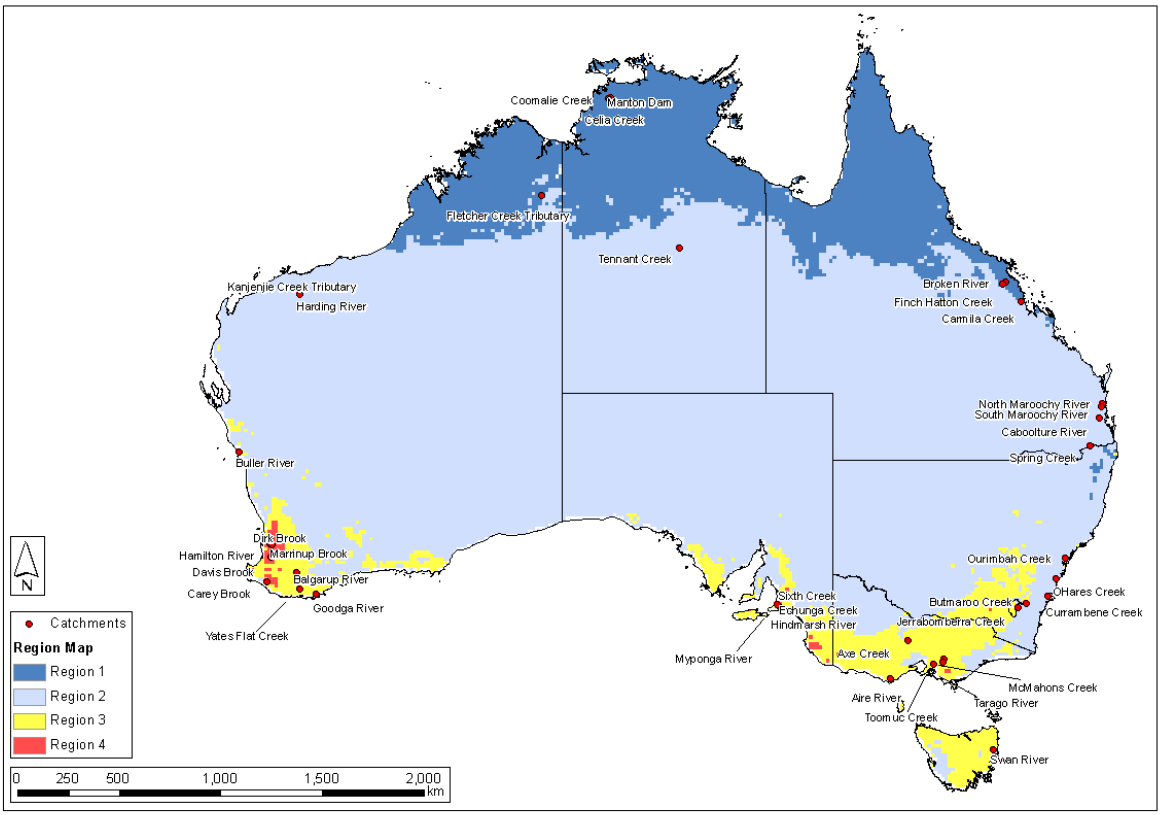

Figure 5.3.16. Regions Adopted for Loss Prediction Equations

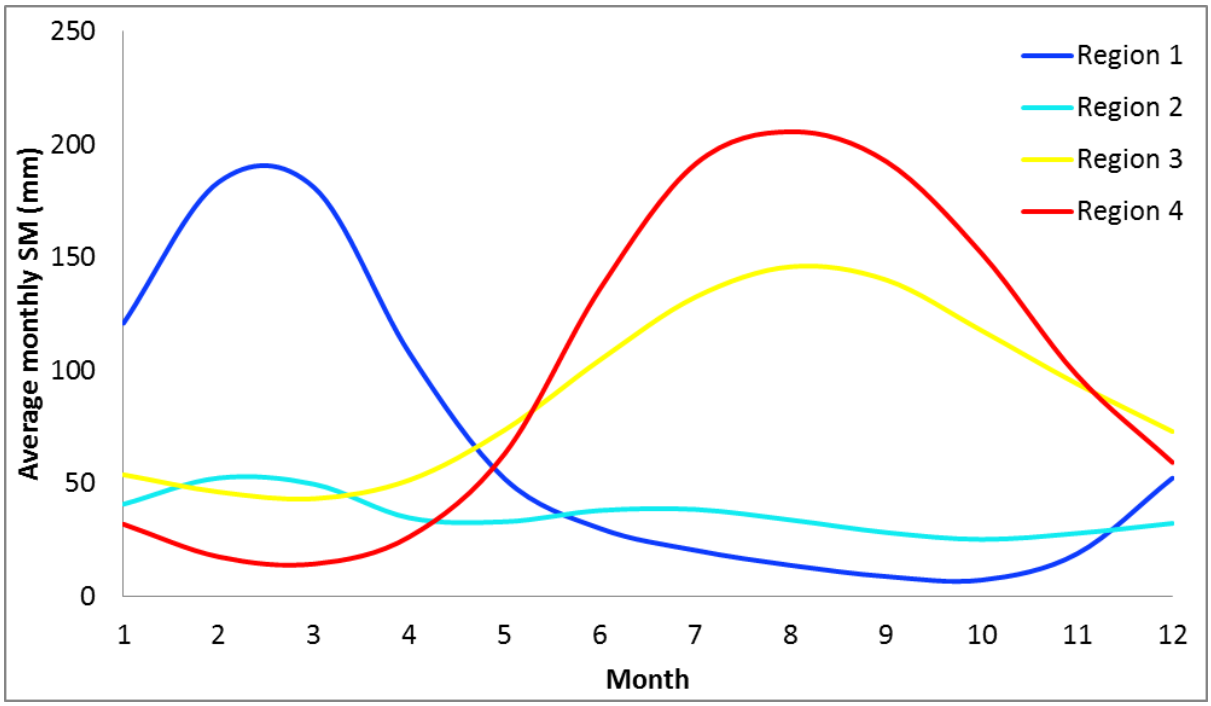

Figure 5.3.17. Seasonality of Average Gridded Soil Moisture in Each Defined Region (Using Gridded Data)

Multi-linear regression was used to develop prediction equations for IL_s and CL in each of the four regions. Given the relatively small number of catchments in each region, the number of independent variables was limited to a maximum of two. The resulting prediction equations are:

Region 1

There are 7 catchments in Region 1 and the prediction equations of loss parameters are displayed below. Initial loss is a function of maximum storage capacity of the shallow soil layer while CL is a function of mean annual PET and surface soil hydraulic conductivity.

$$IL_s = -0.37 * Ssmax + 136.0, R^2 = 0.77, SE = 23\% \quad (5.3.6)$$

$$CL = 2.20 * meanPET - 0.0015 * KO_{sat} - 3.2, R^2 = 0.67, SE = 36\% \quad (5.3.7)$$

Where:

IL_s is the storm Initial Loss (mm)

CL is the Continuing Loss (mm/h)

S_{smax} is the maximum storage of the shallow soil layer (mm)

meanPET is the mean annual potential ET (mm/d)

KO_{sat} is the saturated hydraulic conductivity of surface soil layer (mm/d)

Region 2

9 catchments are in Region 2 and most of them are located near the coast. The prediction equations for this region are:

$$IL_s = 7.89 * meanPET + 0.44 * SOLPAWHC - 47.1, R^2 = 0.68, SE = 24\% \quad (5.3.8)$$

$$CL = 0.77 * KS_{sat} + 0.29 * SO\max - 12.7 \quad (5.3.9)$$

Where:

IL_s is the storm Initial Loss (mm)

CL is the Continuing Loss (mm/h)

meanPET is the mean annual potential ET (mm/d)

SOLPAWHC is the average plant available water holding capacity across catchment (mm)

$KS_{sat}$is the saturated hydraulic conductivity of shallow soil layer (mm/d)

SO_{max} is the maximum storage of the surface soil layer (mm)

Region 3

There are 11 catchments in Region 3 and their loss parameters were estimated as follows:

$$IL_s = -1.57 * s0\_wtr + 0.14 * DES\_RAIN\_24HR + 18.8, R^2 = 0.71, SE = 18.3\% \quad (5.3.10)$$

$$CL = 0.03 * DES\_RAIN\_24HR + 0.06 * SO\max + 5.1, R^2 = 0.38, SE = 45\% \quad (5.3.11)$$

Where:

IL_s is the storm Initial Loss (mm)

CL is the Continuing Loss (mm/h)

s0_wtr is the soil moisture in the surface store in winter season (mm)

DES_RAIN_24HR is the design Rain Intensity (I24,50) (mm)

SO_{max} is the maximum storage of the surface soil layer (mm)

Region 4

There are 8 catchments in this region and the prediction equations are presented as follows:

$$IL_s = -56.2 * slope + 0.28 * SO\max + 16.4, R^2 = 0.47, SE = 21\% \quad (5.3.12)$$

$$CL = 0.088 * SOLPAWHC - 4.9, R^2 = 0.88, SE = 19\% \quad (5.3.13)$$

Where:

IL_s is the storm Initial Loss (mm)

CL is the Continuing Loss (mm/h)

slope is the average slope of catchment (radians)

SO_{max} is the maximum storage of the surface soil layer (mm)

SOLPAWHC is the average plant available water holding capacity across catchment (mm)

The above equations were applied to the relevant regions in Australia using independent variables derived for a grid size of 15 km x 15 km. Given the uncertainty in the prediction equations and the desire to have smooth variations in loss across catchment areas, the gridded values were smoothed using a window of 45 km x 45 km.

Based upon the range of values used in the derivation of the prediction equations, the median loss values were constrained so that the IL_s varied between 0 and 80 mm and the CL constrained between 0 and 10 mm/h.

The range of values for the independent variables and the loss values for the 35 catchments used to derive the prediction equations is summarised in Table 5.3.5 and Table 5.3.6.

Table 5.3.5. Range of Values Used in developing IL_s Prediction Equations

Region	N	Equation	Parameter	Min	Max	Median
Region 1	7	5.5.6	ssmax	180.6	315.4	258.6
			IL_s	22.5	70.0	41.5
Region 2	9	5.5.8	meanPET	3.26	8.61	4.09
			SOLPAWHC	88.48	147.00	118.29
			IL_s	20.0	60.0	37.5
Region 3	11	5.5.10	s0_wtr	0.9	15.9	3.0
			DES_RAIN_24HR	106.1	238.9	137.7
			IL_s	17.0	47.0	27.5
Region 4	8	5.5.12	slope_rad	0.1	0.2	0.1
			s0max	18.2	45.0	29.5
			IL_s	14.0	25.0	18.0

Table 5.3.6. Range of Values Used in Developing CL Prediction Equations

Region	N	Equation	Parameter	Min	Max	Median
Region 1	7	5.5.7	meanPET	4.8	7.7	6.2
			K0_sat	476.5	4153.5	3036.2
			CL	1.6	10.4	5.4
Region 2	9	5.5.9	KS_sat	1.55	9.27	3.37
			S0max	41.37	56.19	46.03
			CL	1.4	8.3	2.7
Region 3	11	5.5.11	DES_RAIN_24HR	1.6.1	238.9	137.7
			S0max	17.2	62.8	42.6
			CL	0.5	6.0	3.1
Region 4	8	5.5.13	SOLPAWHC	82.8	136.9	103.4
			CL	2.2	8.1	3.5

3.5.2.2. Recommended Loss Values

The recommended loss values are shown in Figure 5.3.18 and Figure 5.3.19 and were derived using the prediction equations in the preceding section. For arid areas with mean

annual rainfalls less than 350 mm (shown in grey in both figures) there are no recommendations for design loss information because the prediction equations were developed using data from wetter catchments. Recommended loss values can be accessed via the ARR Data Hub (Babister et al (2016), accessible at http://data.arr-software.org/).

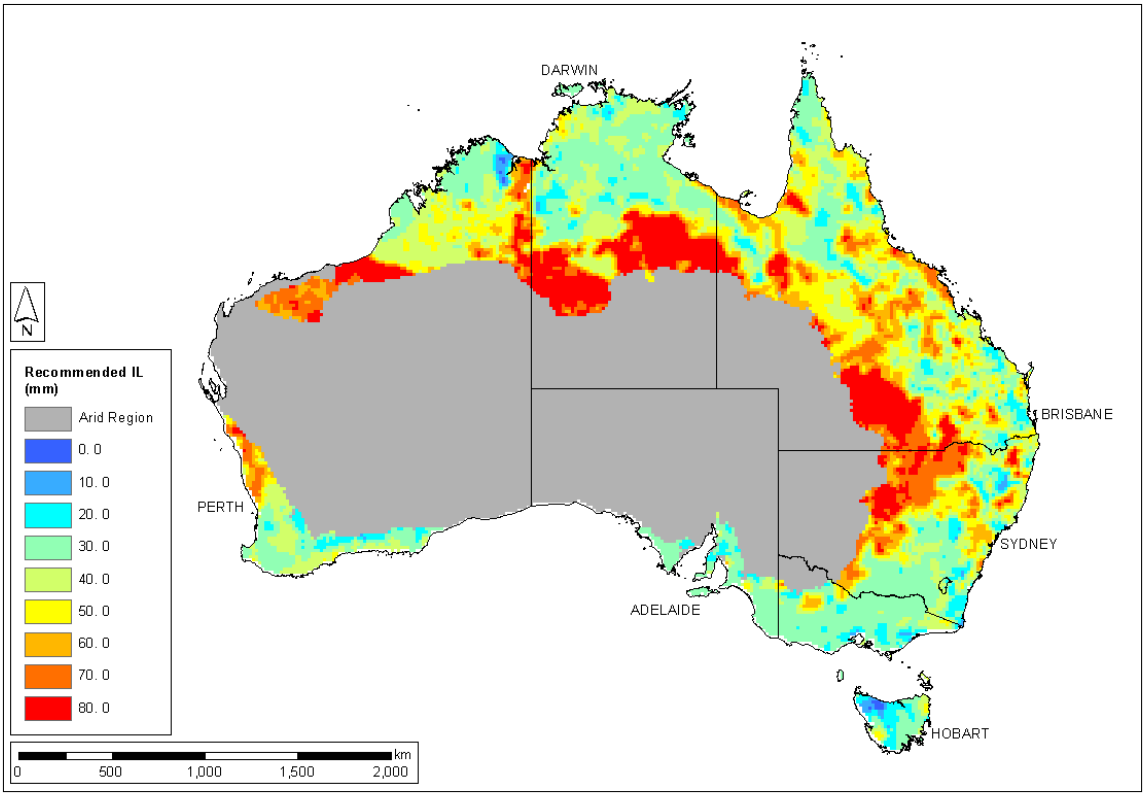

Figure 5.3.18. Recommended Median IL_s (mm)

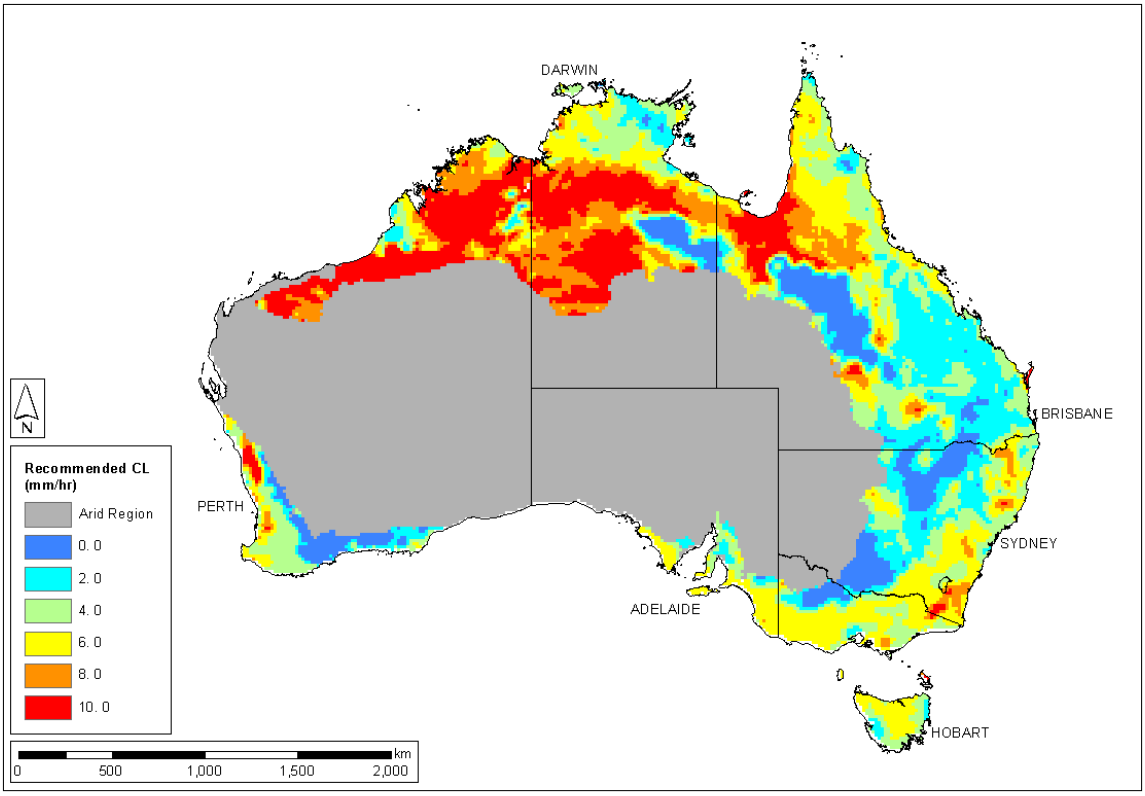

Figure 5.3.19. Recommended Median CL (mm/hr)

It should be noted that the recommended values were derived based upon only 35 catchments and the standard error of the estimates range between 20% and 50%.

Because of the limited number of catchments available, the prediction equations are based upon one or two independent variables. However, it is anticipated that a wide range of characteristics combine to influence the loss values for a particular catchment and therefore judgement is recommended when selecting suitable values for use in design. For example for catchments with very dense vegetation, it would be expected that the loss values would be higher. Similarly, steep catchments with little vegetation would be expected to have lower loss values. Any such adjustment from the regional values should be done giving consideration to the range of loss values obtained in Hill et al. (2014a) and other studies and the implications on the design flood estimates.

Lastly, it is important to note that the recommended loss values in the above figure relate to the *median* for a particular catchment. It is expected that the loss for any particular event could lie well outside of this range. For many catchments, the storm initial loss for any particular event could range from nearly zero, if the storm occurs on a wet catchment, to more than 100 mm if there is little antecedent rainfall.

3.5.2.3. Loss Values for the Arid Region

There is generally a lack of suitable catchments to estimate loss values for the arid regions of Australia.

Kemp and Wright (2014) noted high loss rates for the Gammon Ranges in mid-north South Australia. They attributed the high values to the runoff processes being dominated by the

large amounts of storage within the gravel bed of the tributaries and main streams which absorbs a significant amount of runoff from the hillsides. Thus the initial loss represents loss in the tributaries and main stream in addition to that occurring within the catchment. This explanation is supported by observations in arid western New South Wales (Cordery et al, 1983).

Board et al. (1989) estimated losses for the Emily Creek and Todd River catchments in central Australia by calibrating a RORB model to 3 floods. The IL_s varied from 10 to 60 mm and the CL varied from 1.5 to 4.5 mm. It should be noted that the events were selected based upon the largest floods and hence the sample is likely to be biased to wet antecedent conditions which would indicate that the IL_s values are likely to underestimate the median value.

The median loss values in the Pilbara are some of the highest in Australia. There was only 1 catchment from the Pilbara included in the Hill et al. (2014a) study but information is also available from Pearcey et al. (2014) which documents the calibration of RORB models to 19 catchments in the Pilbara region. Although the events in Pearcey et al. (2014) were selected on the basis of streamflow rather than rainfall (and hence potentially biased towards wet antecedent conditions), they support high values of loss.

For the Pilbara, Flavell and Belstead (1986) recommended IL values of approximately 40 to 50 mm and a CL of 5 mm/h. It should be noted that the loss values were derived from reconciling rainfall based estimates with flood frequency analysis and thus the IL reflects a burst initial loss and a higher initial loss would be expected if complete storms are adopted so the range of IL reported by Flavell and Belstead (1986) should be considered a lower limit of expected IL_s values.

3.5.2.4. South-Western WA

The runoff characteristics of much of south-west Western Australia are different from that found in many other parts of Australia. The highly permeable soils and large soil water storages of the south-west landforms means that the continuing loss rates tend to be high.

The dominate contribution to runoff is believed to be saturated areas in the broad valley floors which represent a relatively small proportion of the total catchment. For catchments where runoff is predominately generated via this mechanism, then a storage capacity loss model such as SWMOD should be applied to estimate the rainfall excess (Refer Book 5, Chapter 3, Section 2). For other catchments in south-west WA the IL/CL model is recommended.

For Southwest WA the rainfall and losses are markedly seasonal in nature and it should be noted that the 160 events analysed by Hill et al. (2014a) were biased towards the winter months with 70% of them occurring in May, June or July. Considerations for the selection of seasonal loss values is discussed in Book 5, Chapter 3, Section 7.

3.5.2.5. Collation of Loss Values

To support the recommended loss values, values from a range of studies have been collated and summarised in Appendix A. The loss values have been drawn from the following studies: Waugh (1991), Hill et al. (1996), Ilahee (2005), Rahman et al. (2002), El-Kafagee and Rahman (2011), Hill et al. (2014a) and Loveridge (Unpublished). These studies have been selected on the basis that the loss values were derived directly from the analysis of rainfall and streamflow (rather than reconciliation of design flood estimates with flood frequency quantiles) to ensure that the values are independent of the design inputs used in

their derivation. Furthermore, in each study the sample of events was selected based upon rainfall rather than streamflow (to avoid any bias towards wet antecedent conditions).

For some studies the CL was estimated as the volume of loss (less the IL_s) divided by the duration of the event post the commencement of surface runoff. As discussed in Book 5, Chapter 3, Section 2 this will underestimate the CL as there are likely to be timesteps where rainfall is less than the CL rate. Values of CL from such studies were removed from the dataset and hence there are less values of CL than IL_s provided in Book 5, Chapter 3, Section 8.

3.5.3. Urban Catchments

As identified, in Book 5, Chapter 3, Section 4, the urban catchments have been conceptualised as EIA, Indirectly Connected Areas (a combination of Indirectly Connected Impervious and Pervious Areas) and Pervious Areas. The following provide guidance on the losses to apply to these areas.

3.5.3.1. Losses for Effective Impervious Areas

3.5.3.1.1. Research

Phillips et al (2014) estimated initial loss based on the EIA analysis undertaken (refer to Book 5, Chapter 3, Section 4), plotting the runoff volume against the rainfall volume. The intersection of the best fit line with the x-axis represents the initial loss on the EIA. Should data be available for a catchment, then this provides a way in which the initial loss can be estimated.

The analysis in Phillips et al (2014) had initial losses ranging from 1 to 3 mm across the country, with no real identifiable trend between the different regions (although the data was limited). A similar approach was undertaken by Kemp and Lipp (1999), Ball and Zaman (1994) and Chiew and McMahon (1999), and these studies identified typical values in the order of 0 to 1mm

Bufill and Boyd (1992) analysed 16 catchments, 10 within Australia and 6 international catchments. Their analysis identified initial loss by estimating the mean initial loss across all events for these catchments. It is important to note that this is a slightly different way of undertaking the analysis from Phillips et al (2014), and therefore can result in slightly different results. However, this study found that typical initial loss rates for the 10 catchments within Australia are around 0 to 1 mm. These catchments were subsequently re-analysed using the EIA technique in Boyd et al. (1993).

Bufill and Boyd (1992) also analysed 6 international catchments, using the method noted above, and found an initial loss ranging from around 0.5 to 1 mm. Boyd et al. (1993) had 17 international catchments in their analysis, with initial loss values typically ranging from 0 to 1.3 mm, although two catchments in the US had 3.7 mm and 6.1 mm.

A summary of the different initial loss estimates available for the different studies are provided in Book 5, Chapter 3, Section 8. It is important to note that there is only one catchment from the northern parts of Australia (i.e. Monsoonal North, Wet Tropics, Pilbara) or the central portion of Australia (Rangelands). However, given the consistency of the estimates across the regions, and with international estimates, it is unlikely that the initial loss for EIA in these areas will be significantly different.

All studies assumed that the ongoing losses on the EIA were effectively zero.

3.5.3.1.2. Recommended Loss Value for EIA

It is recommended to adopt a storm initial loss of between 1 to 2 mm for EIA. Continuing losses for EIA can be assumed to be zero.

3.5.3.2. Losses for Indirectly Connected Areas

3.5.3.2.1. Initial Losses

Literature

One of the key challenges in urban catchments is the lack of gauged urban catchments with reasonable records and relatively stable development. In addition to this, many rainfall events do not produce any Indirectly Connected Area runoff, which can make it difficult to obtain sufficient data to determine appropriate losses.

Phillips et al (2014) used the same catchments as those identified in Book 5, Chapter 3, Section 4 for EIA. In order to isolate events with flow generated from the Indirectly Connected Area, they selected events where the flow generated was 10% higher than the flow estimated by calculating the runoff from the EIA area alone. A number of other criteria were adopted. Further details on the storm event selection are identified in Phillips et al (2014). A summary of the number of events identified for each of the catchments is summarised in Table 5.3.7.

Two catchments from the EIA analysis in Phillips et al (2014) were excluded:

- Parra Hills (SA) – only a limited number of storms were identified. The number of storms was too small to provide any meaningful analysis of the losses.
- Kinkora Road (VIC) – further analysis of the data suggested some unusual behaviour, with periods of runoff with no rainfall and vice versa for the selected events. This catchment was therefore not included in any further analysis.

Table 5.3.7. Total Storms identified for Analysis Phillips et al (2014)

	Giralang (ACT)	Powells Creek (NSW)	Albany Drain (WA)	McArthur Park (NT)	Argyle St (TAS)
Total Identified Storms	41	14	30	20	49

One of the key challenges in the use of the urban data in Phillips et al (2014), and with many other studies, is that the length of record is relatively small. This, together with the filtering method, reduces the number of large storm events to estimate losses. Figure 5.3.20 shows the storm magnitude from the selected events from Phillips et al (2014), based on the ARR 1987 AEPs (storms not shown are less than 63% AEP or 1 EY).

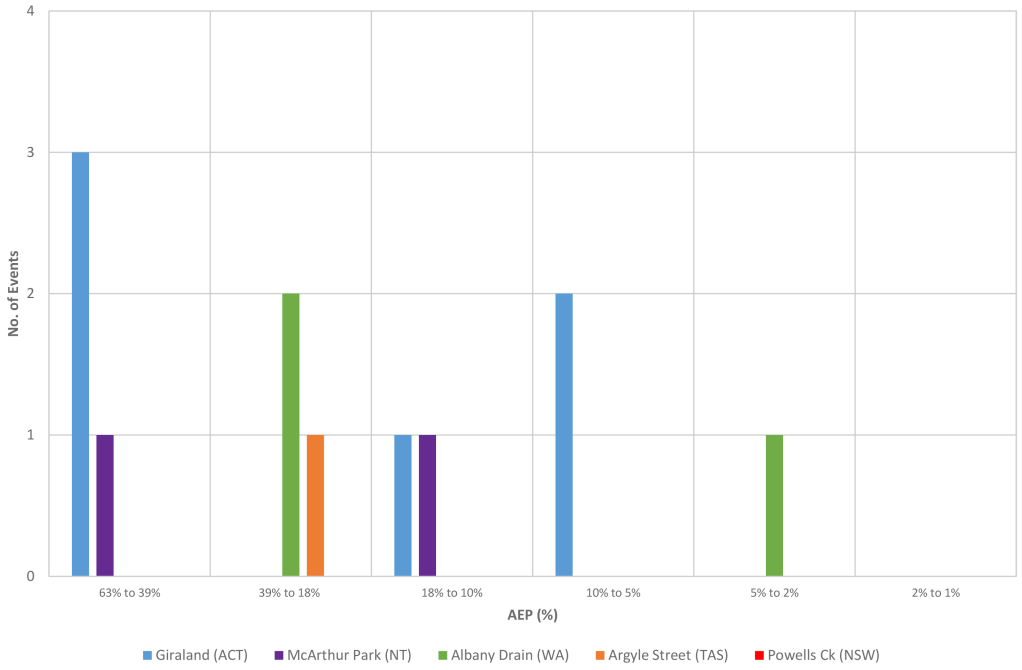

Figure 5.3.20. Storm Magnitude from Phillips et al (2014)

Based on the selected storms, Phillips et al (2014) identified that mean storm initial losses across the range of storms for the catchments analysed were generally in the range of 20 to 30 mm, with the majority between 10 and 40 mm, and would appear fairly consistent across most of the catchments. A summary of the results is provided in Figure 5.3.20, providing an indication of the ranges. Phillips et al (2014) noted that the Argyle Street (TAS) was not well suited to the analysis that was undertaken, due to large pervious areas and bushland. As with the rural catchments, there is significant variation in the results, which is driven by numerous factors such as antecedent conditions and temporal pattern of the storm.

The storms in Phillips et al (2014) were real storms, and may differ to the design storm temporal patterns. Furthermore, the higher loss values may be skewed by rainfall events that occurred where low depths continued for a prolonged period of time at the start of the event. On this basis, the storm initial loss for design storms may be lower than the range estimated in Phillips et al (2014).

Boyd et al. (1994) fitted a model for urban catchment runoff to 3 catchments in Australia (all in ACT). This model conceptualised that the urban catchment was comprised of EIA, pervious area that contributed for small rainfall events (<40 mm) and pervious areas that contributed for larger rainfall events (>40mm). For the “small pervious” area, the study indicated initial losses of 0 to 4 mm, while for the “large pervious” area, the study indicated 30 to 50 mm. It is noted that in other studies the “small pervious” area is effectively lumped into the EIA (such as Phillips et al (2014)), so that the 30 to 50 mm initial loss would be generally consistent with the initial loss concept for the Indirectly Connected Area in this chapter. However, key challenges with the Boyd et al. (1994) catchments is that they are low density (5 to 25% total impervious fraction), and the model applied effectively incorporates a proportional loss into the fraction of “small pervious” and “large pervious” areas.

Kemp and Lipp (1999) analysed three catchments in South Australia. For the Indirectly Connected Areas, they were not able to identify any clear runoff events from these areas for these catchments. Based on the available research, this paper recommended 45 mm of initial loss be adopted for Adelaide, although this could go as high as 60 mm. However, these estimates were identified as preliminary, and there was no runoff records to verify this. Interestingly, Phillips et al (2014) were also unable to identify sufficient events with runoff from the Indirectly Connected Area for South Australia.

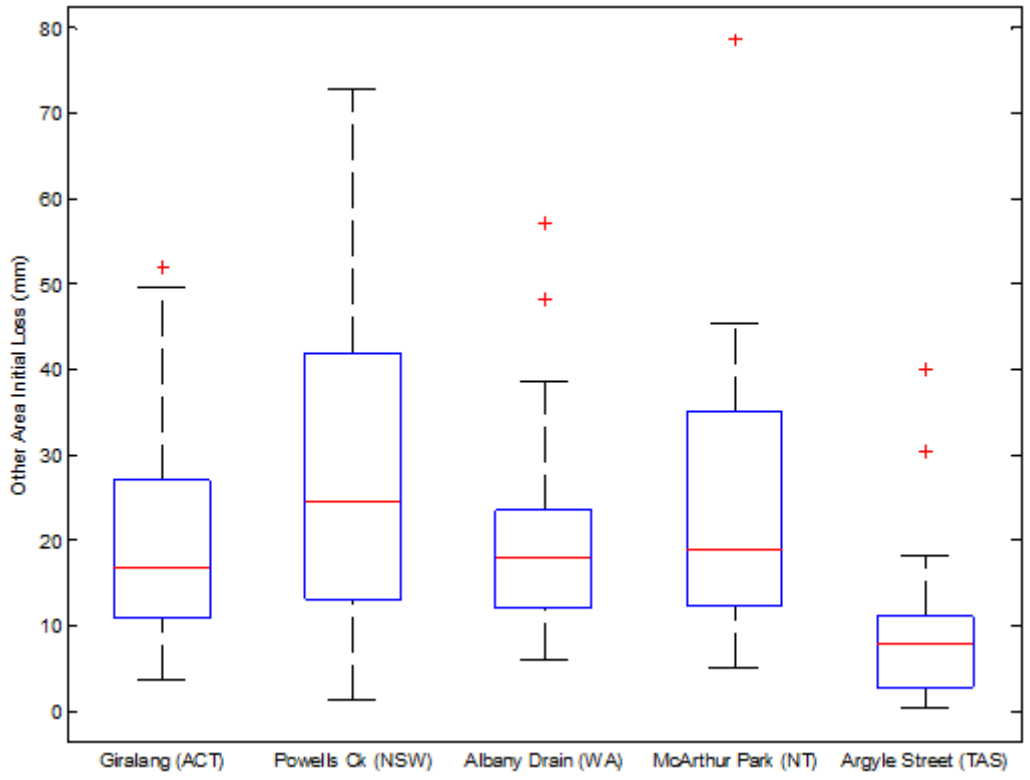

Figure 5.3.21. Summary of Initial Losses for Urban Catchments (from Phillips et al (2014))

Conceptualisation

As per the conceptualisation in this chapter, the Indirectly Connected Area is composed of impervious and pervious areas interacting with each other. The pervious area would be expected to tend towards the rural losses, although will be modified due to urban pervious area modification (such as import of top-soil, differing vegetation etc). However, the impact of the impervious area would be expected to lessen the initial loss across the combined area.

A comparison of the initial loss derived in the literature with the recommended IL_s for Rural catchments is provided in Table 5.3.8. This table also provides the ratio of the Indirectly Connected Impervious Area over Indirectly Connected Area. Key points:

- The initial loss values are similar to the recommended rural loss values although obviously there is significant scatter in both data sets;
- The initial loss values are similar to the recommended rural loss values. Generally, the values are in the order of 60 to 80% of the recommended median Rural IL_s, although obviously there is significant scatter in both data sets;
- There is insufficient data to determine any appropriate relationships with ICIA/ICA with initial loss and its relation to the recommended median rural loss.

- The catchments from Boyd et al. (1994) have almost no ICIA, and the median values for IL_s are in the range of the recommended median rural loss.
- There is insufficient data covering all regions as identified in the rural section.

Table 5.3.8. Comparison of Initial Loss Literature Values with Rural Recommended Values

Catchment	Region	Median IL_s (mm)	Reference	Recommended Rural IL_s (mm)	ICIA/ ICA
Giralang (ACT)	Murray Darling	17	Phillips et al (2014)	23	9%
Powells Creek (NSW)	East Coast	24.5	Phillips et al (2014)	33	43%
Albany Drain (WA)	South-West WA	18	Phillips et al (2014)	31	18%
McArthur Park (NT)	Monsoonal North	18.9	Phillips et al (2014)	25	17%
Argyle Street (TAS)	South-East Coast	7.9	Phillips et al (2014)	27	6%
Long Gully Creek (ACT)	Murray Darling	34	Boyd et al. (1994)	23	0%
Mawson (ACT)	Murray Darling	49	Boyd et al. (1994)	23	5%
Curtin (ACT)	Murray Darling	31	Boyd et al. (1994)	18	0%
South Australia (3 catchments)	South-Central SA	45	Kemp and Lipp (1999)	23	

Recommendation

Based on the limited available information, it is recommended that a median IL_s of 60 to 80% of the recommended rural catchment IL_s be adopted.

It is noted that this may trend towards 100% as the proportion of impervious area in the Indirectly Connected Area reduces. Based on the data that is available, this might occur when the impervious area drops below 5% of the total Indirectly Connected Area.

3.5.3.2.2. Continuing Loss

Literature

The constant continuing losses estimated in Phillips et al (2014) ranged generally from 0 to 4 mm/h across the catchments. However, this excludes the catchment in Northern Territory which was influenced by the presence of a large detention basin that affected results. However, more recent analysis of this catchment with regards to timestep (see Book 5, Chapter 3, Section 7), would suggest that for a 6 minute interval the CL estimate is 2.8 mm/h, which is within the range of the other catchments. Phillips et al (2014) also cautioned with the results of the Tasmanian catchment (Argyle Street), which is influenced by a large bushland area component, significantly larger than the urban area of the catchment.

Both NSW and ACT had median constant continuing loss values in the order of 2.5 mm/h. WA exhibited higher continuing losses, with a median value close to 4mm/h.

A comparison of the median continuing loss values with those of the recommended values for the rural catchments is provided in Table 5.3.9. It is difficult to draw any real conclusions based on the limited data set, other than to note that they are generally in the same range.

Table 5.3.9. Urban Continuing Loss Values Compared with Rural Continuing Loss Values

Catchment	Median CL(mm/h)	
	Phillips et al (2014)	Regional rural estimate from Book 5, Chapter 3, Section 5
Giralang (ACT)	2.5	3.6
Powells Creek (NSW)	2.6	1.8
Albany Drain (WA)	3.8	3.3
McArthur Park (NT)	5.1	4.1
Argyle Street (TAS)	1.4	3.8

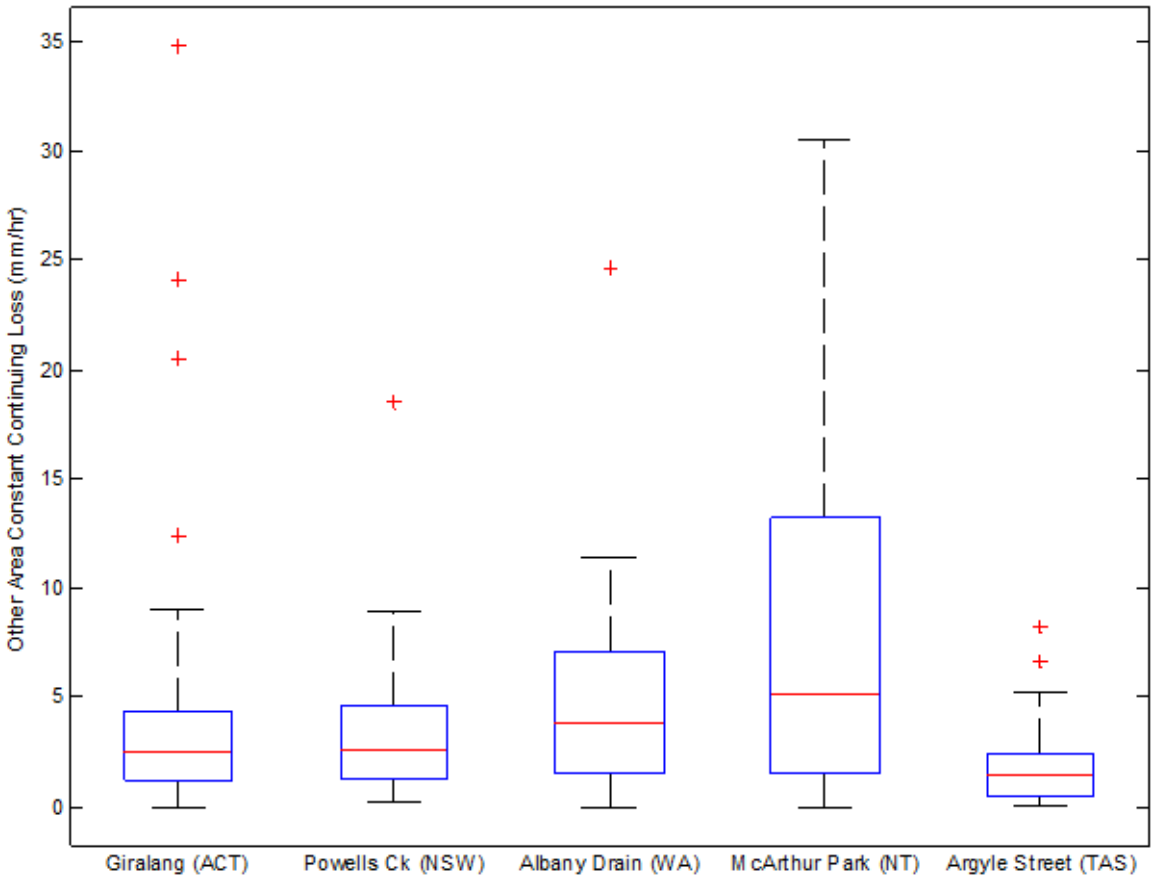

Figure 5.3.22. Indirectly Connected Area Continuing Loss Estimates (from Phillips et al (2014))

Recommendations

In the absence of other data, the following is recommended where appropriate gauging data is not available:

- For southeastern Australia, a typical value of 2.5mm/h, with a range of 1 to 3 mm/h, would be appropriate. The value should be adjusted based on engineering judgement and reviewing the catchment characteristics such as soil types, interaction of indirectly connected impervious areas with pervious areas etc.
- For other areas, adopt a range of 1 to 4 mm/h.
- Similar to initial losses, where the impervious proportion of the indirectly connected area is very low, it may be appropriate to adopt the rural continuing losses. However, there is insufficient data to confirm this.

3.5.3.3. Losses for Urban Pervious Areas

Urban pervious areas represent areas that do not interact directly with impervious areas (i.e. those not within the Indirectly Connected Area), such as pockets of bushland, parks, recreational ovals etc. Traditionally, practitioners have adopted similar loss values for these areas as for those they would adopt in rural areas.

The challenge in the research for these areas is identifying the runoff component from these portions, which are typically dominated by runoff from impervious areas. However, there is nothing to say that these areas will behave the same as rural areas. Areas like parks and sporting fields are highly disturbed from their natural state, and therefore may exhibit very different characteristics. However, with little research and information available, the losses for the rural catchment provide the best estimate that is available at this time.

Therefore, in the absence of better information, it is recommended to adopt the loss values for rural catchments from Book 5, Chapter 3, Section 5.

3.5.3.4. Alternative Loss Models for Indirectly Connected Areas

As noted in Book 5, Chapter 3, Section 5, the recommended loss model for urban catchments is the IL/CL model, based on the results of Phillips et al (2014). However, it is also recognised that a number of other loss models have been and are in use in Australia. Furthermore, there is insufficient data to categorically identify one loss model over another as being preferred, and there are circumstances where specific loss models may suit a particular catchment well.

Two alternative models that are commonly applied in urban environments are the proportional loss models and the Horton loss models. These two loss models are described in the following sections.

Initial Loss - Proportional Loss Model

The initial loss proportional loss model is described in Book 5, Chapter 3, Section 2.

The initial loss for the model should be adopted as per Book 5, Chapter 3, Section 5.

In addition to testing the IL/CL loss model, Phillips et al (2014) also tested the proportional loss model. A summary of the results from this assessment are provided in Figure 5.3.23. As identified in Book 5, Chapter 3, Section 5, some care should be taken with the interpretation of the results from Tasmania (Argle Street) and Northern Territory (McArthur Park).

The key challenge with the results of this analysis is that the results range from median proportional losses of around 45% through to 80%. This makes it difficult to provide a general guidance for catchments.

As discussed in Book 5, Chapter 3, Section 3, the greatest challenge in applying the IL/PL model for design flood estimation is understanding how the proportional loss varies with AEP. Great care should therefore be exercised if the IL/PL is to be applied to events outside of the range of events used in the derivation of the values. For this reason it is generally not considered appropriate for estimating rare or extreme events (ie AEP < 1%).

Therefore, it is recommended that this method only be used where suitable data is available to calibrate the loss model, either for a specific catchment or for a similar catchment nearby. Alternatively, should more research become available this could assist in informing appropriate parameters for design.

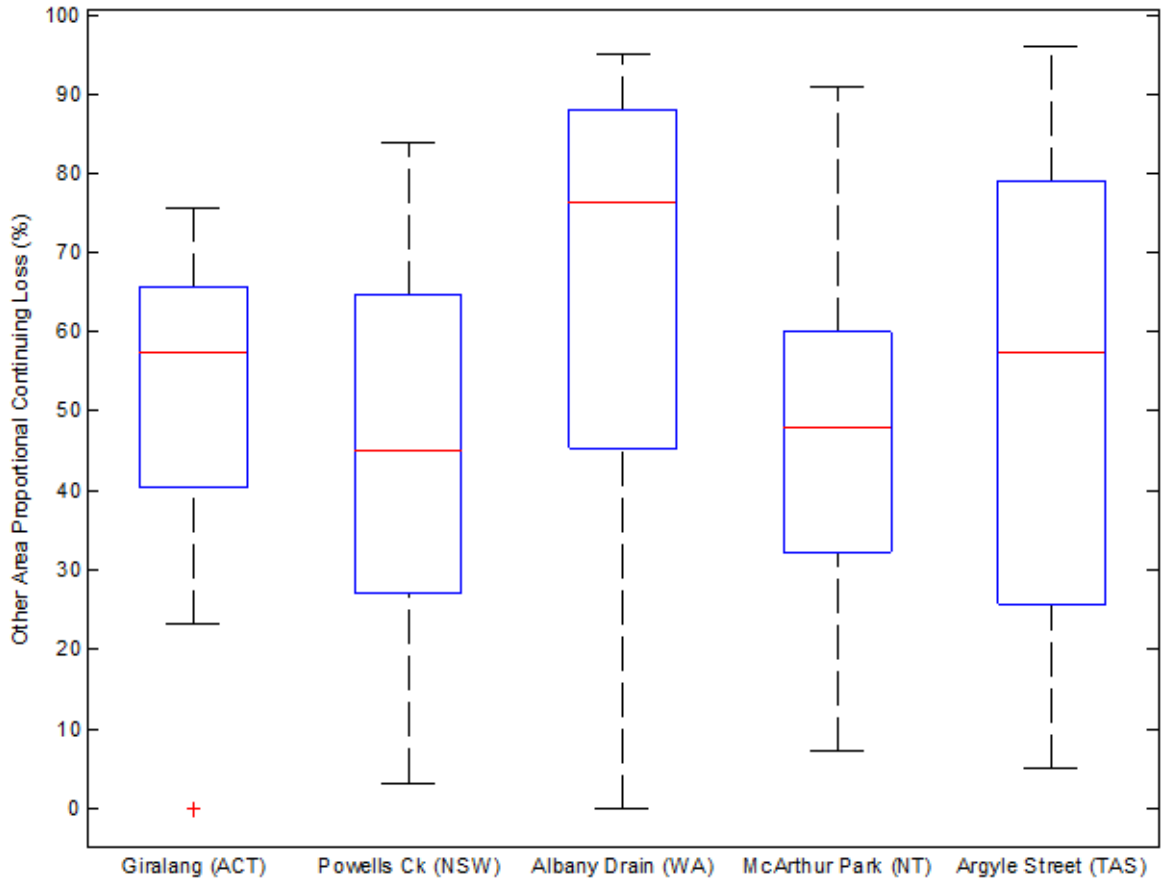

Figure 5.3.23. Indirectly Connected Area Proportional Loss Estimates (from Phillips et al (2014))

Horton Loss Model

The Horton loss model is described in Book 5, Chapter 3, Section 2, with the equation below repeated for reference.

$$f_t = f_c + (f_0 - f_c)e^{-kt} \tag{5.3.14}$$

where:

f_t is the infiltration capacity (mm/h)

f_c is the minimum or ultimate value of f_t

f_0 is the maximum or initial value of f_t (mm/h)

k is a decay coefficient (per hour)

t is the time from the beginning of the storm (h)

This model is for pervious areas only. The hydrological models that use this model separate out the Indirectly Connected Impervious Areas from the Indirectly Connected Pervious Areas, treating the losses separately. An examples of this is ILSAX, as detailed in O'Loughlin and Stack (2014). O'Loughlin and Stack (2014) has been used as the key reference for this section of the chapter, and the parameters reported here are based on this reference.

The Horton model assumes that the losses (or infiltration) of runoff decreases over the duration of the storm. The shape of this decay function is described by the k value, which is typically assumed to be 2 (h-1). The remaining parameters to describe the decay curve are the initial infiltration rate (f_0) and the final infiltration rate (f_c). These are defined by the soil characteristics. Soil classifications that are used are described in Table 5.3.10, which are based on numerous reference and reproduced from O'Loughlin and Stack (2014).

Table 5.3.10. Soil Classifications in Horton Model

Soil Classification	Description
A	low runoff potential, high infiltration rates (consists of sand and gravel)
B	moderate infiltration rates and moderately well-drained
C	slow infiltration rates (may have layers that impede downward movement of water);
D	high runoff potential, very slow infiltration rates (consists of clays with a permanent high water table and a high swelling potential).

In applying the model, a “starting point” is required for the analysis. This represents the infiltration rate at the start of the storm, which is based on the Antecedent Moisture Condition (AMC). The AMC can be categorised from Table 5.3.11 (based on O'Loughlin and Stack (2014)).

Using the soil classification and the AMC number, the Horton Loss Model parameters can be defined based on Table 5.3.12. The resulting loss models for the different classifications, together with the AMC numbers, are shown in Figure 5.3.24.

Table 5.3.11. Antecedent Moisture Condition Number

Number	Description	Total rainfall in 5 days preceding the storm (mm)
1	Completely Dry	0
2	Rather Dry	0 to 12.5
3	Rather wet	12.5 to 25
4	Over Saturated	> 25

Table 5.3.12. Horton Loss Model Parameters

	Soil Type			
	A	B	C	D
Initial Rate (f_0) (mm/hr)	250	200	125	75
Final rate (f_c) (mm/hr)	25	13	6	3
Shape Factor (k) (h^{-1})	2	2	2	2
Initial Infiltration Rates (mm/h) for AMCs				
1	250	200	125	75
2	162.3	130.1	78	40.9
3	83.6	66.3	33.7	7.4
4	33.1	30.7	6.6	3.0

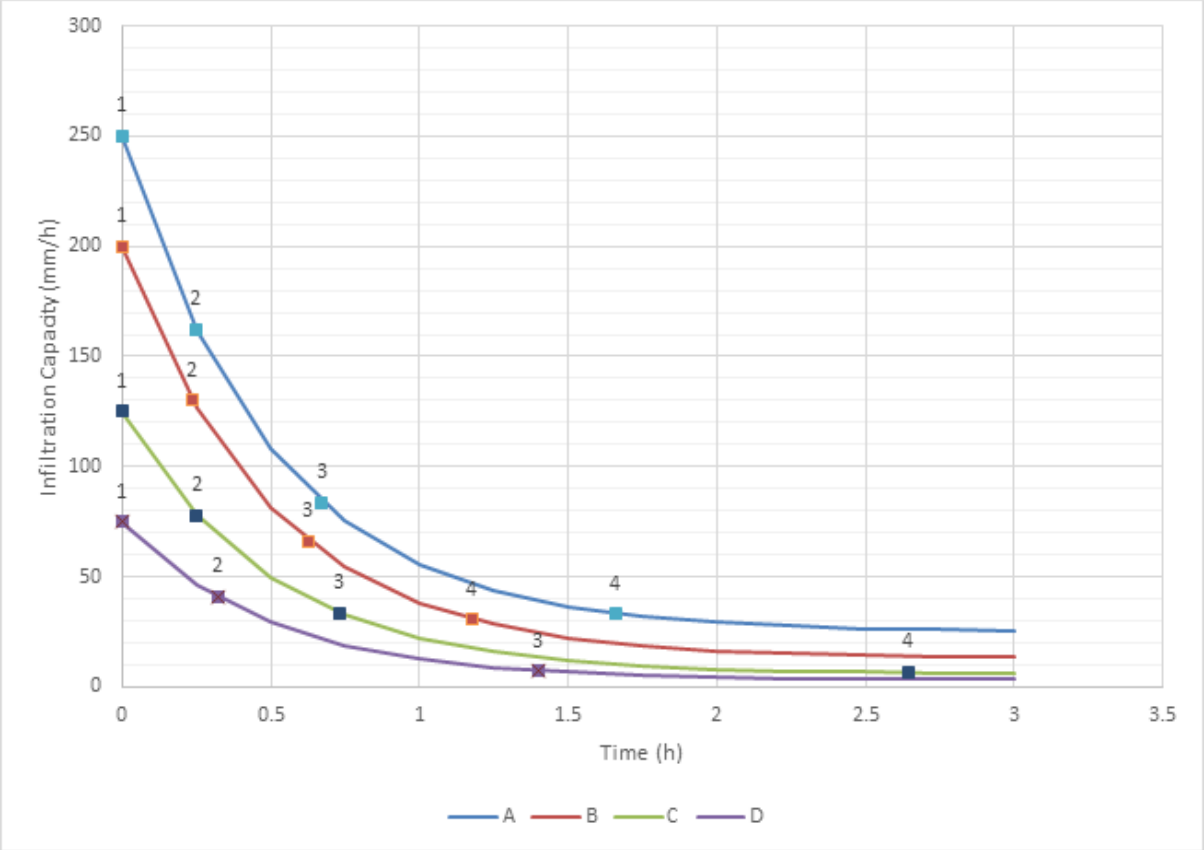

Figure 5.3.24. Horton Loss Model with Different Soil Classifications & AMC Numbers

O'Loughlin and Stack (2014) report that this method has been used in the calibration of a number of ILSAX models to gauged catchments. While no references are provided, it is anticipated that this calibration is for whole hydrological and hydraulic models, which includes a number of parameters not just isolated to losses.

O'Loughlin and Stack (2014) report that Siriwardene et al. (2003) compared the infiltration rates from with those measured with infiltrometers at eight urban gauged catchments in

Victoria. These rates suggested slightly higher rates than those reported in Table 5.3.12. However, the research only focused on the soils, and did not look at the other components that loss models are trying to represent (such as those identified in Book 5, Chapter 3, Section 2).

More research is required to compare the effectiveness of this loss model in comparison to constant continuing loss model.

3.6. Distribution of Loss Values

The discussion in the previous sections concentrates on a single representative (median) value of loss. However, joint probability approaches to design flood estimation allow a distribution of loss values rather than simply some measure of central tendency (eg (Goyen, 1983; Rahman et al., 2002; Nathan et al., 2003; Kuczera et al., 2006)).

The degree of variability in the loss values reflects both natural variability in the factors contributing to loss (initial state of catchment wetness, seasonal effects on vegetation) and impacts of error in rainfall and streamflow data. As long as these errors are of a random rather than systematic nature, they should not bias the estimated loss distribution.

These approaches can be grouped into parametric and non-parametric and are discussed in the following sections.

3.6.1. Non Parametric Approaches

Nathan et al. (2003) describes the derivation of a standardised loss distribution by standardising the values by the median for each catchment. The concept of how the location of the loss distribution changes but not its shape is discussed in Nathan et al. (2003) and is illustrated in Figure 5.3.25. Thus, if the median loss value can be determined, then these standardised distributions can be applied to estimate the distribution of losses for any given catchment.

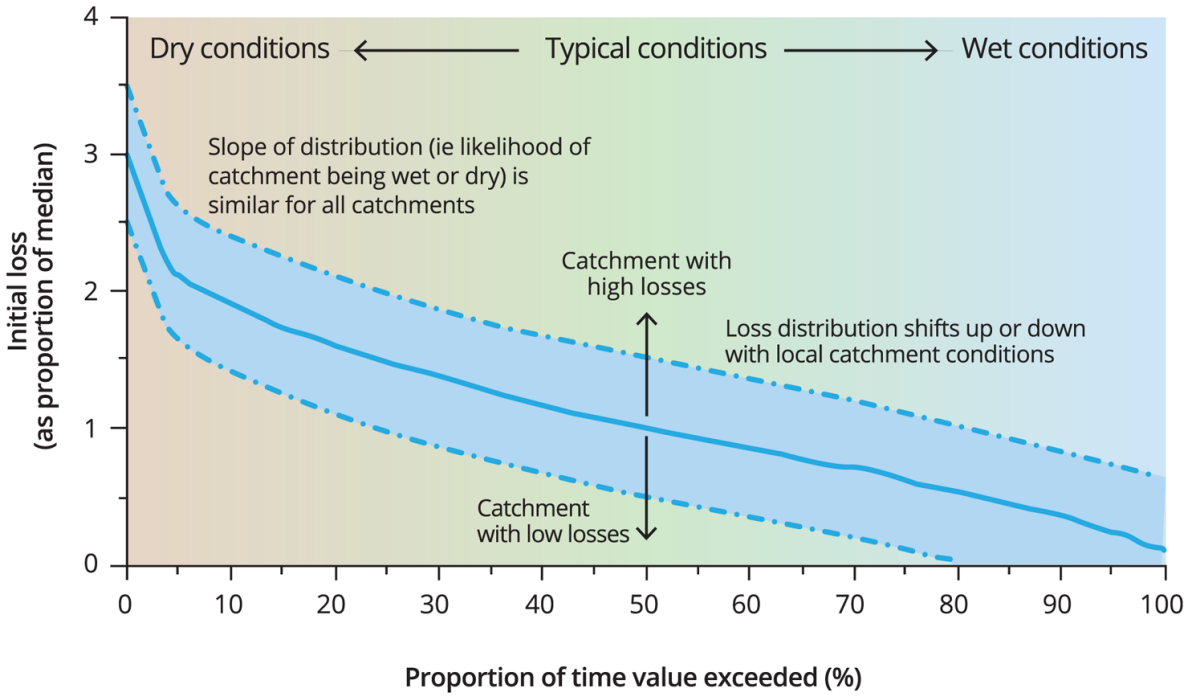

Figure 5.3.25. Variation in Location but Not Shape of Initial Loss Distribution Nathan et al. (2003)

The standardised distributions of storm initial loss and continuing loss from Hill et al. (2014a) are shown in Figure 5.3.26 and the values presented in Table 5.3.13. These standardised loss distributions are remarkably consistent for the different regions across Australia, which demonstrates that while the magnitude of losses may vary between different regions, the shape of the distribution does not.

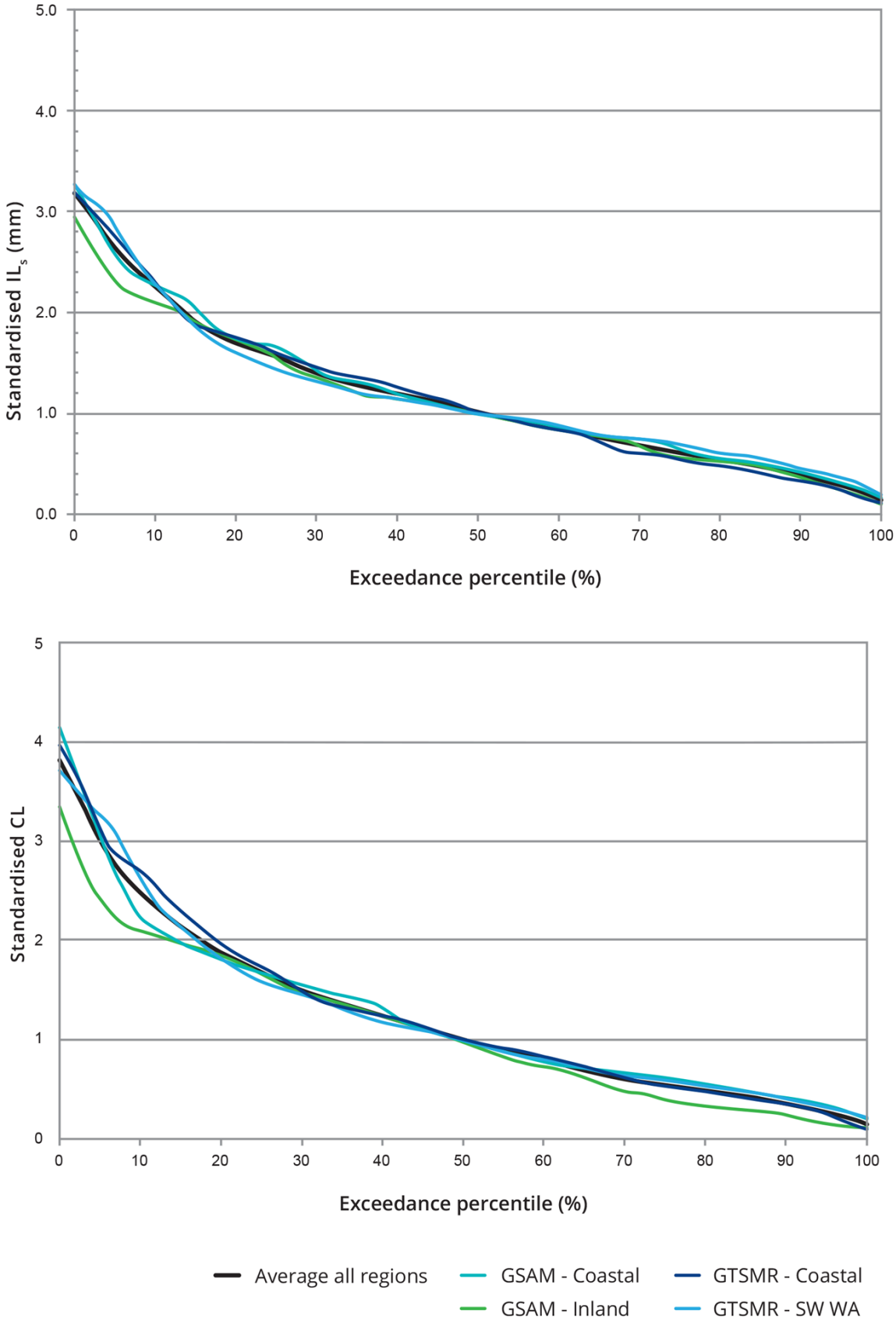

Figure 5.3.26. Regional average standardised loss distributions (Hill et al., 2014a)

Table 5.3.13. Standardised Loss Factors (Hill et al., 2014a)

Percentile	Standardised IL_s	Standardised CL
0	3.19	3.85
10	2.26	2.48
20	1.71	1.88
30	1.40	1.50
40	1.20	1.24
50	1.00	1.00
60	0.85	0.79
70	0.68	0.61
80	0.53	0.48
90	0.39	0.35
100	0.14	0.15

3.6.2. Parametric Approaches

Typical parametric distributions can also be fitted to the sample of loss values derived for a catchment. Parametric distributions provide an efficient means of describing the distribution and help facilitate characterising uncertainty.

A number of studies have investigated different candidate distributions for storm initial loss from samples of catchments from Victoria (Rahman et al., 2002), Queensland (Tularam and Ilahee, 2007) and from around Australia (Hill et al., 2013). Based on these studies the four-parameter Beta distribution is recommended for its flexibility and because its parameters lend themselves readily to physical interpretation. The lower limit can be set to zero, thus reducing the number of parameters to 3.

There has been comparatively less attention paid to the distribution of continuing loss. Based upon a case study of three catchments in Queensland, Ilahee and Rahman (2003) found that the continuing loss values could be approximated by an exponential function. Ishak and Rahman (2006) investigated the probabilistic nature of continuing loss for four Victorian catchments and none of the distributions fitted the observed the distribution satisfactory, however the four-parameter Beta distribution providing the best approximation. Hill et al. (2013) investigated different distributions for 10 catchments from around Australia and concluded that the Gamma (two parameter) distribution was best. Given these different outcomes, further work is required before a preferred distribution for the continuing loss is recommended.

3.6.3. Correlation between Initial and Continuing Loss

The limited number of studies that have explored the correlation between initial and continuing loss values have concluded that there is little systematic dependence between the two. This apparent lack of dependence may reflect reality (for example it might be supposed that variation in continuing loss rates may be more dependent upon rainfall intensity rather than antecedent conditions) or else it may reflect the difficulties of parameter estimation given the limitations of the conceptual model adopted.

It is likely, however, that the observed variation in continuing loss between one event and the next is more due to the propagation of data errors in the analysis rather than differences in

event processes. In applying joint probability approaches to design flood estimation, a number of authors have stochastically modelled the storm initial loss while keeping the continuing loss at a constant value.

The correlation between loss parameter values requires further investigation. In addition to the correlation of loss values for individual events it would be useful to analyse the distribution of total loss.

3.7. Other Considerations for Selecting Loss Values

3.7.1. Variation of Loss with Event AEP

The majority of Australian studies of losses at catchment scale have concluded that both IL_s and CL do not vary systematically with the severity of the event; that is loss is independent of AEP.

This conclusion is not surprising because any potential variation of loss with rainfall severity is difficult to infer from the empirical analysis of data due to the lack of severe rainfall events in the recorded data. This is compounded where the storm severity is characterised as the AEP of the rainfall burst, whereas the loss values relate to the complete storm, and this discrepancy further hinders the identification of any trend with storm severity.

The Australian studies that present loss values that vary with AEP tend to be those where the loss values are derived by verification against flood frequency quantiles. In such studies it is difficult to ascertain whether any variation in loss is meaningful or simply a reflection of the uncertainty in the flood frequency quantiles and the link to the adopted design inputs.

The conclusions that there is no evidence to vary loss with magnitude is supported by the analysis of rainfall antecedent to extreme storms recorded over Southeast Australia which showed that the antecedent rainfall was not significantly greater than normal for the location and time of the year (Minty and Meighen, 1999). The implication of this is that the storm initial losses for large and extreme storms should be similar to those of smaller, more frequent storms".

The recommendation is therefore to keep the IL_s and CL values the same for AEPs unless there is specific evidence to suggest that there is a systematic variation of loss with AEP.

It should be noted that the stores in a storage capacity loss models such as SWMOD fill up during event and hence the proportion of the catchment contributing to the loss increases throughout the event. The net effect of this is an initial loss (which represents the initial filling of the smallest store) following by a variable proportional loss. This proportional loss decreases throughout the event and also decreases for larger rainfall events.

In considering how loss varies with event magnitude it is worth considering that extreme rainfalls may be associated with changed runoff behaviour from that observed for more frequent events with the stripping of vegetation cover.

Book 8 discusses how continuing loss and proportional loss would be expected to vary with event magnitude. The interpretation of proportional loss as the unsaturated proportion of the catchment implies that with larger storm events the unsaturated proportion of the catchment is reducing and the proportional loss reduces. It is however difficult to extrapolate the rate of this reduction to extreme events and hence how proportional loss varies with event magnitude. However, continuing loss is expected to approach a limiting value for saturated

catchment conditions which makes it more suitable for application in extreme flood estimation.

For urban catchments, Phillips et al (2014) undertook an analysis of the correlation between the peak 1 hour intensity after the commencement of indirectly connected area runoff with the continuing loss that was estimated. That study found that for almost all catchments, there was no clear relationship between the two. The one exception to this was the Giralang (ACT) catchment, which showed a strong correlation with the 1 hour peak rainfall intensity after ICA runoff and the continuing loss estimate. The reasoning for this exception was not clear, although it was thought it could be due to the types of storms that fell on the Giralang catchment, which tended to be high intensity in the first hour after the Indirectly Connected Area runoff occurred.

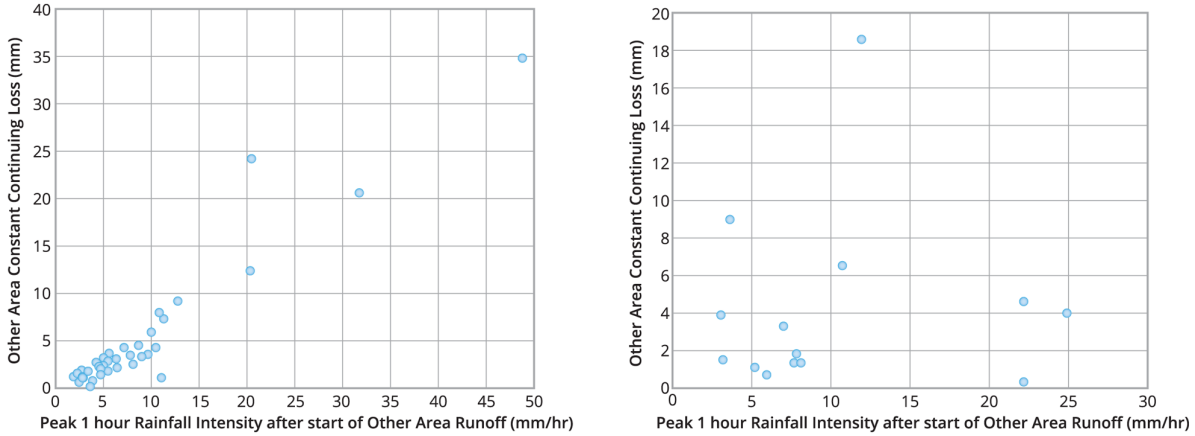

Figure 5.3.27. Correlation between 1 hr Peak Rainfall Intensity and Continuing Loss (left Giralang (ACT) and right Powells Creek (NSW)) (from Phillips et al (2014))

3.7.2. Reduction of Continuing Loss for Long Events

In the application of the IL-CL model it is typically assumed that the loss rates are a constant after the initial loss is satisfied. However for some very large rural catchments where the critical duration is multiple days, it has been noted that the CL reduces throughout the event. This is consistent with the expectation that the loss rates should decrease throughout the event as the catchment becomes wetter and infiltration reduces (as characterised in the Horton model – Book 5, Chapter 3, Section 2) and/or the size of source areas enlarge.

This reduction of continuing loss with duration has also been noted by studies which have analysed a large number of events for rural catchments (e.g. (Ilahee and Imteaz, 2009), and (Ishak and Rahman, 2006)).

Developing a relationship which explains the reduction in CL with duration or infiltrated volume is confounded by the uncertainty in the estimation of CL for specific events. There tends to be very large variation of CL for a particular catchment and a large proportion of this variability is simply likely to be due to uncertainties in the catchment average rainfall depths.

Although potentially important for real-time applications, the potential decrease of CL with duration is not significant for most design applications because the critical duration is typically shorter than a day. For very large rural catchments where the critical duration can be multiple days then it would be reasonable to reduce the CL. Ideally this relationship with duration should be based upon analysis of at site data but can also be informed by

theoretical infiltrations relationships such as Manley-Phillips Loss Model (Manley, 1974). Such an approach in included in the URBS rainfall-runoff model (Carroll, 2012).

For storage capacity loss models such as SWMOD, the moisture content is continuously updated throughout the event which results in a variable proportional loss. This reduction in proportional loss throughout the event may have advantages for modelling of large rural catchments.

3.7.3. Influence of Timestep on the Estimation of Continuing Loss

The definition of Storm Initial Loss as the rainfall depth before surface runoff is generated suggests that its estimation should not be sensitive to the timestep used in the analysis. Similarly, the Proportional Loss and storage capacity loss models such as SWMOD should also not be affected by the timestep.

However, the definition of Continuing Loss as the threshold rate above which rainfall excess is generated, means that it is dependent upon the timestep. This is because as the timestep reduces there is an increased likelihood that there will be some timesteps in which the rainfall depth is less than the Continuing Loss rate threshold. Thus to achieve the same volume of rainfall excess the Continuing Loss will typically need to be increased for shorter timesteps.

This is demonstrated in Figure 5.3.28 for an event at Currambene Creek at Falls Creek in NSW. If the modelling timestep is reduced from 1 hour to 5 minutes the continuing loss rate needs to increase from 4.5 to 7.2 mm/h to maintain the same volume of rainfall excess. This is because for 5 minutes there is a higher proportion of timesteps for which the rainfall depth is less than the threshold value.

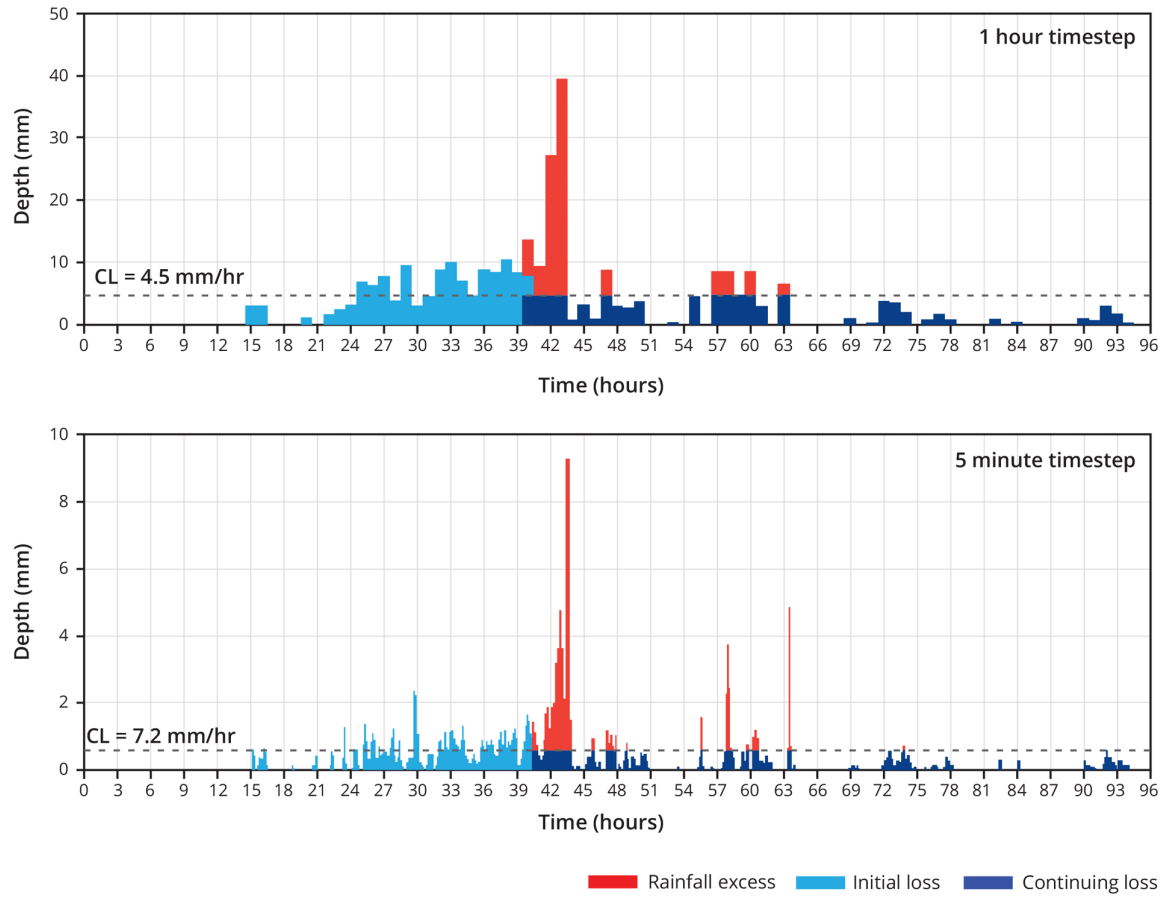

Figure 5.3.28. Example of Continuing Loss Varying with Modelling Timestep (February 1977 event at Currambene Creek at Falls Creek in NSW)

This adjustment of CL is important if the timestep used in the derivation of the loss values is different from that used in design. It should therefore be noted that the timestep used in the derivation of the regional loss information presented in Book 5, Chapter 3, Section 5 was 1 hour for the rural catchments and up to 5 minutes for the urban catchments. If a different timestep is to be adopted in design then the continuing loss should be adjusted accordingly.

3.7.3.1. Rural Catchments

The relationship between CL and the timestep used in the analysis for rural catchments is shown in Figure 5.3.29. The factor relates the CL derived for a timestep less than 1 hour to that for a timestep of 1 hour. The information was based upon the analysis of a number of storms at different timesteps for 18 catchments across Australia. Further details are contained in Lang et al. (2015).

The factor is a function of the rainfall depth with the adjustment factor increasing for smaller rainfall depth. For larger depths, it is more likely that the full CL value can be satisfied in each timestep which reduces the adjustment factor.

This line of best fit can be used to relate continuing losses modelled at sub-hourly time steps to hourly values and vice versa. For example, if the average storm depth is approximately 200 mm and the timestep is reduced from 1 hour to 15 minutes then the continuing loss needs to be increased by 30%.

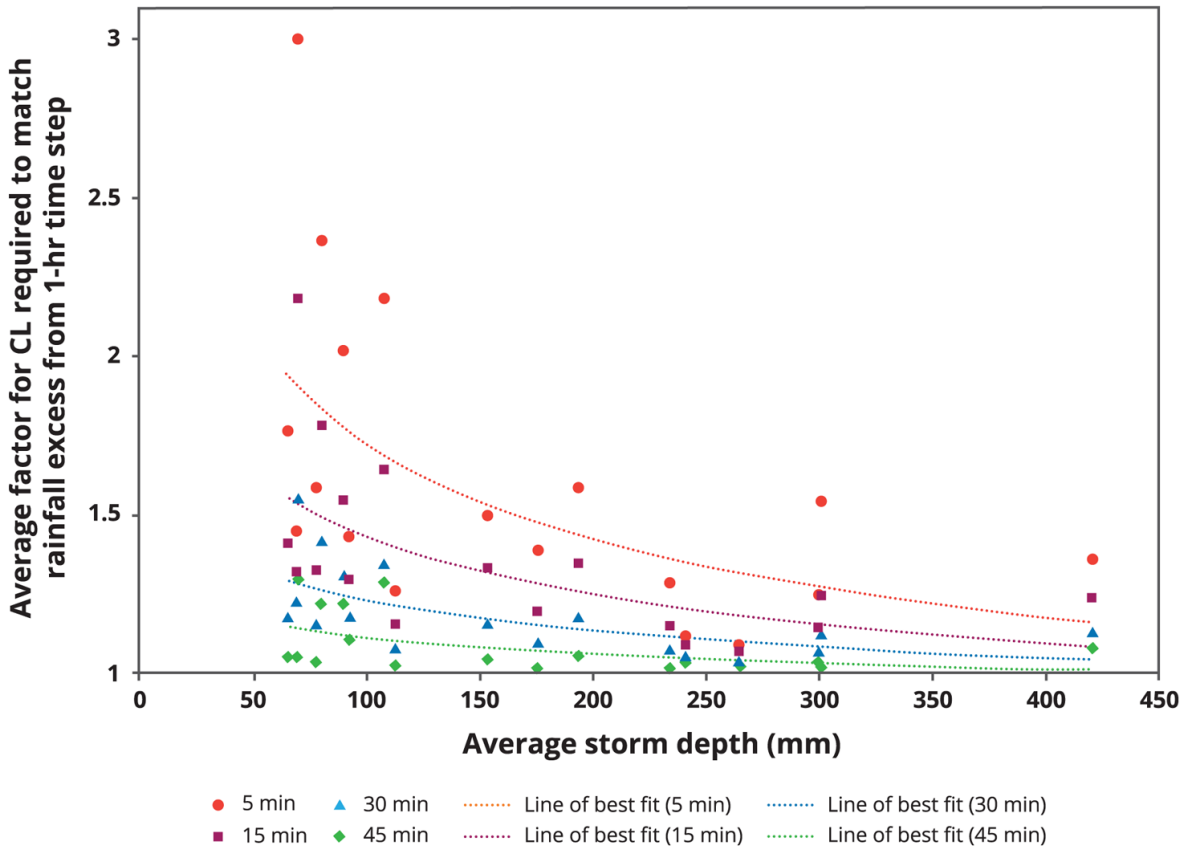

Figure 5.3.29. Variation of Continuing Loss with Modelling Timestep for Rural Catchments

3.7.3.2. Urban Catchments

Urban catchments differ from rural catchments in that generally shorter timestep rainfall data is used. This is in order to represent the fast response that typically occurs in urban catchments. The shorter timestep is required to represent the peak flow appropriately (although the runoff volume may be appropriate).

The urban catchment data derived in Phillips et al (2014) was based on shorter timestep pluviometer data than the rural catchments.

This data was re-analysed comparing with 6 minute time intervals, which is similar to a large majority of the pluviometer data that is available in Australia, and typical of the duration that would be analysed in urban catchments. This re-analysis suggests that there are minimal changes to the CL loss estimates, and well within the error margins of the estimates.

There are insufficient storms for the loss estimates to develop a similar graph to that for the rural catchment (i.e. Figure 5.3.29). Instead, the different catchments were plotted against timestep, and are shown in Figure 5.3.30. This graph shows the percentage change relative to the median CL estimate for 6 minute timestep. A recommended curve is also provided, based on the average of the values provided. The equation of this can be broadly approximated by:

$$\frac{\mathrm{CL}_x}{\mathrm{CL}_{6\mathrm{min}}} = 0.2 \ln t + 1.35 \qquad (5.3.15)$$

Where t=time in minutes

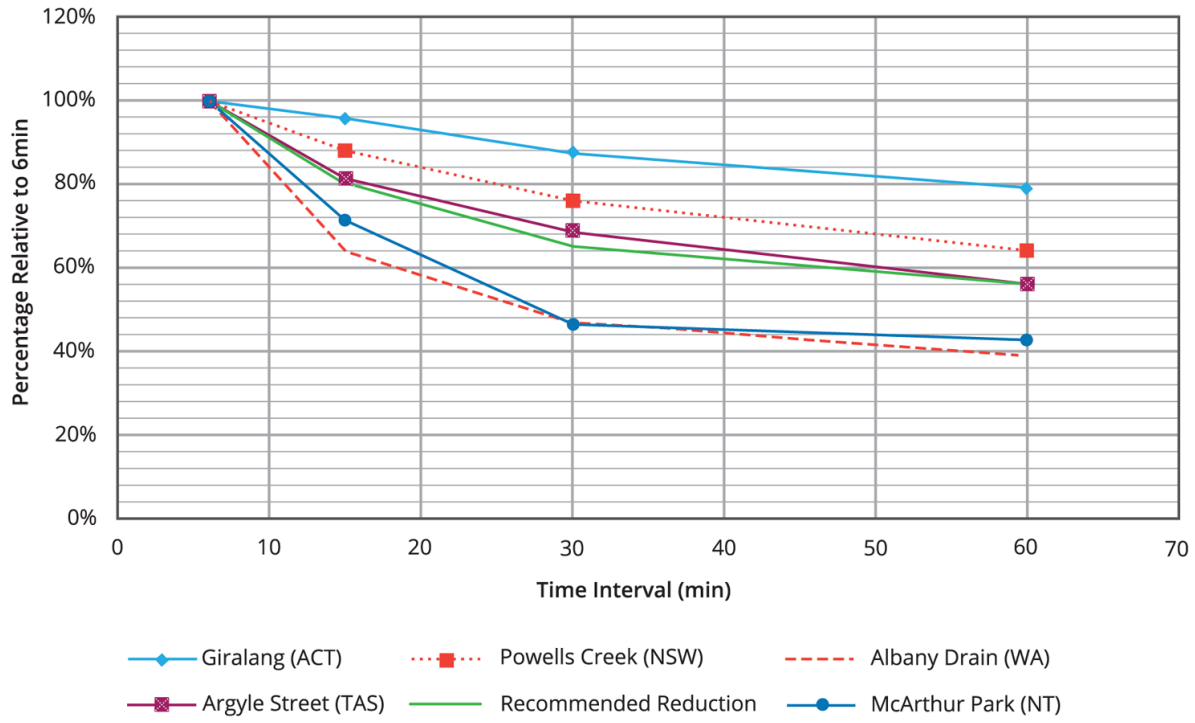

Figure 5.3.30. Relationships of Urban Continuing Loss with Timestep

3.7.4. Antecedent Rainfall and Soil Moisture

3.7.4.1. Antecedent Precipitation

It would be expected that the initial loss, and potentially the CL, is negatively correlated with the antecedent rainfall, as it is a surrogate for the soil moisture.

To avoid the arbitrary selection of the period over which to define the antecedent rainfall, the Antecedent Precipitation Index (API) can be used as a measure of the initial wetness of a catchment. API is calculated by discounting the time series of daily rainfall prior to the event using an empirical decay factor and the basic equation is (Cordery, 1970):

$$\mathrm{API}_d = P_d + \mathrm{k}\, P_{d-1} + k^2 P_{d-2} + \ldots \tag{5.3.16}$$

Where *k* is an empirical decay factor less than unity and *Pd* is rainfall for day *d*. The value of *k* varies typically in the range of 0.85 to 0.98. Linsley et al. (1982) and Cordery (1970) found that the average value for Australian catchments was 0.92. The value of *k* is considered to vary seasonally and has been linked to the variation in potential evapotranspiration (Mein et al., 1995).

Cordery (1970) then related the IL_s to the API using a relationship of the form:

$$\mathrm{IL}_s = \mathrm{IL}_{\max}(N)^{\mathrm{API}} \tag{5.3.17}$$

3.7.4.2. Soil Moisture

There are a number of products that have recently become available that estimate soil moisture over the whole of Australia either from remote sensing, conceptual water balance modelling or a combination of both. One estimate of soil moisture that shows promise for

explaining the variability of loss is AWRA-L (refer Book 5, Chapter 3, Section 5 and Frost et al. (2015)).

There are only a limited number of studies that have investigated the relationship between loss values and these estimates of soil moisture but it is expected that soil moisture will be provide a more useful estimate of loss than indices based only upon rainfall.

3.7.4.3. Rural Catchments

Preliminary results showed that soil moisture conditions in the combined layer over the upper 1m explains the most variation in loss values in most catchments. Accordingly, soil moisture conditions over this depth were adopted for all subsequent analyses.

The results for IL are shown in Figure 5.3.31 and demonstrate that soil moisture has a higher correlation with IL than API for the majority of the catchments. There are still, however, some catchments for which the initial loss is relatively independent of both the API and AWRA-L soil moisture.

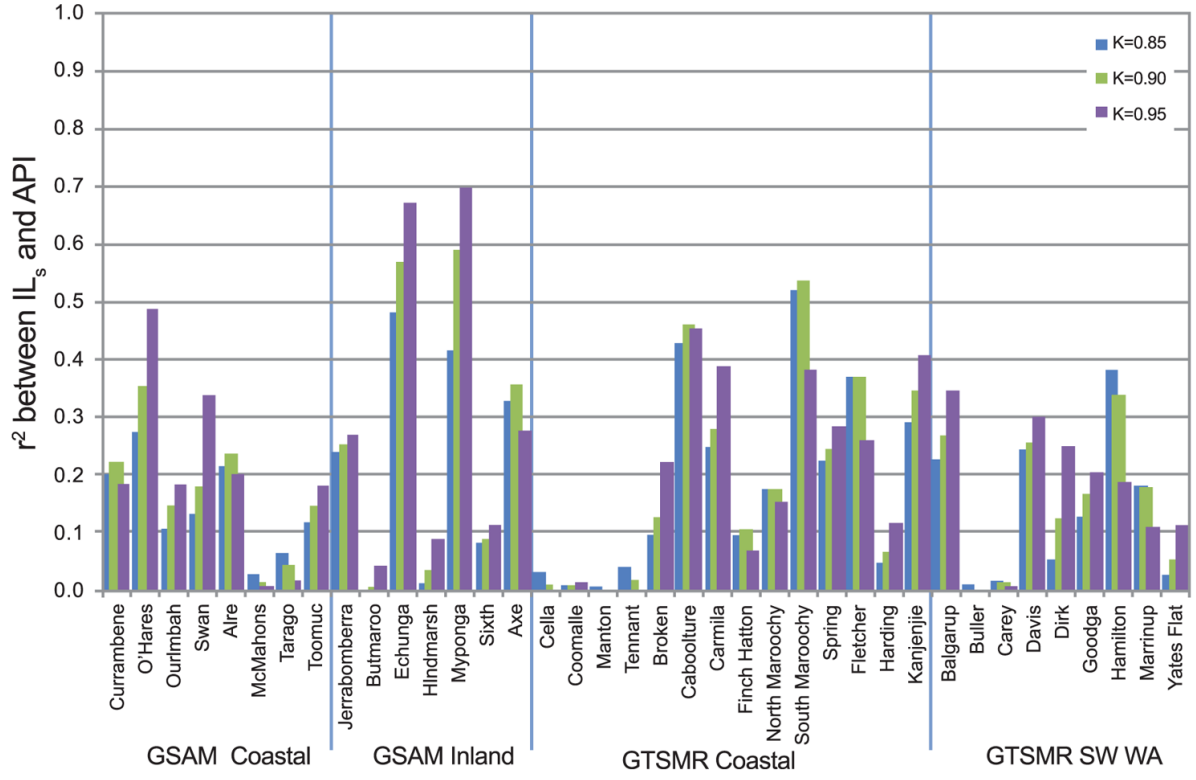

Figure 5.3.31. Proportion of Variance Explained (r^2) between Storm Initial Loss and API (Hill et al., 2014a)

Studies by the Bureau of Meteorology (T. Pagano pers comm.) and Seqwater (D. Pokarier per. comm.) have also found that the storm initial loss is also more highly correlated with soil moisture estimated by AWRA-L than API.

Where such relationships can be established, they can help inform the absolute and seasonal distribution of IL_s.

3.7.4.4. Urban Catchments

In residential areas garden watering may influence antecedent wetness particularly if several dry days occur (Woolmington and Burgess, 1983; Boyd et al., 1994) and therefore measures

of the preceding days rainfall (such as API) may not reflect the true antecedent conditions of the catchment.

Phillips et al (2014) undertook an analysis of the antecedent rainfall in the days leading up to the storms used to estimate the initial loss. They compared the rainfall in 1, 3 and 7 days prior to the event with the initial loss and continuing loss estimates, and found no clear correlation between the two. Samples of this analysis are provided in Figure 5.3.32.

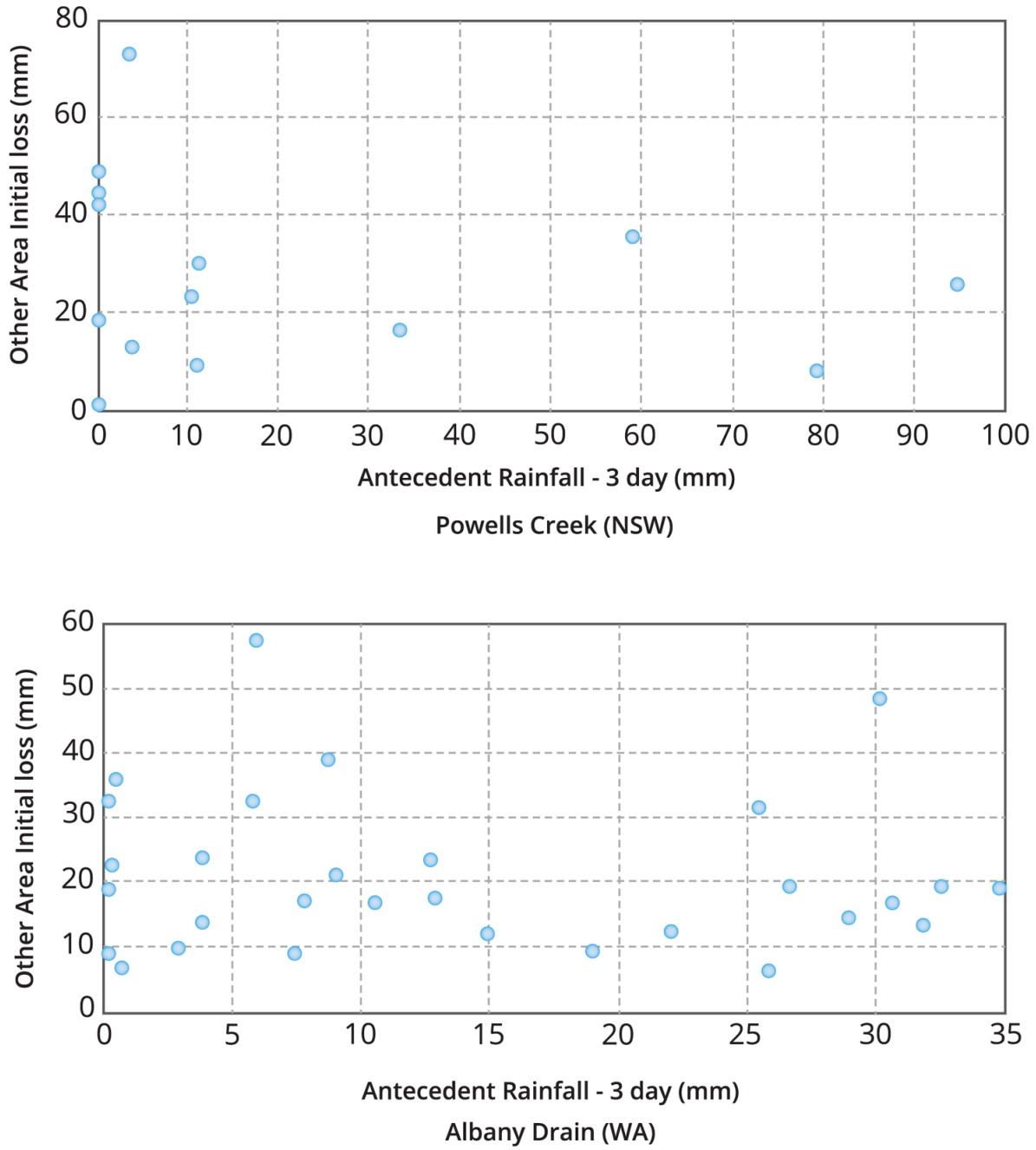

Figure 5.3.32. Plot of Antecedent Rainfall Versus Initial Loss for Indirectly Connected Area (Phillips et al, 2014)

3.7.5. Seasonality

The discussion of losses in the preceding sections has concentrated on the median annual values. However, due to the seasonal variation in rainfall, evapotranspiration (and to a lesser extent vegetation) many regions in Australia are characterised by distinct seasonality in hydrology. The estimation of seasonal design inputs, including loss values, is required in cases where:

- there is a strong seasonal variation in the flood producing mechanisms which need to be accounted for in order to estimate the annual risk; or
- the risk is required to be assessed for a particular period within the year such as the flood risk during construction or upgrade of major infrastructure.

The loss parameters (both initial and continuing loss) can be influenced by antecedent moisture and therefore may display significant seasonal variation. This is likely to primarily reflect changes in antecedent moisture but vegetation change may also contribute in some locations.

The different seasonality across Australia is demonstrated in Figure 5.3.33. This shows the seasonal distribution of the 803 events analysed by Hill et al. (2014a) which were selected on the basis of rainfall. It is clear that in south-eastern Australia the events are reasonably distributed throughout the year, whereas the majority of events in Northern Australia occur in summer and south-west WA is dominated by the winter months.

It is important to consider this seasonal variation when selecting losses for design flood estimation. In some cases the loss values may need to be adjusted to account for a bias in the sample and for some locations it may be necessary to explicitly incorporate the seasonality in the adopted losses and design flood estimation framework.

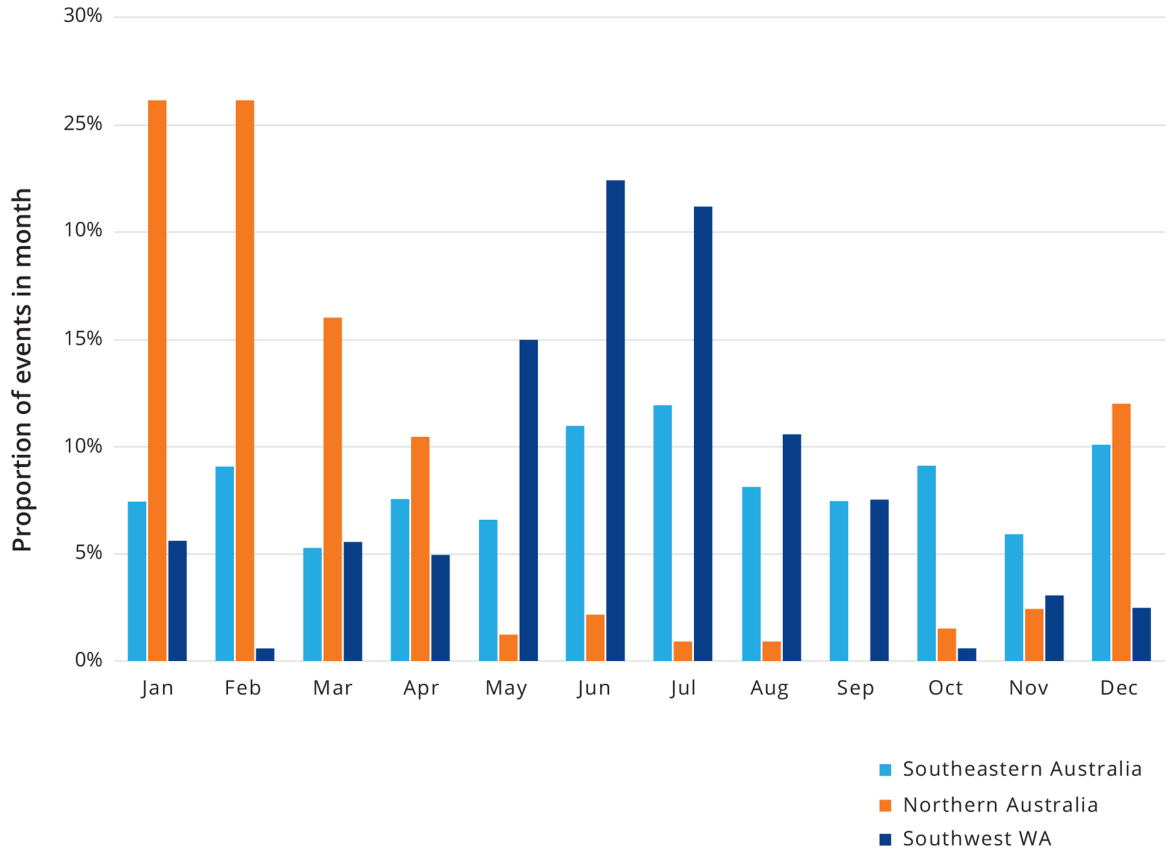

Figure 5.3.33. Seasonal Distribution of Events Analysed by Hill et al. (2014a)

The seasonality of the loss values is demonstrated in Figure 5.3.34. In south-eastern Australia the median losses are lowest in July and steadily increase until summer. For northern Australia the highest losses are at the beginning of the wet season and the losses are slightly lower for late summer and autumn. For south-west WA the highest median losses occur in Summer.

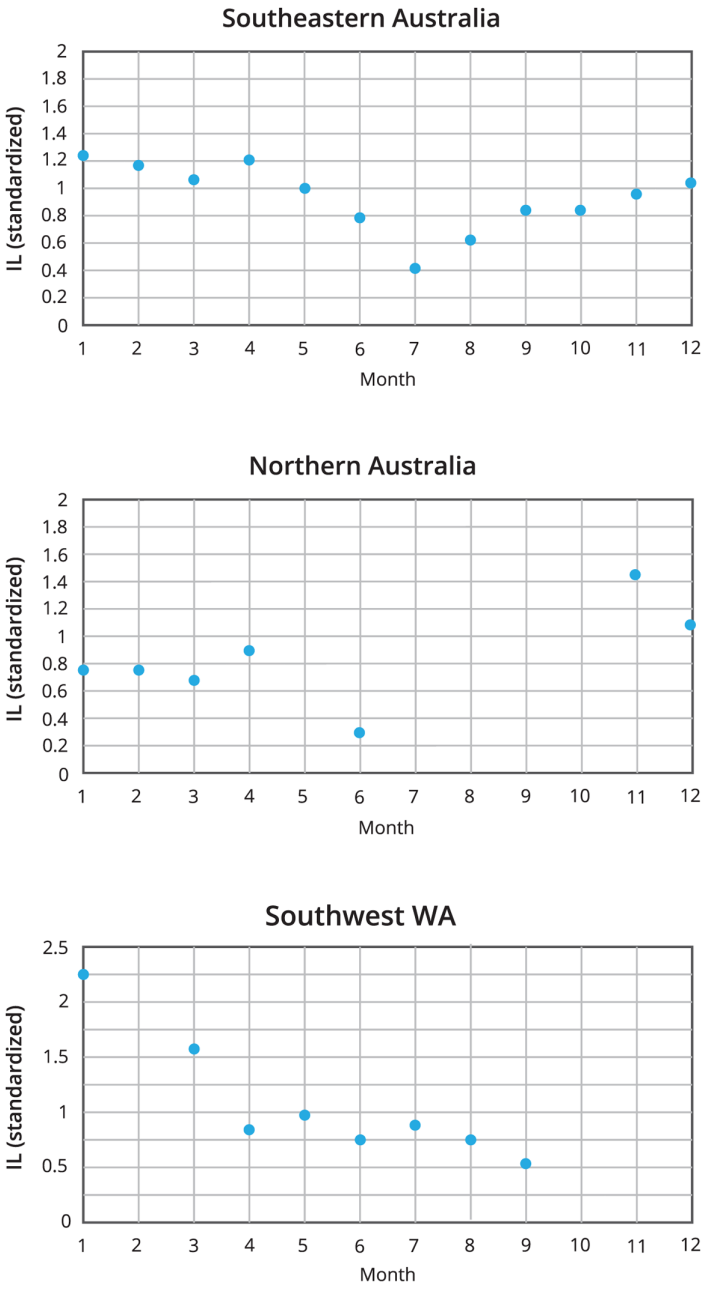

Figure 5.3.34. Seasonality of Standardised Storm Initial Loss Values for Different Regions in Australia

In south-west WA, two different rainfall mechanisms have been identified which result in distinctly seasonal nature of rainfall and losses. The majority of events have been recorded in the winter seasons which are typically associated with lower losses, however the rarer events are more likely to occur in summer when there is typically higher losses. It is therefore important to recognise this in the selection of losses.

This is highlighted by Pearce (2011) which developed seasonal runoff coefficients for south-west WA by generalising the results of the application of SWMOD to a number of catchments (refer to Figure 5.3.35). The results show the important influence of the season and the proportion of the catchment cleared of vegetation (refer to Book 5, Chapter 3, Section 7).

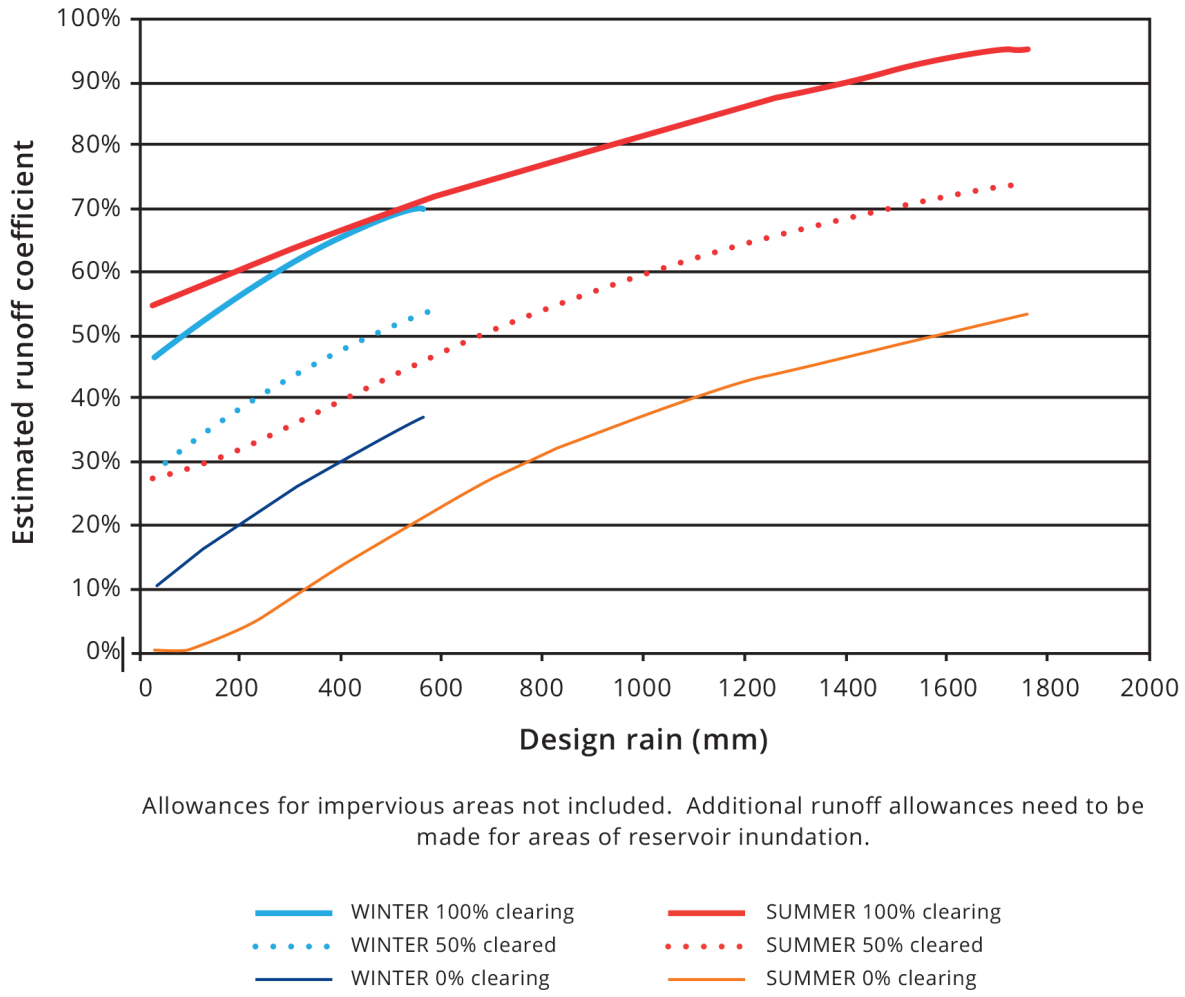

Figure 5.3.35. Regional Runoff Coefficient Curves for South-West Western Australia (Pearce, 2011)

Another approach to deriving seasonal loss values is to verify the rainfall-based estimates from a rainfall runoff model to seasonal flood frequency quantiles. That is, adopt a similar approach as outlined in Book 5, Chapter 3, Section 3 but on a seasonal, rather than annual, basis.

3.7.6. Influence of Vegetation

The presence of vegetation is expected to increase interception and hence loss. However, a number of studies have failed to find a link between the proportion of the catchment vegetated and the loss values (e.g. Cordery and Pilgrim (1983)). This is likely to be due to the uncertainties in estimating both loss values and representatives measures of interception from vegetation at the catchment scale.

One exception to this is south-west WA where the losses have been directly linked to the proportion of the catchment cleared of native vegetation (Pearce, 2011).

3.7.7. Interaction with Routing Parameters

Although it may not be readily apparent, there is an interdependency between the adopted conceptual loss model and the inferences regarding the routing characteristics of the catchment. This is because the different conceptual loss model result in different temporal distributions of loss and hence rainfall excess.

The rainfall excess obtained from loss models where the excess is a proportion of the total rainfall in the timestep (such as IL/PL or SWMOD) will tend to result in a more temporally uniform (less peaky) rainfall excess when compared to IL/CL loss model in which a constant rate of loss is applied. This is because a greater volume of loss is extracted in the timesteps of greatest rainfall.

This means that more attenuation is required for the rainfall excess resulting from the IL/CL loss models than those for the IL/PL or SWMOD.

For example, Australian Rainfall and Runoff Revision Project 6 (Hill et al., 2014a) considered the routing parameters for IL/CL and SWMOD for 38 catchments from across Australia and demonstrated that the adopted loss model affected the selection of the C0.8 value (non-dimensional routing parameter in RORB). With the C0.8 value for SWMOD being typically 75% of that for the IL/CL model (refer Figure 5.3.36).

Therefore, the routing parameters derived using one conceptual loss model are not necessarily applicable for an alternate loss model. This is important if different loss models are to be applied to flood models than those used in calibration.

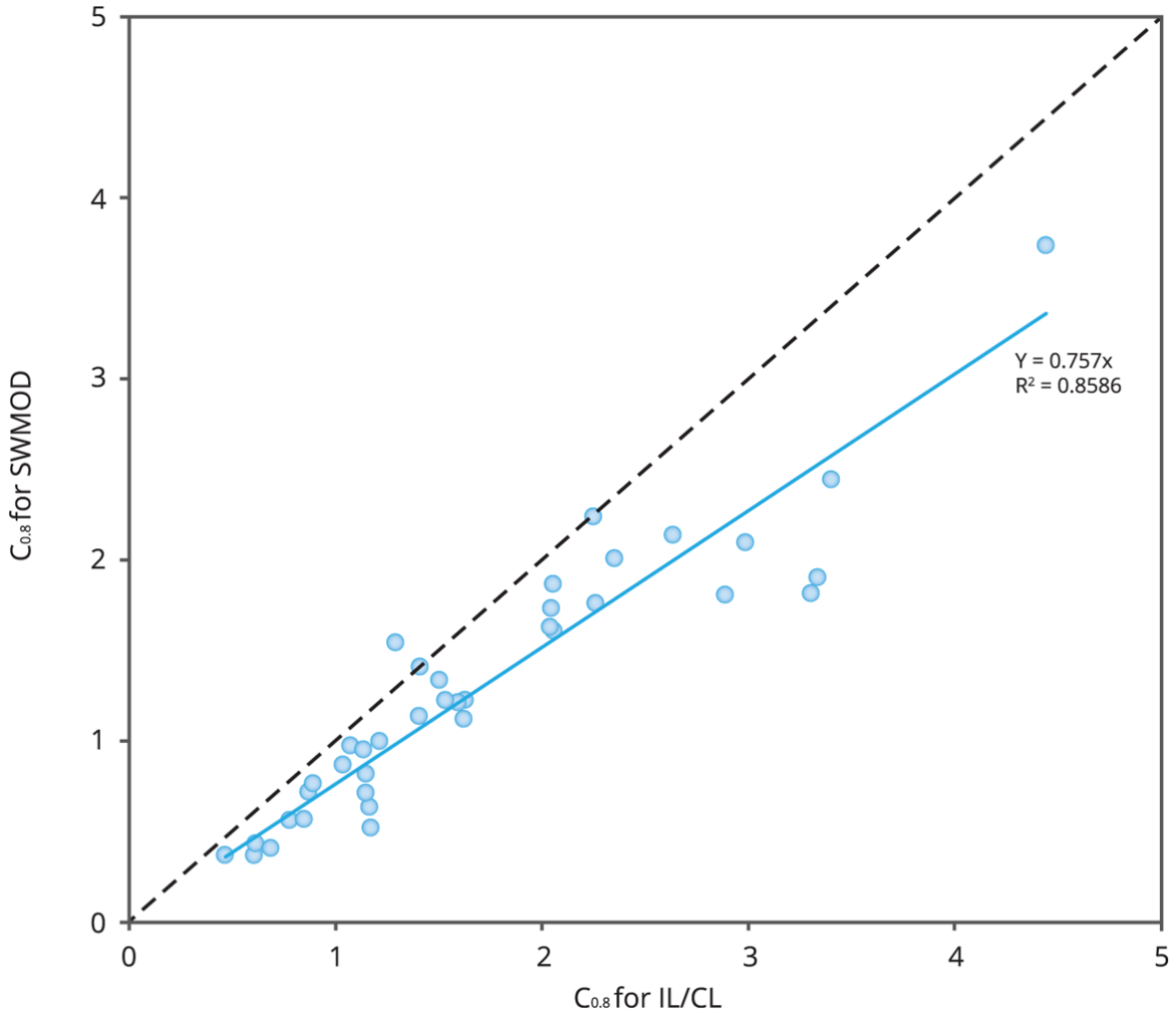

Figure 5.3.36. Comparison of Adopted Routing Parameters for IL/CL and SWMOD

3.7.8. Influence of Snowpack

There is only a relatively small proportion of Australia that experiences substantial snow cover, and even for these catchments this only occurs for a portion of the year. These catchments in parts of south-eastern Australia are typically above an elevation of approximately 1,500 mAHD. The presence of a snowpack influences the losses, runoff generation and routing characteristics of a catchment. With respect to losses, there is typically low losses for rain on the snowpack and therefore it can be assumed that there are low losses for the proportion of the catchment covered by snowpack. For example USACE (1998) adopts a continuing loss of 1 mm/h for rain on snowpack.

3.7.9. Link to Climate Drivers and Change

There has been little research on the potential role that large scale climate drivers such as El Niño/Southern Oscillation (ENSO), Interdecadal Pacific Oscillation (IPO), Indian Ocean Dipole (IOD) and Southern Annular Mode (SAM) have on influencing antecedent rainfalls and hence loss rates.

A number of studies have shown significant dependence of annual maxima floods in Eastern Australia on the Interdecadal Pacific Oscillation (IPO). However, the annual maxima

precipitation does not exhibit a similar level of dependency on the IPO. Pui et al (2009) hypothesize that the difference in flood characteristics as a function of the IPO is a result of catchment antecedent conditions prior to the rainfall event. From the analysis of 88 daily rainfall stations in Eastern Australia they found that the antecedent conditions prior to storm events varied significantly across the two IPO phases.

The influence of these key climate drives on loss rates warrants further research.

3.8. Appendix

Table 5.3.14. Median Loss Values for Rural Catchments

Region	Method	Gauge	River	Name	Area	N	Median IL_s (mm)	Median CL (mm/hr)	Study
East Coast	QLD	141001	South Maroochy	Kiamba	33	22	38	2.7	Hill et al. (2014a)
East Coast	QLD	141009	North Maroochy	Eumundi	41	23	20	2.2	Hill et al. (2014a)
East Coast	NSW	201001	Oxley River	Eungella	218	53	50	2.6	Loveridge (Unpublished)
East Coast	NSW	203010	Leycester River	Rock Valley	179	48	65	0.3	Loveridge (Unpublished)
East Coast	NSW	204017	Bielsdown Creek	Dorrigo No. 2 & No.3	82	57	50	1.4	Loveridge (Unpublished)
East Coast	NSW	204025	Orara River	Karangi	135	37	71	4	Loveridge (Unpublished)
East Coast	NSW	208007	Nowendoc River	Nowendoc	218	37	50	2.3	Loveridge (Unpublished)
East Coast	NSW	210068	Pokolbin Creek	Pokolbin Site 3	25	36	40	2.0	Loveridge (Unpublished)
East Coast	NSW	211013	Ourimbah Creek	Upstream Weir	83	25	40	3.7	Hill et al. (2014a)
East Coast	NSW	213200	O'Hares Creek	Wedderburn	73	22	60	1.6	Hill et al. (2014a)
East Coast	QLD	136108A	Monal Creek	Upper Monal	92	12	13		Ilahee (2005)
East Coast	QLD	141009A	N. Maroochy River	Eumundi	38	22	42		Ilahee (2005)
East Coast	QLD	142001A	Caboolture	Upper Caboolture	94	20	50	1.4	Hill et al. (2014a)
East Coast	QLD	143110A	Bremer River	Adams Bridge	125	37	39		Ilahee (2005)
East Coast	QLD	145003B	Logan River	Forest Home	175	42	31		Ilahee (2005)

Region	Method	Gauge	River	Name	Area	N	Median IL_s (mm)	Median CL (mm/hr)	Study
East Coast	QLD	145010A	Running Creek	5.8 km Deickmans Bridge	128	20	32		Ilahee (2005)
East Coast	QLD	145011A	Teviot Brook	Croftby	83	37	30		Ilahee (2005)
East Coast	QLD	145101D	Albert River	Lumeah Number 2	169	35	44		Ilahee (2005)
Monsoonal North	WA	809312	Fletcher	Frog Hollow	30.6	19	30	10.4	Hill et al. (2014a)
Monsoonal North	QLD	118003A	Bohle River	Hervey Range Road	143	24	29		Ilahee (2005)
Monsoonal North	QLD	120014A	Broughton River	Oak Meadows	182	19	18		Ilahee (2005)
Monsoonal North	QLD	120216A	Broken	Old Racecourse	78	34	68	6.2	Hill et al. (2014a)
Monsoonal North	QLD	916003A	Moonlight Creek	Alehvale	127	7	29		Ilahee (2005)
Monsoonal North	QLD	917114A	Routh Creek	Beef Road	81	7	30		Ilahee (2005)
Monsoonal North	NT	G8150151	Celia	U/S Darwin R Dam	52	15	25	5.4	Hill et al. (2014a)
Monsoonal North	NT	G8170066	Coomalie	Stuart HWY	82	30	50	8.1	Hill et al. (2014a)
Monsoonal North	NT	G8170075	Manton	upstream Manton Dam	29	32	42	1.6	Hill et al. (2014a)
Murray Darling	VIC	403226	Boggy Creek	Angleside	108	33	15	3.7	Hill et al. (1996)
Murray Darling	VIC	404208	Moonee Creek	Lima	91	28	19	6.5	Hill et al. (1996)
Murray Darling	VIC	405229	Wanalta Creek	Wanalta	108	24	31	1.4	Hill et al. (1996)
Murray Darling	VIC	405257	Snobs Creek	Snobs Creek Hatchery	51	12	8	11	Hill et al. (1996)
Murray Darling	VIC	405261	Spring Creek	Fawcett	60	17	27	4.2	Hill et al. (1996)
Murray Darling	VIC	406208	Campaspe River	Ashborne	33	7	48	6.2	Hill et al. (1996)
Murray Darling	VIC	406216	Axe Creek	Sedgewick	34	12	28	6	Hill et al. (2014a)

Region	Method	Gauge	River	Name	Area	N	Median IL_s (mm)	Median CL (mm/hr)	Study
Murray Darling	VIC	407258	Myers Creek	Myers Flat	55	9	36	2.7	Hill et al. (1996)
Murray Darling	ACT	410736	Orroral River	Crossing	90	36	18	7.1	Hill et al. (1996)
Murray Darling	ACT	410739	Tidbinbilla Creek	Mountain Creek	25	31	10	8.8	Hill et al. (1996)
Murray Darling	ACT	410743	Jerrabomberra Creek	Four Mile Creek	52	20	22	2.1	Hill et al. (2014a)
Murray Darling	ACT	410751	Ginninderra Creek	u/s Barton Highway	48	20	38	6.5	Hill et al. (1996)
Murray Darling	NSW	411003	Butmaroo Creek	Butmaroo	65	21	40	2.6	Hill et al. (2014a)
Murray Darling	QLD	422321	Spring	Killarney	32	27	30	5.1	Hill et al. (2014a)
Pilbara	WA	709007	Harding	Marmurrina Pool U-South	49.4	17	60	8.3	Hill et al. (2014a)
Rangelands	NT	G0290240	Tennant	Old Telegraph Stn	72.3	24	0	5.2	Hill et al. (2014a)
South-west WA	WA	602199	Goodga River	Black Cat	49.2	27	30	4.8	Hill et al. (2014a)
South-west WA	WA	603190	Yates Flat Creek	Woonanup	53	17	27	0.8	Hill et al. (2014a)
South-west WA	WA	608002	Carey Brook	Staircase Rd	30.3	19	20	3.8	Hill et al. (2014a)
South-west WA	WA	609005	Balgarup River	Mandelup Pool	82.4	13	25	2.5	Hill et al. (2014a)
South-west WA	WA	612004	Hamilton River	Worsley	32.3	13	47	3.3	Hill et al. (2014a)
South-west WA	WA	613003	Harvey	Paganini Farm	148		16		Waugh (1991)
South-west WA	WA	613013	Bancell Creek	Wagerup	13		11		Waugh (1991)
South-west WA	WA	614003	Marrinup Brook	Brookdale Siding	45.6	19	16	7.3	Hill et al. (2014a)
South-west WA	WA	614003	Marrinup Brook	Brookdale Siding	46		12		Waugh (1991)
South-west WA	WA	614005	Dirk Brook	Kentish Farm	36	20	14	6.7	Hill et al. (2014a)

Region	Method	Gauge	River	Name	Area	N	Median IL_s (mm)	Median CL (mm/hr)	Study
South-west WA	WA	614005	Dirk Brook	Kentish Farm	36		15		Waugh (1991)
South-west WA	WA	614016	North Dandalup River	Nth Dandalup Dam	153		20		Waugh (1991)
South-west WA	WA	614047	Davis Brook	Murray Valley Plntn	65.7	18	25	8.1	Hill et al. (2014a)
South-west WA	WA	701006	Buller River	Buller	33.9	14	32	3.8	Hill et al. (2014a)
South-Central SA	SA	A5040523	Sixth Creek	Castambul	44	24	15	3.3	Hill et al. (2014a)
South-Central SA	SA	AW501500	Hindmarsh River	Hindmarsh Vy Res Offtake	56	33	15	3.2	Hill et al. (2014a)
South-Central SA	SA	AW502502	Myponga River	upstream Dam and Rd Br	77	15	23	2.6	Hill et al. (2014a)
South-Central SA	SA	AW503506	Echunga Creek	upstream Mt Bold Res.	34	13	25	2.2	Hill et al. (2014a)
South-east Coast	TAS	2219	Swan River	upstream Hardings Falls	38	19	40	0.5	Hill et al. (2014a)
South-east Coast	NSW	214003	Macquarie Rivulet	Albion Park	35	26	69	2.9	Loveridge (Unpublished)
South-east Coast	NSW	214003	Macquarie Rivulet	Albion Park	35	26	69		Loveridge (Unpublished)
South-east Coast	NSW	216004	Currambene Creek	Falls Creek	95	17	35	3.9	Hill et al. (2014a)
South-east Coast	NSW	216004	Currambene Creek	Falls Creek	95	37	37		Loveridge (Unpublished)
South-east Coast	VIC	224209	Cobbannah Creek	Bairnsdale	106	13	52	1.7	Hill et al. (1996)
South-east Coast	VIC	226222	La Trobe River	Near Noojee	62	7	19	3.4	Hill et al. (1996)
South-east Coast	VIC	227226	Tarwin River East Branch	Dumbalk Nth	127	5	41	1.7	Hill et al. (1996)
South-east Coast	VIC	227228	Tarwin River East Branch	Mirboo	43	5	21	3.6	Hill et al. (1996)
South-east Coast	VIC	228217	Toomuc Creek	Pakenham	42	25	24	2.5	Hill et al. (2014a)

Region	Method	Gauge	River	Name	Area	N	Median IL_s (mm)	Median CL (mm/hr)	Study
South-east Coast	VIC	229106	McMahons Creek	Upstream Weir	40	21	20	3.7	Hill et al. (2014a)
South-east Coast	VIC	231213	Lerderderg River	Sardine Creek	153	9	25	1.1	Hill et al. (1996)
South-east Coast	VIC	231219	Goodman Creek	above Lerderderg Tunnel	32	19	35	2.4	Hill et al. (1996)
South-east Coast	VIC	233223	Warrambine Creek	Warrabine	57	17	26	1.5	Hill et al. (1996)
South-east Coast	VIC	235212	Chapple Creek	Chapple Value	28	23	28	2.6	Hill et al. (1996)
South-east Coast	VIC	235219	Aire River	Wyelangta	90	17	19	3	Hill et al. (1996)
South-east Coast	VIC	235219	Aire River	Wyelangta	90	30	17	3	Hill et al. (2014a)
South-east Coast	VIC	235229	Ford River	Glenaire	56	23	21	2.6	Hill et al. (1996)
South-east Coast	VIC	238231	Glenelg River	Big Cord	57	17	24	5.1	Hill et al. (1996)
South-east Coast	VIC	228206B	Tarago River	Neerim	78	22	24	3.9	Hill et al. (2014a)
Wet Tropics	QLD	125006	Finch Hatton	Dam Site	36	30	23	5.2	Hill et al. (2014a)
Wet Tropics	QLD	112003A	N. Johnston River	Glen Allyn	173	15	34		Ilahee (2005)
Wet Tropics	QLD	114001A	Murray River	Upper Murray	155	23	66		Ilahee (2005)
Wet Tropics	QLD	116008B	Gowrie Creek	Abergowrie	124	61	22		Ilahee (2005)
Wet Tropics	QLD	116015A	Blunder Creek	Wooroora	127	48	71		Ilahee (2005)
Wet Tropics	QLD	116017A	Stone River	Running Creek	157	55	33		Ilahee (2005)
Wet Tropics	QLD	124002A	St. Helens Creek	Calen	129	11	54		Ilahee (2005)
Wet Tropics	QLD	126003A	Carmila	Carmila	82	19	70	3.1	Hill et al. (2014a)
Wet Tropics	QLD	922101B	Coen River	Racecourse	166	59	25		Ilahee (2005)
Wet Tropics	QLD	926003A	Bertie Creek	Swordgrass Swamp	130	8	1		Ilahee (2005)

Table 5.3.15. Summary of EIA Results from (Boyd et al., 1993)

Catchment	Country	Area	Impervious Fraction	EIA/TA	EIA/TIA	Urban Area (%)
Maroubra	NSW, Australia	57.3	52%	16%	30%	100%
Strathfield	NSW, Australia	234	50%	29%	58%	100%
Jamison Park	NSW, Australia	22.1	36%	21%	58%	100%
Fishers Ghost	NSW, Australia	226	36%	25%	70%	100%
Giralang	ACT, Australia	94	25%	35%	140%	85%
Long Gully	ACT, Australia	490	5%	6%	118%	16%
Mawson	ACT, Australia	445	26%	21%	80%	86%
Curtin	ACT, Australia	2690	17%	17%	102%	57%
Vine Street	Vic, Australia	70	37%	31%	83%	100%
Pompano Beach	USA	15.4	44%	7%	16%	100%
Sample Road	USA	23.5	36%	27%	74%	100%
Fort Lauderdale	USA	7.7	98%	96%	98%	100%
Kings Creek	USA	5.26	71%	75%	106%	100%
Gray Haven	USA	9.4	52%	48%	93%	100%
Malvern	Canada	23.3	34%	34%	99%	100%
East York	Canada	155	49%	48%	98%	100%
Clifton Grove	UK	10.6	40%	24%	60%	100%
St Marks Road	UK	10.3	56%	30%	53%	100%
Porsoberg	Sweden	13	40%	21%	52%	100%
Munkerispa rken	Denmark	6.44	46%	35%	76%	100%
Livry Gargan	France	235.5	33%	17%	53%	78%
Miskole	Hungary	25.4	15%	13%	89%	52%
Luzzi	Italy	1.73	85%	58%	68%	100%

Catchment	Country	Area	Impervious Fraction	EIA/TA	EIA/TIA	Urban Area (%)
Vika	Norway	10.1	97%	65%	67%	100%
Miljakovic	Yukoslavia	25.5	37%	20%	54%	100%
Kotta	Japan	1281	23%	32%	137%	84%

Table 5.3.16. EIA Initial Loss Estimates from Various Studies

Catchment	Initial Loss Estimate (mm)	Reference
Dee Why Creek (NSW)	1	Chiew and McMahon (1999)
Fishers Ghost Ck (NSW)	0.9	Bufill and Boyd (1992)
	0	Boyd et al. (1993)
Ithaca Creek (QLD)	2.8	Phillips et al (2014)
Jamison Park (NSW)	0.8	Bufill and Boyd (1992)
	0	Boyd et al. (1993)
Maroubra (NSW)	0.3	Bufill and Boyd (1992)
	0	Boyd et al. (1993)
Powells Creek (NSW)	2.6 to 2.9	Phillips et al (2014)
	0.7	Bufill and Boyd (1992)
	0	Boyd et al. (1993)
Upper Salt Pan Creek (NSW)	0.8	Ball and Zaman (1994)
McArthur Park (NT)	5.0[a]	Phillips et al (2014)
Curtin (ACT)	1	Bufill and Boyd (1992)
	0	Boyd et al. (1993)
Giralang (ACT)	1.3 to 1.6	Phillips et al (2014)
	0.9	Bufill and Boyd (1992)
	3.26	Boyd et al. (1993)
Long Gully Creek (ACT)	1	Bufill and Boyd (1992)
	0	Boyd et al. (1993)
Mawson (ACT)	0	Boyd et al. (1993)
Paddocks Catchment (SA)	1.3	Kemp and Lipp (1999)
Parra Hills Drain (SA)	1	Phillips et al (2014)
Argyle Street (TAS)	0.9	Phillips et al (2014)
Blackburn Lake (VIC)	1	Chiew and McMahon (1999)
Elster Creek (VIC)	1	Bufill and Boyd (1992)
Kinkora Road (VIC)	2.5	Phillips et al (2014)

Catchment	Initial Loss Estimate (mm)	Reference
Vine Street (VIC)	1	Bufill and Boyd (1992)
	0	Boyd et al. (1993)
Albany Drain (WA)	1.4	Phillips et al (2014)

[a]Phillips et al (2014) notes that this catchment had a large detention basin that may have influenced results

3.9. References

Alley, W.M. and Veenhuis, J. E. (1983), 'Effective impervious area in urban runoff modeling.'J. Hydraul. Eng., 109(2), 313-319.

Babister, M., Trim, A., Testoni, I. and Retallick, M. 2016. The Australian Rainfall and Runoff Datahub, 37th Hydrology and Water Resources Symposium Queenstown NZ

Ball, J.E. and Powell, M. (1998), Inference of catchment modelling system control parameters, Proc. UDM '98: Developments in Urban Drainage Modelling, London, UK, 1, 313-320.

Ball, J.E. and Zaman, S. (1994) 'Simulation of small events in an urban catchment', National Conference Publication - Institution of Engineers, Australia, pp: 353-358.

Beard, L.R. and Shin Chang. (1979), Urbanization impact on streamflow, Journal of the Hydraulics Division ASCE, 105: 647-59.

Black, D.C. and Aitken, A.P. (1977), Simulation of the Urban Runoff Process, Australian Government Publishing Service, 75/82.

Board, R.J., Barlow, F.T.H. and Lawrence, J.R. (1989), Flood and Yield Estimation in the Arid Zone of the Northern Territory. Hydrology and Water Resources Symposium 1989. Christchurch, New Zealand, pp: 367-371

Boughton, W.C. (2015), Master recession analysis of transmission loss in some Australian streams [online]. Australian Journal of Water Resources, 19(1), 43-51. Available at http://search.informit.com.au/

Boughton, W.C. (1989), A Review of the USDA SCS Curve Number Method. Australian Journal of Soil Research, 27: 511-523

Boughton, W.C. and Hill, P.I. (1997), A Design Flood Estimation Procedure using Data Generation and a Daily Water Balance Model. CRC for Catchment Hydrology. Report 97/8.

Boughton, W.C., Muncaster, S.H., Srikanthan, R., Weinmann, P.E., Mein, R.G. (1999) Continuous Simulation for Design Flood Estimation - a Workable Approach. Water 99: Joint Congress; 25th Hydrology & Water Resources Symposium, 2nd International Conference on Water Resources & Environment Research; Handbook and Proceedings; pp: 178-183.

Boyd, M.J., Bufill, M.C. and Knee, R.M. (1993), Pervious and Impervious Runoff in urban catchments, Hydrological Sciences Journal, 38(6), 463-478.

Boyd, M.J., Bufill, M.C. and Knee, R.M. (1994), Predicting Pervious and Impervious Storm Runoff from Urban Drainage Basins, Hydrological Sciences Journal, 39(4), 321-332.

Bufill, M.C. and Boyd M.J. (1992), A sample flood hydrograph model for urban catchment, Proceedings of the International Symposium on Urban Management, 98: 98-103, Sydney.

Carroll, D.G. (2012), URBS (Unified River Basin Simulator) A Rainfall Runoff Routing Model for Flood Forecasting and Design. Version 5.00 Dec, 2012.

Chapman, T.G. (1968), Catchment Parameters for a Deterministic Rainfall-Runoff Model in 'Land Evaluation' (ed G.A. Stewart), Macmillan, Melbourne, pp: 312-323.

Chapman, T.G. (1970), Optimisation of a rainfall-runoff model for an arid zone catchment, in Symposium on the results of research on representative and experimental basins, pp. 126-144, IASH Publ. No. 96, Wellington, New Zealand.

Cherkaver, D.S. (1975), The hydrologic response of small watersheds to suburban development: Observations and modeling in urbanization and water quality control, in Whiple Jr. (Eds), Proceedings of the American Water Resources Association (pp: 110-119), Herndon,VA.

Chiew, F.H.S. and McMahon, T.A. (1999), Modelling Runoff and diffuse pollution loads in urban areas. Water Science Technology, 39(12), 241-248.

Chu, S.T. (1978), Infiltration during an Unsteady Rain. Water Resources Research. 14(3), 461-466.

Cordery, I. (1970)' Antecedent Wetness for Design Flood Estimation, Civil Engineering Transaction, Institution of Engineers, Australia, CE12(2), 181-184.

Cordery, I. and Pilgrim, D.H. (1983), On the Lack of Dependence of Losses from Flood Runoff on Soil and Cover Characteristics, IAHS Pub., (140), 187-195.

Cordery, I., Pilgrim, D.H. and Doran, D.G., (1983), Some Hydrological Characteristics of Arid Western New South Wales. Hydrology and Resources Symposium. I.E.Aust. Nat. Conf. Pub., (83/13), 287-292.

Dayaratne, S.T. (2000), Modelling of Urban Stormwater Drainage Systems using ILSAX, PhD Thesis, Victoria University of Technology, August.

Dyer, B.G., Nathan, R.J., McMahon, T.A. and O'Neill, I.C. (1994), Development of Regional Prediction Equations for the RORB Runoff Routing Model. CRC for Catchment Hydrology Report 94/1. March 1994.

Eastgate, W.I., Swartz, G.L. and Briggs, H.S. (1979), Estimation of Runoff Rates for Small Queensland Catchments, Department of Primary Industries, Queensland Technical Bulletin No.15.

El-Kafagee, M. and Rahman, A. (2011), A study on initial and continuing losses for design flood estimation in New South Wales. In Chan, F., Marinova, D. and Anderssen, R.S. (eds) MODSIM2011, 19th International Congress on Modelling and Simulation, (pp: 3782-3787), Perth, Australia.

Flavell, D.J. and Belstead, B.S. (1986), Losses for Design Flood Estimation in Western Australia, Hydrology and Water Resources Symposium, Griffith University, pp: 203-208.

Fleming, P.M. (1974), The Australian Representatives Basins Programme, Journal of Hydrology, 13(1), 21-31.

Fleming, P.M. and Smiles, D.E. (1975), Infiltration of Water into Soil. In Chapman, T.G. and Dunin, F.X. eds. Prediction in Catchment Hydrology. Canberra. Australian Academy of Science. Pp: 83-110.

Frost, A., Ramchurn, A., Hafeez, M., Zhao, F., Haverd, V., Beringer, J., and Briggs, P. (2015), Evaluation of AWRA-L: the Australian Water Resource Assessment model. Modsim 2015 - 21st International Congress on Modelling and Simulation, 29 Nov - 4 Dec 2015, Gold Coast, 0, 2047–2053.

Goyen, A.G. (2000), Spatial and Temporal Effects on Urban Rainfall / Runoff Modelling. PhD Thesis. University of Technology, Sydney. Faculty of Engineering.

Goyen, A.G. (1983), A Model to Statistically Derive Design Rainfall Losses Hydrology and Water Resources Symposium 1983: Preprints of Papers; pages: 220-225. Institution of Engineers, Australia, National conference publication, No.83/13.

Goyen, A.G., O'Loughlin, G.G. (1999a), The Effects of Infiltration Spatial and Temporal Patterns on Urban Runoff. Water 99: Joint Congress; 25th Hydrology & Water Resources Symposium, 2nd International Conference on Water Resources & Environment Research; Handbook and Proceedings, pp: 819-822.

Goyen, A.G., O'Loughlin, G.G. (1999b), Examining the basic building blocks of urban runoff. Urban Storm Drainage - 8th International Proceedings. Sydney, 30 Aug.-3 Sept. 1999, 3: 1382-1390.

Green, R.E. and Ampt, G.A. (1911), Studies on Soil Physics: 1. Flow of Air and Water through Soils. Journal of Agricultural Science, 4: 1-24

Heneker, T.M, Lambert, M.F. and Kuczera, G. (2003), Overcoming the Joint Probability Problem Associated with Initial Loss Estimation in Design Flood Estimation. Australian Journal of Water Resources, 7(2), 101-109.

Hill, P.I., Graszkiewicz, Z., Sih, K. and Rahman, A. (2013), Revision project 6: Loss models for catchment simulation. Stage 2 Report P6/S2/016A.

Hill, P.I., Maheepala, U. and Mein, R.G. (1996), Empirical Analysis of Data to Derive Losses: Methodology, Programs and Results. CRC for Catchment Hydrology Working Document 96/5.

Hill, P.I., Graszkiewicz, Z., Loveridge, M., Nathan, R.J. and Scorah, M. (2015), Analysis of loss values for Australian rural catchments to underpin ARR guidance. Hydrology and Water Resources Symposium 2015, Hobart, 9-10 December 2015.

Hill et al

Hill, P.I., Graszkiewicz, Z., Taylor, M. and Nathan, R.J. (2014a), ARR Revision Project 6 Loss models for catchment simulation. Stage 4 Analysis of rural catchments. May 2014.

Hill, P.I., Graszkiewicz, Z., Nathan, R.J., Stephens, D.A. and Pearce, L. (2014b), Testing the Suitability of a probability distributed storage capacity loss model for design flood estimation. 2014 Hydrology and Water Resources Symposium, Perth.

Ilahee, M. (2005), Modelling Losses in Flood Estimation, A thesis submitted to the School of Urban Development Queensland University of Technology in partial fulfilment of the requirements for the Degree of Doctor of Philosophy, March 2005.

Ilahee, M. and Imteaz, M.A. (2009), Improved Continuing Losses Estimation Using Initial Loss-Continuing Loss Model for Medium Sized Rural Catchments. American J. of Engineering and Applied Sciences, 2(4), 796-803.

Ilahee, M. and Rahman, A. (2003), Investigation of Continuing Losses for Design Flood Estimation: A Case Study in Queensland. 28th International Hydrology and Water Resources Symposium, 10-14 November 2003,Wollongong, NSW, 1: 191-197.

Ishak, E., and Rahman, A. (2006) Investigation into Probabilistic Nature of Continuing Loss in Four Catchments in Victoria. In: 30th Hydrology & Water Resources Symposium: Past, Present & Future; pages: 432-437.

Janke, B. and Wilson, N. (2011), Development of techniques to quantify effective impervious cover.

Jensen, M. (1990), Rain-runoff parameters for six small gauged urban catchments. Nordic and drol., 21: 165-184.

Kemp, D.J. and Lipp, W.R. (1999), Predicting Stormwater Runoff in Adelaid - What do we Know?, Living with Water Seminar, The Hydrological Society of South Australia, Adelaide.

Kemp, D.J. and Wright, C. (2014), Flood Hydrology in an Arid Area - Findings from the Gammon Ranges Project. 2014 Hydrology and Water Resources Symposium, Perth. 24-27 February 2014, pp: 109-116.

King, K.W. (2000), Response of Green-Ampt Mein-Larsen Simulated Runoff Volumes to Temporally Aggregated Precipitation. Journal of the American Water Resources Association, 36(4), 791-797

Kjeldsen, T.R., Stewart, E.J., Packman, J.C., Folwell, S.S. and Bayliss, A.C. (2005), Revitalisation of the FSR/FEH rainfall-runoff method. Joint Defra/EA Flood and Coastal Erosion Risk Management R&D Programme. R&D Technical Report FD1913/TR.

Knighton, A.D. and Nanson, G.C. (1994), Flow transmission along an arid zone anastomosing river, Cooper Creek, Australia. Hydrological Processes, 8: 137-154.

Kuczera, G., Lambert, M., Heneker, T., Jennings, S., Frost, A. and Coombes, P. (2006), Joint probability and design storms at the crossroads, Australian Journal of Water Resources, 10(1), 63-79.

Lang, S.M., Hill, P.I. Scorah, M. and Stephens, D.A. (2015), Defining and calculating continuing loss for flood estimation, Proceedings of the 2015 Hydrology and Water Resources Symposium, Hobart.

Lee, J. and Lim, W.H. (1995), Green-Ampt Equation and the Soil Water Storage Depth in a Watershed Model, Proceedings of the Second International Symposium on Urban Stormwater Management, pp: 157 -161, 11-13 July, Melbourne.

Linsley, R.K., Kohler, M.A. and Paulhus, J.L. (1982), Hydrology for Engineers, ed 3, NewYork: McGraw-Hill.

Loveridge, M. (unpublished), Evaluation of Monte Carlo simulation for flood frequency curve derivation using an event-based rainfall-runoff model, Doctoral Thesis, University of Western Sydney.

Mag, V.S. and Mein, R.G. (1994), A flood forecasting procedure which combines the RORB and TOPOG models, Proceedings of the Hydrology and Water Resources Symposium, I.E. Nat. Conf. 94/15: 217-222.

Maidment, D.R. (1992), Handbook of Hydrology, New York: McGraw-Hill.

Manley, R.E. (1974), Catchment models for river management, MSc Thesis, University of Birmingham.

Mein, R.G. and Goyen, A.G. (1988), Urban Runoff. Transactions of the Institution of Engineers, Australia: Civil Engineering, CE30(4), 225-238.

Mein, R.G. And Larson, C.L. (1973), Modeling infiltration during a steady rain, Water Resources Research, 9: 384-394.

Mein, R. G. and McMahon, T. A. (1982), Review of the role of process modelling in the Australian Representative Basins Program, In Review of the Australian Representative Basin Program. Rep. Basin Ser. Rep.4.

Mein, R.G. and O'Loughlin, E.M. (1991), A new approach to flood forecasting, Proceedings of the Hydrology and Water Resources Symposium, I.E.Aust. Nat. Conf. Pub. No. 91/12, pp: 219-224, Perth.

Mein, R.G., Nandakumar, N. and Siriwardena, L. (1995), Estimation of initial loss from soil moisture indices (Pilot Study), Working Document 95/1, Cooperative Research Centre for Catchment Hydrology.

Melanen, M. and Laukkanen, R. (1981), Dependence of runoff coefficient on area type and hydrological factors, Proceedings of the 2nd International Conference on Urban Storm Drainage, Water Resources Publications, pp: 404-410, Littleton, Colorado, USA.

Minty, L.J. and Meighen, J. (1999), Development of temporal distributions of rainfall antecedent to large and extreme design bursts over southeast Australia, Hydrology Report Series HRS Report No. 6, Hydrometeorological Advisory Service, Melbourne: Bureau of Meteorology.

Moore, R.J. (1985), The probability-distributed principle and runoff production at point and basin scales, Hydrological Sciences Journal, 30(2), 273-297.

Muncaster, S.H., Weinmann, P.E. and Boughton, W.C. (1999), The representation of loss in continuous simulation models for design flood estimation, Proceedings of Water 99 Joint Congress, Institution of Engineers, Australia, pp: 184-189, 6-8 July, Brisbane.

Nathan, R.J., Weinmann, P.E. and Hill, P.I. (2003), Use of a Monte-Carlo Simulation to estimate the Expected Probability of large to extreme floods, Proceedings of the 28th International Hydrology and Water Resources Symposium, pp: 1105-1112, 10-14 November, Wollongong.

O'Loughlin, G. and Stack, R. (2014), DRAINS User Manual - a manual on the DRAINS program for urban stormwater drainage system design and analysis, Available at: <http://www.watercom.com.au/DRAINS%20Manual.pdf>.

Pearce, L.J. (2011), Regional runoff coefficients for summer and winter design flood events in south-west Western Australia, Proceedings of the 24th IAHR World Congress - Balance and Uncertainty, 26 June - 1 July, Brisbane, Australia.

Pearcey, M., Pettett, S., Cheng, S., and Knoesen, D. (2014), Estimation of RORB Kc parameter for ungauged catchments in the Pilbara Region of Western Australia, Proceedings of the 2014 Hydrology and Water Resources Symposium, 24 - 27 February, Perth.

Phillips, B., Goyen, A., Thomson, R., Pathiraja, S. and Pomeroy, L. (2014), Australian Rainfall and Runoff Revision Project 6: Loss models for catchment simulation - Urban Losses Stage 2 Report, February.

Pui, A., Lall, A. and Sharma, A. (2009), How does the interdecadal pacific oscillation affect design floods in Eastern Australia, Proceedings of H2009 - 32nd Hydrology and Water Resources Symposium, November, pp: 266-274.

Rahman, A., Weinmann, P.E. and Mein, R.G. (2002), The use of probability-distributed initial losses in design flood estimation, Australian Journal of Water Resources, 6(1), 17-29.

Rajendran, R., Mein, R.G. and Laurenson, E.M. (1982), A spatial model for the prediction of losses on small rural catchments, Department of Civil Engineering, Monash University, Australian Water Resources Council Technical Paper, No.75, Canberra.

Ren-Jun., Z (1992) The Xinanjiang model applied in China. Journal of Hydrology. 135: 371-381

Rigby, E.H. and Bannigan, D.J. (1996), The embedded design storm concept - a Critical Review, Proceedings of the Hydrology and Water Resources Symposium 1996: Water and the Environment, Preprints of Papers, National Conference Publication, (96/05), 453-459.

Riley, S.J. and Fanning, P.C. (1997), Spatial patterns of infiltration in suburban developments in the Hawkesbury-Nepean catchment,Science and Technology in the Environmental Management of the Hawkesbury-Nepean Catchment, Institution of Engineers, Australia, NCP 97/01, 10-11 July, Nepean.

Ruprecht, J.K. and Schofield, N.J. (1993), Infiltration characteristics of a complex lateritic soil profile, Hydrological Processes, 7(1), 87-97.

Shuster, W.D., Bonta, J., Thurston, H., Warnemuende, E. and Smith, D.R. (2005), Impacts of impervious surface on watershed hydrology: A review, Urban Water Journal, 2(4), 263-275.

Siriwardene, N.R., Cheung, B.P.M. and Perera, B.J.C. (2003), Estimation of soil infiltration rates of urban catchments, Proceedings of the 28th International Hydrology and Water Resources Symposium, Institution of Engineers, Australia, Wollongong.

Skukla, M.K., Lal, R. and Unkefer, P. (2003), Experimental validation of infiltration models for different land use and soil management systems, Journal of Soil Science, 168(3), 178-191.

Smith, A., Rahman, J., Baron-hay, S., and Shipman, D. (2016), A new web based water information service leveraging the Australian Water Resources Assessment Modelling System Australian Water Resources Assessment Modelling System, (January).

Stewart, B.J. and Boughton, W.C. (1983), Transmission losses in natural streambeds - a Review, Proceedings of the Hydrology and Water Resources Symposium 1983, Institution of Engineers, Australia, preprints of papers, pp: 226-230.

Stokes, R.A. (1989), Calculation file for Soil Water Model - Concept and theoretical basis of soil water model for the south west of Western Australia, Unpublished Report, Water Authority of W.A. Water Resources Directorate.

Tularam, G.A. and Ilahee, M. (2007), Initial loss estimates for tropical catchments of Australia, Environmental Impact Assessment Review, 27(6), 493-504.

United States Army Corps of Engineers (USACE) (1998), Runoff from snowmelt, engineering manual, 31 March, Washington: USACE.

Van Mullem, J.A., Woodward, D.E., Hawkins, R.H., and Hjelmfelt, A.T. Jr. (2002), Runoff curve number method: beyond the handbook. In: Hydrologic Modeling for the 21st Century, Proceedings of the Second Federal Interagency Hydrologic Modeling Conference, July 28 - August 1, Las Vegas.

Walsh, M.A., Pilgrim, D.H. and Cordery, I. (1991), Initial losses for design flood estimation in New South Wales, Proceedings of the International Hydrology and Water Resources Symposium, I.E.Aust. Nat. Conf. Pub. (91/19), 283-288.

Ward, T.J., Hawkins, R.H., Van Mullem, J.A., Woodward. D.E. (2009), Curve number hydrology: state of the practice, College Park: American Society of Civil Engineers.

Water and Rivers Commission (2003), SWMOD A rainfall loss model for calculating rainfall excess - user manual (version 2.11), Prepared by Hydrology and Water Resources Branch Resource Science Division, September.

Waugh, A.S. (1991), Design losses in flood estimation, Proceedings of the International Hydrology and Water Resources Symposium, I.E.Aust. Nat. Conf. Pub. No.91/19, pp: 629-630, Perth.

William, J. (1994), Preliminary report on the use of the Green Ampt Infiltration Model for measuring surface runoff on rural catchments,unpublished report 18 February 1994, CRC for Catchment Hydrology.

Woodward, D.E., Hawkins, R.H. and Quan, Q.D. (2002), Curve number method: origins, applications and limitations, Proceedings of Hydrologic Modeling for the 21st Century, Second Federal Interagency Hydrologic Modeling Conference, July 28 - August 1, Las Vegas.

Woolmington, E. and Burgess, J.S. (1983), Hedonistic water use and low-flow runoff in Australia's national capital, Urban Ecology, 7(3), 215-227.

Zaman, S. and Ball, J.E. (1994), Simulation of small events in an urban catchment, Proceedings of the 1994 Hydrology and Water Resources Conference - Water Down Under '94, I.E.Aust. Nat. Conf. Pub. No.94/15, pp: 353 - 358, Adelaide.

Chapter 4. Baseflow Models

Peter Hill, Rachel Brown, Rory Nathan, Zuzanna Graszkiewicz

Chapter Status	Final
Date last updated	14/5/2019

4.1. Introduction

Streamflow consists of two components based on response timing, following a rainfall event. Water that enters a stream rapidly is termed as quickflow and is sourced from rainfall excess, after the loss has been satisfied (representing a range of processes such as interception, infiltration and depression storage). On the contrary, water that takes longer to reach a river is termed as baseflow and is sourced primarily from groundwater discharge into the river. Also, different locations have varying degrees of baseflow contribution to streamflow, based on regional hydrogeological conditions.

According to Nathan and McMahon (1990) and Brodie and Hostetler (2005), the baseflow hydrograph has the following features:

- The low flow before the start of a flood event is assumed to consist entirely of baseflow;
- The rapid rise of river during a rainfall event increases the volume of water held as bank storage, which returns to the main streamflow after a delay and creates a baseflow peak after the main flood peak;
- The recession of the baseflow peak continues after the recession of the streamflow peak;
- The baseflow recession generally follows an exponential decay function; and
- The baseflow hydrograph rejoins the total hydrograph as the quickflow ceases.

The majority of design flood estimation in Australia utilises flood event models that focus on surface runoff processes. In such models the baseflow component is either ignored or incorporated after the surface runoff has been estimated. The conceptualisation of some continuous models or fully integrated surface water - groundwater models explicitly incorporate the estimation of the baseflow component. However, given the prevalence of flood event models for design flood estimation, the following guide concentrates on estimating a baseflow hydrographs to combine with an existing estimate of surface runoff.

ARR Revision Project 7 - Baseflow for Catchment Simulation, developed a method to calculate and incorporate the baseflow contribution to design flood estimates. Stage 1 of the project (Murphy et al., 2009; Murphy et al., 2011a; Graszkiewicz et al., 2011), focussed on the physical processes of groundwater-surface water interaction and theoretical approaches to baseflow separation. The identified methods were applied to eight case study catchments across Australia in order to develop a suitable approach for wide scale application. Stage 2 of Project 7 (Murphy et al., 2011b) covered the analysis of 236 catchments across Australia, the development of prediction equations to estimate baseflow parameters and the development of a method for their application to design estimates for catchments across Australia.

This document utilises the method developed in ARR Revision Project 7 to provide guidance on how to estimate baseflow for design flood estimation.

The remainder of this chapter is structured as follows:

- Book 5, Chapter 4, Section 2 describes those characteristics of the baseflow that need to be estimated;
- Book 5, Chapter 4, Section 3 discusses considerations when selecting the approach to estimating baseflow;
- Book 5, Chapter 4, Section 4 outlines the different approaches to estimating the baseflow contribution to design hydrographs; and
- Book 5, Chapter 4, Section 5 provides 2 worked examples.

4.2. Guiding Principles

This guide on baseflow draws upon a significant body of work undertaken through ARR Revision Project 7, and provides advice on how to estimate baseflow for design flood estimation.

Users should consider the characteristics of the particular catchment with respect to the underlying assumptions that form the basis of the method outlined in this chapter. The following approach is applicable across the vast majority of Australian catchments. However, users should draw upon their understanding of the particular catchment of interest to make an informed decision regarding the relevance of each step, considering the following issues:

- **Snow melt**, which is not considered in this approach.
- Significant farm dam development or other flow regulations in the catchment, which can mask the contribution of baseflow.
- **Design flood estimation for Rare to Extreme events.** The method outlined below is only relevant to events up to approximately the 1% AEP and guidance for baseflow contribution to very rare and extreme events is provided in Book 8.
- **Seasonality of events,** Seasonality is not explicitly considered in this approach. Region-specific analysis should be undertaken where seasonality of flood producing factors is important. Kinkela and Pearce (2014) describe such a study for the south-west of Western Australia.
- **Urbanised catchments.** The approach and catchments considered in developed of the method were selected to represent rural conditions, therefore the approach is not applicable to urban catchments (flood estimation for urban catchments is covered in Book 9). Baseflow is typically a small contribution to the flows.
- **Small catchments away from the main stem of the river network.** The regional estimates relate to a location on the main stem of the river and reflect the characteristics of all the contributing catchments. The baseflow characteristics of individual tributaries may be different from those in the larger contributing catchment.
- **Estimation of historic events.** The approach in this chapter has been developed for application in design flood estimation, but not for the estimation of the baseflow component of streamflow for individual historic events.

- **Estimation of baseflow for extended periods.** This guide is relevant for design events only. Users should refer to the technical documents supporting ARR Revision Project 7 for more general information on baseflow estimation for longer sequences.

If any of the above factors are deemed to be important for the catchment of interest, it is recommended that the user considers the suitability of this approach to their catchment of interest. It is also relevant to interpret the outcomes in the light of underlying assumptions, and draw on local data to supplement the approach or to consider alternative methods, where these assumptions are not fully met.

Users should refer to the technical reports and analyses undertaken for ARR Revision Project 7 (Murphy et al., 2009; Murphy et al., 2011b) for full details of the data analysis and assumptions that form the basis of the method outlined in this chapter. Users may also like to refer to these supporting documents and data to draw further local conclusions from the significant body of work undertaken through the study.

4.3. Baseflow Characteristics

For design flood estimation in Australia, baseflow has traditionally been considered to be a relatively minor contributor to the flood hydrograph, but baseflow can potentially be significant in more frequent events. This is particularly the case where the catchment geology consists of high yielding aquifers.

For instance, for a 10% AEP, about two-thirds of Australian unregulated rural catchments have baseflow contributions that are estimated to be between approximately 5% and 30% of the peak flow. There are only about 5% of catchments that have a higher proportion of baseflow, which these tend to be located in south-west WA, south-east SA and some areas in the tropics. In just less than a third of unregulated rural catchments, the baseflow is estimated to be less than 5% of the peak (for a 10% AEP). Baseflow is typically insignificant in urban catchments due to the degree of channel modifications and extent of impervious areas.

The variation of baseflow with exceedance probability is discussed in Book 5, Chapter 4, Section 2. For events more frequent than a 10% AEP, the baseflow can represent a significant proportion of the peak flow, particularly volume. For rarer events, baseflow makes up a smaller relative contribution to the surface runoff. For the majority of catchments, it is likely that the contribution of baseflow for extreme events will be less important; although, for volume dependent systems, the baseflow volume may still be significant. Guidance for baseflow contribution to very rare and extreme events is provided in Book 8.

This chapter concentrates on the estimation of baseflow contribution to be included with surface runoff estimated from a flood event model, rather than separating baseflow from recorded streamflow. Approaches for separating baseflow are described in the ARR Revision Project 7 Stage 1 report (Murphy et al., 2009).

In the context of design flood estimation, a surface runoff hydrograph will typically be generated using a flood event model that excludes baseflow. It is therefore necessary to estimate the baseflow contribution in order to represent the total event peak and volume, and to generate a total streamflow hydrograph. This concept is represented in Figure 5.4.1, which depicts the following features of an event hydrograph:

- *Surface runoff peak* - the maximum flow associated with the surface runoff event.
- *Time to the surface runoff peak* - measured from the start of the event to the surface runoff peak.

- *Volume of surface runoff for the event* - event volume, represented by the area under the hydrograph.
- *Baseflow peak* - maximum baseflow associated with the event.
- *Time to the baseflow peak* - measured from the start of the event to the baseflow peak.
- *Baseflow under the surface runoff peak* - baseflow that occurs at the time of the surface runoff peak.

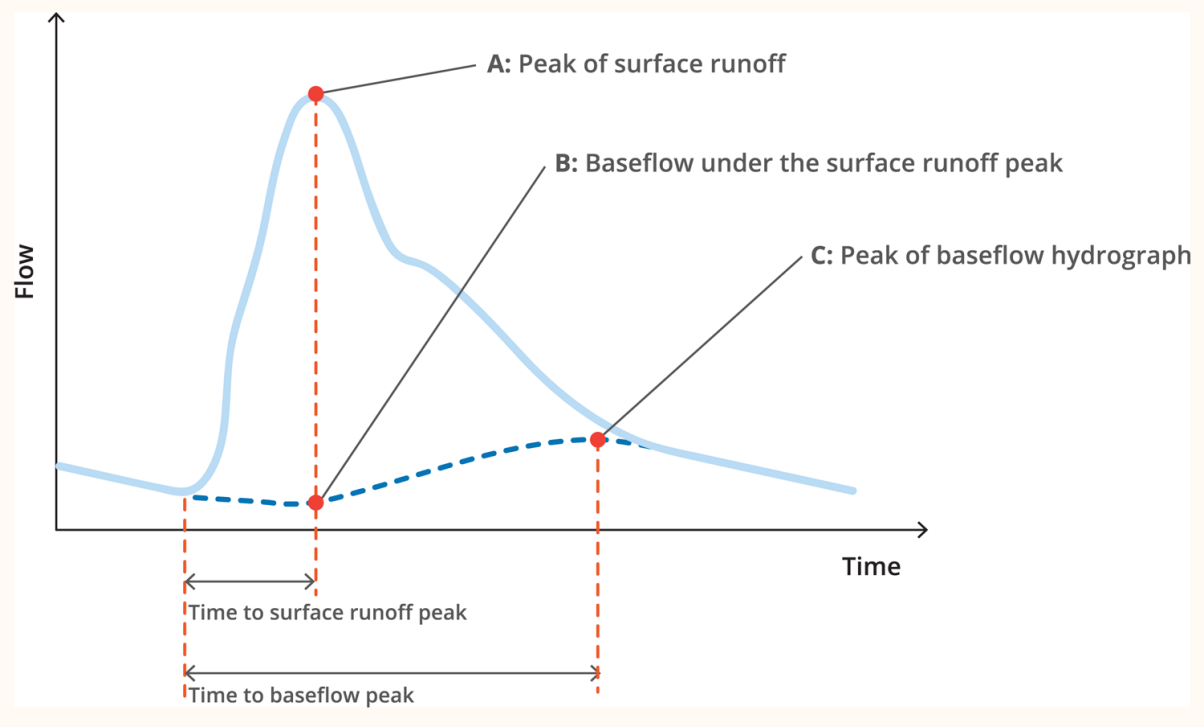

Figure 5.4.1. Key Characteristics for Calculation in a Flood Hydrograph

4.4. Selection of Approach

The recommended approach to quantifying baseflow is dependent on the catchment characteristics, data availability and baseflow characteristics of the catchment. Figure 5.4.2 provides a decision pathway to determine the most suitable approach to estimate baseflow contribution to design flood events, based on site specific criteria.

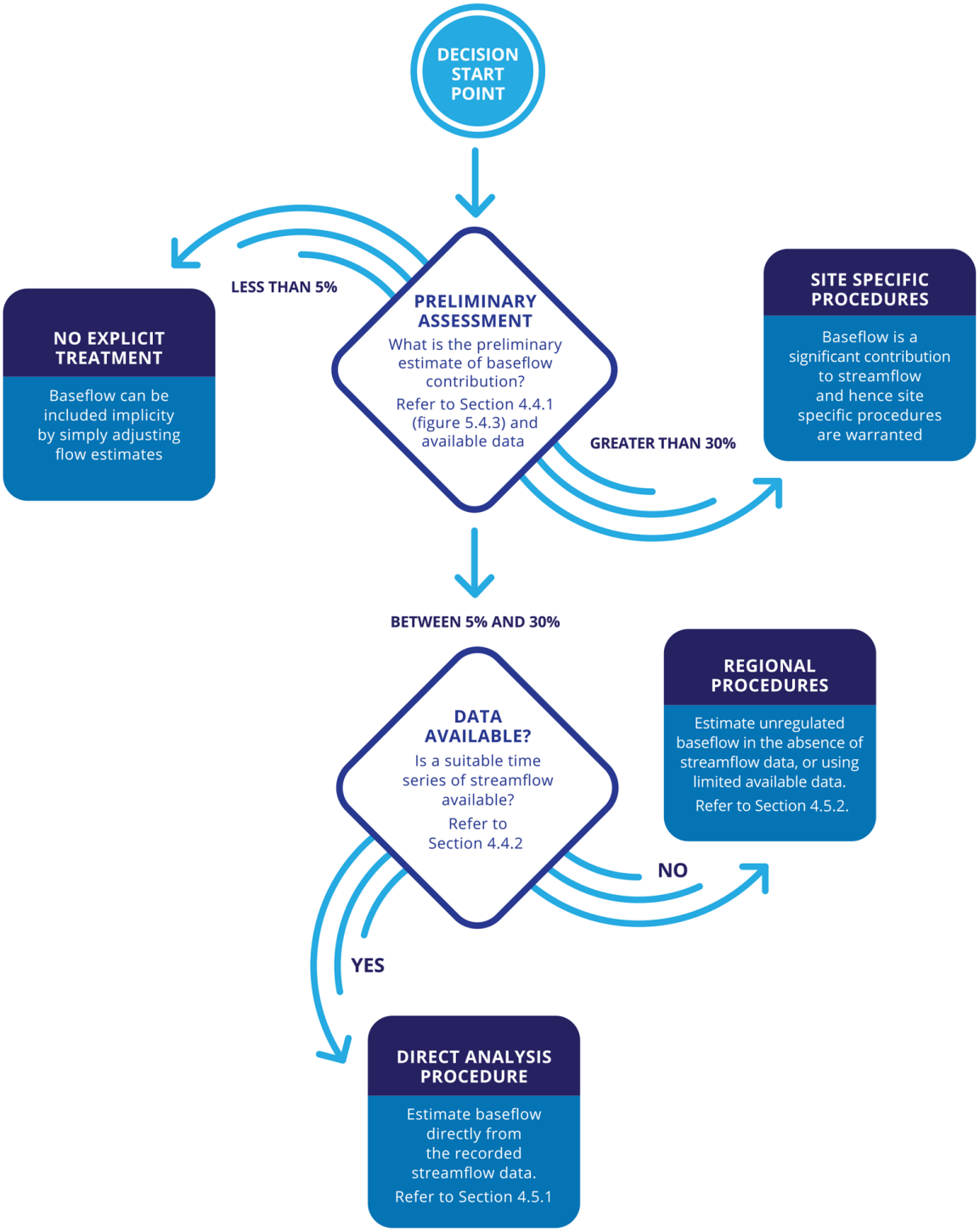

Figure 5.4.2. Decision Tree for Method to Estimate Baseflow Contribution to Design Flood

4.4.1. Preliminary Assessment of Baseflow

A preliminary assessment should be undertaken, in order to consider whether baseflow is likely to be a significant component of the design flood hydrograph. However, a detailed analysis is not suggested at this point,instead, this assessment is intended to be a coarse screening test to help determine the most appropriate approach in estimating baseflow for the catchment of interest based on the expected baseflow characteristics. A number of tools are available to support this assessment:

- Figure 5.4.3 is provided to readily identify the relative magnitude of baseflow compared to surface runoff for catchments across Australia for a 10% AEP event. Practitioners can identify their catchment of interest within this data set and note the value of Baseflow Peak Factor. This map shows catchments to match with the screening criteria identified below, while Figure 5.4.5 provides a more detailed estimate of the baseflow. The data used to generate these figures is available in Geographic Information System (GIS) format, to assist locating catchments/points of interest.

- If available, streamflow data for the catchment should be reviewed. The magnitude of flows between flood events relative to peaks can be used to determine whether baseflow is likely to be an important component of the design flood hydrograph.

Where baseflow is expected to be a small component compared to the surface runoff, the design flood peak can be adjusted up to approximately 5% to make an allowance for baseflow. Catchments with a Baseflow Peak Factor less than 0.05 are considered suitable for this approach. This reflects approximately 30% of the catchments mapped in Figure 5.4.3.

It is suggested that catchments that have a baseflow contribution greater than approximately 5% of the surface runoff should explicitly incorporate the baseflow component into the design flood, using a more rigorous approach.

While baseflow is a very large component of the event (a contribution of more than approximately 30% is suggested, reflected by a Baseflow Peak Factor greater than 0.3), the baseflow contributions should be estimated using techniques that are suited to the nature and availability of local data (e.g. Brodie and Hostetler (2005), Chapman and Maxwell (1996), Nathan and McMahon (1990), and Ladson et al. (2013)). Approximately 5% of Australian catchments, generally the areas of tropical north Australia, south-west Western Australia and the south-east coastline of South Australia, fall into this category. The specific approach of relevance will depend on local conditions and the user is guided to the above references to determine the most appropriate baseflow estimation technique.

Where baseflow is between approximately 5% and 30% of the surface runoff (Baseflow Peak Factor between 0.05 and 0.3), the approach outlined below is recommended. This relates to approximately 65% of the catchments mapped in Figure 5.4.3.

4.4.2. Suitability of Stream Flow Data

Where possible, recorded streamflow data should be used directly to quantify baseflow. However, ideally more than 10 years of continuous streamflow data would be required to undertake detailed site-specific analyses. Appropriate data quality checks should be undertaken prior to ascertaining the period of record available for analysis. Preferably, the streamflow data should extend over a period of record that enables the identification of an event of similar magnitude to the design flood of interest. Some subjectivity may be required to determine the suitability of available streamflow for this approach, depending on the period of record and the events represented within this data, with reference to event magnitude and duration of interest.

Additionally, there are various activities that can impact upon the flow characteristics associated with the baseflow. These activities include:

- *Flow regulation from upstream reservoirs* – reservoirs that release outflows that are different to inflows will produce a low flow response that can be misinterpreted as baseflow at downstream flow gauges.

- *Catchment farm dams* – high concentration of catchment farm dams could influence baseflow but only where the dams are located in a manner where they intercept and store flows arising from long-term depletion of catchment storage.
- *Major diversions* – diversions for consumptive use such as irrigation channels, urban diversions, etc. These diversions decrease low flows and hence appear to reduce estimates of baseflow. Allowances can be made for those diversions where they are metered.
- *Urbanisation* – in urban areas, features such as excess garden or sports field watering can increase low flows during summer that appear similar to baseflow in streamflow data.
- *Return flows* – water can be returned to rivers from sewage treatment plants or from industry,increasing low flows and appearing similar to baseflow.

Where present, these activities will influence the observed flow characteristics making it difficult to identify and quantify baseflow. While it is possible to estimate baseflow in these locations using the regional approach, the baseflow estimate will reflect the unregulated baseflow conditions.

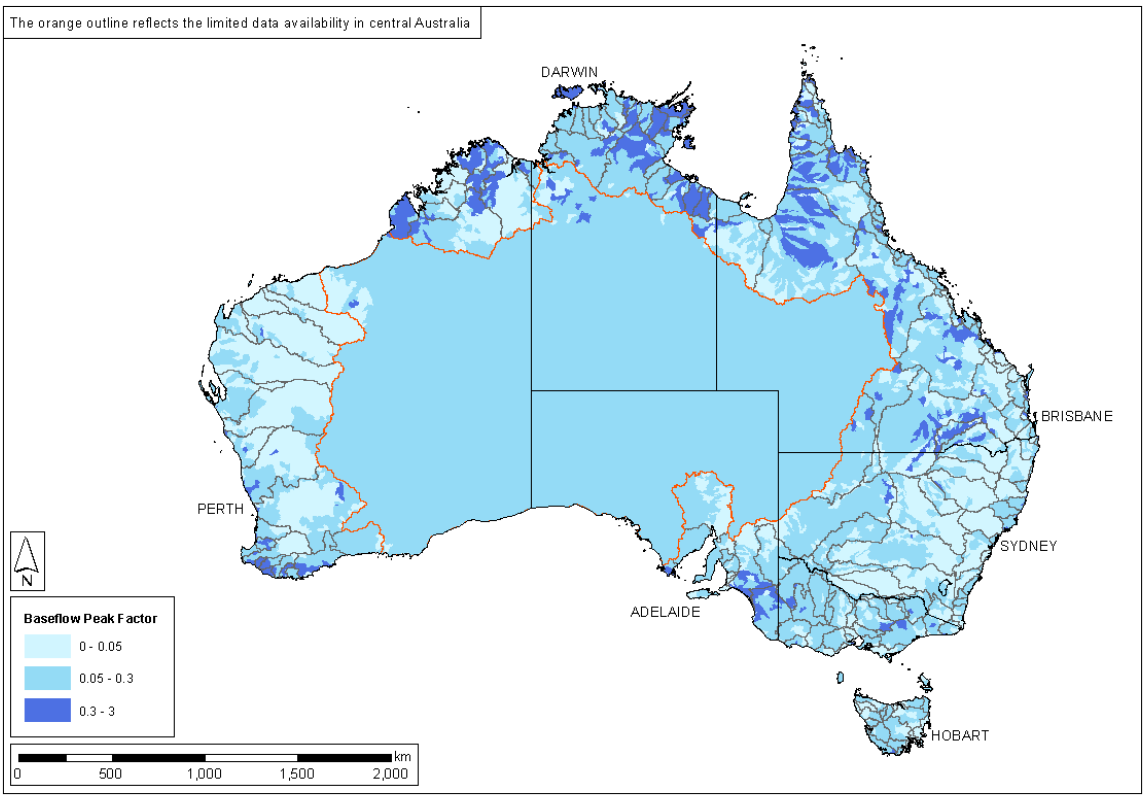

Figure 5.4.3. Preliminary Assessment of Baseflow Peak Factor for a 10% AEP Event

4.5. Quantifying Baseflow Contribution to Design Flood Estimates

4.5.1. Estimating Baseflow Using Streamflow Data

As outlined in Book 5, Chapter 4, Section 4, available streamflow data should meet a number of conditions, to be considered suitable for application to assess baseflow. If

streamflow data does not meet these criteria, this approach is not relevant and practitioners are directed to the regional approach outlined in Book 5, Chapter 4, Section 5.

To estimate baseflow directly from available streamflow data, the following steps should be followed:

a. **Review Data Quality**

Review the streamflow data and eliminate any poor quality data, as determined using the quality codes for each time step.

b. **Check Record Length**

Determine the resulting period of record available for analysis. If less than 10 years of data is available, the regional approach in Book 5, Chapter 4, Section 5 may be more appropriate for application. If more than approximately 10 years of data is available, the following steps can be applied.

c. **Flood Frequency Analysis**

Extract a series of peak flows from the recorded streamflow data and undertake a flood frequency analysis as described in Book 3, Chapter 2. It is recommended that as a minimum, the 10% AEP event should be identified. If the streamflow data record is suitable, identify events of similar magnitude to the design flood of interest.

d. **Estimate Baseflow from Recorded Floods**

Estimate the baseflow for flood events identified above. Literature, such as Nathan and McMahon (1990), Chapman and Maxwell (1996) and Brodie and Hostetler (2005), provides guidance on key features of the baseflow hydrograph. If the streamflow data is suitable, the baseflow should be estimated for events of similar magnitude to the design flood of interest.

e. **Adjust for Different AEPs**

If the above step has been applied to events of similar magnitude to the design flood of interest, the estimated baseflow magnitude and volume can be used directly with the design flood surface runoff hydrograph to generate the total streamflow estimate. Refer to Book 5, Chapter 4, Section 5 for a description of how to generate the total streamflow hydrograph. In this case, the key baseflow features, including timing, should be taken from baseflow estimated above .

If the design events are outside of the range of recorded events it is necessary to scale the baseflow contribution to reflect the AEP of interest. The method outlined in Book 5, Chapter 4, Section 5 should be applied, with the key baseflow characteristics determined from the recorded streamflow rather than the regional approach, as outlined in the following section.

4.5.2. Estimating Baseflow in the Absence of Streamflow Data

A regional method to estimate baseflow contribution to design flood events has been developed so that it is applicable for unregulated catchments across Australia. This method was developed using catchments across Australia with catchment areas between 7 and 7800 km^2, and as such the approach is considered most suitable for application for

catchments within this range. Practitioners should be mindful of these constraints when applying and interpreting the outcomes from this method.

The following three parameters are defined to characterise the contribution of baseflow to design flood hydrographs:

1. **Baseflow Peak Factor:** This factor is applied to the estimated surface runoff peak flow to give the value of peak baseflow for a 10% AEP event.

2. **Baseflow Volume Factor:** This factor is applied to the estimated surface runoff volume to give the volume of the baseflow for a 10% AEP event.

3. **Baseflow Under Peak Factor:** This factor is applied to the estimated surface runoff peak flow to give the baseflow at the time of the peak surface runoff and can be determined from the Baseflow Peak Factor, such that the Baseflow Under Peak Factor = 0.7 x Baseflow Peak Factor.

The Baseflow Peak Factor and Baseflow Volume Factor are presented in Figure 5.4.5 and Figure 5.4.6, which covers the whole of Australia. It should be noted that the maps represent the values for the total area upstream of the main stem of the river, rather than any smaller sub-catchments. As baseflow characteristics may vary from the main stream, the estimation of baseflow in subcatchments may require the approach to be supplemented with additional local data or through an alternative approach, such as transposition from another location.

ARR Revision Project 7 developed a series of regression relationships to estimate the Baseflow Peak Factor and Baseflow Volume, based on catchment characteristics (Murphy et al., 2011a). The resulting values are presented in Figure 5.4.5, Figure 5.4.6 and supporting spatial data for use with GIS, and can be used to determine the Baseflow Peak Factor and the Baseflow Volume Factor for a 10% AEP event for the catchment of interest. This data is available on the ARR Data Hub (Babister et al (2016), accessible at http://data.arr-software.org/).

These factors provide information on baseflow contribution to design flood events for a 10% AEP event. Table 5.4.1 shows the AEP scaling factors that should be applied to the 10% AEP Baseflow Peak Factor and Baseflow Volume Factor to scale relevant factors to reflect events of other AEPs.

Table 5.4.1. AEP Scaling Factors, F_{AEP}, to be applied to the 10% AEP Baseflow Peak Factor and the Baseflow Volume Factor to determine the Baseflow Peak Factor for events of various AEPs

EY	AEP (%)	Baseflow Peak Factor	Baseflow Volume Factor
2	86.47	3.0	2.6
1	63.21	2.2	2.0
0.5	50	1.7	1.6
0.2	18.13	1.2	1.2
0.11	10	1.0	1.0
0.05	5	0.8	0.8
0.02	2	0.7	0.7
0.01	1	0.6	0.6

For events of AEPs not shown in Table 5.4.1, Figure 5.4.4 can be used to determine an appropriate AEP factor. This is to be multiplied by the 10% AEP Baseflow Peak Factor or the

Baseflow Volume Factor as relevant, to determine the factor for other event magnitudes. Guidance for baseflow contribution to Rare and Extreme Events is provided in Book 8.

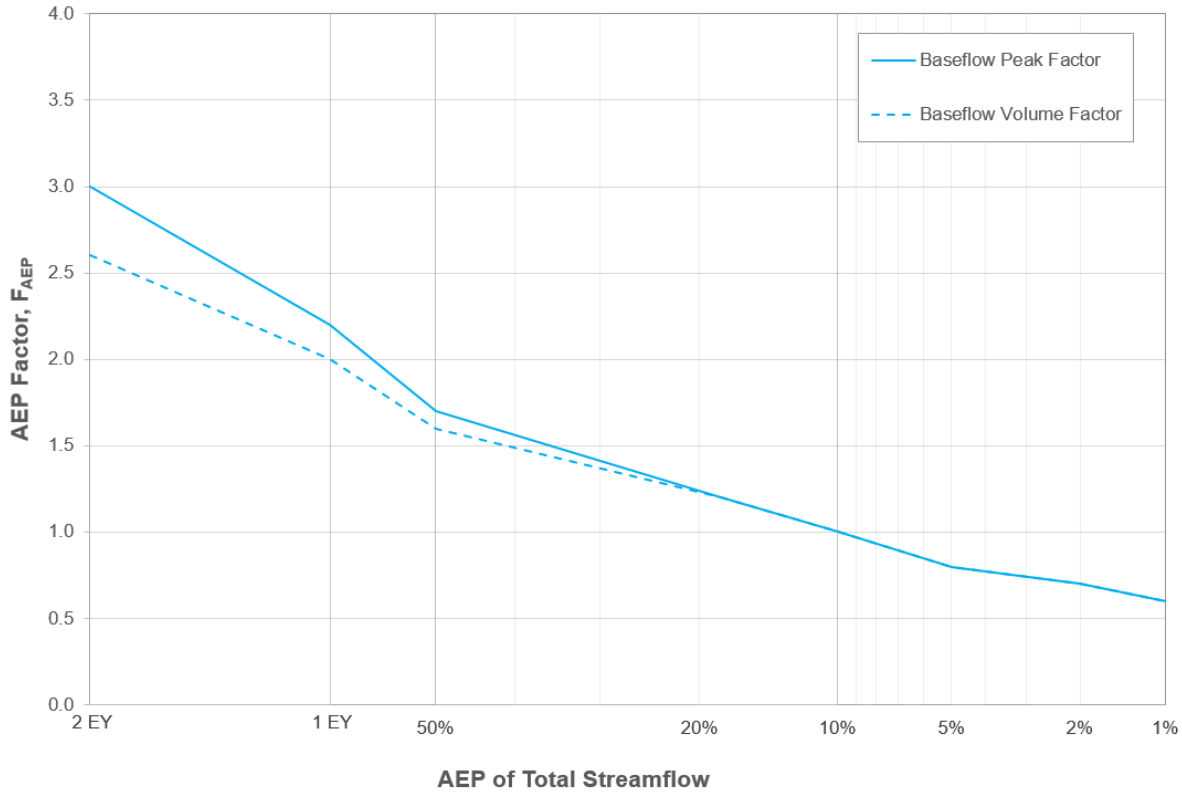

Figure 5.4.4. AEP Factors, F_{AEP} to be applied to the 10% AEP Baseflow Volume Factor to determined the Baseflow Volume Factor for events of various AEPs

This information is applied to the design flood event using the procedure outlined in the relationships below that relate to the typical flood hydrograph in Figure 5.4.1.

To Calculate the Peak Baseflow (Point C in Figure 5.4.1):

1. Determine the Baseflow Peak Factor for a 10% AEP ($R_{\mathrm{BPF,10\%AEP}}$) from Figure 5.4.5.

2. Determine the AEP factor, corresponding to the event AEP using Table 5.4.1 or Figure 5.4.4. Scale the 10% AEP Baseflow Peak Factor appropriately to determine the Baseflow Peak Factor for the event severity of interest.

3. Apply the Baseflow Peak Factor to the calculated peak surface runoff as in Equation (5.4.1).

$$Q_{\mathrm{Peak\ baseflow}} = R_{\mathrm{BPF}} Q_{\mathrm{Peak\ surface\ runoff}} \tag{5.4.1}$$

4. Calculate the timing of the baseflow peak using Equation (5.4.2). The time to the peak surface runoff should be applied in units of hours from the start of the event.

$$T_{\mathrm{Peak\ baseflow}} = 0.92\ \mathrm{T}_{\mathrm{Peak\ surface\ runoff}} + 33.4 \tag{5.4.2}$$

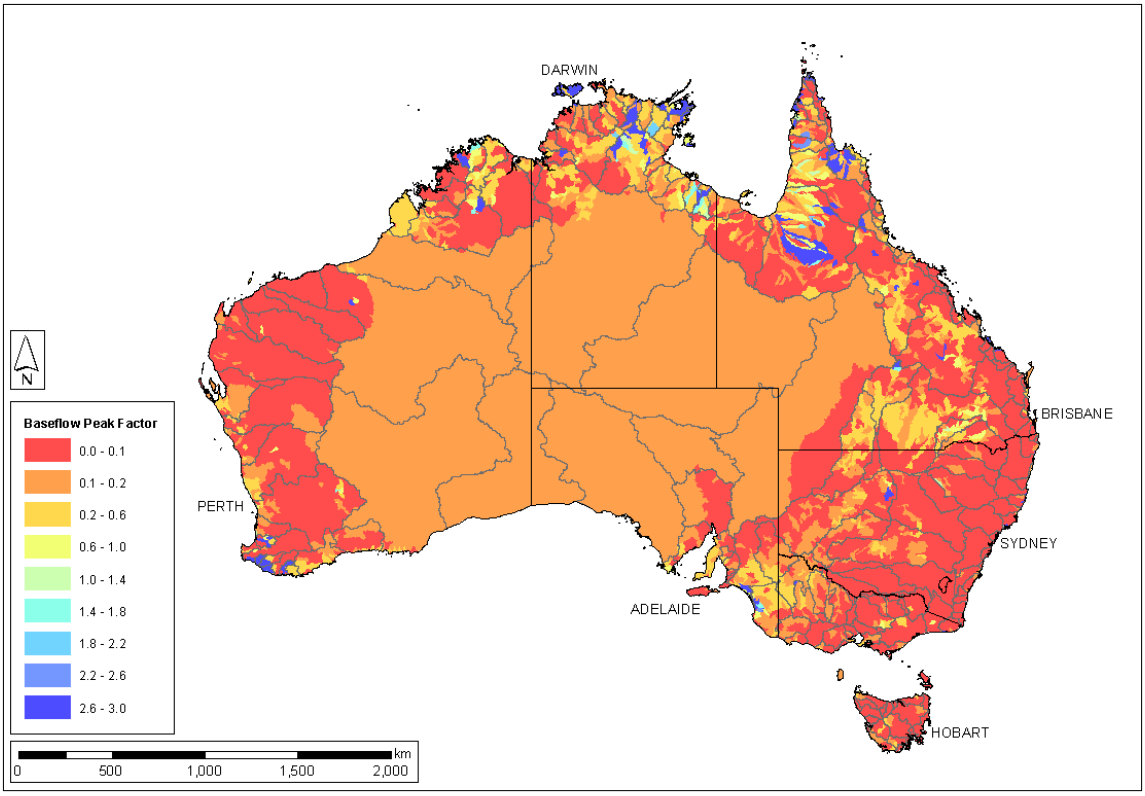

Figure 5.4.5. Map of Baseflow Peak Factor for a 10% AEP

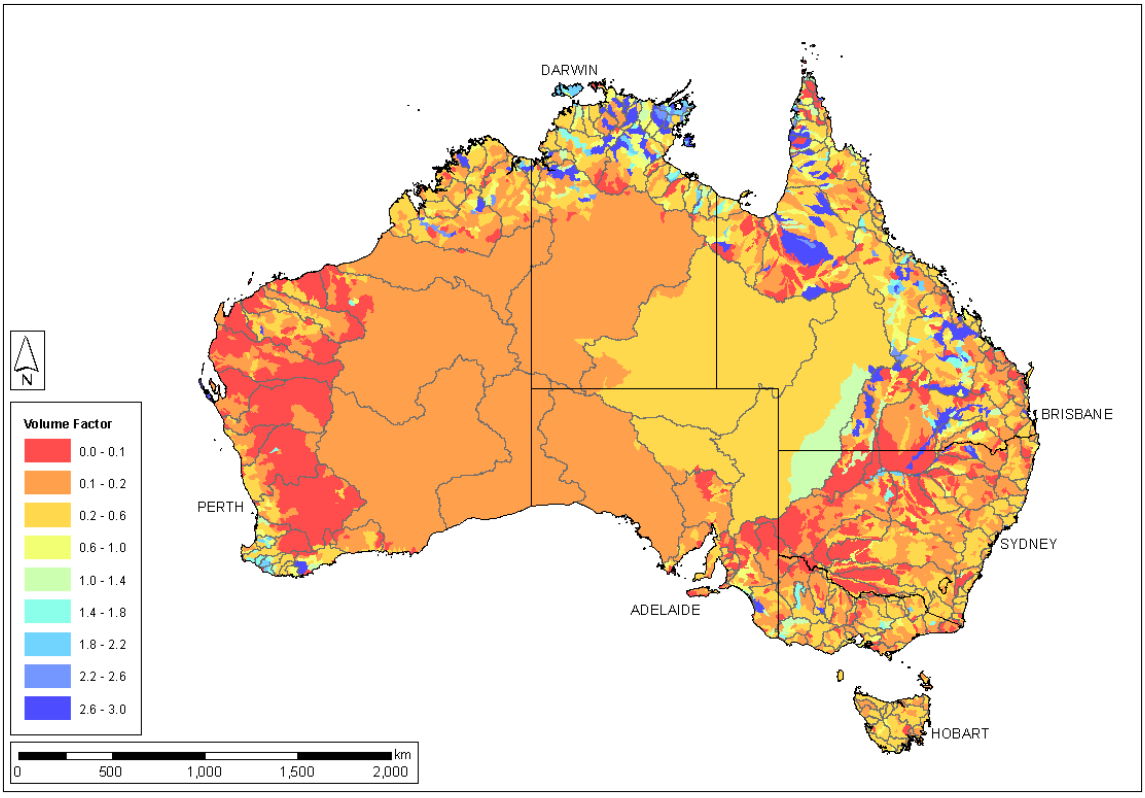

Figure 5.4.6. Map of Baseflow Volume Factor for a 10% AEP

To calculate the baseflow under the peak streamflow (Point B in Figure 5.4.1):

1. The Baseflow Peak Factor (R_{BPF}) calculated for the appropriate AEP event as above should be used in Equation (5.4.3) to calculate the Baseflow Under Peak Factor (R_{BUPF}).

$$R_{\text{BUPF}} = 0.7 \times R_{\text{BPF}} \tag{5.4.3}$$

2. R_{BUPF} should be used as in Equation (5.4.4) to calculate the baseflow under the peak streamflow.

$$Q_{\text{Baseflow under peak streamflow}} = R_{\text{BUPF}} Q_{\text{Peak surface runoff}} \tag{5.4.4}$$

To Calculate the Total Streamflow Peak (Point A in Figure 5.4.1):

1. Calculate the baseflow under the streamflow peak for the appropriate AEP as above.

2. Add the baseflow under the streamflow peak calculated using Equation (5.4.4), to the calculated peak surface runoff as in Equation (5.4.5).

$$Q_{\text{Peak streamflow}} = Q_{\text{Peak surface runoff}} + Q_{\text{Baseflow under peak streamflow}} \tag{5.4.5}$$

To Calculate the Total Baseflow Volume for an Event:

1. Determine the Baseflow Volume Factor for a 10% AEP ($R_{BVF,10yrARI}$) from Figure 5.4.5.

2. Determine the AEP factor corresponding to the AEP event using Table 5.4.1 or Figure 5.4.4. Scale the 10% AEP Baseflow Volume Factor appropriately to determine the Baseflow Volume Factor (R_{BVF}) for the event.

3. Apply the Baseflow Volume Factor to the calculated surface runoff volume as in Equation (5.4.6).

$$V_{\text{Baseflow}} = R_{\text{BVF}} V_{\text{Surface Runoff}} \tag{5.4.6}$$

To Calculate the Total Streamflow Volume for an Event:

1. Calculate the baseflow volume for the event using the appropriate AEP factors.

2. The baseflow volume calculated using Equation (5.4.6) should be added to the calculated surface runoff as in Equation (5.4.7).

$$V_{\text{Total streamflow}} = V_{\text{Surface runoff}} + \text{V}_{\text{Baseflow}} \tag{5.4.7}$$

This approach can be directly applied to estimate the baseflow contribution to any event between a 2 EY and a 1% AEP.

4.5.3. Generating the Total Streamflow Hydrograph

The characteristics of surface runoff, baseflow and total streamflow can be used to estimate the hydrograph for the event. For simplicity, a linear approach can be used to estimate the baseflow at each time step, by fitting between the data values estimated through the process described above and matching the baseflow volume. This time series can be manually added to the surface runoff time series data to generate a time series for the total streamflow, which is generated through this process and should be reviewed. It may require

smoothing to produce a more realistic temporal distribution of baseflow. This process is presented in Figure 5.4.7.

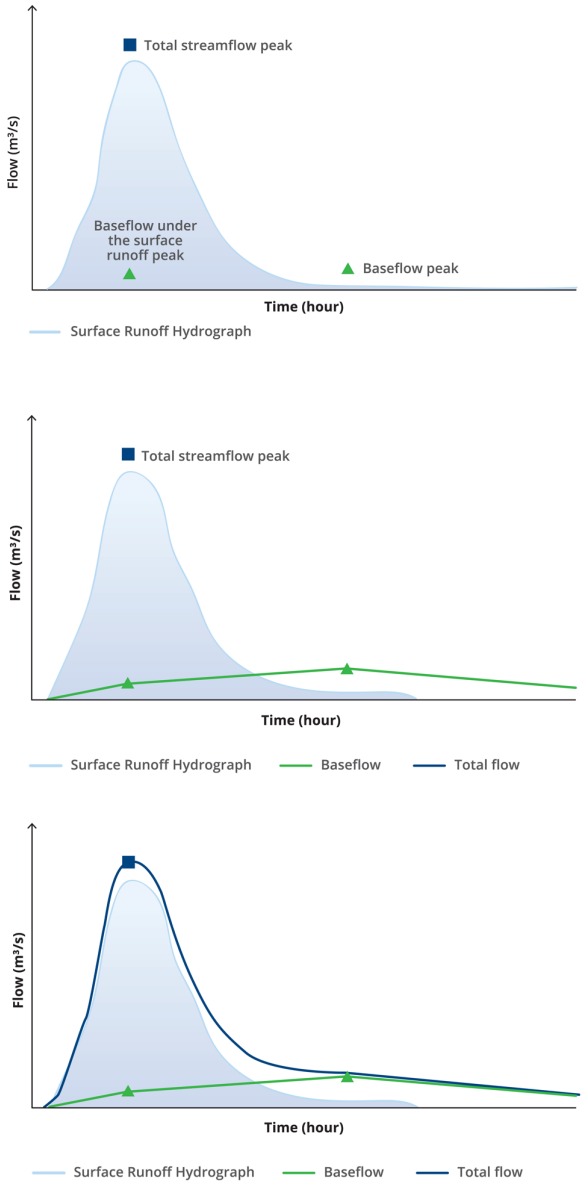

Figure 5.4.7. Total flow hydrograph generation approach, where (a) the data values calculated through the baseflow estimation process are plotted; (b) linear interpolation between the baseflow data points and matching the area under the curve to the baseflow event volume is used to estimate the baseflow time series, which is plotted on the hydrograph in green; and (c) the total streamflow time series is generated by summing the surface runoff and baseflow time series values, with the streamflow hydrograph plotted in dark blue.

4.6. Example

The process described in Book 5, Chapter 4, Section 5 is worked through in a number of different case study examples.

4.6.1. North Maroochy River at Eumundi, Queensland

Catchment 1 is located in south-east Queensland and has a catchment area of 40 km^2. Hourly flow data has been collected at this location since 1982, providing approximately 30 years of data. Very little data was missing or of poor quality, during this period.

The 10% AEP event is of interest for this case study. The reviewed flow data was used to identify flood peaks, in particular the 10% AEP event. A comparable event was identified in the record in February 1999. The event hydrograph was plotted and key characteristics of the baseflow were identified manually (Figure 5.4.8; manually identified baseflow features shown by green points). Straight lines were used to join the key baseflow features, to estimate the baseflow time series. In this instance, the baseflow peak occurs 18 hours after the peak of the streamflow.

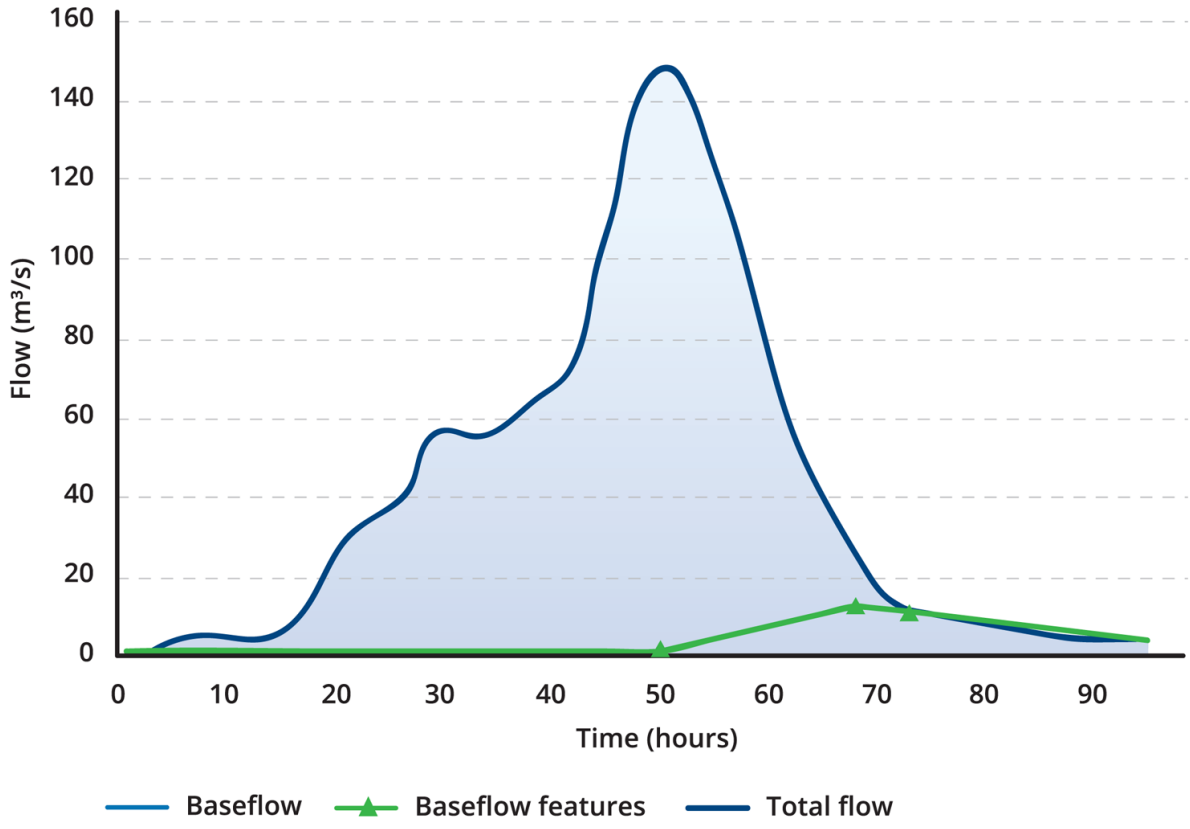

Figure 5.4.8. Streamflow Hydrograph Approximating the 10% AEP Event for the North Maroochy River at Eumundi

The surface runoff hydrograph for the design flood event was generated using a flood event model with a critical duration of 18 hours (Figure 5.4.11, and details in Table 5.4.3).

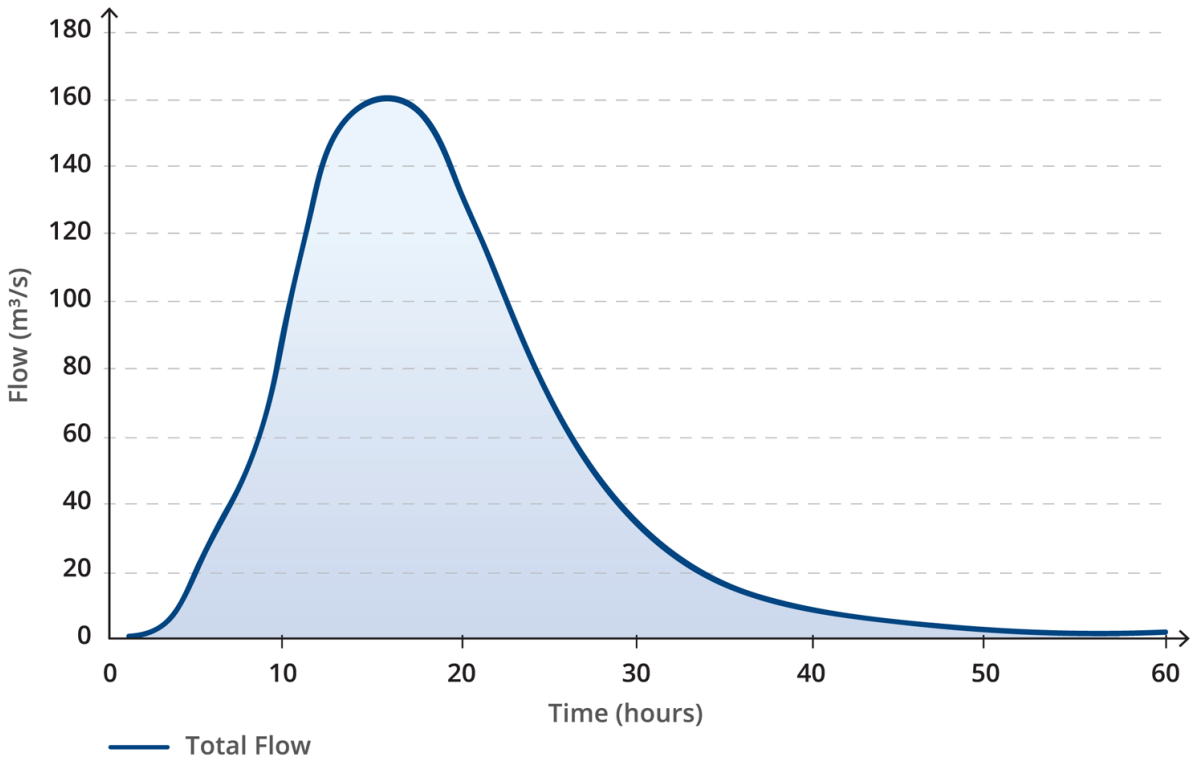

Figure 5.4.9. Surface Runoff Hydrograph for the 10% AEP Design Flood event at Eumundi

Table 5.4.2. Key Surface Runoff Characteristics for the 10% AEP Design Flood Event at Eumundi

Characteristic	Data from design flood
Surface runoff peak flow (m^3/s)	160.6
Time to the surface runoff peak (hours, from the start of the event)	16
Volume of surface runoff for the event (m^3)	9.9×10^6

The baseflow series estimated above was used directly to approximate the baseflow for the 10% AEP design flood event. The baseflow at the time of the streamflow peak (from Figure 5.4.8) was aligned with the Surface Runoff Peak in the design hydrograph (Figure 5.4.11), with the rest of the baseflow hydrograph used to guide the behaviour through the duration of the design event.

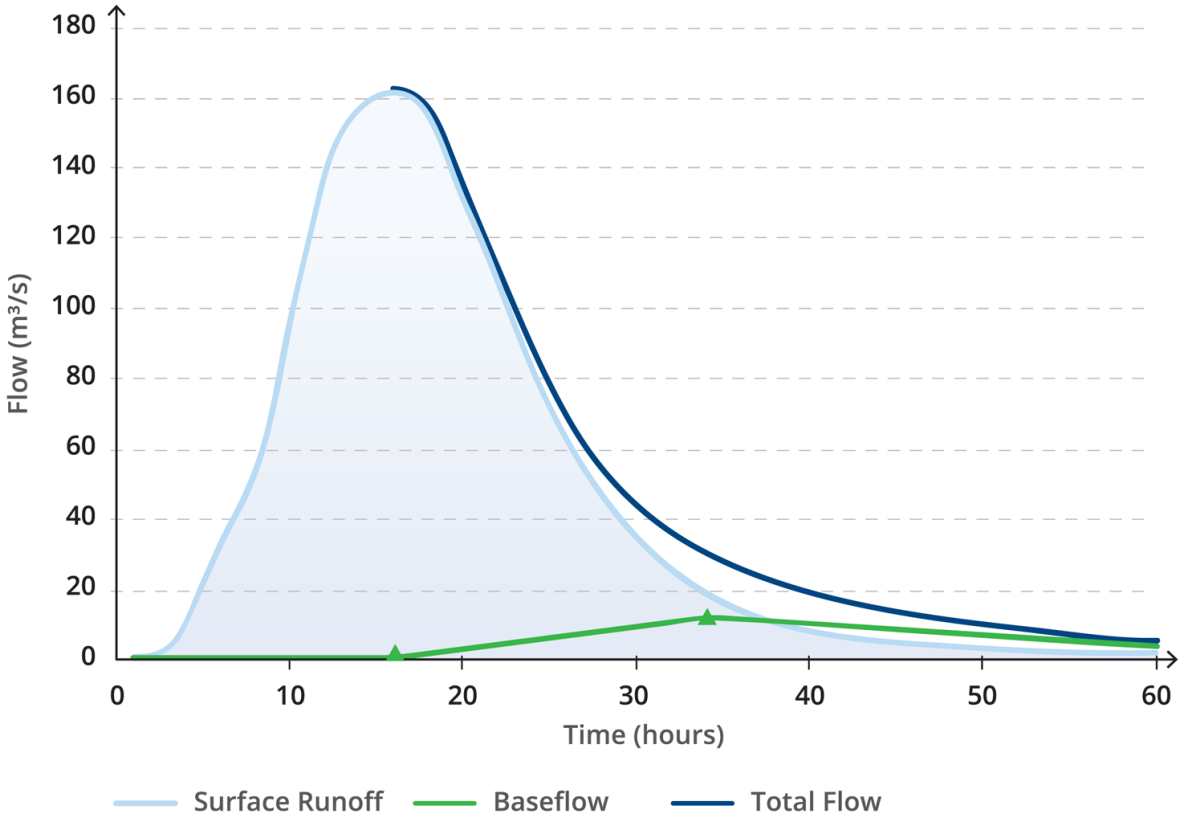

Figure 5.4.10. Surface Runoff, Baseflow and Total Streamflow Hydrographs for the 10% AEP Event at Eumundi

4.6.2. Dirk Brook, Western Australia

Catchment 2 is located in south-west Western Australia. The 1% AEP event is of interest. The Surface Runoff Hydrograph for this event was generated using a flood event model with a critical duration of 18 hours (Figure 5.4.11, and details in Table 5.4.3). This case study assumes that no streamflow data is available for use. The process described in Book 5, Chapter 4, Section 5 has been used to estimate baseflow.

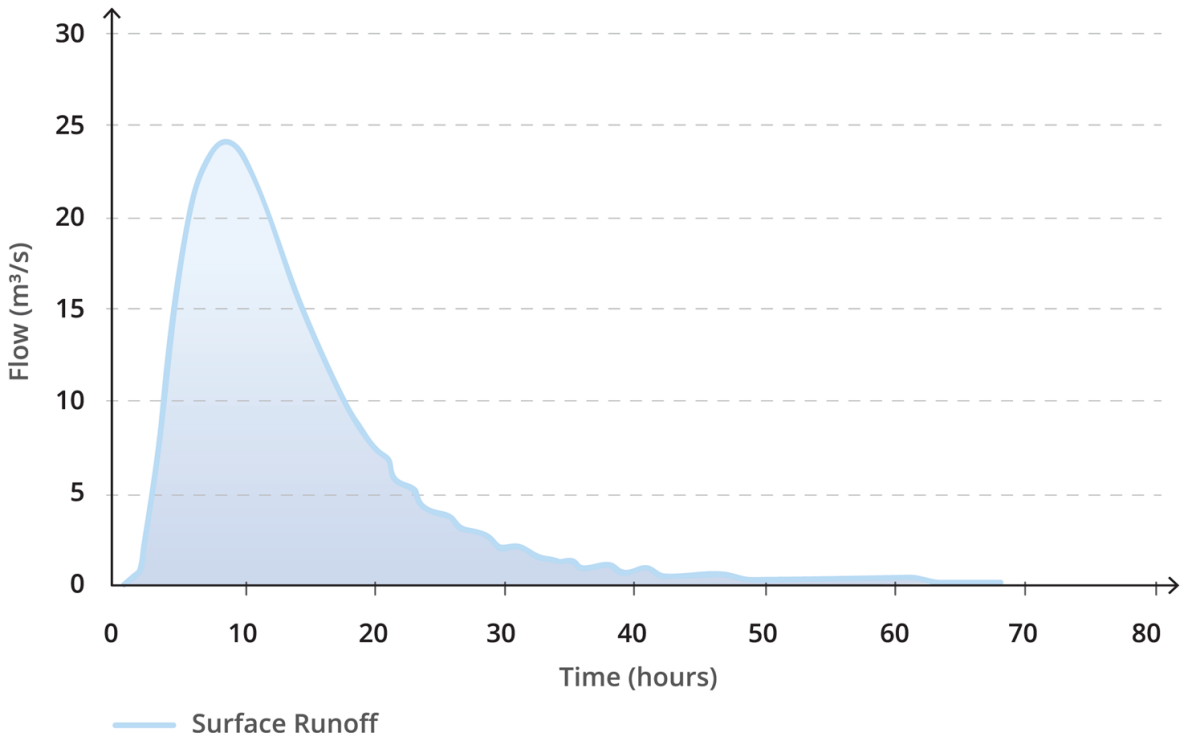

Figure 5.4.11. Surface Runoff Hydrograph for the 1% AEP Design Flood Event at Dirk Brook

Table 5.4.3. Key Surface Runoff Characteristics for the 1% AEP Design Flood Event at Dirk Brook

Characteristic	Data from design flood event
Surface runoff peak flow (m^3/s)	23.9
Time to the surface runoff peak (hours, from the start of the event)	8
Volume of surface runoff for the event (m^3)	1.25×10^6

Aligning the catchment boundary shape file with the spatial data from Figure 5.4.5 allows the Baseflow Peak Factor and Baseflow Volume Factor for the 10% event to be extracted for the catchment area directly:

$R_{BPF\ 10\ \%\ AEP} = 0.186$

$R_{BVF\ 10\ \%\ AEP} = 1.099$

The scaling factor for the 1% AEP event is sourced from Table 5.4.1, with a value of 0.6 for both the peak and volume calculations. Using the relationships described earlier, the final Baseflow Peak Factor, Baseflow Volume Factor and Baseflow Under Peak Factor for application are outlined in Table 5.4.4. These values are applied to calculate the baseflow and total streamflow characteristics in Table 5.4.5, and plotted in Figure 5.4.12.

Table 5.4.4. Calculation of Baseflow Factors for the 1% AEP Design Event for the Dirk Brook

Factors for application	Factor values for 1% AEP design event
Final Baseflow Peak Factor	= 0.6 x 0.186

Factors for application	Factor values for 1% AEP design event
$R_{BPF} = F_{AEP}R_{BPF,\ 10\ \%\ AEP}$	= 0.11
Final Baseflow Volume Factor $R_{BVF} = F_{AEP}R_{BVF,\ 10\ \%\ AEP}$	= 0.6 x 1.099 = 0.66
Final Baseflow Under Peak Factor $R_{BUBF} = 0.7 \times R_{BPF}$	= 0.7 x 0.112 = 0.08

Table 5.4.5. Calculation of Baseflow and Total Streamflow Characteristics for the 1% AEP Event for the Dirk Brook Catchment

Baseflow and total streamflow characteristics	Factor values for 1% AEP
Peak Baseflow	
Peak Baseflow Equation (5.4.1) $Q_{Peak\ baseflow} = R_{BPF}\ Q_{Peak\ surface\ runoff}$	= 0.11 x 23.9 = 2.6 m^3/s
Time to Peak Baseflow Equation (5.4.2) $T_{Peak\ baseflow} = 0.92T_{Peak\ surface\ runoff} + 33.4$	= (0.92 x 8) +33.4 = 41 hours
Baseflow Under the Peak	
Baseflow Under the Streamflow Peak Equation (5.4.4) $Q_{Baseflow\ under\ peak\ streamflow} = R_{BUPF}\ Q_{Peak\ surface\ runoff}$	= 0.08 x 23.9 = 1.9 m^3/s
Total Streamflow Peak	
Total Streamflow Peak Flow Equation (5.4.5) $Q_{Peak\ streamflow} = Q_{Peak\ surface\ runoff} + Q_{Baseflow\ under\ peak\ streamflow}$	= 23.9 + 1.9 = 25.8 m^3/s
Baseflow Volume	
Baseflow Volume Equation (5.4.6) $V_{Baseflow} = R_{BVF}\ V_{Surface\ runoff}$	= 0.66 x 1.25 x 10^6 = 0.83 x 10^6
Total Streamflow Volume	
Total Streamflow Volume Equation (5.4.7) $V_{Total\ streamflow} = V_{Surface\ runoff} + V_{Baseflow}$	= 1.25 x 10^6 + 0.83 x 10^6 = 2.08 x 10^6

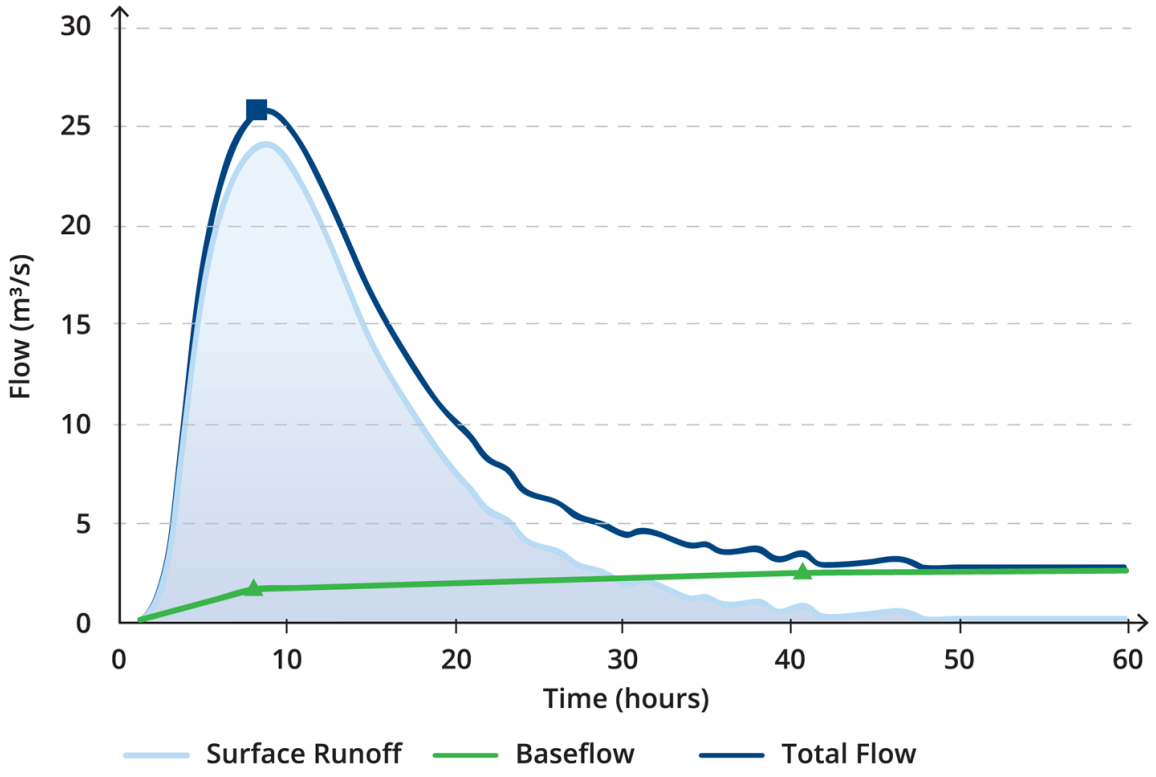

Figure 5.4.12. Surface Runoff, Baseflow and Total Streamflow Hydrographs for the 1% AEP Event at Dirk Brook

4.7. Appendix - Calculation of the Timing of the Baseflow Peak

Analyses undertaken to develop most of the method outlined in Book 5, Chapter 4, Section 5 is described in detail in separate technical documents, available online at the ARR website (Murphy et al., 2010). However, the background behind the calculation of the timing of the baseflow peak is not captured in those documents. A full description of the development of Equation (5.4.2) is provided below. The description below assumes that the reader has an understanding of the work presented in the separate technical documents, and a full background of the broader study concepts is not provided here.

More than 230 suitable catchments across Australia were identified for analysis for ARR Revision Project 7, and hourly streamflow data was collated for each of these locations. A baseflow time series was generated from each flow record using the Lyne and Hollick digital filter, modified to suit hourly streamflow data. The top 4N flood events were identified in the hourly time series data for each catchment, generating a data set of more than 30,000 flood events across the 236 catchments. For each of these events, the magnitude and timing of the total streamflow peak and baseflow peak were identified. The time to these peaks was calculated from the start of the event. At each location, the average time to the streamflow and baseflow peaks were then calculated based on the 4N events.

For the purposes of this assessment, it was assumed that the total streamflow and surface runoff peaks would coincide. This is considered a reasonable assumption since surface runoff is generally the main component of the total streamflow hydrograph.

Analysis of the average time to peak data identified a strong relationship between the time to the surface runoff (and streamflow) and baseflow peaks, as presented in Figure 5.4.13. This relationship provides a direct calculation from which to estimate the timing of the baseflow peak, based upon knowledge of the surface runoff event generated using a flood event model. That is, the time to the baseflow peak (in hours from the start of the event) can be calculated as:

$$T_{\text{Peak baseflow}} = 0.92\ \text{T}_{\text{Peak surface runoff}} + 33.4 \tag{5.4.8}$$

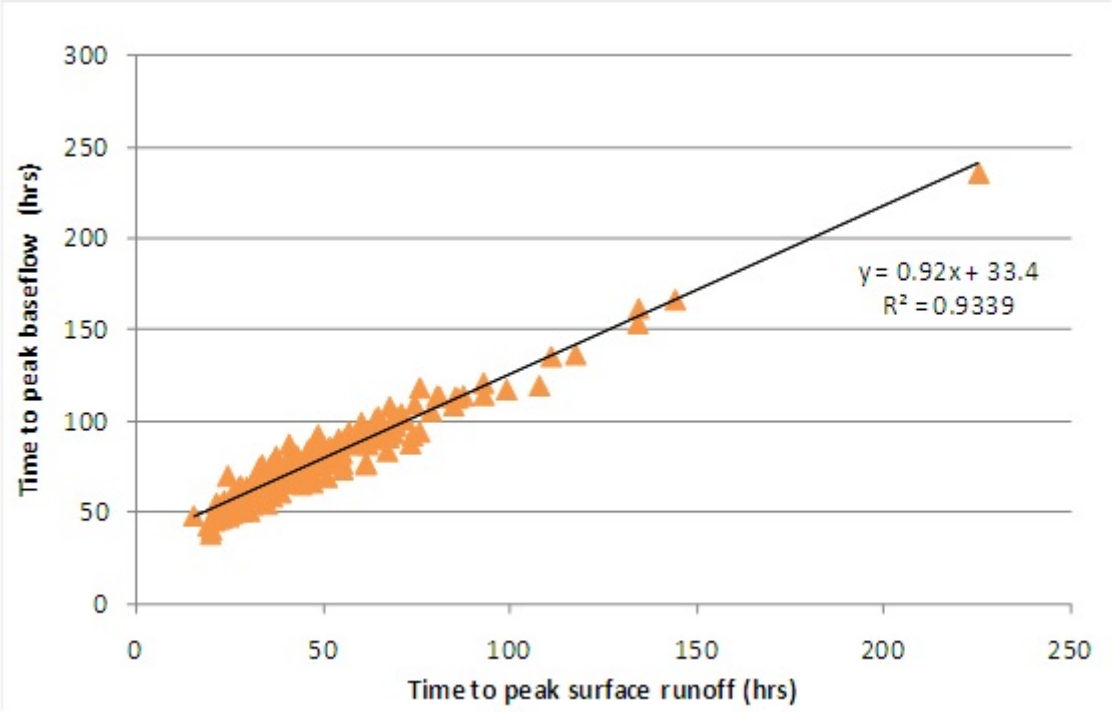

Figure 5.4.13. Comparison of Average Time to Surface Runoff Peak and Time to Baseflow Peak, Based on Analysis of more than 30,000 Flood Events from Catchments across Australia.

4.8. References

Babister, M., Trim, A., Testoni, I. and Retallick, M. 2016. The Australian Rainfall and Runoff Datahub, 37th Hydrology and Water Resources Symposium Queenstown NZ

Brodie, R.S. and Hostetler, S. (2005), A review of techniques for analysing baseflow from stream hydrographs, Proceedings of the NZHS-IAH-NZSSS 2005 conference, 28 November - 2 December, Auckland, New Zealand.

Chapman, T.G. and Maxwell, A.I. (1996), Baseflow separation - Comparison of numerical methods with tracer experiments, Proceedings of the 23rd Hydrology and Water Resources Symposium, 21-24 May, Hobart, Australia.

Graszkiewicz, Z., Murphy, R.E., Hill, P.I., Nathan, R.J. (2011), Review of techniques for estimating the contribution of baseflow to flood hydrographs, Proceedings of the 34th IAHR World Congress, 26 June - 1 July Brisbane, Australia.

Kinkela, K., Pearce, L.J. (2014), Assessment of baseflow seasonality and application to design flood events in southwest Western Australia, Australian Journal of Water Resources, 18(1), 27-38.

Ladson, A.R., Brown, R., Neal, B. and Nathan, R. (2013), A standard approach to baseflow separation using the Lyne and Hollick filter. Aus J Water Resour., 17(1), 25-33.

Murphy, R., Graszkiewicz, Z., Hill, P., Neal, B., Nathan, R., and Ladson, T. (2009), Project 7: Baseflow for catchment simulation, Phase 1 - selection of baseflow separation approach. Report prepared for the Australian Rainfall and Runoff Technical Committee by Sinclair Knight Merz, AR&R Report Number P7/S1/004, ISBN 978-085825-9218.

Murphy, R., Graszkiewicz, Z., Hill, P. and Nathan R. (2010), Project 7: Baseflow for catchment simulation, Data collection and catchment characteristics, Report prepared for Engineers Australia. Avaliable at http://arr.ga.gov.au/downloads-and-software/revision-project-reports

Murphy, R.E., Graszkiewicz, Z., Hill, P.I., Neal, B.P., Nathan, R.J. (2011a), Predicting baseflow contributions to design flood events in Australia, Proceedings of the 34th IAHR World Congress, 26 June - 1 July , Brisbane, Australia.

Murphy, R., Graszkiewicz, Z., Hill, P., Neal, B., and Nathan, R. (2011b), Project 7: Baseflow for catchment simulation, Phase 2 - development of baseflow estimation approach. Report prepared for the Australian Rainfall and Runoff Technical Committee by Sinclair Knight Merz, ARR Report Number P7/S2/017, ISBN 978-0-85825-916-4.

Nathan, R.J. and McMahon, T.A. (1990), Evaluation of automated techniques for base flow and recession analyses, Water Resources Research, 26(7), 1465-1473.

Chapter 5. Flood Routing Principles

James Ball, Erwin Weinmann, Michael Boyd

Chapter Status	Final
Date last updated	14/5/2019

5.1. Introduction

This chapter deals with the modelling of how the direct runoff and baseflow contributions from different parts of the catchment (derived from the models discussed in Book 5, Chapter 3 and Book 5, Chapter 4) are combined and modified on their movement through the catchment to form a hydrograph at points of interest, both at the catchment outlet and inside the catchment. In Book 5, Chapter 5, Section 2 a number of fundamental concepts relevant to flood routing are introduced. Book 5, Chapter 5, Section 3 then deals with the hydrologic principles and methods of storage routing applied in the most widely used flood hydrograph estimation models. In Book 5, Chapter 5, Section 4 the storage routing principles are expanded from linear to non-linear models. Finally, Book 5, Chapter 5, Section 5 introduces a range of hydraulic flood routing approaches that are based on various forms of the unsteady flow equations.

The focus of the descriptions of flood routing approaches and methods in this chapter is on explaining the background, merits and limitations of the different methods employed in flood hydrograph estimation models. The details of how these flood routing principles and methods are applied in flood hydrograph estimation models are covered in Book 5, Chapter 6. For more details on hydraulic analysis and modelling approaches refer to Book 7.

This chapter focuses on rural catchments. Similar routing approaches also apply for urban catchments, but specific issues in urban hydrology are described in detail in Book 9.

5.2. Fundamental Concepts

The runoff inputs generated by various processes in different subareas or sub-catchments are gradually transformed into a combined flood hydrograph at a downstream location. This process is determined principally by various forms of *temporary flood storage* available in the catchment as well as by transmission losses along the flow route. The different elements of a catchment where temporary flood storage occurs include:

- Catchment surfaces (overland flow segments);
- Stream channels;
- Stream banks;
- Floodplains; and
- Drainage channels (or pipes).

These forms of storage are *distributed* in nature – the storage is spread along these catchment elements. In flood hydrograph estimation modelling the different forms of storage do not need to be represented separately but can be modelled as *combined (conceptual) storage elements*.

In addition to the distributed forms of storage, a catchment may also contain lakes, reservoirs or flood detention basins where the storage occurs in a more concentrated form and is represented in models by *concentrated storage elements*. For these concentrated storage elements a more direct relationship exists between inflow and outflow than for distributed forms of storage, as is explained further in Book 5, Chapter 5, Section 3. It is also possible to use concentrated storage elements as a simplified representation of distributed forms of storage (Book 5, Chapter 5, Section 4).

The effects of the different forms of catchment storage on the transformation of flow inputs are twofold (Figure 5.5.1):

i. *Translation* of the hydrograph peak and other ordinates forward in time or, expressed differently, delaying the arrival of the hydrograph peak at a downstream location; and

ii. *Attenuation* or flattening of the hydrograph as it moves along the stream network; this results in a reduction of the peak flow but also in diffusion (spreading out) of the hydrograph, thus extending its duration.

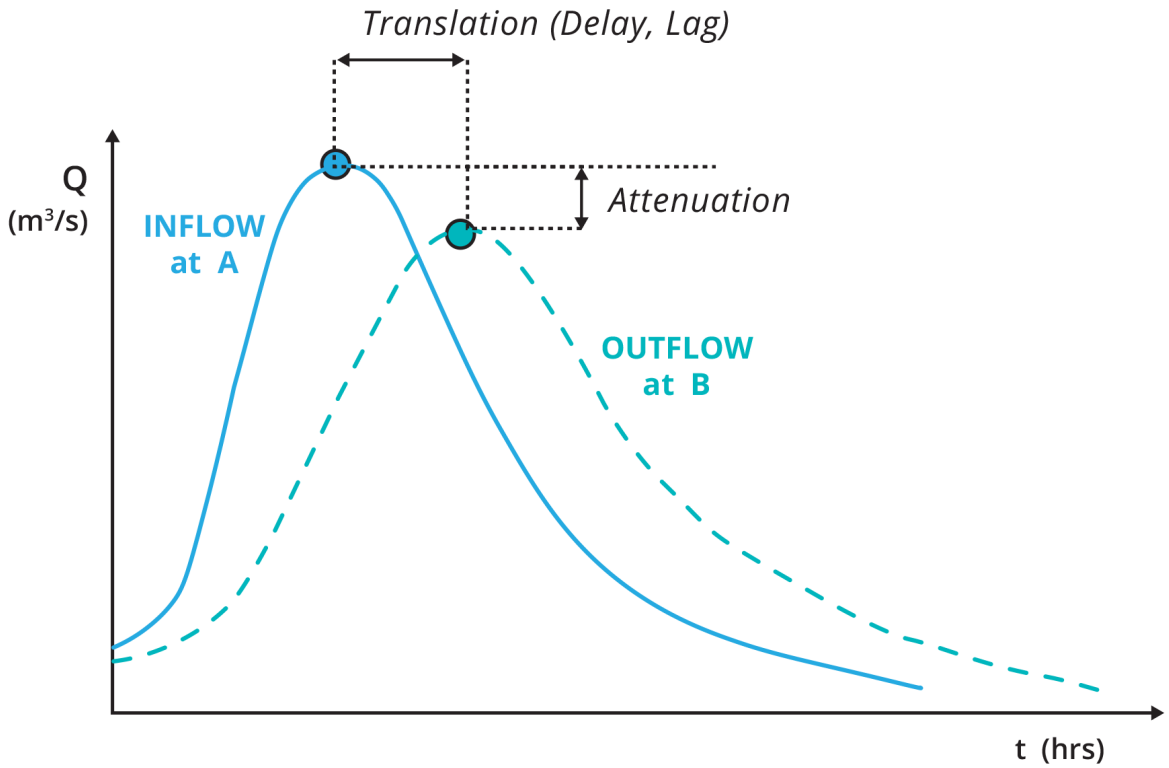

Figure 5.5.1. Effects of Storage on Transforming Inflow Hydrograph

The effects of storage can be modelled through the formulation of the continuity equation for a specific catchment element and over a time interval Δt:

$$I_v = O_v + \Delta S \tag{5.5.1}$$

where I_V is the volume of inflow to the catchment element, O_V is the volume of outflow from the element, and ΔS is the change in the storage during the time interval. The inflow volume (I_V) may represent runoff and baseflow inputs or outflow from an upstream element. While ΔS is positive, the inflow volume to the element is greater than the outflow volume and therefore the storage within the element will increase. Conversely, when ΔS is negative, the

outflow volume is greater than the inflow volume and the storage in the element will decrease.

Due to the principle of mass conservation, the total volumes of inflow to and outflow from the catchment element must be equal. In many situations and particularly in the arid and semi-arid regions of the country, flow in a channel may infiltrate into the banks or bed of the channel; in other words, transmission losses will occur. In these situations, the principle of mass conservation remains, with the volume of the inflow being equal to the volume of the outflow hydrograph plus the volume of the transmission loss.

The application of the continuity equation in the form above refers to *temporary storage* or *detention storage* in different catchment elements. In contrast to this form of storage, where all water is released again during the flood event, there may also be catchment elements with *retention storage* (e.g. reservoirs with a flood storage compartment), where water is retained more permanently and released from the storage mostly after the flood event by controlled releases or, more gradually, through evapotranspiration and seepage losses.

These fundamental flood routing concepts form the basis of the runoff-routing approaches to flood hydrograph estimation discussed in Book 5, Chapter 6, Section 4. Different flood hydrograph estimation modelling systems use flood routing approaches of different complexity, with correspondingly different data requirements. The following Book 5, Chapter 5, Section 3 to Book 5, Chapter 5, Section 5 explain in more detail the theoretical basis and practical application of these different flood routing approaches.

5.3. Hydrograph Translation (Lag)

The simplest method for routing a hydrograph through a channel, pipe, stream or floodplain element is to simply translate all ordinates by a fixed travel time or lag. This method of routing produces pure translation without any attenuation of the hydrograph peak. It is useful for flood routing in systems with little storage (e.g. piped drainage systems) or in situations where the timing of the hydrograph peak is of principal interest (e.g. flood warning systems).

In piped drainage systems the travel time through a pipe segment can be directly determined from the flow velocity through the pipe.

In channels or natural streams the travel time T of a flood hydrograph through a routing reach of length Δx is related to the kinematic wave speed c_k:

$$T = \frac{\Delta x}{c_k} \tag{5.5.2}$$

The travel time or lag is thus directly proportional to the length of the channel reach. For a wide rectangular channel and constant Manning's n, the kinematic wave speed can be approximated as 1.67 times the average flow velocity through the routing reach.

For practical flood routing applications, estimates of the lag time are generally based on systematic analysis of observed flood peak travel times and their variation with flood magnitude. Wong and Laurenson (1983) have examined the variation of the wave speed (reach length divided by travel time of flood peak) with flow magnitude in a number of Australian river reaches. They found that for in-bank flow the wave speed typically increases with flow magnitude but reaches a maximum before bank-full flow and then reduces rapidly, most likely because the effects of bank vegetation become more pronounced. With fully developed floodplain flow the wave speed increases again. This means that travel time

estimates from smaller floods cannot be directly applied to estimate travel times for larger floods and vice versa.

A variation of the simple hydrograph translation approach that also takes into account attenuation effects is the 'Lag and Route' method in which the hydrograph is first translated by the appropriate lag time and then routed through a concentrated linear storage (Fread, 1985).

5.4. Storage Routing

Storage routing methods have been developed as a convenient form of hydrologic routing, to track the movement of a flood wave on its way through a catchment system and to assess the effects of storage on the transformation of an inflow hydrograph to an outflow hydrograph. Storage routing is a lumped approach – it considers only the inputs (inflows) and outputs (outflows) of the system without considering what is happening within the system. Different applications of storage routing principles focus on different types of systems with different forms of storage, e.g. level pool routing methods (concentrated storage as in reservoirs) and river routing methods, including different forms of the Muskingum Method (distributed storage).

Following some basic background on storage routing principles introduced in Section 5.4.1, the main methods in practical use are described in Section 5.4.2 to Section 5.4.4. All the storage routing methods described in these sections are based on a linear relationship between storage and discharge. Some important limitations of the storage routing methods are discussed in Book 5, Chapter 5, Section 4. The non-linear storage routing methods described in Book 5, Chapter 5, Section 5 can overcome some of these limitations.

5.4.1. Basic Equation

The storage routing methods are based on the Conservation of Mass principle which is reflected in the *continuity equation*, expressed as:

$$I - O = \frac{dS}{dt} \tag{5.5.3}$$

Where *I* and *O* respectively are the average rates of inflow and outflow and *dS* is the change in storage during the time interval *dt*. Multiplication of Equation (5.5.3) by the time interval *dt* yields the continuity equation expressed in terms of volumes:

$$\text{INFLOW - OUTFLOW} = \text{CHANGE OF STORAGE} \tag{5.5.4}$$

It is important to note that only the change in storage is considered, rather than the total storage volume; this means that the datum used for the determination of storage volumes is not important as it does not influence the routing calculations.

Storage routing methods do not use a momentum equation (see Book 6, Chapter 2, Section 8) but can reflect the conservation of momentum (dynamic effects) through appropriate selection of their parameters (Koussis, 2009).

5.4.2. Reservoir (Level Pool) Routing

5.4.2.1. Traditional Methods

The category of storage routing approaches commonly referred to as reservoir routing or level pool routing is suitable for systems where storage and outflow are related by a unique

invariant function (ie. a function not subject to hysteresis). These relationships imply that for a given stage (water surface elevation) the outflow is unique and independent of how that stage is developed. Reservoirs or systems with horizontal water surfaces have relationships of this type. For these concentrated storage systems, the peak outflow from the reservoir occurs when the outflow hydrograph intersects the recession limb of the inflow hydrograph, as illustrated in Figure 5.5.2.

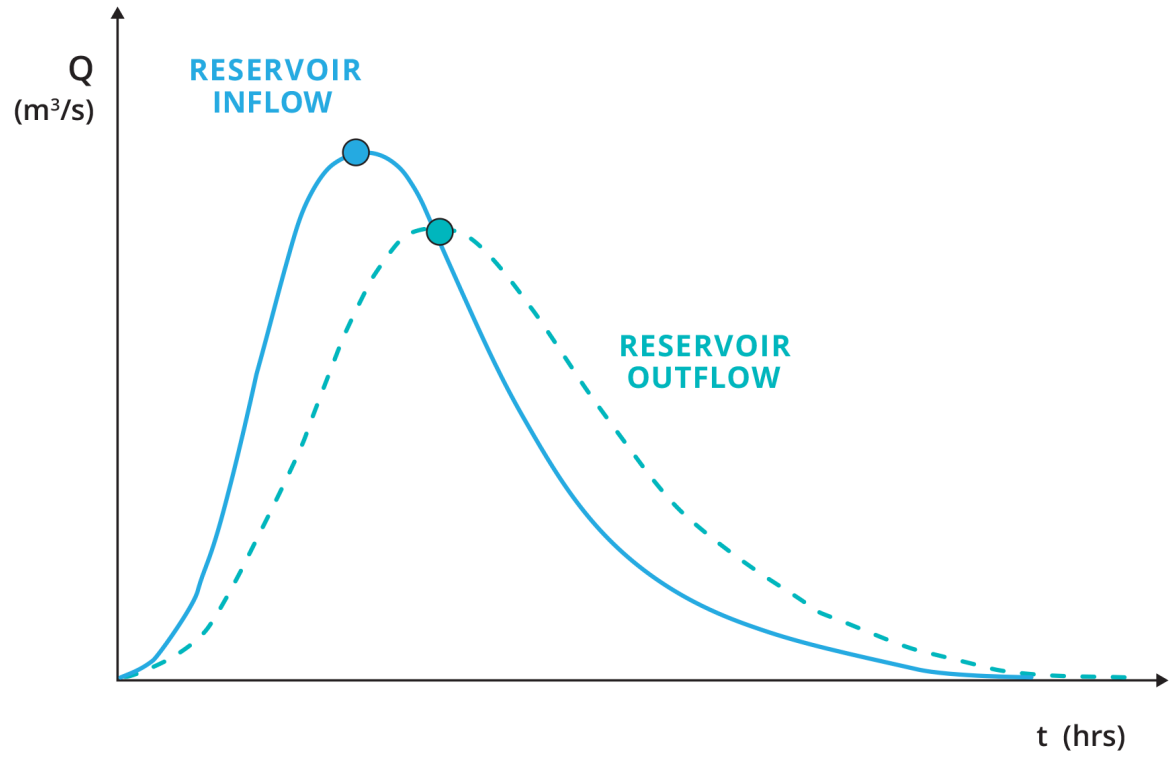

Figure 5.5.2. Effects of Reservoir on Transforming Inflow Hydrograph

The suitability of the assumption of a horizontal water surface during a flood event should be considered when level pool storage routing techniques are applied. If backwater effects create a 'wedge storage' effect (similar to the wedge storage discussed in Book 5, Chapter 5, Section 4) then it might be necessary to develop a storage-discharge relationship for the reservoir where storage depends not only on outflow but also on inflow.

Using a finite difference approximation, Equation (5.5.3) can be written as:

$$\frac{1}{2}(I_1 + I_2)\Delta t - \frac{1}{2}(O_1 + O_2)\Delta t = S_2 - S_1 \qquad (5.5.5)$$

where Δt, is the time increment used for the calculations, and subscripts 1 and 2 refer to the start and end, respectively, of the time period being considered. All variables with the subscript 1 are known either from the initial conditions or from previous calculations. In addition, the inflow at the end of the time period (I_2) is known. Hence, only S_2 and O_2 (ie. the storage and the outflow at the end of the time period) are unknown.

The relationship between storage in a reservoir or detention pond and discharge from it through spillways and outlets is generally highly nonlinear. This means that Equation (5.5.5) cannot be solved analytically but requires a numerical solution method (or traditionally a graphical solution technique).

There are a large number of alternative numerical and graphical techniques for solving Equation (5.5.5); some of these alternatives are presented by Henderson (1966) and Bedient et al. (2008). Possibly, the most commonly used method is the Modified Puls method. The basis of this method is Equation (5.5.5) and the *storage indication curve* given by:

$$\frac{2S}{\Delta t} + Q \text{ vs. } Q \tag{5.5.6}$$

To use the *storage indication curve*, Equation (5.5.5) is rearranged to give:

$$\frac{2S_2}{\Delta t} + O_2 = (I_1 + I_2) + \left(\frac{2S_1}{\Delta t} - O_1\right) \tag{5.5.7}$$

In this equation, all of the known parameters are on the right hand side of the equation while all of the unknown parameters are on the left hand side of the equation. As the value of the right hand side of Equation (5.5.7) is known, Equation (5.5.6) can be used to determine values for $S_2$and O_2. Calculations then proceed to the next time step.

An alternative approach was presented by Henderson (1966) which has the advantage of being self-correcting; in other words, an error in estimating flows at one time period will not flow into subsequent time periods. The approach is based on using a variable *N* defined by:

$$N = \frac{S}{\Delta t} + \frac{O}{2} \tag{5.5.8}$$

Substituting this variable into Equation (5.5.5), after rearranging, results in:

$$N_2 = N_1 + \frac{1}{2}(I_1 - I_2) - O_1 \tag{5.5.9}$$

In this form, all the unknown variables in Equation (5.5.9) are located on the left-hand side of the equation and all the known variables are found on the right-hand side. Equation (5.5.9), therefore, can be solved incrementally for values of N_2 which, with Equation (5.5.8), enables prediction of the unknown outflow rate (O_2).

5.4.2.2. Computer-based Methods

Computer-based solution techniques for the non-linear storage routing equation (Equation (5.5.5)) employ a number of different numerical solution schemes. The first-order Euler scheme produces the following simple expression for reservoir routing (Fenton, 1992):

$$S_2 = S_1 + \Delta t(I_1 - O_1) \tag{5.5.10}$$

Where the outflow *O* is a well-defined function of the storage content *S*. This explicit numerical scheme is stable and accurate if the computational time step Δt is chosen sufficiently small (significantly smaller than the time steps used to define the inflow hydrograph).

If the storage-discharge relationship can be expressed as a power function (Equation (5.5.32)) or other function for which the first derivative can be readily determined, then the Newton-Raphson numerical method can be applied. Other numerical methods such as the Regula Falsi (False Position) method or Runge-Kutta methods are more widely applicable (e.g. Chapra and Canale (2010), Bedient et al. (2008)) give an example of the application of Runge-Kutta numerical solution approaches for detention basin routing.

The general purpose runoff routing modelling systems described in Book 5, Chapter 6, Section 4 incorporate options for routing through reservoirs and detention basins as special cases. Generally the routing routines applied allow for a range of different non-linear formulations of the storage-discharge relationship.

An alternative form of the governing equation for storage routing is given by Fenton (1992), based on expressing both storage content and outflow as a function of *h*, the water surface level in the reservoir (or the head above the spillway crest). The storage increment ΔS can be expressed as the product of the reservoir surface area *A* and level increment Δh. The outflow *O* is then also defined as a function of *h*, and in cases where the outflow depends on operational decisions (e.g. for gated spillways), also as a function of time. Numerical solution methods discussed by Fenton (1992) range from a first order approximation by Euler's method to second order and higher order Runge-Kutta methods.

5.4.2.3. Reverse Routing

At many smaller reservoirs there is no gauging of reservoir inflows but records of reservoir levels (and corresponding storage volumes) and outflows are available from the reservoir operation. In these situations inflow hydrographs can be derived by the process of reverse routing. Reverse reservoir routing is also based on the solution of Equation (5.5.5) but in this case for the unknown inflow I_2. However, most numerical solution schemes exhibit instabilities in the form of severe oscillations in the calculated inflow hydrograph (Boyd et al., 1989). These oscillations arise from relatively small variations in the measured reservoir level, which include random fluctuations due to the effects of wind, waves and measurement inaccuracies.

Boyd et al. (1989) and Zoppou (1999) showed that the following centred explicit finite difference scheme produces stable estimates of the inflow hydrograph without the need for any filtering or smoothing of the calculated hydrograph:

$$I(t) = Q(t) + \frac{S(t+\Delta t) - S(t-\Delta t)}{2\Delta t} \tag{5.5.11}$$

However, as demonstrated by (Boyd et al., 1989), some oscillations may still be introduced if the time step selected is too small, requiring the application of a simple smoothing algorithm to the calculated hydrograph ordinates.

5.4.3. Muskingum Hydrologic Routing

The Muskingum Method of routing flood waves along channels was developed by the US Army Corps of Engineers during a study of the Muskingum River Basin in Ohio, USA (McCarthy, 1938). The basis of the technique is the application of the continuity equation to a control volume and relating the storage within the control volume to the discharge from the control volume. Due to its simplicity, the Muskingum Method is a widely used flood routing technique and also forms the basis of the procedures used in many flood hydrograph estimation models for routing direct runoff to the catchment outlet.

Despite this apparent simplicity, the Muskingum Method, with appropriate selection of its parameters, can be shown to be equivalent to the solution of the convective diffusion equation, the simplest physically-grounded flood routing model (Koussis, 2009). There are many papers in the technical literature discussing its strengths and limitations, as well as proposed enhancements to the classical Muskingum Method. Among these is the classical paper by Cunge (1969) which led to the development of the now widely used Muskingum-Cunge flood routing procedure (Book 5, Chapter 5, Section 4).

5.4.3.1. Muskingum Storage-Discharge Relationship

For level pool flood routing, it is assumed that there is a unique relationship between the storage (*S*) at a given pool level and the discharge or outflow (*O*) from the pool. In contrast, for Muskingum routing, this is replaced by an assumption that the outflow from the control volume will depend on the water level at both the upstream and downstream ends of the control volume. It then follows that the storage within the control volume will depend on the inflow as well as the outflow, and there will be no unique relationship between storage and outflow.

Using this concept, it is common to subdivide the storage within the control volume into prism and wedge storage. These two conceptual storages are schematically illustrated in Figure 5.5.3. The prism storage is formed by a volume of constant cross-section along the length of the prismatic section which is dependent only on the outflow. Wedge storage is dependent on the difference between the inflow and the outflow from the control volume. During the rising limb of the hydrograph, inflow will exceed the outflow and the wedge storage will be positive. Similarly, during the falling limb of the hydrograph outflow will exceed the inflow and the wedge storage will be negative.

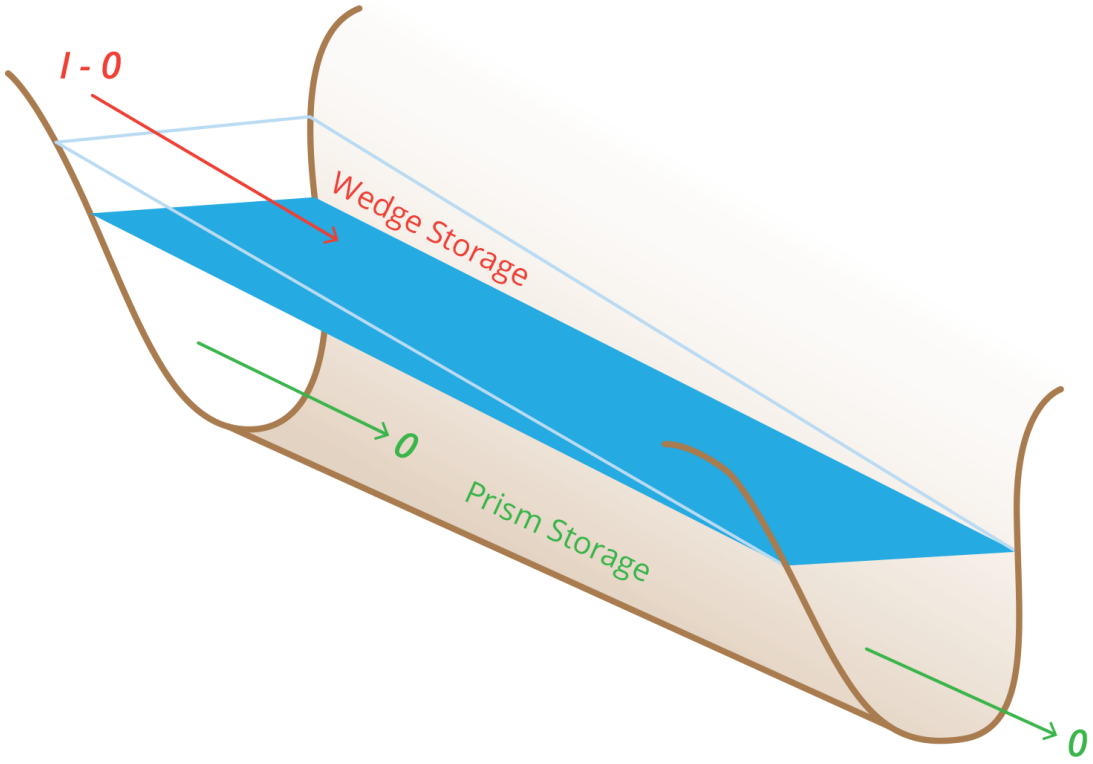

Figure 5.5.3. Prism Storage and Wedge Storage in a River Reach on the Rising Limb of the Hydrograph

The concepts of prism storage and wedge storage can also be applied to non-prismatic natural channels (rivers, streams and floodplains) with prism storage representing uniform flow conditions in the irregular channel.

Assuming a linear relationship between the storage and outflow from the control volume, the prism storage can be shown to be equal to *KO* while the wedge storage will be *KX(I-O)*

where *K* is a proportionality coefficient and *X* is a weighting factor in the range *0 ≤ X ≤ 0.5*. The total storage, which is the sum of the two components, is then given by:

$$S = K[O + X(I - O)] \tag{5.5.12}$$

which can be rearranged to give:

$$S = K[XI + (1 - X)O] \tag{5.5.13}$$

This is the standard form of the storage-discharge relationship used with the Muskingum Method.

The two coefficients, *X* and *K*, can be related to physical characteristics of the routing element. The 'weighting coefficient' *X* depends on the shape of the wedge storage and *K* reflects the travel time of the flood wave through the routing element (given by the time lag between the centroids of the inflow and the outflow hydrographs). The value of *X* varies from 0 for a reservoir type storage to 0.5 for a full wedge (or fully distributed storage). When *X* is equal to 0, there is no wedge and, hence, the inflow has no influence on the storage volume; this being the implicit assumption made with level pool routing. In this case the Muskingum equation reduces to *S = KQ*, the storage-discharge (S-Q) relationship for a fully concentrated storage. In most natural streams, *X* is approximately 0.2 but can vary from 0 to 0.3. A value of *X* equal to 0.5 corresponds to fully distributed storage, where the hydrograph is translated with little attenuation. Great accuracy in determining the value of *X* is not necessary as the predicted hydrograph is relatively insensitive to the value of this parameter.

The storage coefficient (*K*) has dimensions of time and represents the average travel time of the flood wave through the reach; this time can be estimated by considering the centroids of the inflow and outflow hydrographs. The relationship of *K* with the physical characteristics of the routing element is further discussed in Book 5, Chapter 5, Section 4.

5.4.3.2. Muskingum Equation – Classical Coefficients

The development of the Muskingum Method is based on a finite difference approximation to the continuity equation (Equation (5.5.3)), ie:

$$\frac{I_n + I_{n+1}}{2} - \frac{O_n + O_{n+1}}{2} = \frac{S_{n+1} - S_n}{\Delta t} \tag{5.5.14}$$

together with Equation (5.5.11) expressed for time t_n and time t_{n+1} respectively as:

$$S_n = K[XI_n + (1 - X)O_n] \tag{5.5.15}$$

$$S_{n+1} = K[XI_{n+1} + (1 - X)O_{n+1}] \tag{5.5.16}$$

where Δt is the time increment between times t and n t_{n+1}. Subtracting Equation (5.5.13) from Equation (5.5.14) gives the change in storage over time Δt as:

$$S_{n+1} - S_n = K\{[XI_{n+1} + (1 - X)O_{n+1}] - [XI_n + (1 - X)O_n]\} \tag{5.5.17}$$

Combining Equation (5.5.15) with Equation (5.5.12) results in the routing equation for the Muskingum Method which usually is expressed as:

$$O_{n+1} = C_1 I_{n+1} + C_2 I_n + C_3 O_n \tag{5.5.18}$$

where the Muskingum coefficients (C_1, C_2 and C_3) are given by:

$$C_1 = \frac{\Delta t - 2KX}{2K(1-X) + \Delta t}$$
$$C_2 = \frac{\Delta t + 2KX}{2K(1-X) + \Delta t} \qquad (5.5.19)$$
$$C_3 = \frac{2K(1-X) - \Delta t}{2K(1-X) + \Delta t}$$

It should be noted that summation of the Muskingum coefficients should give a value of unity ($C_1 + C_2 + C_3 = 1$). This provides an easy and a quick check that the coefficient values have been calculated correctly.

Example: Muskingum Flood Routing – Werribee River (after Laurenson (1998))

The outflow hydrograph from Melton Reservoir is to be routed through a 20 km reach of the Werribee River to Werribee Weir. As described in Book 5, Chapter 5, Section 4, analysis of an observed flood event has produced the following routing parameter estimates: K = 4.64 hours, X = 0.25. The routing calculations use a time step Δt = 2 hours. The Muskingum coefficients C_1, C_2 and C_3 are calculated from Equation (5.5.19) and are shown at the top of Table 5.5.1.

Table 5.5.1. Calculations for the Muskingum Routing Example

Time (hours)	Inflow (m^3/s)	C_1 -0.036	C_2 0.482	C_3 0.554	Outflow (m^3/s) Actual	Outflow (m^3/s) Calculated
14:00	0				**0**	**0**
16:00	66	-2	0	0	**8**	**-2**
18:00	150	-5	32	-1	**34**	**25**
20:00	253	-9	72	14	**64**	**77**
22:00	325	-12	122	43	**147**	**153**
0:00	391	-14	157	85	**245**	**227**
2:00	420	-15	189	126	**310**	**299**
4:00	309	-11	203	166	**356**	**357**
6:00	247	-9	149	198	**330**	**338**
8:00	211	-8	119	187	**290**	**299**
10:00	166	-6	102	165	**245**	**261**
12:00	139	-5	80	145	**216**	**220**
14:00	88	-3	67	122	**185**	**185**
16:00	86	-3	42	103	**150**	**142**
18:00	82	-3	41	79	**122**	**117**
20:00	63	-2	40	65	**104**	**102**
22:00	55	-2	30	57	**96**	**85**
0:00	54	-2	27	47	**90**	**72**
2:00	52	-2	26	40	**76**	**64**
4:00	50	-2	25	35	**68**	**59**
6:00	49	-2	24	32	**62**	**55**

Time (hours)	Inflow (m^3/s)	C_1 -0.036	C_2 0.482	C_3 0.554	Outflow (m^3/s) Actual	Calculated
8:00	48	-2	24	30	**59**	**52**
10:00	47	-2	23	29	**57**	**50**
12:00	37	-1	23	28	**55**	**49**
14:00	36	-1	18	27	**53**	**44**
16:00	36	-1	17	24	**50**	**40**
18:00	36	-1	17	22	**42**	**38**
20:00	36	-1	17	21	**36**	**37**

Figure 5.5.4 shows the inflow hydrograph and the observed and calculated outflow hydrographs. The inflow hydrograph at Melton Reservoir (Column 1) has a peak flow of 420 m^3/s at 2.00 am of Day 2, while the calculated outflow peak at the end of the 20 km reach (Column 7) is 357 m^3/s occurring at 4.00 am on the same day. This is close to the actual (observed) peak flow of 356 m^3/s (Column 6).

The calculated hydrograph has a small 'initial dip' (negative flow values) at time 16.00 hour on Day 1. Such a dip results for values of X > 0 if the time step is shorter than the travel time through the reach (in other words, the outflow is calculated before the change in inflow has travelled through the reach).

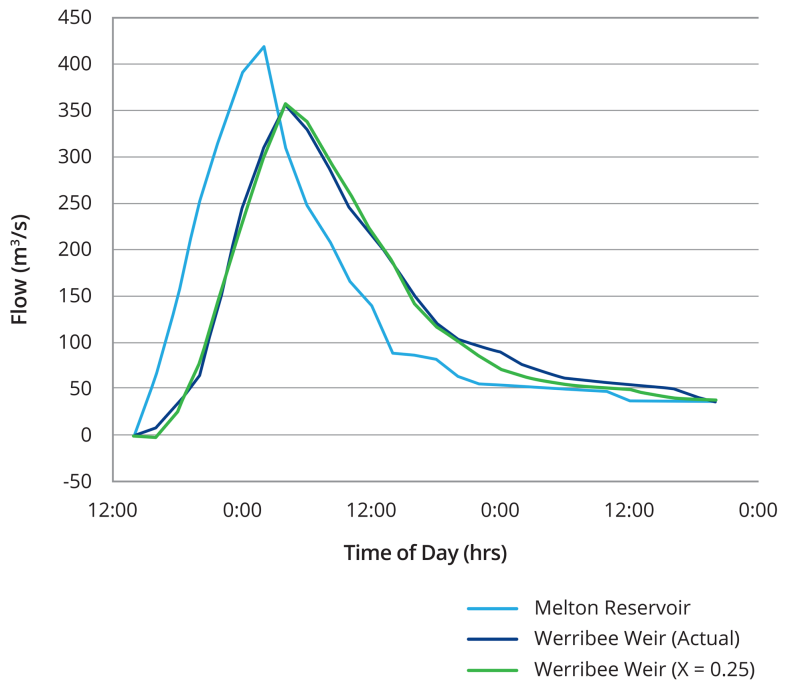

Figure 5.5.4. Werribee River Example – Inflow Hydrograph and Observed and Calculated Outflow Hydrographs

Figure 5.5.5 illustrates the impact of changing the routing parameter *X* from the optimum value of *X* = 0.25 to *X* = 0 (concentrated or reservoir-type storage) and *X* = 0.5 (fully distributed storage). It can be seen that a concentrated storage results in greater attenuation, with the peak of the outflow hydrograph on the falling limb of the inflow hydrograph, while fully distributed storage results in almost pure translation of the inflow hydrograph. With *X* = 0.5, there is a very noticeable initial dip in the outflow hydrograph.

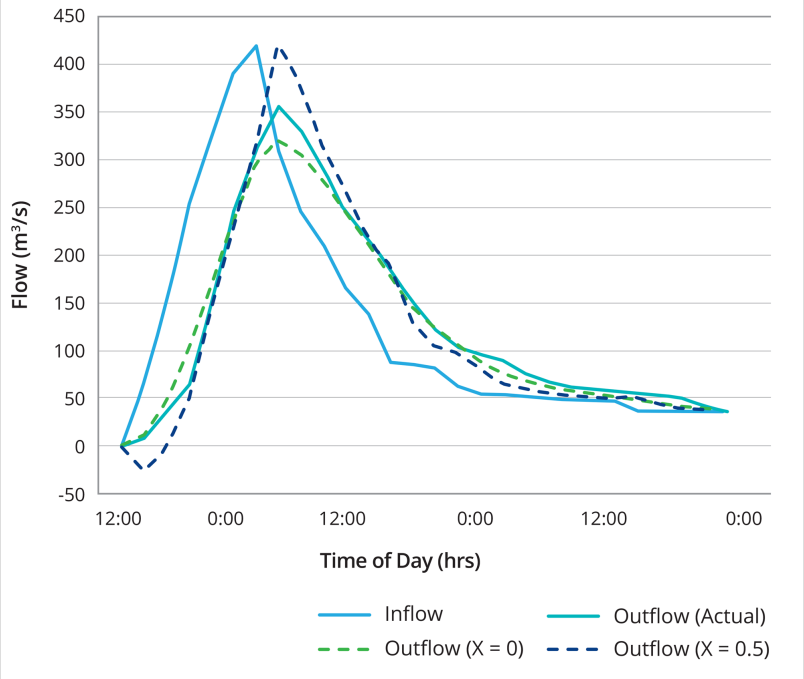

Figure 5.5.5. Werribee River Example – Impact of Routing Through Concentrated Storage (X = 0) or Fully Distributed Storage (X = 0.5)

5.4.3.3. Muskingum Equation – Nash Coefficients

An alternative development of the coefficients in the Muskingum routing equation was presented by Nash (1959). These alternative coefficients are:

$$C_1 = 1 - \frac{K(1-c)}{\Delta t}$$
$$C_2 = \frac{K(1-c)}{\Delta t} - c \qquad (5.5.20)$$
$$C_3 = c$$
$$c = e^{\frac{-\Delta t}{K(1-X)}}$$

Pilgrim (1987) suggests that these coefficients are more accurate than the classical coefficients. The basis of this suggestion is that the coefficients proposed by Nash (1959) do not require the ratio *Δt/K* to be small and, furthermore, the coefficients are not based on the finite difference approximation to the continuity equation (Equation (5.5.12)) but rather on the differential form of the continuity equation.

When *Δt/K* is small, the two alternative estimates of the routing coefficients should converge.

Given that current approaches to implementation of any flood routing approach are based on computer applications, the historical need for large *Δt* and hence large ratios of *Δt/K* due to the use of hand calculations is no longer relevant. Therefore, those applying Muskingum techniques within computerised applications should not notice any difference between use of the classical and Nash formulations of the coefficients, so long as an appropriately short time step is adopted for the simulations.

For the Werribee River example, replacing the standard Muskingum coefficients with Nash coefficients results in an outflow peak of 353 m^3/s, a difference of only about 1% from the original result.

5.4.3.4. Estimation of Muskingum Parameters X and K

When the Muskingum flood routing method is used, it is necessary to determine the values of two parameters; these are the parameters *K* and *X*. In general, estimation of the values for these coefficients requires recorded flood hydrograph information.

There are a number of methods by which the recorded flood information can be used to derive values for *K* and *X*. These vary from graphical approaches as outlined below to optimisation approaches as presented by Stephenson (1979) and Chang et al. (1983).

A classical graphical method is based on combining Equation (5.5.14) and Equation (5.5.17) which, after rearrangement, results in:

$$K = \frac{0.5\Delta t\left[\left(I_{n+1} + I_n\right) - \left(O_{n+1} + O_n\right)\right]}{X\left(I_{n+1} - I_n\right) + (1 - X)\left(O_{n+1} - O_n\right)} \tag{5.5.21}$$

The numerator represents the change in storage during the time interval *Δt* and the denominator is the weighted discharge for a selected value of *X*. The computed values of the cumulative storage values are plotted against the weighted discharge for each time interval, with the usual result being a graph in the form of a loop. The value of *X* that produces a loop closest to a straight line is adopted as the value for *X*. The value for *K* is given by the slope of the line.

Figure 5.5.4 illustrates typical results obtained with this technique for the Werribee River example introduced in Book 5, Chapter 5, Section 4 (Laurenson, 1998). In this example a value of *X* = 0.25 produced the narrowest loop. The *K* value is computed as the slope of the fitted line:

$$K = \frac{1}{3600}\frac{5750000 - (-100000)}{350 - 0} = 4.64 hours \tag{5.5.22}$$

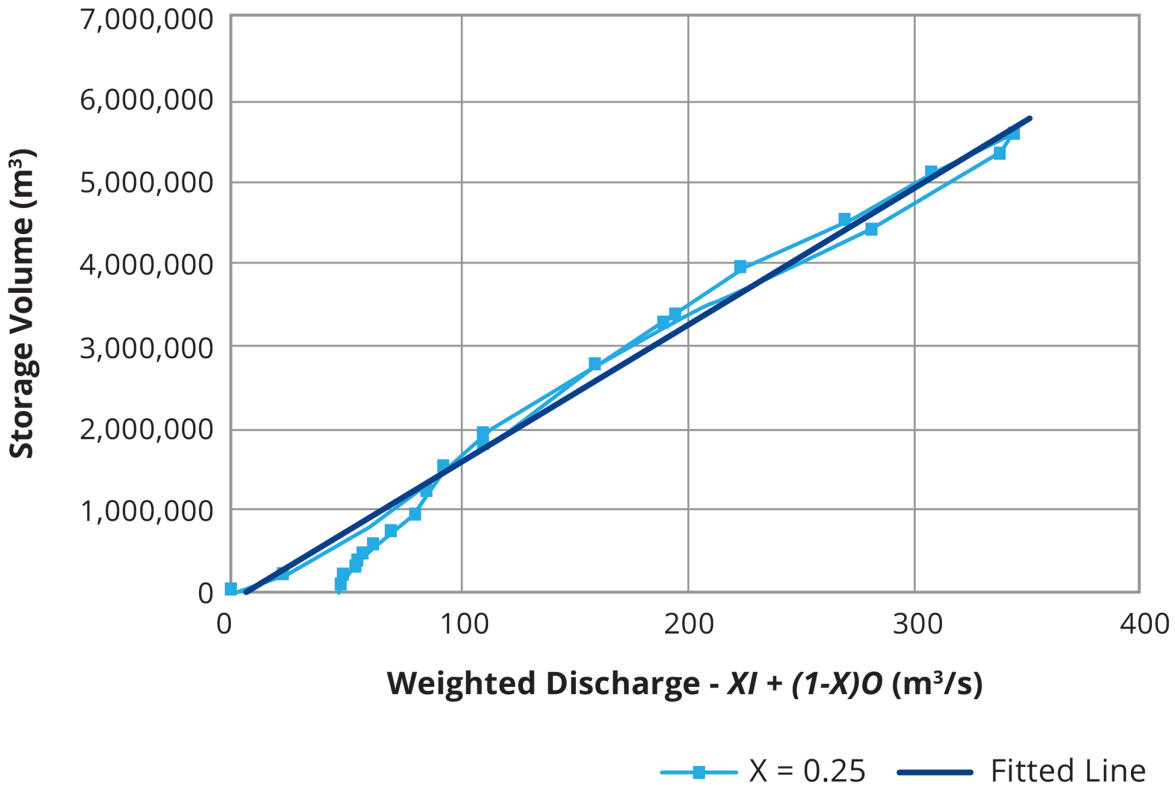

Figure 5.5.6. Graphical Estimation of X and K (after Laurenson (1998))

Some points to note with respect to the estimation of *X* and *K* are:

- Failure to collapse to a straight line indicates that the length of the reach being considered is too long;
- Inflow and outflow hydrograph peaks of similar magnitude indicates that *X* will be close to 0.5;
- A peak of the outflow hydrograph much smaller than the peak inflow indicates that *X* will be close to zero;
- An inconsistent slope of the line after evaluation of *X* indicates a change in the storage characteristics. This change may be due to, for example, inundation of the floodplains adjacent to the river channel. In these circumstances, the practitioner needs to use the slope of the line most appropriate for the problem being investigated to select the value of *K*; and
- As discussed in Book 5, Chapter 5, Section 3, flood travel times vary substantially with flood magnitude. If floods of different magnitudes are to be routed, the storage analysis needs to be carried out for a range of floods and the flood routing parameters varied accordingly.

In a discussion of determining the Muskingum coefficients, Chang et al. (1983) suggested the use of classical approaches based on the best fit between weighted storage and discharge need not result in optimal values of the routing coefficients; in other words, the classical approaches for determining the Muskingum coefficients may not result in values that minimise the error between observed and predicted hydrographs. The alternative to the classical approaches for determining the values of the two routing coefficients in the Muskingum method is the application of optimisation techniques.

Stephenson (1979) presents one such application where linear programming was used to minimise the difference, or error, between a predicted and recorded hydrograph for a recorded inflow hydrograph. The error function used in this application was the sum of the absolute values of the differences between the recorded and predicted hydrographs; values of the routing coefficients that minimised this error function were assumed to be the appropriate values for the coefficients. It was noted, however, that use of alternative error functions would result in different values for the routing coefficients.

5.4.3.5. Reverse Routing in River Reach

In some situations it may be desirable to determine a hydrograph at an upstream river location from an observed hydrograph at a downstream location. As shown by (Boyd et al., 1989) this can also be achieved by the solution of Equation (5.5.14) by a Muskingum-type numerical scheme, but to avoid numerical oscillations, the reverse routing calculations need to be carried out backward in time, starting at the end of the hydrograph. An equivalent to Equation (5.5.18) can then be written as:

$$I_{n-1} = \frac{1}{C_2} Q_n - \frac{C_s}{C_2} Q_{n-1} - \frac{C_1}{C_2} I_n \tag{5.5.23}$$

5.4.4. Muskingum-Cunge Storage Routing

5.4.4.1. Introduction

The Muskingum-Cunge technique was developed from a discussion of the Muskingum Method by Cunge (1969). The basis of this discussion was an attempt to explain the apparent attenuation of a flood wave when the Muskingum technique is used to route a hydrograph through a river reach. The Muskingum technique assumes that there is a singular relationship between the storage and the discharge. This assumption leads to a differential equation whose analytical solution does not allow for wave damping (attenuation of the flood wave).

However, application of the Muskingum technique results in attenuation of the flood wave as it moves downstream. This contradiction between the analytical and the numerical applications required investigation. It is worthwhile noting that other methods, such as numerical solutions of the kinematic wave equation, also demonstrate similar characteristics, ie. application of the method results in attenuation of flood waves despite theoretical considerations indicating that no flood wave attenuation should occur.

Since its proposal by Cunge (1969), the Muskingum-Cunge technique has achieved widespread usage; for example, it is an option available in several flood hydrograph modelling systems for routing of flows along channels. One advantage of the Muskingum-Cunge technique is that its application does not require the use of historical flood events for estimation of the lag parameter or the weighting coefficient.

5.4.4.2. Derivation of Muskingum-Cunge Routing Scheme

As explained in Koussis (2009), Cunge showed in his seminal 1969 paper that the Muskingum flood routing scheme can be derived either from a second order approximation of the *convective diffusion (Equation (5.5.21)*) or by a particular discretisation of the *kinematic wave equation* – equation Equation (5.5.21) with the right hand side (the diffusion term) set to zero (the derivation of equation Equation (5.5.21) is further explained in Book 5, Chapter 6, Section 5):

$$\frac{\partial Q}{\partial t} + C_k \frac{\partial Q}{\partial x} = D \frac{\partial^2 Q}{\partial x^2} \tag{5.5.24}$$

with

$$C_k = \frac{\partial Q}{\partial A} \tag{5.5.25}$$

representing the kinematic wave celerity, and

$$D = \frac{Q}{2BS_o} \tag{5.5.26}$$

the diffusion coefficient.

where *Q* is the discharge, *x* the distance along the channel, *A* the cross-sectional area, *B* the water surface width and S_o the channel slope.

Through the diffusion term, the convective diffusion equation allows for the diffusive effects of the flood wave movement (attenuation of the flood peak) on its movement downstream. It should be noted that, through inclusion of the 'pressure term' from the complete momentum equation, the diffusion wave equation allows for backwater effects to be reflected in the flood routing. However, this feature is lost through the second order approximation in the Muskingum-Cunge method.

5.4.4.3. Muskingum-Cunge Coefficients

The Muskingum-Cunge technique uses the same coefficient equation as the classical Muskingum Method:

$$O_{n+1} = C_1 I_{n+1} + C_2 I_n + C_3 O_n \tag{5.5.27}$$

However, the direct link to the hydraulically-based convective diffusion or kinematic wave equation now allows the coefficients given by Equation (5.5.17) or Equation (5.5.18) to be determined using the hydraulic characteristics of the channel reach.

The Muskingum lag parameter *K* (which has the dimensions of time) is directly linked to the kinematic wave celerity C_k:

$$K = \frac{\Delta x}{C_k} \tag{5.5.28}$$

where Δx is the length of the routing reach and C_k is as defined by Equation (5.5.25). When *Q* is calculated from the Manning Equation, and the cross-sectional area, wetted perimeter and the roughness parameter are known functions of depth or stage, the derivative *dQ/dA* in Equation (5.5.25) can be evaluated. For a wide rectangular channel and Manning's *n* constant with changing flow depth, the kinematic wave celerity can be approximated as 1.67 times the average flow velocity through the routing reach.

To avoid confusion with the distance (*x*), the Muskingum weighting coefficient (*X*) is now labelled θ and evaluated as:

$$\theta = \frac{1}{2}\left(1 - \frac{Q}{C_k B S_o \Delta x}\right) \tag{5.5.29}$$

where Q is a representative discharge for the hydrograph being routed and the other terms are as defined before (corresponding to the same representative discharge).

The direct links of the Muskingum-Cunge coefficients to physical routing reach characteristics allows the application of the method in ungauged catchments and in situations where the routing characteristics are modified from those experienced during model calibration.

For the Werribee River example from Example: Muskingum Flood Routing – Werribee River (after Laurenson (1998)) the relevant routing reach characteristics are as follows:

Δx = 20 km

C_k = 1.2 m/s

Q = 210 m^3/s

B = 35 m and

S_0 = 0.0005.

Application of Equation (5.5.28) and Equation (5.5.29), respectively, gives values of K = 4.63 hours and

X = 0.25. As these values are almost identical to the values used in the original calculations, there is little difference in the results obtained with the Muskingum-Cunge method.

5.4.4.4. Representing Distributed Storage by a Series of Concentrated Storages

It has been shown by Kalinin and Miljukov (1958) and Laurenson (1962) that a similar representation of the translation and attenuation effects of distributed storage as in the Muskingum Method can be achieved by routing through a series of concentrated storages (ie. with the Muskingum weighting coefficient X = 0). However, for this method to be essentially equivalent to the Muskingum-Cunge Method, the length of the routing reaches represented by a concentrated storage (Δx) has to be selected in accordance with the following criterion (Weinmann, 1977; Wong , 1985):

$$\Delta x^* = \frac{Q}{S_o B C_k} \tag{5.5.30}$$

where Δx^* is the characteristic reach length proposed by Kalinin and Miljukov (1958). The optimum number of sub-reaches represented by a concentrated storage(N^*) can then be calculated as $L/\Delta x^*$, where L is the total length of channel to be routed through.

This means that the steeper the channel and the faster the flood wave travels for a given discharge per unit width, the shorter the routing reaches and thus the larger the number of routing reaches required. For very flat channels and slow moving flood waves, the number of sub-reaches required approaches one; the whole river reach can thus be expected to act like a concentrated storage. Using a number of storages less than N^* will tend to overestimate the degree of attenuation compared to translation, while using a larger number of storages will have the opposite effect.

Wong (1985) confirmed that using too few concentrated storages resulted in underestimation of both the peak flow and the travel time. Conversely, using a greater number of concentrated storages enhances the translation effects and increases the peak flow. However, beyond a certain number of storages the lag time does not increase any further but the peak flow will still increase.

These findings have implications for the application of runoff-routing models using a series of linear or nonlinear storages, as discussed in Book 5, Chapter 6, Section 4.

Werribee River Flood Routing Example – Kalinin-Miljukov Method

For this example the total routing reach of 20 km is divided into two sub-reaches of 10 km length, each being represented by a concentrated storage (X = 0). If the same wave speed of c_k = 1.2 m/s is used as for the Muskingum-Cunge Method, the routing parameter is calculated as $K = \Delta x/c_k$ = 2.31 hours.

Figure 5.5.7 shows the outflow hydrographs for the two sub reaches; it indicates that routing through a cascade of two linear storages (ie. the application of the Kalinin-Miljukov Method) results in slightly greater attenuation of the peak flow than obtained with the single reach Muskingum Method. The calculated peak flow is 338 m^3/s, which is 5% less than the actual observed flow at Werribee Weir.

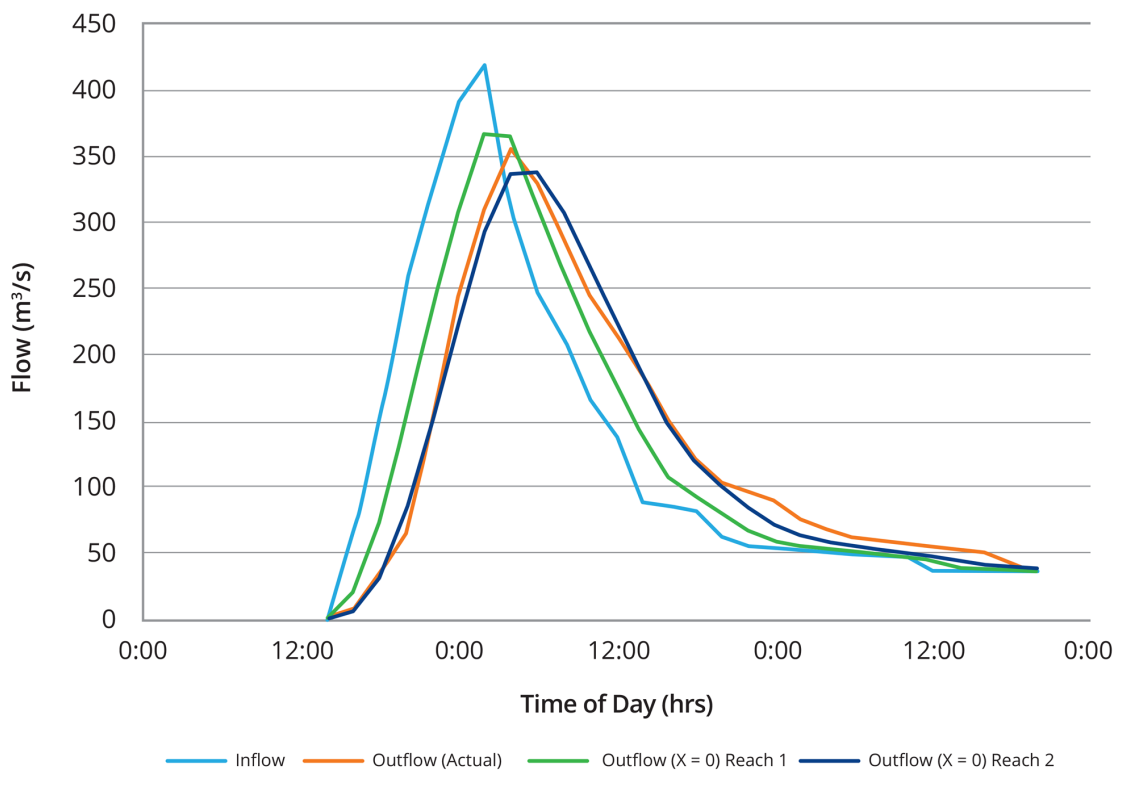

Figure 5.5.7. Werribee River Example – Application of the Kalinin-Miljukov Method (Two Routing Reaches of 10 km Length)

5.4.5. Limitations of the Muskingum Method

While the Muskingum Method of flood routing in its various forms has become very popular, due to its relative simplicity when compared to the more complete flood routing techniques, there are some limitations to its usage. Among these limitations are:

i. The assumption of a linear relationship between *S*, *I* and *O*. Although, in many instances, the actual relationships approximate a straight line when suitable values of *X* and *K* are selected, there is no physical or theoretical justification for this assumption. The linear assumption limits the degree of extrapolation to flood events similar in magnitude to those used in the calibration of the routing parameters (approaches to overcome this limitation are discussed in Book 5, Chapter 5, Section 5);

ii. For the classical Muskingum Method the evaluation of *X* and *K* requires the use of historic flood data and therefore is based on the channel geometry within the limited range of that flood data. Extrapolation for higher flood levels may require modification of the values for *X* and *K* to reflect any significant changes in channel characteristics. The Muskingum-Cunge Method can at least partly overcome this limitation;

iii. The need for the volume of the inflow hydrograph to equal the volume of the outflow hydrograph, which means that lateral inflows have to be added at either end of the routing reach;

iv. The method has an inherent problem in that it may produce physically unrealistic negative outflows (an 'initial outflow dip') when the inflow hydrograph rises steeply. This can be overcome by specifying a minimum routing time step Δt of $2KX$;

v. The inability of the method to consider downstream disturbances that propagate upstream (backwater effects). This places limitations on the application of the method in relatively flat stream reaches; and

vi. The limited ability to deal with fast rising hydrographs, due to the neglect of the acceleration terms in the momentum equation.

Limitations (ii) to (vi) also apply to the non-linear storage routing methods described in Book 5, Chapter 5, Section 5.

5.5. Non-linear Storage Routing

5.5.1. Introduction

All the methods discussed in Book 5, Chapter 5, Section 3 involved the assumption that the storage (*S*) in a routing element is related to the characteristic discharge (*Q*) in a linear fashion, in other words doubling the discharge corresponds to a doubling of storage. For concentrated forms storage (as in the level pool routing methods discussed in Book 5, Chapter 5, Section 4) the linear *S*-*Q* relationship is based on the outflow from the storage, while for the distributed forms of storage (as in the different forms of the Muskingum Method discussed in Book 5, Chapter 5, Section 4 to Book 5, Chapter 5, Section 4) the *S*-*Q* relationship uses a weighted average between inflow to and outflow from the routing reach.

The linear storage-discharge relationship can be expressed in general form as:

$$S = KQ \tag{5.5.31}$$

The constant coefficient *K* represents the *lag time* between inflow and outflow (or the average travel time through the routing element).

As shown in the Book 5, Chapter 5, Section 5, hydraulic analysis of various routing elements indicates that their *S*-*Q* relations are typically non-linear and that they can be approximated by a power function relationship of the following form:

$$S = kQ^m \tag{5.5.32}$$

where, *k* is a dimensionless coefficient and the exponent *m* is a dimensionless constant. Depending on the storage and discharge characteristics of the routing element, the exponent *m* can be smaller or greater than the value of 1.0 (which applies to the linear form of the *S*-*Q* relationship). The formulation in Equation (5.5.32) implies also a lag time *K* that varies with discharge:

$$K = \frac{S}{Q} = kQ^{m-1} \tag{5.5.33}$$

Non-linear storage routing methods require an iterative numerical procedure for their solution, such as the Regula Falsi (False Position) method or the Newton-Raphson method (e.g. Chapra and Canale (2010)). A numerical method for non-linear flood routing has been developed by Laurenson (1986) and is summarised in Pilgrim (1987).

5.5.2. Different Forms of Non-linearity

To examine different form of non-linearity in the *S*-*Q* relationship it is useful to express Equation (5.5.32) in logarithmic form:

$$\log S = \log k + m \log Q \tag{5.5.34}$$

This relationship plots as a straight line on log-log paper, and the exponent *m* represents the slope of the line. For any two points on the line:

$$m = \frac{\Delta \log S}{\Delta \log Q} \tag{5.5.35}$$

The exponent *m* can thus be interpreted as indicating the relative efficiency of storage and discharge with increasing water level (or increasing flood magnitude). Furthermore, Equation (5.5.33) indicates how the lag time changes for different values of *m*. Three different cases can be distinguished:

i. *m* = 1 (equivalent to the linear *S*-*Q* relationship) means that storage and discharge increase at a similar rate – the lag time remains constant;

ii. *m* < 1 represents relatively efficient flow and storage increasing slowly – the lag time decreases with increasing flood magnitude; and

iii. *m* > 1 indicates that flow is relatively inefficient and storage increases rapidly – the lag time increases with increasing flow.

An example of case (ii) is discharge and storage in a wide rectangular channel of Length *L* with water depth *y* (Mein et al., 1975):

$$S = yBL \tag{5.5.36}$$

$$Q = \frac{S_o^{1/2}}{n} B y^{5/3} \tag{5.5.37}$$

Substitution of y from Equation (5.5.37) into Equation (5.5.36) yields:

$$S = \frac{n^{0.6} B^{0.4} L}{S_o^{0.3}} Q^{0.6} \tag{5.5.38}$$

In this case the exponent *m* is 0.6 (efficient flow compared to storage) and the coefficient *k* is represented by the fraction before Q in Equation (5.5.38). A similar analysis for a triangular cross-section will yield an exponent *m* = 0.75.

In contrast to this, the analysis of storage and discharge for a rectangular channel being blocked by an embankment with a culvert, where discharge occurs as flow through an orifice of fixed size (inefficient flow), will yield a value of the exponent *m* substantially greater than 1.0.

Examples of *S*-*Q* curves with different values of the exponent *m* are illustrated in Figure 5.5.8, where values of S are plotted against Q on logarithmic scale axes. The different curves are plotted so that they cross at a representative discharge of about 30 m^3/s (representing the middle of the range of flood magnitudes used in model calibration).

It follows from the examples plotted in Figure 5.5.8 that different combinations of *k* and *m* can give similar values of storage for a given discharge. Calibration of a runoff-routing model over a limited range of flood magnitudes can thus only give a broad indication of the appropriate degree of non-linearity when the model is applied for the flow conditions of a different flood magnitude, and application in the extrapolated range needs to be guided by consideration of the physical characteristics of the routing reach.

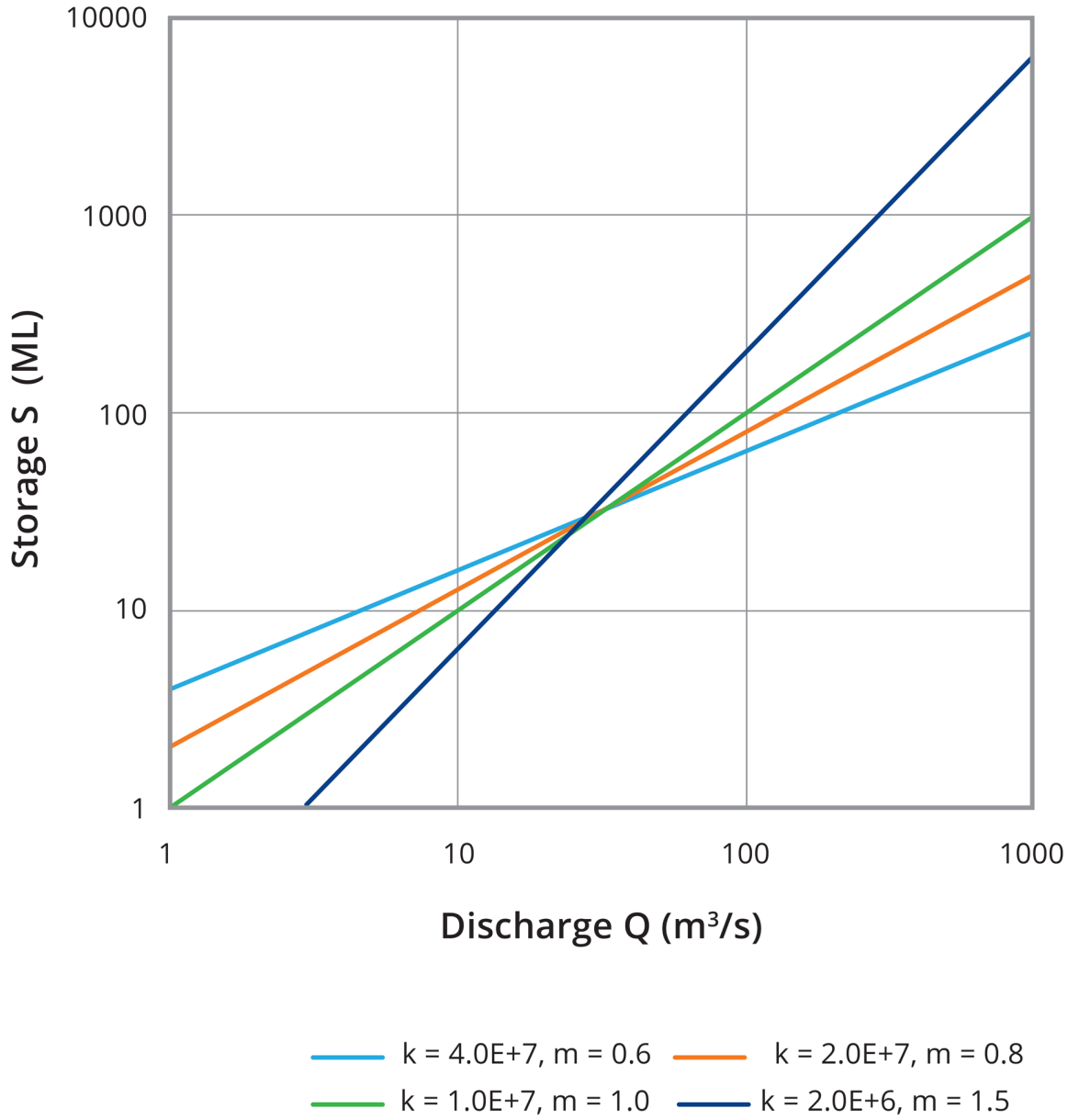

Figure 5.5.8. Storage-Discharge Relationships with Different Degrees of Non-linearity

The non-linear nature of catchment storage and values of the exponent *m* for application in runoff-routing applications are further discussed in Book 5, Chapter 6. Application of runoff-routing models for the range of Very Rare to Extreme floods is discussed in Book 8.

5.5.3. Non-linear Distributed Storage

The distributed form of the S-Q relationship used in the Muskingum equation (Equation (5.5.27)) can also be applied as a nonlinear relationship:

$$S = k[XI + (1 - X)O]^m \tag{5.5.39}$$

or more simply:

$$S = kQ_w^{\ m} \tag{5.5.40}$$

where Q_w is the weighted discharge for the routing reach.

An example of the application of the non-linear Muskingum Method for routing hydrographs through river reaches is in the URBS runoff routing model (Carroll, 2012).

The translation and attenuation effects of non-linear distributed storage represented by Equation (5.5.39) can also be replicated by routing through a number of non-linear storages placed in series. This is the approach incorporated in the RORB runoff-routing model (Laurenson et al., 2010). However, as discussed for the case of linear routing methods (Book 5, Chapter 5, Section 4), for accurate representation of the attenuation characteristics of a river reach, the number of sub-reaches used for routing needs to be carefully selected.

The effect of different non-linearity assumptions used for routing hydrographs through non-linear distributed storage (or a series of concentrated non-linear storages) is to produce different degrees of attenuation when the calibrated *k* and *m* parameters are applied to routing floods of different magnitude. This is illustrated in Figure 5.5.9 for the case where the non-linear routing model is applied to a flood hydrograph twice the magnitude of the observed flood used for calibrating the model. It is shown that a lower value of *m* (with a correspondingly higher value of *k*) produces a higher peak that occurs earlier than if a *k* and *m* parameter combination for a linear model had been used.

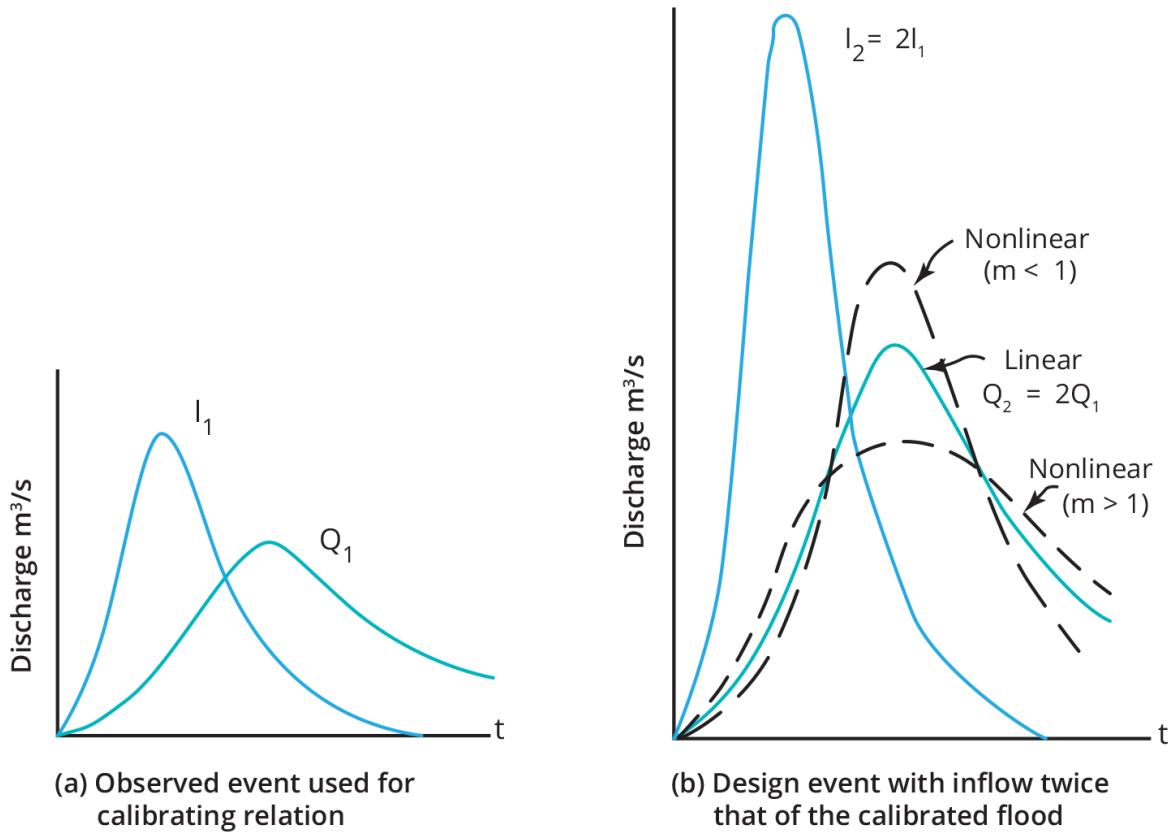

Figure 5.5.9. Effect of Non-linearity of Storage-Discharge Relationship on Routed Hydrographs (after Pilgrim (1987))

5.6. Hydraulic Routing Approaches

5.6.1. Introduction

The hydraulic routing approaches are based on various forms of unsteady flow equations. The *full dynamic wave equations* (or St Venant equations) introduced in Book 6, Chapter 2, Section 8 and Book 6, Chapter 4, Section 6 describe the conservation of mass (continuity equation) and the conservation of momentum (momentum equation).

For application in flood hydrograph estimation models it is most useful to present the one dimensional unsteady flow equations in terms of the discharge *Q* and stage *z* (Weinmann, 1977; Fread, 1985):

Continuity:

$$\frac{\partial A}{\partial t} + \frac{\partial Q}{\partial x} - q = 0 \tag{5.5.41}$$

Momentum:

$$\frac{\partial A}{\partial t} + \frac{\partial}{\partial x}\left(\frac{Q^2}{A}\right) + gA\left(\frac{\partial z}{\partial x} + S_f\right) = 0 \tag{5.5.42}$$

where q is the rate of lateral inflow to the routing reach, g the gravitational acceleration, z the water level or stage and S_f the average friction slope of the routing reach. The friction slope can be determined from a uniform flow resistance formula (Book 6, Chapter 2, Section 5) as $S_f = Q^2/C^2$, where C is the conveyance of the cross-section.

This system of equations can be applied in flood hydrograph estimation models to track the movement of a flood hydrograph through river and floodplain reaches. The equations have no analytical solution and flood routing methods based on the full dynamic equations thus need to apply one of the numerical solution procedures described in Book 6, Chapter 4, Section 7. Explicit numerical solution schemes provide a more direct and more computationally efficient solution than implicit schemes but, to avoid computational stability problems, they require the time and space steps to be selected in accordance with the Courant stability criterion.

The particular advantage of the application of the full dynamic wave equations is in their ability to allow for backwater effects or tidal influences and to deal more accurately with rapidly rising or falling flood hydrographs. The flood routing models based on the full dynamic equations can also produce flood level hydrographs and rating curves at points of interest.

The application of hydraulic routing approaches requires the geometry of the channel and floodplain system to be defined by cross-sectional information obtained from river surveys or Digital Elevation Models. The representation of the actual river and floodplain system in the model is highly conceptualised, as the computational cross-sections are generally quite widely spaced and a smooth variation of the hydraulic characteristics over the model reach is assumed.

Traditionally the application of the full dynamic wave equations has been limited by the fact that their numerical solution is more demanding on computer resources but this is no longer an important factor.

Two dimensional forms of the unsteady flow equations are introduced in Book 6, Chapter 2, Section 9 and Book 6, Chapter 4, Section 7. This form of the dynamic wave equations (or a simplified form of the equations) is applied in the rainfall-on-grid models discussed in Book 5, Chapter 6, Section 5.

5.6.2. Kinematic and Diffusion Wave Routing

The basic equations used for kinematic wave and diffusion wave routing are derived from the full dynamic wave equations introduced in Book 5, Chapter 5, Section 6 by neglecting some terms of the complete momentum equation (Equation (5.5.42)).

5.6.2.1. Diffusion Wave Routing

By neglecting the first two terms of the momentum equation (Equation (5.5.42)), which represent the effects of local and convective acceleration respectively, but keeping the terms representing the pressure and friction forces, the following simplified form of the momentum equation is obtained:

$$S_f = S_0 - \frac{\partial z}{\partial x} \tag{5.5.43}$$

The inclusion of the pressure term ∂z/∂x allows for the effects of a downstream boundary condition (backwater, tidal influences) to be included in the routing computations.

By combining this simplified momentum equation with the continuity equation (Equation (5.5.41)) the form of the *convective-diffusion (diffusion wave) equation* (Equation (5.5.44)) used in hydrologic flood routing models is obtained:

$$\frac{\partial Q}{\partial t} + C_k \frac{\partial Q}{\partial x} = D \frac{\partial^2 Q}{\partial x^2} + C_k q \tag{5.5.44}$$

with $C_k = \frac{\partial Q}{\partial A}$ the kinematic wave celerity

and $D = \frac{Q}{2BS_o}$ the diffusion coefficient

where *Q* is the discharge, *q* the rate of lateral inflow, *x* the distance along the channel, *A* the cross-sectional area, *B* the water surface width and S_o the channel slope.

The diffusion term in Equation (5.5.44) allows explicitly for the diffusion and peak attenuation effects observed in the movement of flood waves through river and floodplain reaches. This is in contrast to the Muskingum Method where the diffusion effects are only introduced through judicious choice of the numerical solution scheme and determination of parameter values.

5.6.2.2. Kinematic Wave Routing

The kinematic wave equation is obtained from Equation (5.5.44) by omission of the diffusion term:

$$\frac{\partial Q}{\partial t} + C_k \frac{\partial Q}{\partial x} = C_k q \tag{5.5.45}$$

The term ‘kinematic wave’ was introduced by Lighthill and Witham (1955) to describe the motion of waves in time and space without considering mass and force. Equation (5.5.45)

can be obtained from the full unsteady flow equations by replacing the momentum equation (Equation (5.5.42)) by a uniform flow relationship.

Kinematic waves are theoretically not dispersive (ie. they travel without attenuation) but the variation of the travel speed C_k with Q produces a change of wave form, resulting in a gradual steepening of the wave front as it travels downstream, eventually leading to a 'kinematic shock' (Henderson, 1966). Analytical solutions for the kinematic wave equations exist only for a few idealised situations (Miller, 1984). Numerical solution schemes for the kinematic wave equation introduce some degree of dispersion/attenuation of the flood wave, and thus match more closely the behaviour of actual flood waves.

As indicated in Book 5, Chapter 5, Section 4, the Muskingum Method can be understood to be a numerical solution scheme for the kinematic wave model. Various other numerical solution techniques are described in the literature and applied in practical flood routing models (e.g. Miller (1984), HEC (1993)) The application of kinematic wave principles in runoff routing models is discussed in Book 5, Chapter 6, Section 4.

5.7. References

Bedient, P.B., Huber, W.C. and Vieux, B.E. (2008), Hydrology and floodplain analysis, ed. 4, Upper Saddle River: Prentice Hall.

Boyd, M.J., Pilgrim, D.H., Knee, R.M. and Budiawan, D. (1989), Reverse Routing to Obtain Upstream Hydrographs. Hydrology and Water Resources Symposium. Christchurch, NZ, 23-30 November. Preprints of Papers (p: 372). Institution of Engineers, Australia.

Carroll, D.G. (2012), URBS (Unified River Basin Simulator) A Rainfall Runoff Routing Model for Flood Forecasting and Design. Version 5.00 Dec, 2012.

Chang, C.N., da Motta Singer, E. and Koussis, A.D. (1983), On the mathematics of storage routing, Jounral of Hydrology, 61(4), 357-370.

Chapra, S.C. and Canale, R.P. (2010), Numerical methods for engineers, New York: McGraw Hill.

Cunge, J.A. (1969), On the subject of a flood propagation method, Journal of Hydrology Research, 7(2), 205-230.

Fenton, J.D. (1992), Reservoir routing, Hydrological Sciences Journal, 37(3), 233-246.

Fread, D.L. (1985), Channel routing. In 'Hydrological Forecasting', Chichester: John Wiley and Sons Ltd.

HEC (1993). Introduction and application of kinematic wave routing techniques using HEC-1. US Army Corp of Engineers, Hydrologic Engineering Centre, http://www.hec.usace.army.mil/publications/TrainingDocuments/TD-10.pdf.

Henderson, F.M. (1966), Open Channel Flow, Macmillan Publishing Co., New York

Kalinin, G. P. and Miljukov, P. I. (1958), Approximate methods for computing unsteady flow movement of water masses (in Russian), Transactions Central Forecasting Institute, 66 p.

Koussis, A.D. (2009), Assessment and review of the hydraulics of storage routing 70 years after the presentation of the Muskingum method. Hydrological Sciences Journal, 54(1), 43-61, available at <http://dx.doi.org/10.1623/hysj.54.1.43>.

Laurenson, E.M. (1998), Hydrology CIV3263 Course Notes, Monash University, Department of Civil Engineering.

Laurenson, E.M. (1962), Hydrograph synthesis by runoff routing, Report No. 66, Sydney: Water Research Laboratory, University of New South Wales.

Laurenson, E.M. (1986), Variable time-step nonlinear flood routing, In Hydrosoft '86; Hydraulic Engineering Software, Proceeding sof the 2nd International Conference, Computational Mechanics Publns, Springer-Verlag, 9-12 September, pp: 61-72, Berlin.

Laurenson, E.M., Mein, R.G. and Nathan, R.J. (2010). RORB Version 6 Runoff Routing Program - User Manual.

Lighthill, M.J. and Witham, G.B. (1955), On kinematic waves I, Proceedings of the Royal Society of London, 229: 281-316.

McCarthy, G.T. (1938), The unit hydrograph and flood routing, Manuscript presented at a conference of the North Atlantic Division, United States Army Corps of Engineers, 24 June (unpublished).

Mein, R.G., Laurenson, E.M. and McMahon, T.A. (1975), Simple nonlinear model for flood estimation, Journal of Hydrology, 100(HY11), 1507-1518.

Miller, J.E. (1984), Basic concepts in kinematic wave models. U.S. Geological Survey Professional Paper 1302, Washington: United States Government Printing Office.

Nash, J.E. (1959), A note on the Muskingum flood-routing method, Journal of Geophysical Research, 64(8), 1053-1056.

Pilgrim, DH (ed) (1987) Australian Rainfall and Runoff - A Guide to Flood Estimation, Institution of Engineers, Australia, Barton, ACT, 1987.

Stephenson, D. (1979), Direct optimization of Muskingum routing coefficients, Journal of Hydrology, 41: 161-165.

Weinmann, P.E. (1977), Comparison of flood routing methods for natural rivers, Civil Engineering Research Report No.2/1977, Clayton: Monash University.

Wong, T.H.F. (1985), Reach subdivision for storage routing in rivers, Proceedings of the 21st IAHR Congress, 19-23 August, Melbourne.

Wong, T.H.F. and Laurenson E.M. (1983), Wave speed-discharge relations in natural channels, Water Resources Res., 19: 701-706.

Zoppou, C. (1999), Reverse routing of flood hydrographs using level pool routing, Journal of Hydrologic Engineering, 4(2), 184-188.

Chapter 6. Flood Hydrograph Modelling Approaches

James Ball, Erwin Weinmann

Chapter Status	Final
Date last updated	14/5/2019

6.1. Introduction

This chapter deals with a range of approaches available to calculate design flood hydrographs at the catchment outlet and other points of interest. It therefore integrates the previous chapters in Book 5 and also links to Book 7, where practical applications are discussed.

The time-area approaches (Book 5, Chapter 6, Section 2) and unit hydrograph approaches (Book 5, Chapter 6, Section 3) allow a relatively simple transformation of rainfall excess inputs to flood hydrograph outputs and are directly applicable to a lumped representation of the flood formation process in a catchment, where the inputs and processes can be assumed to be spatially uniform (or at least spatially consistent between different events). These “traditional” approaches have generally been replaced by more flexible approaches. However, they also find application to represent the overland flow phase of hydrograph formation in some of the node-link type models discussed in subsequent sections.

The most widely used flood hydrograph estimation models are based on the runoff routing approach, in which both the runoff production and hydrograph formation phases can be represented in a distributed fashion, reflecting the spatial variation of rainfall inputs and flood processes in a catchment. The two principal groups of models are the network (node-link type) models described in Book 5, Chapter 6, Section 4 and the rainfall-on-grid (or direct rainfall) models described in Book 5, Chapter 6, Section 5.

The routing methods incorporated in these models have their foundations in the open channel hydraulics introduced in Book 6 and apply the flood routing principles outlined in Book 5, Chapter 5 of this book. The descriptions in Book 5, Chapter 6, Section 4 and Book 5, Chapter 6, Section 5 focus on the specific way these principles are applied to represent different parts of the flood hydrograph formation process.

The discussion of flood hydrograph modelling in this chapter is intended to introduce readers to the different approaches used and the assumptions made in different modelling approaches and different runoff routing modelling systems. Guidance on the practical application of flood hydrograph models to different flood estimation problems, including estimation of model parameters, is provided in Book 7.

As with other chapters of Book 5, this chapter deals primarily with rural catchments, and while the principles apply also for urban catchments, urban catchment hydrology is covered in detail in Book 9.

6.2. Time-Area approaches

6.2.1. Time-Area Theory

Time-area approaches can be seen as an extension of the *travel time* concept used in the Rational Method. However, instead of using a single travel time or *time of concentration* for flow from the most remote point on the catchment to its outlet to calculate a peak discharge, time-area approaches use travel times from all parts of the catchment and calculate a complete flood hydrograph. Early development of the approach was carried out by Hawken (1921) and Ross (1921), while examples of time-area approaches are given in Bedient et al. (2008).

The basic principle of time-area approaches, as illustrated in Figure 5.6.1, is that rainfall excess at any time *t-tt* after the start of the storm that occurs at a point on the catchment with a travel time of *tt* to the catchment outlet will influence flow at the catchment outlet at time *t*. A fundamental assumption involved in this is that flow at the catchment outlet is influenced only when the runoff reaches the catchment outlet, i.e. when the individual water particles reach the catchment outlet.

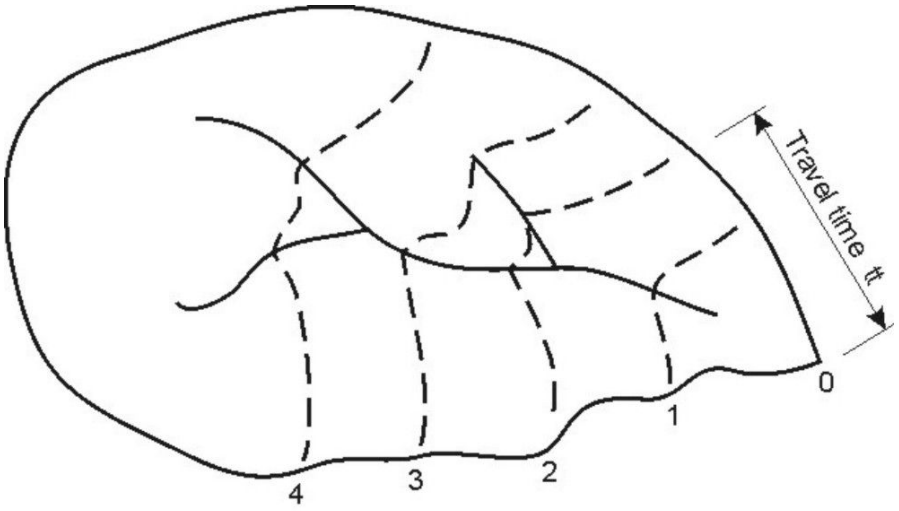

(a) Isochromes of travel time

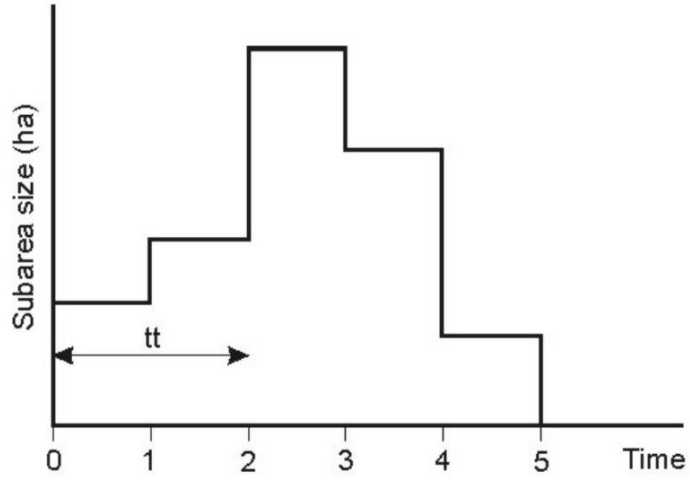

(b) Time-area curve

Figure 5.6.1. Isochrones and Time-Area Curve

Points on the catchment which have equal travel times to the outlet can be joined to form isochrones. Application of the time-area method requires isochrones to be drawn for the catchment being considered; note that many computerised applications assume that the area increases in a linear manner on small subcatchments to avoid the need for delineation of isochrones.

When construction of isochrones is required, a common assumption is that the travel time is related to the travel length (*L*) and slope (*S*) of the catchment by the following relationship:

$$t_t = \frac{L}{S^{0.5}} \tag{5.6.1}$$

Equation (5.6.1) follows directly from Manning's equation, in which flow velocity is related to the square root of stream slope which is assumed to be the same as the energy gradient. However, as the flow moves downstream to the catchment outlet, the flatter stream slopes are accompanied by greater water depths, which may compensate for the decreasing stream slope in the Manning equation. Studies by Leopold et al. (1964) and Pilgrim (1977) indicate that stream velocities essentially remain constant along the length of the stream and may even increase in a downstream direction. If velocities remain constant along the stream, the travel time would be directly related to travel distance by:

$$t_t = L \tag{5.6.2}$$

A plot of the area between adjacent isochrones against the travel time produces a time-area curve. An example of a time-area curve is presented in Figure 5.6.1.

Since there are many points on the catchment with travel times t_t and corresponding times t-t_t after the start of the storm, the flowrate at the outlet at time t is the sum of all possible combinations. As a simple example, if the catchment is divided into five segments using isochrones (A_i), and a storm has three periods of rainfall excess (P_j in mm/h) with both the isochrones and rainfall having the same time step, then the total time of the hydrograph is eight time steps. Also, the discharges from the catchment at successive time steps (equal to the isochrone interval) for this example are given by:

$$\begin{aligned}
Q_0 &= 0 \\
Q_1 &= kA_1P_1 \\
Q_2 &= k(A_1P_2 + A_2P_1) \\
Q_3 &= k(A_1P_3 + A_2P_2 + A_3P_1) \\
Q_4 &= k(A_2P_3 + A_3P_2 + A_4P_1) \\
Q_5 &= k(A_3P_3 + A_4P_2 + A_5P_1) \\
Q_6 &= k(A_4P_3 + A_5P_2) \\
Q_7 &= kA_5P_3 \\
Q_8 &= 0
\end{aligned} \tag{5.6.3}$$

where k is an appropriate unit conversion factor (k varies with the units of Q and A).

In general, Equation (5.6.3) can be expressed as:

$$Q_t = k \sum_{i=1}^{t} A_i P_{j-i+1} \tag{5.6.4}$$

where Ai is the area between the i-1 and i isochrones, Pj is the rainfall excess depth in the jth period of the storm event, and k is a conversion factor. As the conversion factor (k) will vary with the isochrone interval, it is recommended that the intensity of rainfall excess (mm/h) be used; details of the conversion factors for different combinations of discharge, area units and rainfall excess intensity in mm/h are given in Table 5.6.1.

Table 5.6.1. Conversion Factors

Discharge	Area	Rainfall Excess Intensity	Conversion Factor
m^3/s	ha	mm/h	1/360
m^3/s	km^2	mm/h	1/3.6
L/s	ha	mm/h	1/0.36

6.2.2. Limitations of Time-Area Approaches

Despite the use of the time-area approach in various models, the time-area concept has several limitations, including:

- Isochrones of travel time usually are not known, except in a few experimental studies and must be estimated. These experimental catchments include those monitored by (Pilgrim, 1966a; Pilgrim, 1966b) using tracers to ascertain travel times. To overcome this disadvantage, many applications adopt a simplified time-area relationship. A common simplified relationship is based on a linear growth in area with time (in essence, an assumption of a rectangular shape with a length given by the response time and a width defined by the catchment area), and thus there is a need only to estimate a representative travel time for the conceptualised catchment.

- The time-area curve cannot be easily derived from recorded rainfall and streamflow data.

- Construction of the direct runoff hydrograph assumes that flow is translated to the outlet with a lag but without attenuation. In other words, a kinematic response is assumed. As a result of this, time area methods are more likely to be applicable to estimation of flows from small catchments and particularly to estimation of surface flows in urban catchments.

- The method is linear, i.e. a doubling of rainfall excess results is a doubling of predicted discharges, whereas data from many catchments, particularly the larger rural catchments, demonstrates a nonlinear response to changes in rainfall excess.

6.2.3. Worked Example

The example below illustrates the application of the time-area method to a small rural catchment. The steps in the method remain similar when applied to an urban catchment but the time-area diagram then needs to reflect differences in travel time over different types of catchment surfaces and different types of drainage systems.

Example - Hydrograph Calculation for Triangular Time-Area Curve

A 5 hectare catchment has a time of concentration of 15 minutes. The time-area curve is assumed to be triangular in shape. (This is similar to the time-area curve used with the Cordery-Webb approach for development of synthetic unit hydrographs). The surface runoff hydrograph is to be estimated for a 21 minute storm event with the details of this event shown in Table 5.6.2.

Since the storm event has 7 periods, each of 3 minutes duration, the catchment will be divided into 5 subareas by isochrones spaced at 3 minute intervals. The hydrograph base length is given by the catchment time of concentration plus the storm duration, ie 15 minutes + 21 minutes = 36 minutes. The total depth of rainfall excess is 8.1 mm (see Column 3 in Figure 5.6.2). Using this depth of rainfall excess and the catchment area, the volume of direct runoff from the catchment is 405 m^3.

The subarea sizes between each adjacent pair of 3 minute isochrones, proceeding from the outlet of the catchment to the top of the catchment, are 0.33, 0.67, 1.00, 1.33 and 1.67 ha. The resultant time-area relationship is shown in Figure 5.6.2.

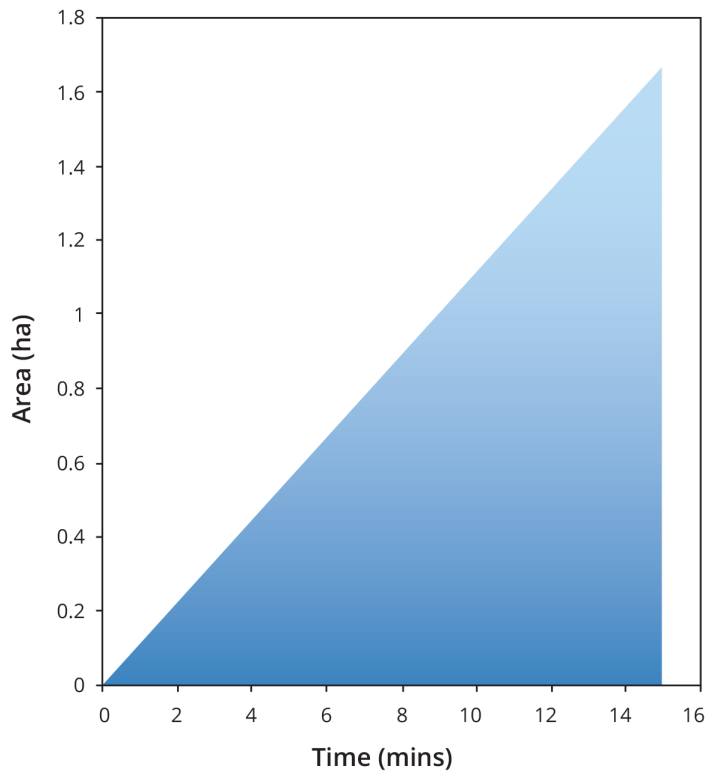

Figure 5.6.2. Time-Area Relationship for Example 2

Table 5.6.2. Calculation of Surface Runoff Hydrograph using Triangular Time-Area Curve

Time (minutes)	Subarea (ha)	Rainfall Excess (mm)	Rainfall Excess Intensity (mm/h)	Surface Runoff (m^3/s)
0	0	0	0	0
3	0.33	0.3	6	0.006
6	0.67	0.6	12	0.022
9	1	1.8	36	0.072
12	1.33	3.6	72	0.189
15	1.67	0.9	18	0.322
18		0.3	6	0.428
21		0.6	12	0.506
24				0.439
27				0.139
30				0.072
33				0.056
36				0
∑		**8.1**		**2.25**

Application of Equation (5.6.4) allows the direct runoff hydrograph ordinates to be calculated (see Column 5 in Table 5.6.2). Figure 5.6.3 summarises the time-area calculations and shows the resulting surface runoff hydrograph.

As a check, from Column 5 in Table 5.6.2, the volume of the direct runoff hydrograph 1 is given by

$$\text{Volume} = \sum Q\Delta t = 2.25m^3/s \text{ x } 180s = 405m^3 \quad (5.6.5)$$

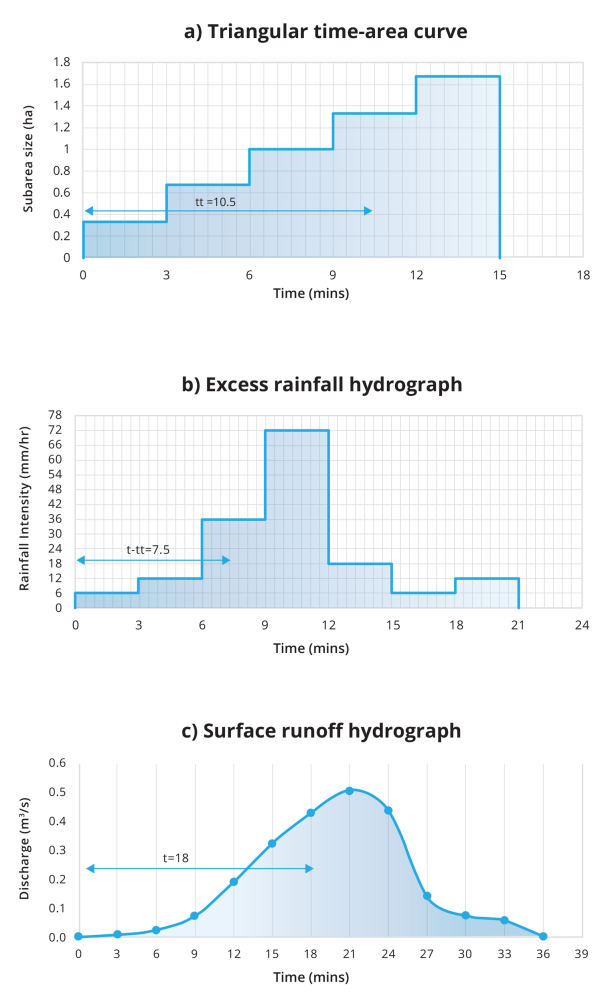

Figure 5.6.3. Calculation of Surface Runoff Hydrographs using Time-Area Approach

6.3. Unit Hydrograph Approaches

6.3.1. Introduction

This section of Australian Rainfall and Runoff is based on the chapter on unit hydrographs prepared by Cordery (1987) for the previous edition of Australian Rainfall and Runoff. However, as the unit hydrograph approaches are no longer widely applied in Australia, only a brief introduction is given here. For a more detailed description of the unit hydrograph method and worked examples the reader is referred to Cordery (1987).

6.3.2. Unit Hydrograph Theory

6.3.2.1. Basic Concepts

Development of the unit hydrograph approach is generally attributed to Sherman (1932). Unit hydrographs represent an advance over time-area procedures because, rather than constructing a time-area curve from isochrones of travel time, which requires assumptions regarding the travel times from all points on the catchment, the unit hydrograph represents

the actual flood response of the catchment to rainfall, and can be directly determined or estimated from recorded rainfall and streamflow data. As a consequence, the resulting unit hydrograph incorporates the effects of both translation and attenuation, and so reduces the assumptions needed in the time-area approaches.

6.3.2.2. Definition of a Unit Hydrograph

A unit hydrograph is defined as the direct runoff hydrograph resulting from 1mm depth of rainfall excess, where the rainfall excess occurs over a particular time period and is uniformly distributed across the catchment. The time period of the rainfall excess sets the period of the unit hydrograph. Thus a rainfall burst which lasts 2 hours and has an average rainfall excess intensity of 0.5mm/h will produce a 2 hour unit hydrograph. It is important to note that the rainfall excess intensity should be uniform over the period of the burst, and that it also should be spatially uniform across the catchment.

Direct runoff hydrographs result from the interaction between two important factors:

- the time varying storm rainfall hyetograph; and
- the translation and attenuation properties of the catchment storage

In the special case of the unit hydrograph, a standardised rainfall excess (1 mm) is used, and the unit hydrograph, therefore, represents the effects of the catchment in delaying and attenuating rainfall excess as it flows from all points on the catchment to the catchment outlet. Use of this standardised rainfall excess provides the opportunity to relate the size and shape of the unit hydrograph to the catchment's geophysical properties such as area, stream length and slope, and thus enables synthetic unit hydrographs to be estimated for catchments where no recorded streamflow data exists.

Each unit hydrograph reflects the unique geophysical properties of the catchment and, hence, each catchment should have its own unique unit hydrograph. Bernard (1935) pioneered this concept by developing a dimensionless unit hydrograph which reflected the geophysical properties of the catchment.

The basic principle of unit hydrograph theory is that the catchment responds in a linear manner to rainfall excess and, hence, superposition is feasible. As unit hydrographs form a linear system, the ordinates of the direct runoff hydrograph are linearly proportional to the depth of rainfall excess. For example, if the rainfall excess is doubled, each ordinate of the direct runoff hydrograph will be doubled. As another example, if a sequence of several periods of rainfall excess occurs, one after another, the resulting direct runoff hydrograph is equal to the sum of the runoff from each individual period of rain (see Figure 5.6.4).

6.3.2.3. The Specified Period of the Unit Hydrograph

The specified period of the unit hydrograph must be short enough to provide good definition of both the rainfall excess hyetograph and the resulting direct runoff hydrograph. This means the specified period should be short enough to provide a reasonable representation of all major changes of the rainfall excess intensity and should be less than a quarter of the time of rise of the unit hydrograph. Large rural catchments could have unit hydrographs with specified periods of 3 or more hours, whereas small urban catchments may require specified periods of 5 minutes or less.

For a given catchment the unit hydrograph for a particular specified period will be different from those with different time specified periods. For example, a 1 hour unit hydrograph

results from 1mm of rainfall excess falling over 1 hour at a rate of 1mm/h, whereas a 2 hour unit hydrograph results from 1mm of rainfall excess falling over 2 hours at a rate of 0.5 mm/h. In general, the peak discharges of unit hydrographs with longer specified periods will be lower and will occur later in time. This decrease in peak discharge arises as a result of the lower intensity of rainfall excess as the specified period of the unit hydrograph increases.

The 1 hour unit hydrograph will be applied to a rainfall hyetograph with 1 hour rain periods, and will produce a direct runoff hydrograph with the ordinate values predicted every hour. The 2 hour unit hydrograph will be applied to a rainfall hyetograph with 2 hour rain periods.

6.3.2.4. Changing the Specified Period of a Unit Hydrograph

To change the specified time period of the unit hydrograph two approaches are available, depending on whether a longer or a shorter specified period is needed.

Calculation of a unit hydrograph of longer time period from one of a shorter period is accomplished by the addition of several short period unit hydrographs with each sequential unit hydrograph delayed by the specified period. Thus, the sum of four 15 minute unit hydrographs, each of which is delayed in time by 15 minutes, will produce a direct runoff hydrograph resulting from 4 mm of rainfall excess during a 1 hour period. Since a unit hydrograph is the result of 1 mm of rainfall excess during the specified time period, the 1 hour unit hydrograph is derived from this runoff hydrograph by dividing all ordinates in the runoff hydrograph by four.

Another situation in which the specified time period needs to be changed is where an instantaneous unit hydrograph has been obtained, as occurs in some synthetic unit hydrograph methods. The instantaneous unit hydrograph (IUH) represents the direct runoff hydrograph produced by 1 mm of rainfall excess which occurs at an instant in time. The ordinates of a specified period unit hydrograph at each time t are obtained by integrating the ordinates of the IUH over an interval from t-T to T, where T is the specified time period, then dividing this result by T. Practically, this is achieved by averaging the IUH ordinates at times t and t-T. For example, each ordinate of a 1 hour unit hydrograph is the average of the IUH ordinates at this time and 1 hour before this time (Boyd, 1982).

The derivation of a unit hydrograph of shorter specified time period from one of a longer period is less direct, but can be attempted using an S-curve. Data errors will often produce oscillations in the S curve and it is often difficult to obtain good results when this method is applied to real data. (Details of the S-curve method are given in many textbooks, e.g. Bedient et al. (2008))

6.3.3. Calculating Direct Runoff Hydrographs Using Unit Hydrographs

Since superposition is assumed to be feasible with unit hydrographs, a storm with j periods of rainfall excess will produce j direct runoff hydrographs, with the ordinates of each direct runoff hydrograph factored in proportion to the depth of rainfall excess. The direct runoff for the storm is then the sum of all j hydrographs. For the summation, the period of the unit hydrograph must be the same as incremental time period of the rainfall hyetograph.

If the unit hydrograph has k ordinates and there are j periods of rainfall excess, the number of direct runoff ordinates will be given by $n = j + k - 1$. Shown in Equation (5.6.6) is the determination of the direct runoff hydrograph for the case where there 3 periods of rainfall excess and 5 unit hydrograph ordinates.

$$
\begin{aligned}
Q_0 &= 0 \\
Q_1 &= P_1U_1 \\
Q_2 &= P_1U_2 + P_2U_1 \\
Q_3 &= P_1U_3 + P_2U_2 + P_3U_1 \\
Q_4 &= P_1U_4 + P_2U_3 + P_3U_2 \\
Q_5 &= P_1U_5 + P_2U_4 + P_3U_3 \\
Q_6 &= P_2U_4 + P_3U_4 \\
Q_7 &= P_3U_5 \\
Q_8 &= 0
\end{aligned}
\tag{5.6.6}
$$

The first column on the right hand side represents the direct runoff hydrograph from P_1 mm of rainfall excess in the first period of the storm, while the second and third columns represent the direct runoff from the subsequent periods in the storm. Note that each direct runoff hydrograph is delayed by one time period, because the rainfall excesses P_1, P_2 and P_3 occur in successive periods of the storm. Note also that the rainfall excess period, the period of the unit hydrograph, and the time step at which the unit hydrograph ordinates are listed, are all equal.

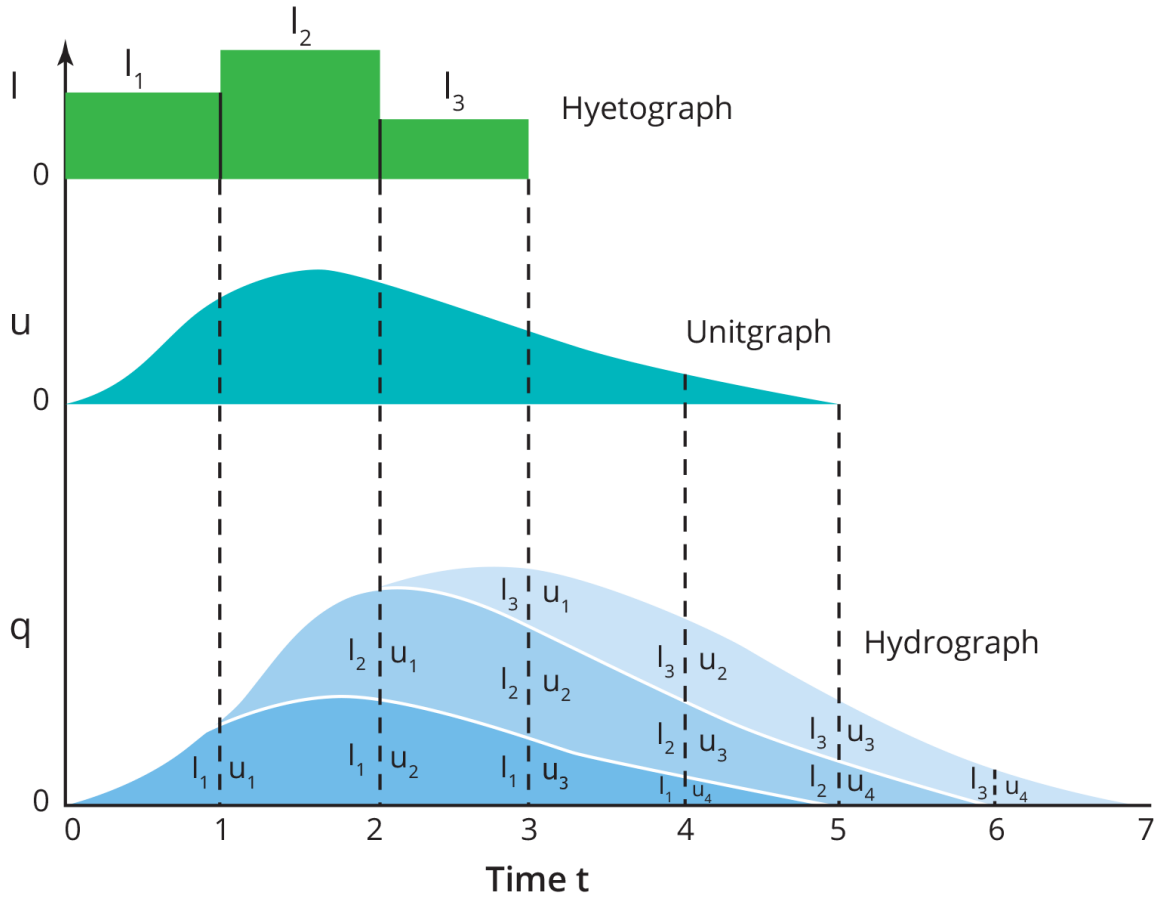

Figure 5.6.4. Unit Hydrograph Calculation – example with 3 periods of rainfall excess and unit hydrograph with 5 ordinates (after Laurenson (1998)).

This figure needs to be redrawn but still referenced to Laurenson.

Equation (5.6.6) can be written in a general form as

$$Q_m = \sum_{i=1}^{j} P_i U_{m-i+1} \tag{5.6.7}$$

where Q_m is any ordinate of the direct runoff hydrograph.

6.3.4. Derivation of Unit Hydrographs from Rainfall and Streamflow Data

6.3.4.1. General Concepts

Recorded rainfall and streamflow data can be used to derive unit hydrographs. Steps in the process are:

1. Select a range of significant flood events for which the direct runoff hydrograph and suitable rain gauge data are available. Only floods with a 50% AEP or less should be used in order to ensure that the data properly reflects the processes which occur during significant flood events. Furthermore, the rainfall during the selected events should be spatially and temporally uniform over the catchment. If an insufficient number of large events is available then it may be necessary to use smaller floods. In this case it must be borne in mind that small floods will tend to produce unit hydrographs which have lower peaks and longer times of rise than are appropriate for use in the estimation of large floods.

2. Separate baseflow as described in Book 5, Chapter 4 to obtain the direct runoff hydrograph.

3. Calculate the volume of direct runoff.

4. Calculate a spatial average rainfall hyetograph for the storm, using hyetographs from all available rainfall stations on or near to the catchment.

5. Calculate the rainfall excess hyetograph, by subtracting losses so that the depth of rainfall excess equals the depth of direct runoff. Rainfall losses can be assumed either as an initial loss-continuing loss model, or an initial loss-proportional loss model (see Book 5, Chapter 3).

Once the recorded streamflow and rainfall data have been analysed to extract the direct runoff hydrograph and rainfall excess hyetograph, derivation of the unit hydrograph can proceed. Unit hydrographs can be derived from single period storms, or from multi-period storms.

6.3.4.2. Selection of an Average Unit Hydrograph for the Catchment

In principle, every unit hydrograph derived from various recorded storms on a catchment should be the same (since each catchment is considered to have a unique unit hydrograph). In practice, however, various factors such as spatial variation in rainfall, errors in data, or limited data (for example insufficient rain gauge coverage of the catchment) means that the unit hydrographs derived from different storms will be somewhat different from one another. Titmarsh and Cordery (1991) found that the peak discharge of unit hydrographs derived from a range of storms on a catchment varied by a factor of 4, while Boyd (1975) found that the mean absolute deviation of the peak discharge was on average 31%.

It is important, therefore, to derive several unit hydrographs for a catchment, selecting the larger storms. All derived unit hydrographs should be compared for consistency, and inconsistent ones rechecked or deleted.

A plot of unit hydrograph peak discharge against the peak discharge of the recorded direct runoff hydrograph from which it was derived may reveal a trend for unit hydrograph peaks to increase for the larger floods. Any such trend is an indication that the catchment is not behaving in a linear manner. In these circumstances, it may be more appropriate to use an alternative technique for estimation of the direct runoff hydrograph. Catchments displaying a nonlinear response to storm events can still use the unit hydrograph approach, but it may be desirable to derive several unit hydrographs for the catchment, each one derived from, and being applicable to a particular range of flood sizes, as discussed by Body (1962).

The unit hydrographs which are considered to be acceptable can be averaged to produce a more representative unit hydrograph for the catchment. Averaging unit hydrographs in this way also has the benefit of reducing any oscillations on the recessions of unit hydrographs derived from multi-period storms.

The recommended approach to calculate the average unit hydrograph is to align the peaks of all unit hydrographs, then average their ordinates at each successive time step (Titmarsh and Cordery, 1991). This method produces a unit hydrograph whose time to peak is the average of all times to peak, and peak discharge which is the average of all peak discharges. A simple average of all unit hydrographs, without regard for the occurrence of the peak is not recommended, as this can produce an average unit hydrograph which is quite different from the individual unit hydrographs (see Figure 5.6.5).

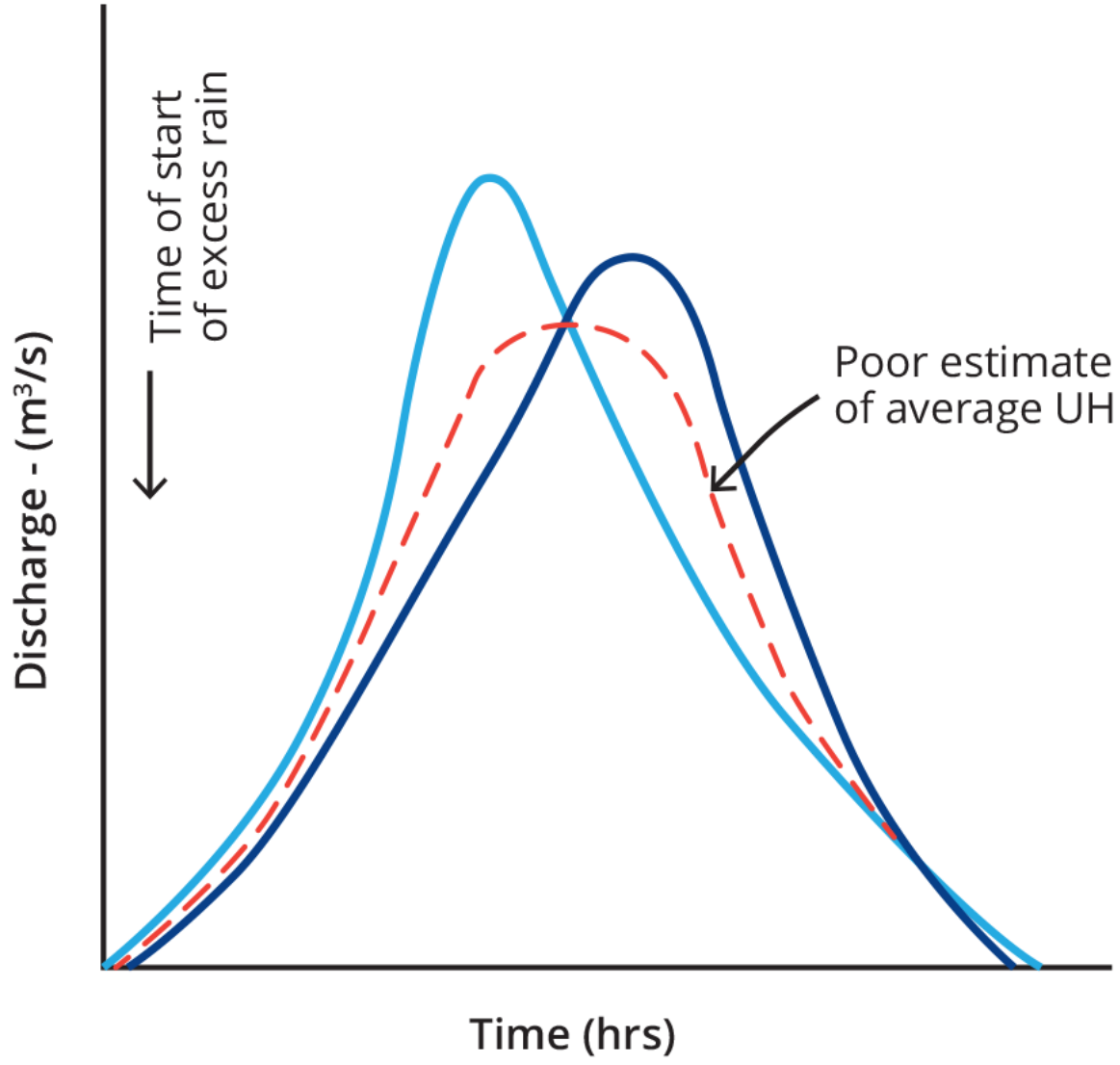

Figure 5.6.5. Poor Averaging of Unit Hydrographs

6.3.5. Synthetic Unit Hydrographs

The synthetic unit hydrograph approach provides a means of estimating unit hydrographs for ungauged catchments. In essence the approach involves estimating the parameters of the unit hydrograph from relationships between these parameters and the physical characteristics of the catchment. These relationships may be derived by considering a number of catchments in a reasonably homogeneous area (with similar climatic and geomorphologic characteristics) for which unit hydrographs have been derived from recorded rainfall and streamflow data. These relationships are empirical and as such cannot be expected to be universally applicable. In general their application should be restricted to the region in which the relationships were derived.

Of the various synthetic unit hydrograph approaches available, the only ones to have found widespread use in Australia are those based on the model of Clark (1945), commonly referred to as the Clark- Johnstone model. The Clark-Johnstone method has been simplified by Cordery and Webb (1974) to produce a model which is suitable for some limited applications.

The Clark-Johnstone model involves the translation of rainfall excess to the outlet and routing this translated flow through a lumped concentrated storage at that location. It has been used quite widely for synthetic unit hydrograph derivation and has been shown to be applicable to most of the east coast of Australia (Cordery et al., 1981). The basic assumption is that the shape of the unit hydrograph may be determined from two parameters, namely the base length of the time-area curve (C) and the catchment storage factor (K).

For more detailed description of these synthetic unit hydrograph approaches and examples of their application the reader is referred to Cordery (1987).

6.3.6. Limitations of the Unit Hydrograph Approach

The unit hydrograph is arguably the most direct way of characterising the response of a catchment to storm rainfall, as it takes account of all factors which influence the flood response to a particular rainfall excess input. The basic concept underlying the approach is simple to understand and easy to apply, being suited to both hand and spreadsheet calculations. The unit hydrograph approach can be applied with some confidence where its main assumptions are at least approximately satisfied: spatial uniformity of rainfall excess and linearity of catchment response.

However, the simplifying assumptions made in the unit hydrograph approach impose the following limitations for its application in many practical situations:

- Catchments generally respond in a non-linear fashion to rainfall excess inputs. This means that the travel time (or lag) varies with discharge or flood magnitude rather than being constant as implied by the linearity assumption. This limitation is particularly important when a significant degree of extrapolation is required from the magnitude of the observed events used in the derivation of the unit hydrograph to the magnitude of floods to be estimated.

- Particularly in larger catchments the spatial distribution of rainfall and rainfall excess is generally non-uniform, and in very large catchments heavy rainfall may only occur over part of the catchment. In such catchments the unit hydrograph approach would be likely to produce flood hydrographs that are biased both in terms of their peak flow and in their time to peak.

- In common with other lumped modelling approaches, the unit hydrograph approach produces only hydrographs at the catchment outlet and not at internal points of interest.

- The unit hydrograph approach and other lumped hydrograph estimation approaches are unsuitable for application in catchments where significant differences in flood response of different parts of the catchment require a more distributed modelling approach (e.g. urban catchments).

- Being based on a range of observed hydrographs for a particular catchment condition, the unit hydrograph approach is not suited to determine flood behaviour for changed catchment conditions (e.g. storage development, significant urbanisation or other major land use changes).

On the basis of these recognised limitations and the ready availability of more flexible runoff routing approaches (Book 5, Chapter 6, Section 4), the unit hydrograph approaches are not recommended for practical applications.

6.4. Runoff Routing Approaches

6.4.1. Introduction

The general term ‘runoff routing’ refers to flood hydrograph modelling approaches where a simplified conceptual representation is used to model the actual processes involved in the conversion of rainfall inputs to direct runoff (using a loss model – Book 5, Chapter 3), the contributions of baseflow (Book 5, Chapter 4) and the translation of runoff from different points in the catchment to a flood hydrograph at the catchment outlet (using a routing model – Book 5, Chapter 5).

The actual flood formation processes in a catchment are complex and highly distributed in nature. Direct runoff generated from storm rainfall in the upper parts of the catchment initially moves downhill as shallow overland flow and is modified by the effects of various forms of detention storage as it moves over the catchment surface. It is then gradually concentrated into minor drainage pathways and successively combined with baseflows and flows from other pathways. These flows eventually reach well defined water courses, creeks or rivers and move downstream, being combined with other tributary flows on their way to the catchment outlet.

A significant degree of simplification in the representation of the actual processes in models is made possible by the fact that catchments act on rainfall inputs as systems with a high degree of damping. This means that the streamflow hydrograph output at the catchment outlet does not reflect the ‘high frequency’ variations of the input in either the time or space dimensions. Similarly, small errors in modelling the various catchment processes may have little effect on the outflow hydrograph. This enables surprisingly accurate and useful results to be obtained from relatively simple models (Laurenson, 1975).

The different groups of models developed in Australia and in other countries have adopted different conceptualisations of the actual flood formation processes, with different levels of simplifications and assumptions in terms of:

- areal variability of runoff inputs over the catchment – lumped, semi-distributed and fully distributed models (see Book 5, Chapter 2)
- variation of routing processes from hillslopes to channel and floodplain reaches (Book 5, Chapter 2, Section 3)
- flood routing techniques (Book 5, Chapter 2, Section 3 and Book 5, Chapter 6, Section 5)
- model parameters and links with physical catchment characteristics.

However, all models are only approximations of reality and require care and expertise in their application and interpretation.

The major types of runoff routing models are described firstly in terms of how they deal with the distributed nature of the flood formation and the variation of routing processes along the flow path from the top to the bottom of the catchment (Book 5, Chapter 6, Section 4). The different model representations of the hillslope or overland flow phase of the hydrograph formation are introduced in Book 5, Chapter 6, Section 4, while Book 5, Chapter 6, Section 4 deals with flood routing in the various forms of channel, natural stream and floodplain segments of the catchment. Finally, Book 5, Chapter 6, Section 4 describes how areas of significant extra flood storage, such as natural lakes or swamps, extensive floodplain areas, reservoirs or flood retention/detention basins are modelled.

6.4.2. Representing the Distributed Nature of Flood Formation

6.4.2.1. Relative Importance of Overland Flow and Channel Routing Phases

As described in Book 5, Chapter 2, the detail of catchment representation in flood hydrograph estimation models ranges from lumped models to fully distributed models. This section focuses on semi-distributed or node-link type models introduced in Book 5, Chapter 2, Section 3.

A number of investigators (e.g. Robinson et al. (1995)) have examined the relative roles of 'hillslope' (overland flow) processes and channel routing in the modelling of hydrologic response. Their conclusions indicate that in *relatively small catchments* the emphasis should be on appropriate modelling of the *hillslope response* to rainfall inputs, while the spatial variation of rainfall inputs and hillslope responses is less important. Lumped models (Book 5, Chapter 6, Section 4) or semi-distributed models with relatively simplistic representation of spatial variations (Book 5, Chapter 6, Section 4) can thus produce acceptable flood hydrograph estimates.

In contrast, in *large (>1000 km^2) to very large (>10,000 km^2) catchments* the flood response is governed primarily by the *network geomorphology* and the *spatial distribution of runoff inputs*. In these larger catchments, and in catchments with significant storage development, it is thus important to model the distributed nature of runoff inputs and to give a realistic representation of the actual drainage network in node-link type models (Book 5, Chapter 6, Section 4).

In catchments of intermediate size, the overland flow and channel routing phases may be of similar importance in the overall catchment response to rainfall inputs, and it is thus desirable to model the flow routing in the overland flow segments separately from the flow routing in the drainage network segments. Similar considerations apply in catchments with significantly different land uses (e.g. urban or partly urbanised catchments), where runoff from subareas of different type is routed separately before routing in the pipe or channel network.

6.4.2.2. Lumped Runoff Routing Models

By definition, lumped models do not allow for the distributed nature of flood hydrograph formation in catchments. At the time of their development the application of hydrograph estimation models was restricted to hand calculations, requiring relatively simple models. However, lumped models can still play a useful role as a component of node-link type models, to represent the formation of runoff hydrographs from hillslope or overland flow segments as an input to the streamflow network.

Apart from the Time-Area Method (Book 5, Chapter 6, Section 2) and the Unit Hydrograph Method (Book 5, Chapter 6, Section 3), the best known lumped runoff routing models are the Clark model (Clark, 1945) and the Nash model (Nash, 1960) illustrated in Figure 5.6.6. The Clark model represents the translation and attenuation through a linear storage placed at the catchment outlet. By placing a number of linear storages in series and routing the rainfall excess input successively through this cascade of storages, the Nash model provides more flexibility in matching the routing response of the model to both the hydrograph translation and attenuation characteristics of the catchment.

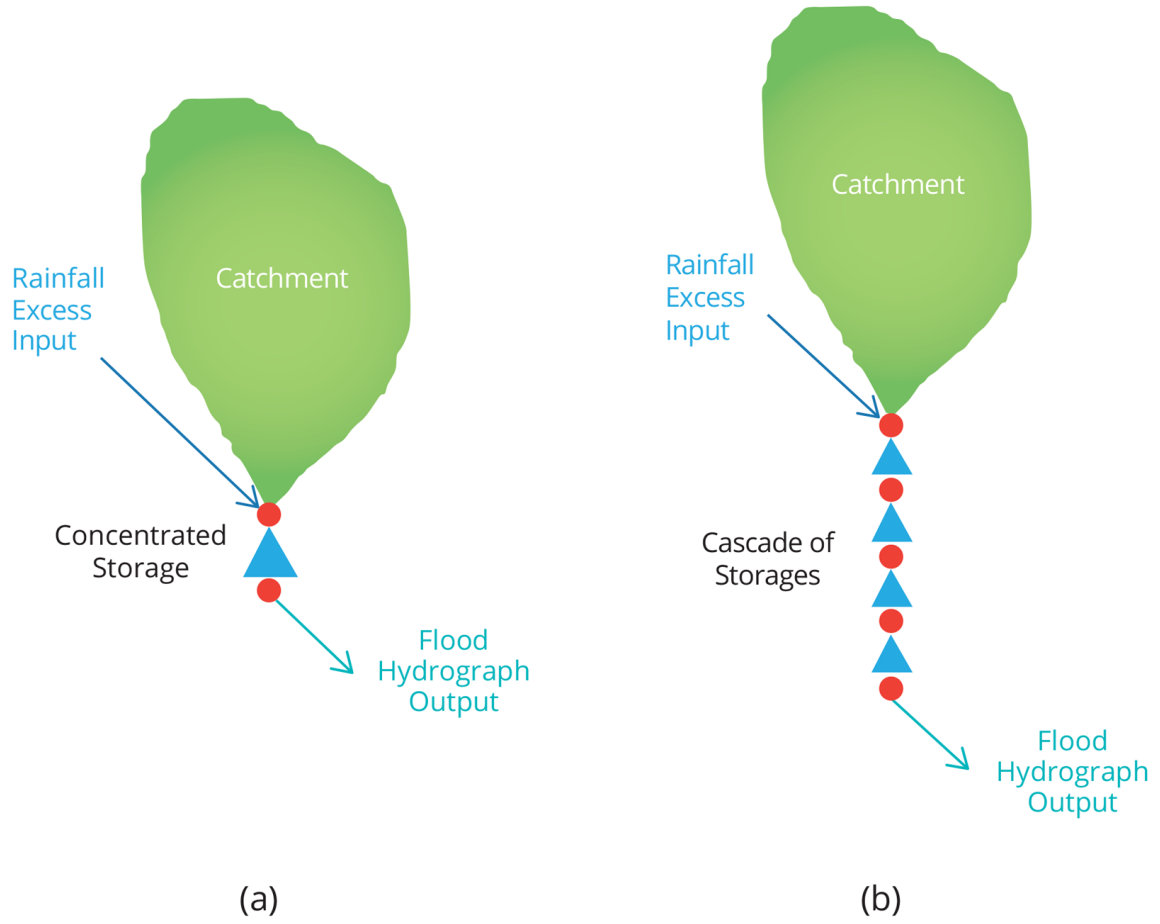

Figure 5.6.6. (a) Clark and (b) Nash models of runoff routing

The example below illustrates the application of a simple runoff routing model to estimate design flood hydrographs for an ungauged catchment of medium size. In most practical applications the simple Clark model would be replaced by a node-link type runoff routing model, implemented through one of the readily available runoff routing modelling systems referred to in Table 5.6.3 and Table 5.6.4. However, the steps of estimating model parameters and model inputs for the design application remain similar. The example also illustrates the application of the critical rainfall duration concept.

Example: Clark Runoff Routing Model

An ungauged catchment west of Melbourne has an area of 56 km^2 and a main stream length of 20 km. A flood hydrograph for a 1% AEP design event is required as the basis of defining flood prone land for a planned subdivision.

The Clark runoff routing model is being used to obtain an initial flood estimate for planning purposes. For the concentrated linear storage representing the catchment's routing characteristics in this model, the Muskingum routing equation (Equation (5.5.18)) can be written as

$$O_{n+1} = 2C_1\left(\frac{I_n + I_{n+1}}{2}\right) + C_3 O_n \tag{5.6.8}$$

C_1 and C_3 are calculated from Equation (5.5.19) which for X = 0 simplifies to

$C_1 = \frac{0.5\Delta t}{K + 0.5\Delta t}$ and $C_3 = \frac{K - 0.5\Delta t}{K + 0.5\Delta t}$

The coefficient K of the can be calculated as a function of the main stream length to the catchment boundary (L) using the equation proposed by Cordery et al. (1981):

$$K = 0.70L^{0.57} \tag{5.6.9}$$

For a main stream length of 20 km this gives a value of K = 3.86 hours.

The critical rainfall duration for this catchment is not known *a priori*, so a range of rainfall durations from 3 to 24 hours are trialled to find the duration than produces the highest peak flow. The design rainfall depths and temporal patterns have been selected in accordance with Book 2.

Based on experience with neighbouring catchments, the following design loss values have been adopted: IL = 15 mm, CL = 2.5 mm/h.

The resulting hydrographs for the five different durations are shown in the Figure below. This indicates that the critical rainfall duration for this catchment is about 9 hours. The estimated peak flow for the 1% AEP design flood event is 155 m^3/s.

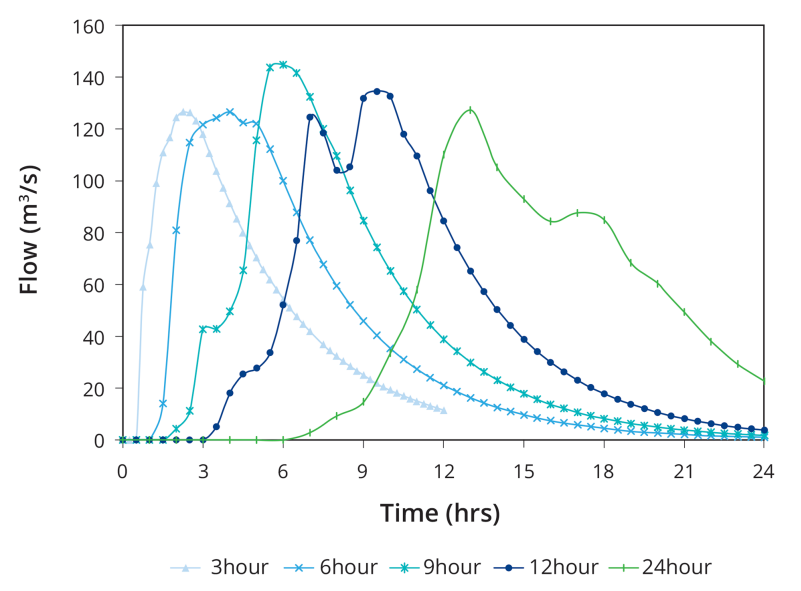

Figure 5.6.7. Clark Runoff Routing Example- resulting hydrographs for the five different durations

6.4.2.3. Simple Semi-distributed Models

The original Laurenson Runoff Routing Model – LRRM (Laurenson, 1962; Laurenson, 1964) illustrated in Figure 5.6.8 is an example of simple semi-distributed flood hydrograph estimation models. Similar to the time-area method, the LRRM divides the catchment into a number of sub-areas (typically 10) on the basis of equal travel time to the catchment outlet (isochrones). However, it assigns a separate storage to each of the subareas, and runoff from a sub-area is then routed through the series of downstream storages to the catchment outlet. The division into sub-areas and the detailed representation of travel time in the catchment allows the effects of spatial variation of catchment rainfall to be modelled explicitly.

The model uses nonlinear storages, with the relationship between discharge and storage represented by a power function, as discussed in Book 5, Chapter 5, Section 5 and expressed by Equation (5.5.32).

The catchment representation in the LRRM can be regarded as a linear network of ten rainfall input nodes, ten routing links (each with a nonlinear concentrated storage) and one output node. While the LRRM was originally conceptualised as a runoff routing model for the whole catchment, it is now more typically used as model to represent the routing of overland flow in a hillslope segment to a channel network node, e.g. in the XPRAFTS model (xpsolutions, 2016).

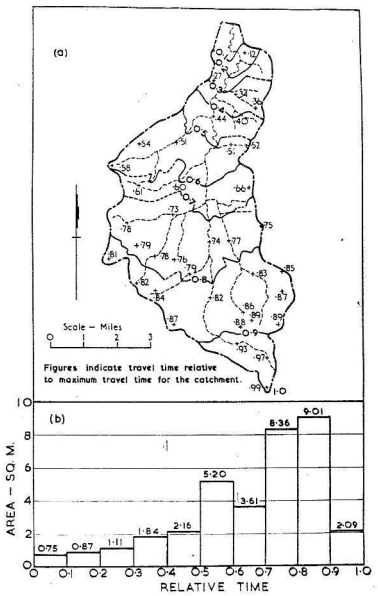

Figure 5.6.8. Original Laurenson Runoff Routing Model (South Creek catchment) (a) Isochrones of storage delay time (b) Time-area diagram

6.4.2.4. Node-link Type Models

The representation of the runoff routing process in a typical node-link type model is shown in Book 5, Chapter 6, Section 4. As shown on the left, the catchment is divided into a number of subareas within which the spatial rainfall distribution can be assumed to be uniform, and the actual drainage network is represented by a simplified network of the main tributary streams. The conceptual representation of this catchment in a runoff routing model is then by a set of nodes and links, as shown for the examples of RORB (centre) and WBNM (right).

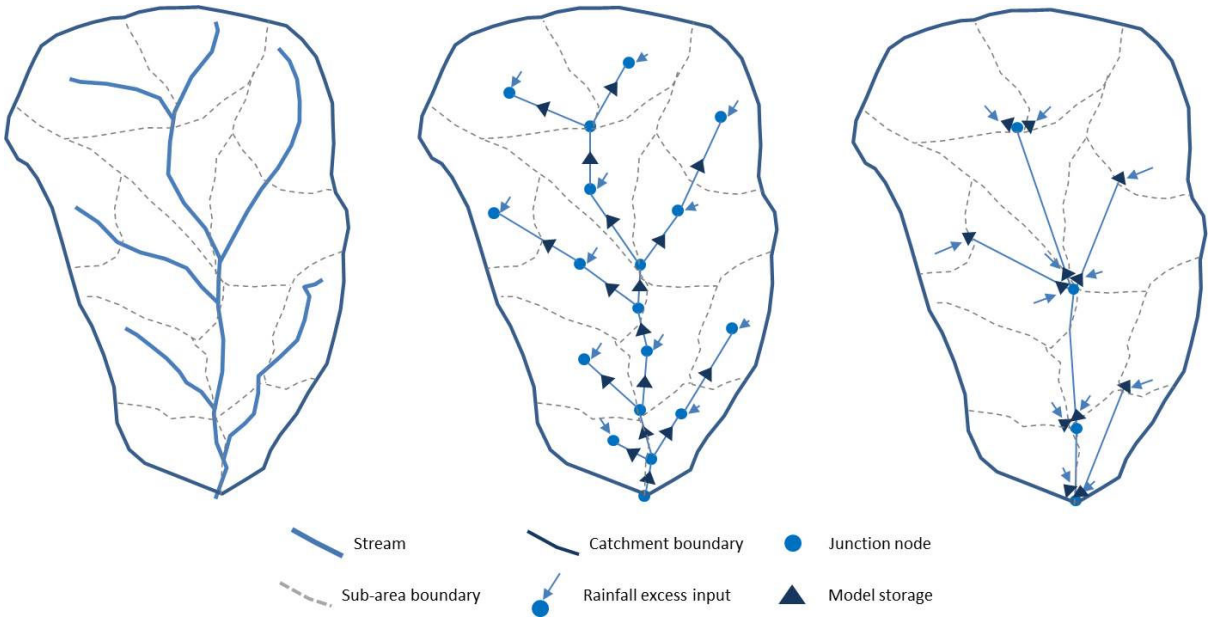

Figure 5.6.9. Node-link type representation of a catchment in runoff routing models: map view and schematic representation of node-link network in RORB and WBNM

As explained in Book 5, Chapter 6, Section 4, there are two distinctly different ways to convert the distributed rainfall excess inputs over a subarea into a runoff hydrograph at the subarea node (placed near the centroid of the subarea). These subarea runoff hydrographs are then routed progressively from one node through a routing link to the next node in the drainage network and eventually to the catchment outlet (Book 5, Chapter 6, Section 4). The concentrated or distributed storages used in these routing links are shown in Book 5, Chapter 6, Section 4 as small black triangles.

Some of the routing links receive the outflow hydrograph from an upstream link as well as a subarea runoff hydrograph. In these links the two hydrographs are combined before they are routed through to the next node in the network. At stream junction nodes the two (or more) tributary hydrographs are combined by simple addition.

The drainage network may also have a branched structure, where flows are diverted by natural or artificial features into a system of distributary or diversion channels, and these flows may or may not join up again with flows in the main channel. Most runoff routing modelling systems have the capability to represent the features controlling diversion and return flows.

If the catchment includes areas with significant extra flood storage, such as natural lakes or swamps, extensive floodplain areas, reservoirs or flood retention/detention basins, these can also be included in the drainage network as ‘special storage’ nodes or links, with separately defined storage and discharge characteristics (Book 5, Chapter 6, Section 4).

The baseflow contributions to the total flood runoff hydrograph (Book 5, Chapter 4) are typically modelled in a lumped fashion and added to the routed hydrograph at the catchment outlet. However, in more complex catchment situations with significant baseflow contributions it is desirable to model the distributed nature of baseflow contributions, by adding them at each runoff input node and routing the combined runoff hydrograph through the drainage network.

Figure 5.6.10 shows schematically how the different modelling components can be combined to convert the distributed rainfall inputs to a hydrograph at the catchment outlet.

The Book 5 chapters and sections providing more detail of the individual components are also indicated in the figure.

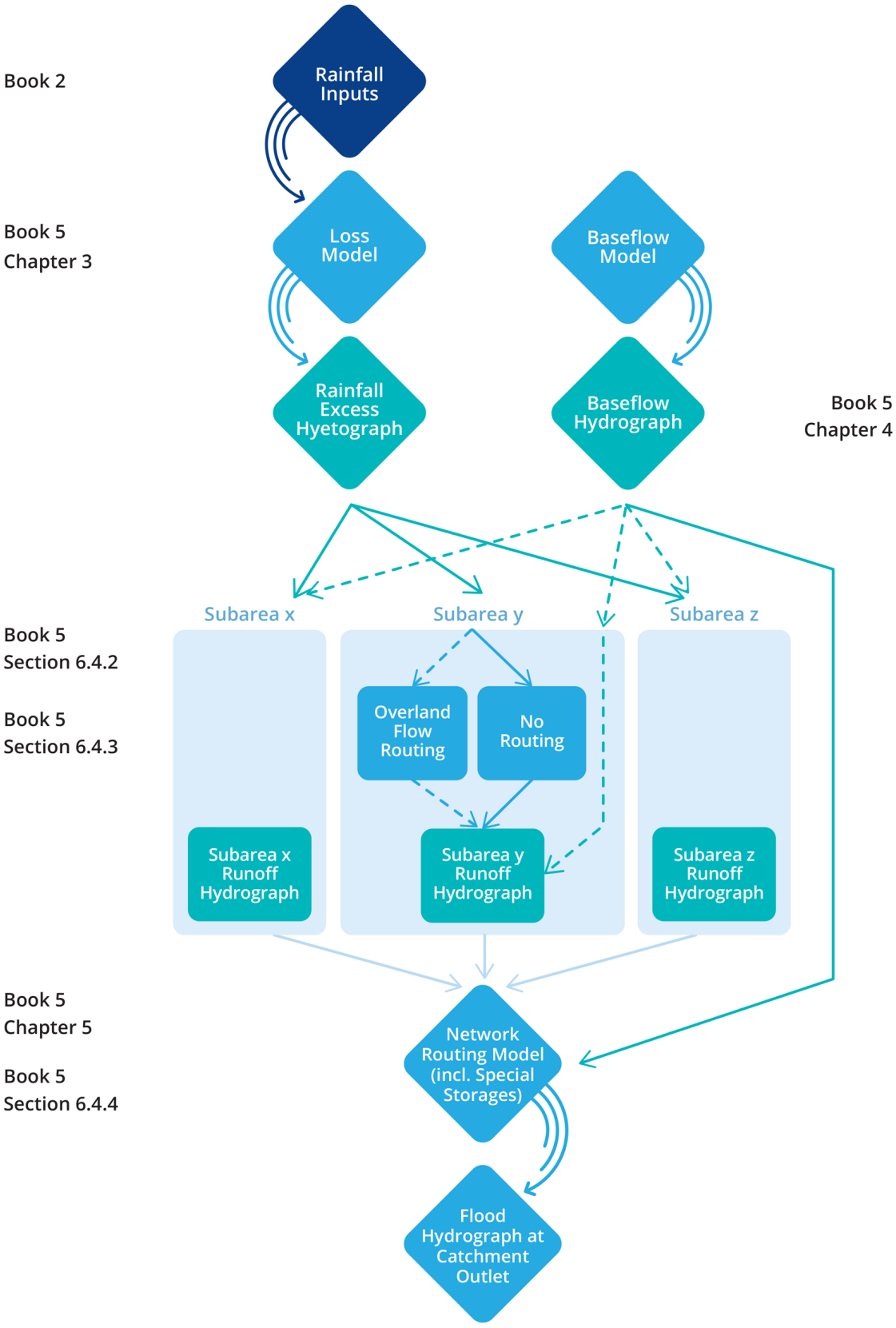

Figure 5.6.10. Components of a runoff routing model

Book 7 provides practical guidance on how these different model elements can best be used to represent the important features of a specific catchment.

6.4.3. Modelling of Hillslope (Overland Flow) Phase

The individual subareas of semi-distributed runoff routing models represent the runoff contributions from a relatively large part of a catchment (see Figure 5.6.9). Runoff from these subareas is the result of a complex and spatially varying set of processes which divide the rainfall inputs into a number of runoff components. These components may then follow different pathways to the model node used to represent their combined input to the modelled stream or channel network (Kemp, 2002). The mix and relative importance of different processes depends on the runoff production characteristics of a particular catchment. The scale of the modelled catchment also plays an important role, as with increasing size of the subareas a greater degree of averaging of the effects of different processes and modification of the runoff hydrograph though routing processes will occur,

As discussed in more detail in Book 4, Chapter 2, the runoff routing models routinely used in Australia employ very simplified representations of the processes involved in runoff production, generally dividing the rainfall inputs into a loss and rainfall excess component, and dealing only indirectly with baseflow contributions. The main distinction in the modelling of runoff from contributing areas is in how the routing of runoff within the subareas is treated.

6.4.3.1. Combined Subarea and Stream/Channel Network Routing

In this form of model conceptualisation the hillslope or overland flow phase of the hydrograph formation is modelled by simply converting the rainfall excess hyetograph into a direct runoff hydrograph:

$$1/3.6 * \text{Rainfall Excess (mm/h)} * \text{Catchment Area}\left(km^2\right) = \text{Runoff}\left(m^3/s\right) \quad (5.6.10)$$

(6.4.1)

This subarea runoff hydrograph is input at a stream network node near the centroid of the subarea and then routed successively along the stream network to the catchment outlet. The modification of the hydrograph as it travels through the stream or channel network is generally modelled by a linear or nonlinear storage for each routing link (Book 5, Chapter 5, Section 4 and Book 5, Chapter 5, Section 5).

Examples of the application of the combined subarea and stream network routing approach include the RORB Runoff Routing Model (Laurenson et al., 2010) and the Basic Model version of URBS (Carroll, 2012).

The key feature of this runoff routing conceptualisation is that all the translation and attenuation effects experienced by the runoff inputs on their way to the catchment outlet have to be represented in the routing through the channel links.

The justification for the combined treatment of overland flow and stream/channel network routing is firstly that the separation of these two phases is somewhat arbitrary, in that the change from shallow distributed flow over hillslope surfaces to concentrated flow in water courses and streams is very gradual. Secondly, if the interest is only on hydrographs at the catchment outlet, the internal separation into different processes is of secondary importance, as long as the overall routing and delay characteristics of the catchment and their variation with flood magnitude can be adequately represented. As discussed in Book 5, Chapter 6,

Section 4, this condition is likely to be satisfied in large catchments with relatively uniform land use.

The main limitation of this modelling approach is that it is designed to produce only an integrated catchment response hydrograph at or near the catchment outlet. As demonstrated by Yu and Ford (1989), this modelling approach does not satisfy the principles of 'self-consistency', as the storage parameter of an individual routing element depends on the size of the total catchment being modelled. While the model can output hydrographs at any internal node, hydrographs produced for the upper parts of the catchment are likely to show positive bias, as they tend to underestimate the degree of attenuation in the routing process.

6.4.3.2. Separate Overland Flow and Stream/Channel Network Routing

The node-link conceptualisation of the catchment in these runoff routing approaches is similar to the one shown in Figure 5.6.9 but the subarea rainfall excess inputs are now first routed through a storage element (or a kinematic wave routing element) to produce the runoff hydrograph inputs to the stream network. Different models use different methods to derive the runoff hydrographs from the hillslope segments, as summarised in Table 5.6.3.

Table 5.6.3. Methods used in different runoff routing modelling systems to derive the overland flow hydrograph

Method	Example	Reference	ARR Section
Time-area method	ILSAX, DRAINS	O'Loughlin and Slack (2014)	Book 5, Chapter 6, Section 2
Unit hydrograph convolution	HEC-HMS	HEC (2000)	Book 5, Chapter 6, Section 3
Cascade of non-linear storages	XPRAFTS	xpsolutions (2016)	Book 5, Chapter 5, Section 5 Book 5, Chapter 6, Section 4
Nonlinear storage routing	SWMM URBS WBNM2000	EPA (2016) Carroll (2012) Boyd et al. (2002)	Book 5, Chapter 5, Section 5 Book 5, Chapter 6, Section 4
Kinematic wave routing	HEC-HMS (Option)	HEC (2000)	Book 5, Chapter 5, Section 6 Book 5, Chapter 6, Section 4

The hydrograph formation methods used by the first three groups of modelling systems have been described in previous chapters, as indicated in the last column of Table 5.6.3, and the methods used to estimate their parameters are described in the relevant user manuals. The catchment conceptualisation used in nonlinear storage routing models and kinematic wave routing models warrants some additional discussion (Book 5, Chapter 6, Section 4 and Book 5, Chapter 6, Section 4 respectively).

The main advantage of modelling the overland flow phase separately is that this modelling approach can deal with different land uses in different parts of the catchment and changes to

these land uses, such as substantial urbanisation. If the variation of the routing response with flood magnitude is quite different for the overland flow and channel routing phases, then a separate modelling approach lends itself better to extrapolation to Very Rare to Extreme flood events.

The disadvantage of the separate overland and channel flow routing approach is that it requires additional parameters to model the contributing area or overland flow component of the overall catchment routing process. If appropriate information is not available to allow separate calibration of the parameters to the overland and channel routing processes, then it may be more appropriate to use a combined routing approach, as described above.

More detailed approaches for modelling runoff from the overland flow segment have also been proposed and applied. The RRR model (Kemp and Daniell, 1996) allows for the generation of the runoff hydrograph by two or more different processes, with different losses and subarea routing delays being applied to each runoff component. Kemp (2002) postulated three different conceptual processes that can contribute to runoff at the subarea scale: baseflow, ‘slow flow’ and ‘fast flow’.

For urban catchments, further sub-division of the overland component on a spatial basis to allotment-size units and subsequent scaling up to the subareas has been proposed by Goyen (2005).

6.4.3.3. Nonlinear Storage Routing of Overland Flow

In the nonlinear storage routing models the attenuation and delay experienced by runoff from a subarea (i.e. a hillslope or overland flow segment) are modelled by routing through a nonlinear storage of the form

$$S = kQ^m \tag{5.6.11}$$

where the coefficient *k* is a delay or lag time parameter related to the lag parameter *K* in linear storage routing models (Book 5, Chapter 5, Section 4) by the following equation

$$k = KQ^{1-m} \tag{5.6.12}$$

and the exponent *m* expresses the degree of nonlinearity of the routing response. Exponent values in the range of 0.6 to 0.8 are typically used.

The coefficient k has been shown to be a function of catchment area A

$$k = CA^b \tag{5.6.13}$$

where *C* is a lag parameter for the subarea of the catchment. Equation (5.6.13) with an exponent value *b* = 0.57 is the basis of the subarea routing elements used in the WBNM2000 model (Boyd et al., 2002).

A similar expression for *k* is used in the URBS model, with an exponent value *b* = 0.5 (Carroll, 2012). URBS also allows adjustments of *k* for the degree of forestation of the subarea (increasing the value of *k*) and for the fraction of the subarea being urbanised (reducing the value of *k*).

The detailed form of the equations used and the adopted numerical solution method are described in the manuals of the respective runoff routing modelling systems.

6.4.3.4. Kinematic Wave Routing of Overland Flow

In the kinematic wave routing approaches the 'hillslopes' are generally conceptualised as two symmetrical rectangular planes of width *W*, inclined at slope *S*, discharging into the stream channel, as shown in Book 5, Chapter 6, Section 4. This simplified representation of the complex hillslope topography focuses on the average properties of the hillslope relevant to runoff generation rather than reflecting the actual physical processes at a smaller scale.

The overland flow discharging from the hillslope segment into the channel (at a node) is computed as flow in a wide rectangular channel, giving the simplified expression

$$q = \frac{s^{\frac{1}{2}}}{n} y^{\frac{5}{3}} \tag{5.6.14}$$

where *q* is the discharge per unit width of the hillslope, *S* is the slope of the hillslope plane, *n* a roughness coefficient and *y* the average flow depth over the plane. It should be noted that the roughness coefficient *n* for overland flow over a particular type of surface and ground cover is typically higher than for channels (Bedient et al., 2008).

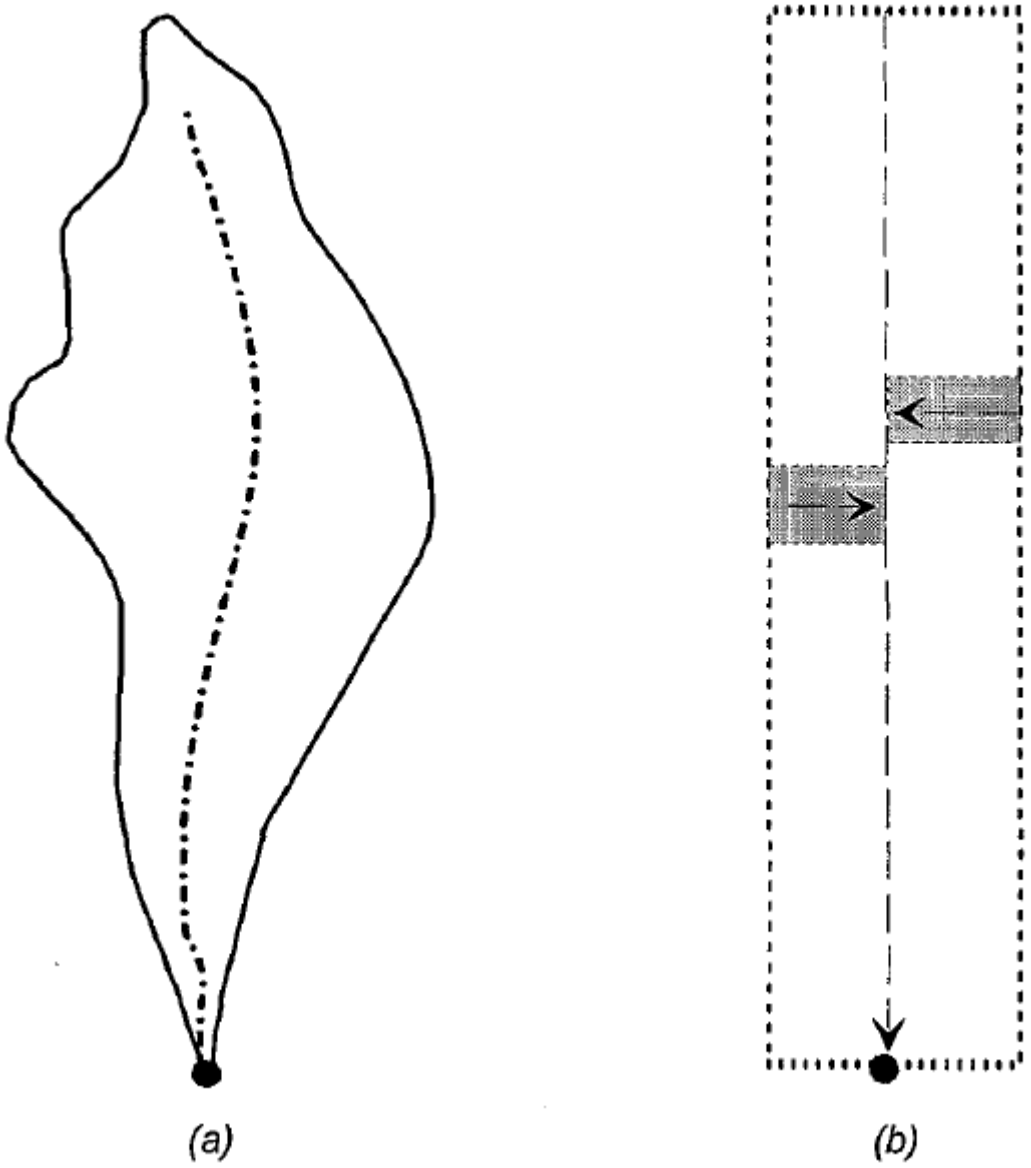

Figure 5.6.11. Hillslope representation in kinematic wave routing models (a) actual catchment (b) model representation (from HEC-HMS Manual)

Equation (5.6.15) is substituted in the appropriate form of the kinematic wave equation

$$\frac{\partial y}{\partial t} + \frac{\partial q}{\partial x} = i \tag{5.6.15}$$

where is *x* is the distance in the direction of the overland flow and *i* the rate of rainfall excess (mm/h) on the hillslope plane.

While analytical solutions are available to solve the overland flow equations, runoff routing modelling systems such as HEC-HMS (HEC, 2000) use a numerical solution scheme to solve the kinematic wave equation for *y* at each time step. This value is then substituted into Equation (5.6.14) and the flow rate *q* per unit width (from one of the planes) is multiplied by twice the width of the hillslope (measured parallel to the channel) to determine the total overland flow hydrograph from the subarea.

A more detailed description of kinematic wave routing techniques and their application in a flood hydrograph estimation model (HEC-1 or HEC-HMS) is given in HEC (1993).

6.4.4. Routing Through Channel, Stream and Floodplain Reaches

As shown in Figure 5.6.9, the inflow hydrographs from the various catchment subareas have to be routed through the drainage network formed by the channel, stream and floodplain reaches. Table 5.6.4 gives an overview of the routing methods of varying complexity available in different runoff routing modelling systems, with corresponding references and links to the relevant sections of Book 5, Chapter 5 that describe these routing methods in more detail.

Table 5.6.4. Routing models used in different runoff routing modelling systems to route flows through channel, stream and floodplain reaches

Routing Model	Example	Reference	ARR Section
Simple lag, Lag and route	RORB (Option) SWMM (Option) XPRAFTS Option)	Laurenson et al. (2010) EPA (2015) xpsolutions (2016)	Book 5, Chapter 5, Section 3
Muskingum-Cunge Method (linear)	XPRAFTS	xpsolutions (2016)	Book 5, Chapter 5, Section 4
Concentrated non-linear storages	ILSAX, DRAINS RORB WBNM2000	O'Loughlin and Slack (2014) Laurenson et al. (2010) Boyd et al. (2002)	Book 5, Chapter 5, Section 5
Nonlinear Muskingum	SWMM URBS	EPA (2015) Carroll (2012)	Book 5, Chapter 5, Section 5
Kinematic wave routing	HEC-HMS (Option) ILSAX, DRAINS XPRAFTS (Option)	HEC (2000) O'Loughlin and Slack (2014) xpsolutions (2016)	Book 5, Chapter 5, Section 6
Dynamic wave routing	SWMM XPRAFTS (Option)	EPA (2015) xpsolutions (2016)	Book 5, Chapter 5, Section 6

The parameters of the simple lag and storage routing models are generally estimated by analysis of or calibration to observed hydrographs in the catchment being modelled, or by transfer of information from gauged catchments in regions with similar streamflow characteristics. In these methods it is generally assumed that the same parameter set applies to the different routing links, except for an adjustment to reflect the different time lag associated with routing reaches of different lengths.

In the Muskingum-Cunge Method, the kinematic wave and the dynamic routing methods the routing parameters can be determined from direct links with stream survey data and hydraulic flow characteristics, e.g. channel slope and hydraulic roughness (Equation (5.5.25) and Equation (5.5.26)). These parameters will thus vary naturally with the topographic and hydraulic characteristics of the routing reaches.

In the modelling systems using the nonlinear storage routing methods described in Book 5, Chapter 5, Section 5, the value of the exponent *m* in the nonlinear storage-discharge relationship found from calibration to observed hydrographs typically varies in the range from 0.6 to 0.8. These values imply that with increasing flood magnitude discharge increases more rapidly than storage. A value of $m = 1.0$ (linear storage) would imply that discharge and storage increase at the same rate).

The expected variation of the exponent with flood magnitude is particularly important when appropriate routing parameter values for the estimation of Very Rare to Extreme floods need to be selected. This question is discussed in more detail in Book 8, Chapter 5, Section 4.

As indicated in Book 5, Chapter 5, Section 4 and Book 5, Chapter 5, Section 5, the translation and attenuation effects of distributed storage, as modelled by the Muskingum-Cunge method, can also be represented by routing through a series of concentrated storages. Figure 5.6.12 illustrates the effect of successive routing of a rainfall excess hydrograph from subarea A through three concentrated nonlinear storages. The peak of the input hydrograph is progressively translated and attenuated on its movement along the channel network.

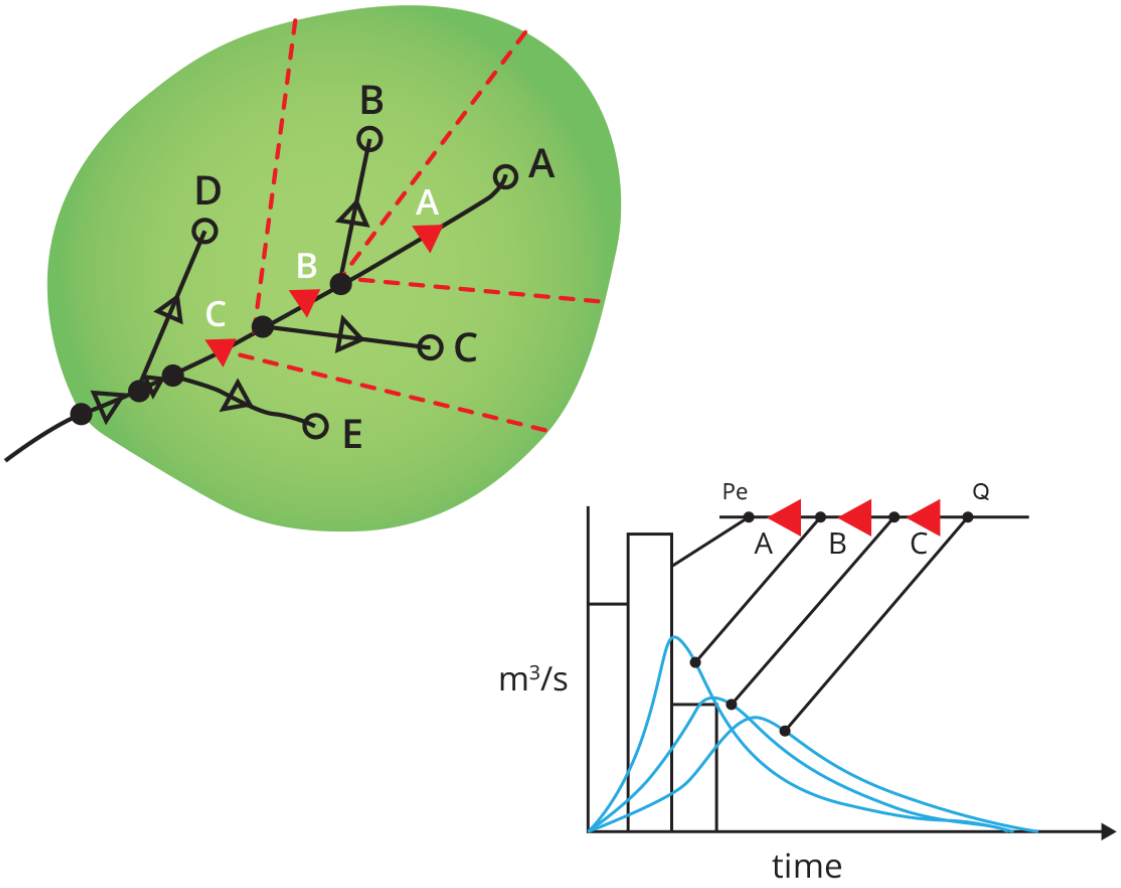

Figure 5.6.12. Routing of rainfall excess hydrograph through a series of nonlinear storages (after Laurenson et al. (2010))

The characteristic reach length criterion expressed by Equation (5.5.28) means that the degree of subdivision of the drainage network into sub-reaches represented by concentrated storages cannot be chosen arbitrarily. Too few or too many sub-reaches will make it difficult to accurately reflect both the translation and attenuation effects experienced by flood waves as they move through the drainage network of the actual catchment. Boyd (1985) has shown empirically that the optimum degree of subdivision of a catchment into subareas and routing reaches increases approximately with the square root of catchment area.

The different methods available to estimate the routing parameters for different runoff routing modelling systems are discussed in Book 7, Chapter 5.

6.4.5. Routing Through Special Storages

The methods used to route hydrographs through channel, stream and floodplain reaches assume similar routing characteristics in different routing links. If the catchment includes areas with significant extra flood storage (e.g. natural lakes or swamps, extensive floodplain areas, reservoirs or flood retention/detention basins), this assumption is no longer satisfied, and these special features will require separate representation in the model. They can be included in the node-link network as ‘special storage’ nodes or links, with separately defined storage-discharge relationships.

The approaches used to represent the routing effects through a special storage range from linear reservoir routing methods (Book 5, Chapter 5, Section 4) to non-linear storage routing methods (Book 5, Chapter 5, Section 5), with different methods being applied to define the S-Q relationship for the storage:

- a linear or nonlinear S-Q relationship derived by calibration to observed hydrographs (after the routing parameters of the normal channel routing links have been determined)

- a nonlinear S-Q relationship for a special channel or floodplain routing link determined from calculations of storage volumes in the link and corresponding flow through the link for different flood magnitudes, or from the analysis of hydraulic modelling results

- a nonlinear S-Q relationship for reservoir or pond determined by combining a stage-storage relationship (e.g. a reservoir storage capacity curve) with a stage-discharge relationship (e.g. a spillway rating curve)

- a set of S-Q relationships for regulated storages with information on the triggers for the application of the individual S-Q relationships

- separate specification of a stage-storage relationship together with details of the levels and hydraulic characteristics that determine the different forms of outflows from the storage (e.g. for flood detention basins)

Details of these different options are provided in the user manuals of the different runoff routing modelling systems.

6.5. Rainfall on Grid Modelling Approaches

6.5.1. Introduction

The following description of the ‘rainfall-on-grid’ or ‘direct rainfall’ modelling approaches to runoff routing is based mainly on the Stage1/2 report from ARR Revision Project 15 ‘Two-dimensional (2D) modelling (Babister and Barton, 2016)

In contrast to the traditional rainfall runoff modelling approaches, the rainfall-on-grid approaches do not require the specification of a node-link type representation of the catchment and its drainage network. Instead they use information from a digital elevation model and hydraulic modelling to define the drainage paths used by floodwaters on their way towards the catchment outlet. In the flatter parts of a catchment the drainage paths may thus change adaptively during a flood event.

The catchment is represented by a large number of grid cells, each with its individual rainfall input and runoff output – in other words, the cells act as the equivalent to subareas in node-link type models. However, the different scales of these basic catchment elements have important implications for the modelling of flood runoff, as they require different representations of the typical properties of the catchment elements. The non-linear nature of runoff generation means that the average response from many different small scale catchment elements cannot be expected to correspond to the lumped response of a subarea with average properties (e.g. a hillslope in a kinematic wave model).

The rainfall-on-grid approaches can be applied in two ways:

- the whole catchment is represented by a 2D grid, or

- a ‘hybrid approach’, where only the flatter parts of the catchment with more complex floodplain topography are represented by a 2D grid; they receive inflow hydrographs from the rest of the catchment produced by a traditional runoff routing approach.

The computational basis of the rainfall-on-grid approaches are the two-dimensional unsteady flow equations introduced in Book 6, Chapter 4, Section 7, or simplified forms of these equations.

Figure 5.6.13 shows how the generation of runoff from a grid cell is conceptualised. Different direct rainfall models vary in the degree of detail adopted in modelling the runoff generated on a grid element, as discussed in Book 5, Chapter 6, Section 5.

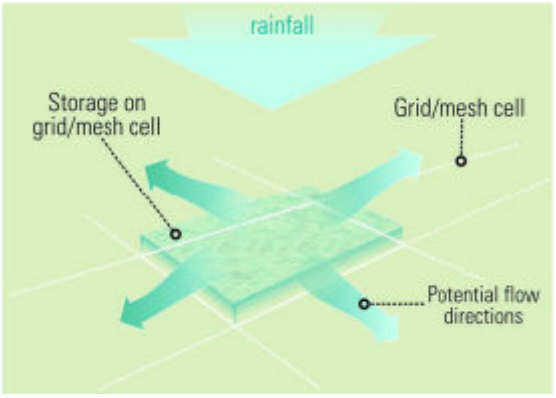

Figure 5.6.13. Conceptualisation of generation of runoff hydrograph from a grid cell

The successive routing of the runoff through other grid cells to the catchment outlet then uses the hydraulic routing approaches incorporated into the modelling package.

6.5.2. Modelling of Runoff from Individual Cells

Similar to traditional runoff routing models, runoff from a grid cell depends on the following factors:

- the area of the grid cell
- the rainfall depth
- the losses and
- the storage volume in the cell

However the amount and direction of outflow from the cell here also depends on additional factors:

- the hydraulic roughness of the cell
- the slope between neighbouring grid cells and
- the water level in neighbouring cells
- inflows from other cells

In principle the model can accept a detailed space-time distribution of the rainfall inputs but in practice limited data availability means that more discretised rainfall inputs need to be used.

The traditional loss models described in Book 5, Chapter 3 can be used but the way these losses are applied may vary in different models, and the traditional design loss values may thus not be directly applicable. Loss models that have a more direct physical basis could also be applied to reflect the varying infiltration, depression storage and transmission losses that reduce the volume of rainfall inputs but the required data and parameters estimates are not readily available. Finally, at least in theory, a groundwater model could be integrated to allow a consistent estimation of losses and baseflow contributions when modelling over an extending time period.

The topographic information included in the model means that the model can include relatively large depression storage areas which interact with losses. A process of 'pre-wetting' these storage areas (priming the model with an artificial rainfall burst to fill depression storages) may have to be used to prevent low bias in modelled flood hydrographs.

The model outputs are quite sensitive to the selection of the hydraulic roughness parameters. Because of the differences in conceptualisation and scale, these grid cell roughness parameters will generally be different from the values used in traditional channel hydraulics. Use of depth varying roughness parameters rather than constant ones may be necessary to reflect the changing hydraulic characteristics of catchment surfaces with flow depth.

The modelling of urban areas requires consideration of the impacts of a mix of different catchment surfaces, buildings, drainage systems and other infrastructure. The model resolution will generally not allow these features to be represented in detail, thus representative cell characteristics need to be adopted, using some form of averaging of the detailed urban area characteristics.

6.5.3. Advantages and Limitations of the Rainfall-on-Grid Approaches

As summarised in ARR (2012) the use of rainfall-on-grid approaches has following advantages and limitations:

Advantages of rainfall-on-grid approaches:

- Where a 2D model extends over the whole catchment, there is no need to develop and calibrate a separate hydraulic model, allowing seamless simulation of flood level outputs from rainfall inputs.
- Assumptions on sub-catchment delineation are not required as these are automatically defined by the topographic information for the cells.
- Overland flow is modelled directly.
- Drainage paths and flow direction do not need to be predefined, which makes the approaches particularly useful for runoff routing in flat areas and where catchment boundaries are not well defined.

Challenges and limitations of rainfall-on-grid approaches:

- Direct rainfall modelling is a new technique, with limited calibration or verification to gauged data. Caution and detailed checking is needed in the application of this approach.

- Potential significant increases in model run times. Hydrological models on their own generate peak flows significantly faster than direct rainfall, which facilitate their use in simulation frameworks that aim to ensure probability neutrality in the transformation of rainfall into floods (as discussed in Book 4, Chapter 3).

- Require digital terrain information. Depending on the accuracy of the results required, there may be a need for extensive survey data, such as aerial survey data.

- Insufficient resolution of smaller flowpaths may impact upon timing of routed flows. The smaller flowpaths higher up in the catchment may not be as well-represented by the 2D model as they may exist on a sub-grid scale. This may affect timing of runoff routing.

- The shallow flows generated in the direct rainfall approach may be outside the typical range of application of Mannings 'n' roughness parameters and will thus require special consideration.

ARR (2012) discusses these challenges/limitations and possible ways to deal with them in more detail.

It is important for both users of rainfall-on-grid models and their clients to realise that greater detail in the representation of catchment physiography can only be expected to translate to greater accuracy of flood estimation results if this is accompanied by appropriate representation of hydrologic flood formation processes at the adopted special scale. Given the present simple representation of such processes and the difficulties of realistically representing shallow overland flows, it is considered that at present the main value of rain-on-grid models is their ability to accommodate the influences of hydraulic controls on flow conditions.

At the current stage of development of these models and with the limited level of experience gained with their practical application, it is considered premature to recommend the general use of rainfall-on-grid models in these guidelines.

However, it is expected that further development and testing will allow rainfall-on-grid models to be more widely applied.

6.6. References

ARR (2012). Australian Rainfall and Runoff Revision Project 15: Two-dimensional modelling in urban and rural floodplains, Stage 1 and Stage 2 Report.

Babister, M. and Barton, C. (eds) (2016). Australian Rainfall and Runoff Support Document: Two dimensional modelling in urban and rural floodplains. Project 15

Bedient, P.B., Huber, W.C. and Vieux, B.E. (2008), Hydrology and floodplain analysis, ed. 4, Upper Saddle River: Prentice Hall.

Bernard, M.M. (1935), An approach to determinate streamflow, Transactions of the American Society of Civil Engineers, 100: 347-395.

Body, D.N. (1962), Significance of peak runoff intensity in the application of the unit graph method to flood estimation, Journal of the Institution of Engineers, Australia, 34: 25-31.

Boyd, M.J. (1982). A note on the Cordery-Webb synthetic unit hydrograph, IEAust. Civil Engineering Transactions, CE24(1), 107-108

Boyd, M.J. (1975), Hydrograph synthesis using mathematical models, Proceedings of the 1975 Hydrology Symposium, Institution of Engineers, Australia, NCP 75/3, pp: 117-121.

Boyd, M.J. (1985), Effect of catchment subdivision on runoff routing models, Civil Engineering Transactions, Institution of Engineers, Australia, 27: 403-410.

Boyd, M.J., Rigby, E.H., VanDrie, R. and Schymitzek, I. (2002), WBMN 2000 for flood studies on natural and urban catchments, In 'Mathematical Models of Small Watershed Hydrology and Applications', pp: 225-258.

Carroll, D.G. (2012), URBS (Unified River Basin Simulator) A Rainfall Runoff Routing Model for Flood Forecasting and Design. Version 5.00 Dec, 2012.

Clark, C.O. (1945), Storage and the unit hydrograph, Transactions of the American Society of Civil Engineers, volume 110, pp.1419-1488.

Cordery, I. (1987), The unit hydrograph method of flood estimation, Chapter 8 in Australian Rainfall & Runoff - A Guide to Flood Estimation, Barton: Engineers Australia.

Cordery, I. and Webb, S.N. (1974), Flood estimation in eastern New South Wales - a design method, Civil Engineering Transactions, Institution of Engineers, Australia, 16: 87-93.

Cordery, I., Pilgrim, D.H. and Baron, B.C. (1981), Validity of use of small catchment research results for large basins, Civil Engineering Transactions, Institution of Engineers, Australia, CE23: 131-137.

United States Environmental Protection Agency (2016), Storm water management model - reference manual, volume 1 - Hydrology (Revised), Washington: United States Environmental Protection Agency, available at: <http://nepis.epa.gov/Exe/ZyPDF.cgi?Dockey=P100NYRA.txt>.

United States Environmental Protection Agency (2015), Storm water management model - user manual version5.1, Washington: United States Environmental Protection Agency, available at: <http://nepis.epa.gov/Exe/ZyPDF.cgi?Dockey=P100N3J6.TXT>.

Goyen, A. (2005), Changes to urban stormwater management from ARR1958 to ARR2008? - 2005 Munro Oration, delivered at the 29th Hydrology and Water Resources Symposium, 20-23 February, Canberra.

HEC (2000), Hydrologic Modelling System HEC-HMS Technical Reference Manual, United States Army Corp of Engineers, Hydrologic Engineering Centre, available at: <http://www.hec.usace.army.mil/software/hec-hms/documentation/HEC-HMS_Technical%20Reference%20Manual_%28CPD-74B%29.pdf>.

HEC (1993). Introduction and application of kinematic wave routing techniques using HEC-1. US Army Corp of Engineers, Hydrologic Engineering Centre, http://www.hec.usace.army.mil/publications/TrainingDocuments/TD-10.pdf.

Hawken, R.W.H. (1921), An analysis of maximum run-off and rainfall intensity, Transactions of the Institution of Engineers, Australia, 2: 193-215.

Kemp, D.J. (2002), The development of a rainfall-runoff-routing (RRR) model. Thesis submitted to the Department of Civil and Environmental Engineering, University of Adelaide.

Kemp, D.J. and Daniell, T.M. (1996), A proposal for a rainfall runoff routing (RRR) model. I.E.Aust. Proceedings of the 23rd Hydrology and Water Resources Symposium, May, Hobart, pp: 15-20.

Laurenson, E.M. (1998). Hydrology CIV3263 Course Notes, Monash University, Department of Civil Engineering.

Laurenson, E.M. (1975), Streamflow in catchment modeling, Proceedings of Prediction in Catchment Hydrology - a national symposium on Hydrology, sponsored by the Australian Academy of Science, 25-27 November, Canberra.

Laurenson, E.M. (1962), Hydrograph synthesis by runoff routing, Research Report 66, Sydney: Water Research Laboratory, University of New South Wales.

Laurenson, E.M. (1964), A catchment storage model for a runoff routing, Journal of Hydrology, 2: 141-163.

Laurenson, E.M., Mein, R.G. and Nathan, R.J. (2010). RORB Version 6 Runoff Routing Program - User Manual.

Leopold, L.B., Wolman, M.G. and Miller, J.P. (1964), Fluvial processes in geomorphology, San Francisco: W.H. Freeman.

Nash, J.E. (1960), A unit hydrograph study with particular reference to British catchments, Proceedings of the Institute Civil Engineers, 17: 249-282.

O'Loughlin, G. and Stack, R. (2014), DRAINS User Manual - a manual on the DRAINS program for urban stormwater drainage system design and analysis, Available at: <http://www.watercom.com.au/DRAINS%20Manual.pdf>.

Pilgrim, D.H. (1977), Isochrones of travel time and distribution of flood storage from a tracer study on a small watershed, Water Resources Research, 13(3), 587-596.

Pilgrim, D.H. (1966a), Radioactive tracing of storm runoff on a small catchment - 1. Experimental technique, Journal of Hydrology, 4: 289-305.

Pilgrim, D.H. (1966b), Radioactive tracing of storm runoff on a small catchment - 2. Discussion of results, Journal of Hydrology, 4: 306-326.

Robinson, J. S., Sivapalan, M. and Snell J. D. (1995), On the relative roles of hillslope processes, channel routing, and network morphology in the hydrologic response of natural catchments, Water Resour. Res., 30(12), 3089-3101.

Ross, C.N. (1921), The calculation of flood discharges by the use of a time contour plan, Transations of the Institution of Engineers, Australia, 2: 85-92.

Sherman, L.K. (1932), Streamflow from rainfall by unitgraph method, Engineering News Record, 108: 501-505.

Titmarsh, G.W. and Cordery, I. (1991), An examination of linear and non linear flood estimation methods for small agricultural catchments, Australian Civl Engineering Transactions, 33(4), 233-242.

Yu, B and Ford, B.R. (1989). Self-Consistency in Runoff Routing Models. IEAust Civil Engg. Trans., CE31(1), 47-53.

xpsolutions (2016), Rafts: Urban and rural runoff routing application, Belconnen, available at: <http://xpsolutions.com/assets/dms/XPRAFTS-tech-desc.pdf>.

Australian Rainfall & Runoff

ENGINEERS
AUSTRALIA

11 national Circuit
BARTON ACT 2600
e | arr_admin@arr.org.au
www.arr.org.au

9 781925 848366